

For Reference

NOT TO BE TAKEN FROM THIS ROOM

Ex libris
UNIVERSITATIS
ALBERTAEASIS



To My Parents

THE UNIVERSITY OF ALBERTA

KINETIC STUDIES ON CARBONATOCOBALT(III) AMMINE COMPLEXES

by



Donald James Francis

A THESIS

SUBMITTED TO THE FACULTY OF GRADUATE STUDIES
IN PARTIAL FULFILMENT OF THE REQUIREMENTS FOR THE DEGREE
OF DOCTOR OF PHILOSOPHY

DEPARTMENT OF CHEMISTRY

EDMONTON, ALBERTA

SPRING, 1971

UNIVERSITY OF ALBERTA
FACULTY OF GRADUATE STUDIES

The undersigned certify that they have read, and recommend to
the Faculty of Graduate Studies for acceptance, a thesis entitled

KINETIC STUDIES ON CARBONATOCOBALT(III) AMMINE COMPLEXES

submitted by Donald James Francis in partial fulfilment of the require-
ments for the degree of Doctor of Philosophy.

..... Sept 1 19

ACKNOWLEDGMENTS

I would like to express my sincere thanks to Dr. Robert B. Jordan for his help and encouragement during the course of these studies.

Special thanks to my wife, Susan, for her patience and understanding throughout my years of study.

A special thank you to my parents, Ed and Mai Francis, to whom this thesis is dedicated.

To my children, Heather and Catherine, goes my appreciation for the use of time which was rightfully theirs.

To Mrs. Gladys Whittal goes my thanks for her secretarial assistance.

Financial assistance from the University of Alberta and the National Research Council of Canada was greatly appreciated.

ABSTRACT

Chapter 1 serves as a brief general introduction to the thesis. The term, "mechanism of a reaction" is defined and the classical kinetic method of investigating a mechanism is discussed. The two major types of classification schemes for inorganic substitution reactions are reviewed. The acid hydrolysis reactions of cobalt(III) ammine complexes are discussed as well as the evidence for a general dissociative mode of activation. Acid catalyzed hydrolysis and dual reaction paths in acid hydrolysis of complexes having chelated ligands are also discussed. The evidence for the S_N1CB base hydrolysis mechanism for mono- and bidentate oxyanion cobalt(III) ammine complexes is summarized.

Chapter 2 is concerned with the base hydrolysis studies on the $(NH_3)_5CoCO_3^+$, $(en)_2CoCO_3^+$ and $(phen)_2CoCO_3^+$ ions where en and phen refer to ethylenediamine and o-phenanthroline, respectively. Specific rate constants, activation parameters and equilibrium constants were obtained for the first two systems. The $(NH_3)_5CoCO_3^+$ base hydrolysis results fitted on a linear free energy plot with other $(NH_3)_5CoX^{n+}$ base hydrolysis results, indicating the large importance of Co-X bond cleavage in this family of reactions. Estimates for the specific rate constant for acid hydrolysis and the acid dissociation constant of the $(NH_3)_5CoCO_3H^{2+}$ ion were also obtained.

The base hydrolysis study of the $(en)_2CoCO_3^+$ ion yielded rate constants, equilibrium constants and activation parameters for both the uncatalyzed and base catalyzed ring-opening/ring-closing reactions.

The base catalyzed path was shown to go largely to *cis*-(en)₂CoOHCO₃ with 100% Co-O bond cleavage. Both the ring-opening and ring-closing base catalyzed reactions were shown to proceed with complete retention of optical activity. Rate constants over the [OH⁻] range, 1.0-3.71 M, at 26°, were obtained for a second reaction involving base catalyzed loss of carbonate from the ring-opened *cis*-(en)₂CoOHCO₃ species as well as for the first, ring-opening/ring-closing equilibration step.

The (phen)₂CoCO₃⁺ base hydrolysis kinetics gave an increase in rate with time which was shown to be caused by a Co(II) complex, *cis*-(phen)₂Co(OH₂)₂²⁺. The product of the Co(II) catalyzed hydrolysis was shown to be the Co(III) complex, *cis*-(phen)₂Co(OH₂)₂³⁺.

Chapter 3 discusses the preparation, characterization, and acid hydrolysis of the (phen)₂CoCO₃⁺ and (bipy)₂CoCO₃⁺ complexes. The results of the elemental analysis, infrared spectral characterization, nmr experiments, and some ion exchange experiments for both complexes are given. Specific rate constants, activation parameters, and bond cleavage positions for the relatively slow acid hydrolysis of the (phen)₂CoCO₃⁺ and (bipy)₂CoCO₃⁺ complexes are given and discussed. A correlation between the rate of acid catalyzed carbonato ring-opening reactions of N₄CoCO₃⁺ complexes with the basicity of the ammine ligand, N, is discussed.

Chapter 4 gives and discusses the results of oxygen-18 studies between water and NaHCO₃, (NH₃)₅CoCO₃⁺ and (en)₂CoCO₃⁺, respectively. The results of the NaHCO₃ and (NH₃)₅CoCO₃⁺ studies are compared and show that the rate controlling reactions in both studies involved

the hydration of CO_2 . A pH dependence was observed for the $(\text{en})_2\text{CoCO}_3^+$ system, but it was not possible to determine whether decarboxylation or water exchange on the ring-opened species was rate determining.

TABLE OF CONTENTS

	<u>Page</u>
Acknowledgments	iii
Abstract	iv
List of Figures	xi
List of Tables	xiv
1. INTRODUCTION	1
2. THE BASE CATALYZED HYDROLYSIS OF CARBONATOCOBALT(III) AMMINE COMPLEXES	12
Introduction	12
Experimental	18
Base Catalyzed Hydrolysis of Carbonatopenta- amminecobalt(III) Ion	18
Base Hydrolysis of Carbonatobis(ethylene- diamine)cobalt(III) Ion	20
- Preparation of Complexes and Reagents	20
- Base Hydrolysis Kinetics	23
- Geometrical Isomerization	24
- Optical Isomerization	25
- Oxygen-18 Tracer Study	26
Base Catalyzed Hydrolysis of Carbonatobis(o-phen- anthroline)Cobalt(III) Ion	26
- Preparation and Characterization of o-Phenanthroline Complexes	26

- Base Hydrolysis of Carbonatobis(o-phen- anthroline)Cobalt(III) Ion	27
Results	29
Base Catalyzed Hydrolysis of Carbonatopenta- amminecobalt(III) Ion	29
Base Catalyzed Hydrolysis of Carbonatobis(ethylene- diamine)cobalt(III) Ion	42
- Base Hydrolysis Kinetics	42
- Geometrical Products of the Base Hydrolysis of $(en)_2CoCO_3^+$	58
- Optical Isomerization	64
- Oxygen-18 Tracer Study	66
Base Hydrolysis of Carbonatobis(o-phenanthroline) Cobalt(III) Ion	69
Discussion	77
3. ACID HYDROLYSIS STUDIES ON THE CARBONATOBIS(O-PHENANTHROLINE) - AND (2,2'-BIPYRIDYL)COBALT(III) IONS	93
Introduction	93
Experimental	99
Preparation of o-Phenanthroline Complexes	99
Characterization of o-Phenanthroline Complexes	101
Preparation of 2,2'-Bipyridyl Complexes	103
Characterization of 2,2'-Bipyridyl Complexes	104

Page

Acid Hydrolysis Kinetics of $(\text{bipy})_2\text{CoCO}_3^+$ and $(\text{phen})_2\text{CoCO}_3^+$ Ions	106
Oxygen-18 Tracer Study	107
Results	109
Characterization of o-Phenanthroline Complexes . . .	109
Characterization of 2,2'-Bipyridyl Complexes . . .	124
Acid Hydrolysis Kinetics of $(\text{bipy})_2\text{CoCO}_3^+$ and $(\text{phen})_2\text{CoCO}_3^+$ Ions	129
 4. OXYGEN EXCHANGE STUDIES ON SODIUM BICARBONATE AND CARBONATO- COBALT(III) AMMINE COMPLEXES	145
Introduction	145
Experimental	152
Oxygen Exchange Between Sodium Bicarbonate and Oxygen-18 Enriched Water	152
Oxygen Exchange Between $(\text{NH}_3)_5\text{CoCO}_3^+$ Ion and Oxygen-18 Enriched Water	156
Oxygen Exchange Between $(\text{en})_2\text{CoCO}_3^+$ Ion and Oxygen-18 Enriched Water	157
Results	158
Oxygen Exchange Between Sodium Bicarbonate and Oxygen-18 Enriched Water	158
Oxygen Exchange Between $(\text{NH}_3)_5\text{CoCO}_3^+$ Ion and Oxygen-18 Enriched Water	169

Oxygen Exchange Between (en) $_2\text{CoCO}_3^+$ Ion and Oxygen-18 Enriched Water	177
Discussion	183
References	185
Appendix A - The Determination of Parameter Confidence Limits and Their Use in Testing the Significance of a Theoretical Model	195
Appendix B - An Exchange Rate Law Derivation	203
Appendix C - Derivations of Expressions and Equations	210
Appendix D - Tables of Data	224

LIST OF FIGURES

<u>Figure</u>		<u>Page</u>
2.1	Electronic Absorption Spectra of $(\text{NH}_3)_5\text{CoCO}_3^+$, (A), $(\text{NH}_3)_5\text{CoOH}_2^{3+}$, (B), and $(\text{NH}_3)_5\text{CoOH}^{2+}$, (C).	30
2.2	Variation of Absorbance with Time for the Reaction of $(\text{NH}_3)_5\text{CoCO}_3^+$ Ion in Aqueous Sodium Hydroxide.	32
2.3	Variation of k_{obsd} with $[\text{OH}^-]$ for the Hydrolysis of $(\text{NH}_3)_5\text{CoCO}_3^+$ in Sodium Hydroxide.	33
2.4	Variation of $[\text{H}^+]^{-1}$ with $[\epsilon_o/(\epsilon_o - \epsilon_\infty)]k_{\text{obsd}}^{-1}$ for the Hydrolysis of $(\text{NH}_3)_5\text{CoCO}_3^+$ at 25.0° and Low pH.	38
2.5	Variation of $[K_1\epsilon_1 - \epsilon_\infty(K_1 + [\text{H}^+])]/[\text{H}^+]$ with $K_w\epsilon_\infty/[\text{H}^+][\text{HCO}_3^-]$ for the $(\text{NH}_3)_5\text{CoCO}_3^+$ ion.	41
2.6	Visible Absorption Spectra of $(\text{en})_2\text{CoCO}_3^+$, (A), <i>cis</i> - $(\text{en})_2\text{Co}(\text{OH}_2)_2^{3+}$, (B), and <i>cis</i> - $(\text{en})_2\text{Co}(\text{OH})_2^+$, (C).	43
2.7	Variation of Absorbance with Time of a Solution of $(\text{en})_2\text{CoCO}_3^+$ in NaOH at 26.0° .	44
2.8	Variation of Absorbance with Time of a Solution of $(\text{en})_2\text{CoCO}_3^+$ in NaOH at 34.0° .	45
2.9	Variation of Absorbance with Time of a Solution of $(\text{en})_2\text{CoCO}_3^+$ in NaOH at 24.5° .	47
2.10	Plot of $[\text{OH}^-]^{-1}$ vs. $bT_o/(A'_{\text{max}} - A_o)$ at 26.0° .	51
2.11	Variation of k_{obsd} with $-\text{Log}[\text{OH}^-]$ for $(\text{en})_2\text{CoCO}_3^+$ in NaOH at 26.0° .	56

<u>Figure</u>		<u>Page</u>
2.12	Variation of Absorbance with Time of Solutions of $(\text{phen})_2\text{CoCO}_3^+$ in Aqueous Sodium Hydroxide.	70
2.13	Variation of Absorbance with Time of Solutions of $(\text{phen})_2\text{CoCO}_3^+$ in NaOH.	73
2.14	Variation of Absorption Spectrum of $(\text{phen})_2\text{CoCO}_3^+$ in Aqueous Sodium Hydroxide.	75
2.15	Plot of Log (specific rate constant) vs. Log (equilibrium constant) for the Base Hydrolysis of $(\text{NH}_3)_5\text{CoX}^{n+}$ Ions at 25°.	80
2.16	Plot of k_{obsd}^N vs. $[\text{OH}^-]$ at High Hydroxide Ion Concentration with No Ionic Strength Control, at 24.5°.	85
3.1	Electronic Absorption Spectra of $(\text{phen})_2\text{CoCO}_3^+$, (A), <i>cis</i> - $(\text{phen})_2\text{Co}(\text{OH}_2)_2^{3+}$, (B), <i>cis</i> - $(\text{phen})_2\text{Co}(\text{OH}_2)_2^{2+}$, (C), and <i>cis</i> - $(\text{phen})_2\text{Co}(\text{OH})_2^+$, (D).	110
3.2	Infrared Spectrum of $[(\text{phen})_2\text{CoCO}_3]\text{Cl}\cdot 3\text{H}_2\text{O}$ in KBr Disk.	113
3.3	60 MHz Nmr Spectrum of o-Phenanthroline Monohydrate in CDCl_3 with TMS as an External Reference and a Schematic ABX Spectrum.	115
3.4	Nmr Spectrum of $[(\text{phen})_3\text{Co}][\text{phen H}][\text{CoCl}_4]_2\cdot\text{HCl}$ in D_2O at 60 MHz.	118
3.5	Nmr Spectra of $[(\text{phen})_2\text{CoCO}_3]\text{Cl}\cdot 3\text{H}_2\text{O}$, (A), and <i>cis</i> - $[(\text{phen})_2\text{Co}(\text{OH}_2)_2]\text{Cl}_3\cdot 2\text{H}_2\text{O}$, (B), at 60 MHz in D_2O .	120

<u>Figure</u>		<u>Page</u>
3.6	100 MHz Nmr Spectrum of $[(\text{phen})_2\text{CoCO}_3]\text{Cl} \cdot 3\text{H}_2\text{O}$ in D_2O with 10% t-Butanol as an Internal Reference.	121
3.7	Visible Absorption Spectra of $(\text{bipy})_2\text{CoCO}_3^+$ in 1 M NaCl , (A), and <i>cis</i> - $(\text{bipy})_2\text{Co}(\text{OH}_2)_2^{3+}$, (B).	125
3.8	100 MHz Nmr Spectrum of $(\text{bipy})_2\text{CoCO}_3^+$ in D_2O .	126
3.9	Variation of k_{obsd} with $[\text{H}^+]$ for the Reaction of $(\text{bipy})_2\text{CoCO}_3^+$ with HCl .	131
3.10	Variation of k_{obsd} with $[\text{H}^+]$ for the Reaction of $(\text{phen})_2\text{CoCO}_3^+$ with HCl .	136
4.1	Schematic Diagram of the Sampling Apparatus used in Oxygen-18 and Tracer Experiments.	155
4.2	Exchange Systems and Chemical Equilibria for the Exchange of Oxygen Between Sodium Bicarbonate and Water.	159
4.3	Variation of $\text{Log}(1-F)$ with Time for the Exchange of Oxygen Between NaHCO_3 and OH_2 at 26° .	164
4.4	Exchange Systems and Chemical Equilibria for the Exchange of Oxygen Between $(\text{NH}_3)_5\text{CoCO}_3^+$ and OH_2 .	173

LIST OF TABLES

<u>Table</u>		<u>Page</u>
2.1	Comparison of the Visible Spectra of $(en)_2CoCO_3^+$ and its Acid Hydrolysis Product, $cis-(en)_2Co(OH_2)_2^{3+}$ to Previously Reported Spectra	22
2.2	Specific Rate Constants and Activation Parameters for the Hydrolysis of $(NH_3)_5CoCO_3^+$	35
2.3	Kinetic and Equilibrium Data for the Hydrolysis of $(NH_3)_5CoCO_3^+$ at 25.0°	37
2.4	Variation of k_{obsd} with $[OH^-]$ for the Complete Hydrolysis of $(en)_2CoCO_3^+$ in NaOH at 24.5°	49
2.5	Variation of K_1 with Temperature	53
2.6	Specific Rate Constants and Activation Parameters for the Base Hydrolysis of $(en)_2CoCO_3^+$	57
2.7	Comparison of Molar Extinction Coefficients of $cis-(en)_2Co(OH_2)_2^{3+}$ and the Acidified Product of the Base Hydrolysis Reaction of $(en)_2CoCO_3^+$ at 44.0°	59
2.8	Comparison of Molar Extinction Coefficients of $cis-(en)_2Co(OH_2)_2^{3+}$ and the Acidified Product of the Base Hydrolysis Reaction of $(en)_2CoCO_3^+$ at 0.40 M NaOH and 26.0°	62
2.9	Comparison of Molar Extinction Coefficients of $cis-(en)_2Co(OH_2)_2^{3+}$ and the Acidified Product of the Base Hydrolysis Reaction of $(en)_2CoCO_3^+$ at 1.00 M NaOH and 26.0°	63

<u>Table</u>		<u>Page</u>
2.10	Tracer Results on the Base Hydrolysis of $(\text{en})_2\text{CoCO}_3^+$ at 26°	68
2.11	Comparison of Spectral Characteristics of a Solution of $(\text{phen})_2\text{CoCO}_3^+$ Ion in Aqueous Sodium Hydroxide at Zero and Infinite Times with Spectral Characteristics of $(\text{phen})_2\text{CoCO}_3^+$ Ion and <i>cis</i> - $(\text{phen})_2\text{Co}(\text{OH})_2^+$ Ion	71
2.12	Comparison of Kinetic Parameters for the Base Hydrolysis of $(\text{en})_2\text{CoCO}_3^+$	83
2.13	Comparison of Ring-Opening Kinetic Parameters for $(\text{en})_2\text{CoC}_2\text{O}_4^+$, $(\text{en})_2\text{CoCO}_3^+$, $(\text{en})_2\text{CoPO}_4$, and $(\text{en})_2\text{CoSO}_4^+$ at 22.5°	88
3.1	Rate Parameters for the Acid Catalyzed Hydrolysis of Various $\text{N}_4\text{CoCO}_3^+$ Ions at 25°	96
3.2	Molecular Weights and, Calculated and Experimental Percentage of Elements for Various Cobalt(III) Complexes of o-Phenanthroline	102
3.3	Molecular Weights and, Calculated and Experimental Percentage of Elements for Dichloro-and Carbonato- bis-(2,2'-bipyridyl)Cobalt(III) Complexes	105
3.4	Visible Spectral Characteristics of <i>cis</i> -Dihydroxy-, <i>cis</i> -Diaquo-, and Carbonatobis-(o-phenanthroline) Cobalt(III) Ions at 25° and 1.0 (NaCl) Ionic Strength	111

<u>Table</u>		<u>Page</u>
3.5	60 MHz Nmr Spectral Data for o-Phenanthroline	116
3.6	Specific Rate Constants and Activation Parameters for the Acid Hydrolysis of $(\text{bipy})_2\text{CoCO}_3^+$	132
3.7	Specific Rate Constants and Activation Parameters for the Acid Hydrolysis of $(\text{phen})_2\text{CoCO}_3^+$	135
3.8	Tracer Experiments on the Bond Breaking in the Acid Hydrolysis of $(\text{bipy})_2\text{CoCO}_3^+$ and $(\text{phen})_2\text{CoCO}_3^+$ at 1.0 M $[\text{H}^+]$	137
3.9	The Basicity of Some Ammine Ligands	141
3.10	Acid Dissociation pK_a 's of Some <i>cis</i> - $\text{N}_4\text{Co}(\text{OH}_2)_2^{3+}$ Complexes at 25°	143
4.1	Experimental and Calculated Data for the Exchange of Oxygen Between NaHCO_3 and OH_2	170
4.2	Best Fit Parameters with 95% Confidence Limits and Fixed Parameters for the Exchange Between Sodium Bicarbonate and Water at 20, 26, and 30°	172
4.3	Experimental and Calculated Data for the Exchange of Oxygen Between $(\text{NH}_3)_5\text{CoCO}_3^+$ and OH_2 at 20, 26, and 30°	178
4.4	Best Fit Parameters with 95% Confidence Limits for the Exchange of Oxygen Between $(\text{NH}_3)_5\text{CoCO}_3^+$ and OH_2 at 20, 26, and 30°	180
4.5	Comparison of Values for Rate Constants of the Reactions of CO_2 with OH_2 and OH^-	184

CHAPTER 1

INTRODUCTION

A thesis¹ is a formal essay whose function is to convey a logical argument upholding a specific point of view, particularly, a solution to a problem.

The types of problems which chemists solve and write about often simply result in an increase in the general store of knowledge. This however, eventually leads to improving the quality of life by helping to solve the specific problems facing mankind, some of which are of our own making.

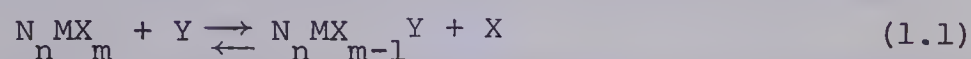
The problem for this thesis concerns the mechanism of a specific type of chemical reaction. Knowledge of the mechanism of a reaction² involves understanding and knowing about all the individual collisional or other elementary processes involving molecules (atoms, radicals, and ions included) that take place simultaneously or consecutively in producing the observed overall reaction, as well as a detailed stereochemical picture of each step as it occurs. Presumably, determining the mechanism will help to control or even prevent a reaction such as that leading to the formation of the antigen-antibody complex³ in allergies.

Up until recently,⁴ it was not possible to directly observe atoms, let alone to observe directly a chemical reaction as it occurred. Nor has theoretical chemistry reached the stage of being able to predict the lowest energy path, and hence the mechanism, of a reaction. Thus the chemist is left with the classical kinetic method as

a way to determine, or at least learn something about, the mechanism of a reaction.

The classical kinetic method usually first involves a study of how the rate of the reaction is varied by changing the experimental variables such as reagent concentrations and possible catalyst concentrations. These data can usually be interpreted by formulating an equation, the rate law, relating the rate of change of concentration of a species with time to the concentrations of all the species involved in the reaction. By itself, this rate law cannot do more than establish a possible reaction sequence for the overall reaction. Additional evidence of the more intimate details of each step are often obtained by studies on the identity of the reaction products, the stoichiometry of the reaction, the geometrical and stereochemical path of the reaction, the position of bond cleavage when more than one possibility exists, the effect of temperature, pressure, and volume changes on the reaction rate, and the identity and features of possible short lived intermediates. The actual determination of the intimate details of a reaction mechanism are often arrived at only by doing complete kinetic studies on many compounds which vary only slightly from each other or by changing other experimental parameters such as the solvent media or the ionic strength. However, the kinetic method can never unequivocally establish any mechanism since a mechanism so arrived at is a theory and must be changed to accommodate new facts. Chapters 1 and 12 of reference (2) provide a good review of some procedures and results of the kinetic method.

The reactions being studied in this thesis are classified generally as ligand substitution reactions of coordination complexes, specifically, as substitution for a ligand by a water molecule or hydroxide ion. A general reaction scheme for these types of reactions may be written as



where Y represents OH_2 or OH^- , M refers to the central atom which is cobalt(III) in this case, N represents various ammine ligands, and X_m represents mono- or bidentate oxyanions.

There are two classifications for the various types of ligand substitution reactions, both of which are useful in certain instances. The more commonly used classification, as discussed by Basolo and Pearson,⁵ allows four different mechanism types, S_{N}^1 , S_{N}^2 , S_{N}^1 lim, and S_{N}^2 lim. S_{N} refers to substitution on an electrophilic center by a nucleophilic species and 1 and 2 refer to the molecularity⁶ of the *rate-determining* step of the total reaction. A S_{N}^1 lim reaction goes by a two step process involving a slow unimolecular dissociation to an *experimentally detectable* intermediate of reduced coordination number followed by a rapid reaction of the intermediate with the entering ligand, Y. For a S_{N}^1 reaction, no reduced coordination number intermediate can be detected although the effect of changing the leaving group, X, on the rate of reaction (i.e. energy of the transition state⁷) is much greater than the effect of changing the entering group, Y. A S_{N}^2 lim reaction involves a bimolecular rate

determining step for which there is *definite experimental evidence* for an intermediate of increased coordination number. When no intermediate is detectable but the effect of the entering group, Y, on the rate is significant, the reaction is classed as S_N2 .

The detection of intermediates of changed coordination number can be accomplished by actually isolating and characterizing them in the case of stable long lived species. More usually, the intermediate is reactive and short lived.

An increase in the rate upon addition of perchlorate ion (the Winstein salt effect) or a common ratio of products, $N_n MY / N_n MZ$, when a theoretically identical intermediate, $N_n M$, is generated from different reactants, $N_n MX'$, $N_n MX''$..., in the presence of some coordinating ligands, Z and Y, (competition experiments) are tests which may be used to detect reactive intermediates of reduced coordination number.

No such tests exist for short lived increased coordination number intermediates.

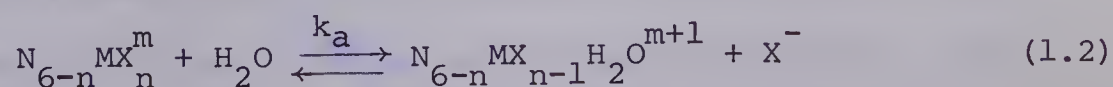
The second type of classification for ligand substitution reactions is due to Langford and Gray⁸ and is based on a division of a reaction mechanism into two phases. The *stoichiometric* mechanism is the sequence of elementary steps by which an over-all reaction proceeds. Knowledge of the *intimate* mechanism involves understanding the magnitudes of the rate constants for the individual steps in terms of the rearrangement of atoms and bonds (electrons) taking place. The three types of stoichiometric mechanism are classed as D, I, or A. D refers to dissociation or loss of a leaving ligand

in the first step resulting in an intermediate of reduced coordination number, I refers to an interchange or concerted process where the leaving group is moving from the inner to outer coordination sphere at the same time that the entering group moves from the outer to the inner, and A refers to association or gain of a ligand in the first step producing an intermediate of increased coordination number.

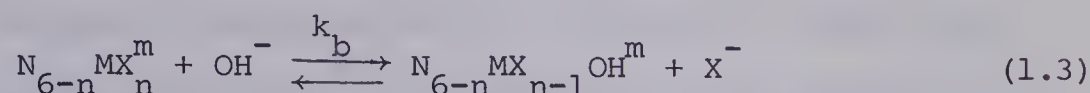
Intimate mechanisms are classified with respect to the effect that the entering group has on the energy of the transition state of each step of the stoichiometric mechanism. If the entering group has an effect on the rate of reaction, the intimate mechanism is classified as α (associative) whereas when the rate is affected more by changing the leaving group than by changing the entering group, a d (dissociative) intimate mechanism exists. The intimate mechanism is indicated by putting the type (α or d) as a subscript to the stoichiometric mechanism (D or I or A).

Because of their relatively easy preparation and their inert⁹ (slow reacting) nature, the complexes of Co(III) have been and are often chosen as model systems on which to develop a knowledge of ligand substitution mechanisms. Cobalt(III) complexes are d^6 and usually spin paired complexes of an octahedral structure whose general bonding schemes are well documented.^{10,11}

The special class of ligand substitution reactions in which water or hydroxide ion are involved are called *hydrolysis* reactions. When an aquo complex is the product, as in equation (1.2),



the reaction is called *acid hydrolysis* (sometimes referred to as aquation). If the experimentally determined rate law has a term in $[H^+]$, the reaction is referred to as an *acid catalyzed hydrolysis*. When the product is a hydroxy complex, as in equation (1.3),



the reaction is called *base hydrolysis*. If the experimentally determined rate law has a term in $[OH^-]$, the reaction is properly referred to as a *base catalyzed hydrolysis*, although the word catalyzed is often omitted.

The acid hydrolysis reactions of cobalt(III) ammine complexes have been extensively studied. Most of the rate laws are first-order in complex concentration. Because of the large excess of water, the rate law does not reveal anything about the role of the entering group, H_2O , in the transition state. Some rate laws show a first-order dependence on $[H^+]$. This is attributed to increased lability of a protonated ligand. Some recent examples of this are studies of the acid hydrolysis of complexes containing acetate¹², nitrite,^{13,14} and phosphate¹⁵ ligands. A $[H^+]$ dependence of the rate law is also often observed in the acid hydrolysis of complexes having chelated leaving ligands. This has been attributed¹⁶ to protonation of the ring opened species which prevents closure and also, as in the above monodendate systems, labilizes the remaining metal-ligand bond. Thus the existence of a $[H^+]$ term in the rate law does not reveal anything about the intimate mechanism although definite knowledge

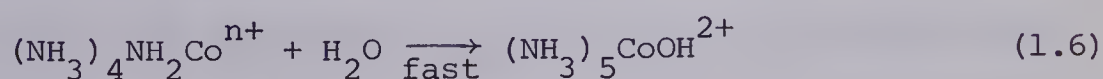
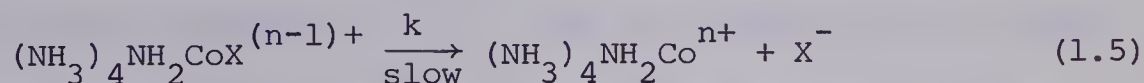
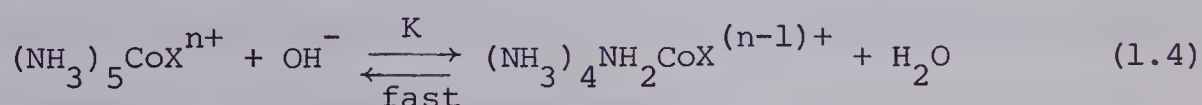
of the proton transfer equilibrium helps define the stoichiometric mechanism.

For the acidopentaammine cobalt(III) complexes, an increase in the rate of acid hydrolysis as the basicity of the leaving group decreases¹⁷ satisfies the criteria for d activation. The linear free energy relationship which is observed for this series^{18,19} is also indicative of a dissociative (d) mode of activation. However, even though the intimate mechanism for acid hydrolysis is probably dissociative, the stoichiometric mechanism is not well defined. Throughout the series, the mechanism could be varied from dissociative interchange (I_d) to dissociative (D). Excellent discussions of this type of acid hydrolysis are given in references (5) and (8).

The reactions discussed above all involve cobalt-ligand bond cleavage. For multi-atom ligands, the possibility of internal ligand bond cleavage exists. For this type of ligand, there exists the possibility of at least two different reaction paths. The mechanisms of the different paths may or may not be different. For example, the position of bond cleavage in the acid hydrolysis of $(\text{NH}_3)_5\text{CoCO}_3^+$ has been shown²⁰ to be the carbon-oxygen bond. Yet the acid hydrolysis of $(\text{NH}_3)_4\text{CoCO}_3^+$ is known²¹ to go via Co-O and then C-O bond cleavage. Thus hydrolysis of coordinated carbonate follows a distinctly different reaction path in the first or ring-opening reaction than it does in the second or decarboxylation reaction. While the mechanism of each path could be the same, the central atom of reference has changed from a Co to a C as the path has changed from Co-O to C-O

bond cleavage. Since there are many mono- and bidentate carbonato-cobalt(III) complexes, a systematic study of the factors which determine the reaction path will help determine the mechanism of both reactions. The study of the acid hydrolysis reactions of $(\text{phen})_2\text{CoCO}_3^+$ and $(\text{bipy})_2\text{CoCO}_3^+$, where bipy and phen refer to 2,2'-bipyridyl and o-phenanthroline, respectively, which are reported in Chapter 3, extends the series of $\text{N}_4\text{CoCO}_3^+$ acid hydrolyses studied to the point where some tentative proposals can be made about the intimate mechanism of the ring-opening step of the reaction.

The base hydrolysis reactions of cobalt(III) ammine complexes involving monodentate leaving groups have been very extensively studied. The rate law normally shows a first-order dependence on both complex and hydroxide ion concentration. Contrary to the acid hydrolysis mechanism, a stoichiometric mechanism for base hydrolysis is generally agreed upon.^{22,23} The reaction sequence below,



involving a unimolecular rate controlling step, has been classified by Basolo and Pearson as $\text{S}_{\text{N}}1\text{CB}$ where CB refers to the equilibrium production of the amido (NH_2) conjugate base. Evidence for reaction (1.4) includes the lack of a $[\text{OH}^-]$ term in the rate laws for base hydrolysis of Co(III) ammines lacking acidic protons,^{24,25} the increase in rate

of production of $\text{trans}-(\text{en})_2\text{Co}(\text{NO}_2)_2^+$ from $\text{trans}-(\text{en})_2\text{CoNO}_2\text{Cl}^+$ and NO_2^- ion in dimethylsulfoxide (DMSO) when small amounts of hydroxide ion are added,²⁶ and the isotope fractionation experiments on some $(\text{NH}_3)_5\text{CoX}^{n+}$ base hydrolyses which showed that the oxygen in the product, $(\text{NH}_3)_5\text{CoOH}^{2+}$, was derived from the solvent and not from the hydroxide ion.²⁷ The existence of a short lived five coordinate intermediate, as given by reaction (1.5), has been shown by competition studies²⁸⁻³⁰ and by studies on the stereochemistry^{31,32} of the products which both indicated a common intermediate which was independent of the nature of the leaving group, X. Studies of the geometrical products of the base hydrolysis of cis - and $\text{trans}-(\text{en})_2\text{CoAX}^{n+}$ complexes showed that for a common A, the amount of $\text{cis}-(\text{en})_2\text{CoAOH}^{n+}$ product is constant, regardless of X, which again indicates a common intermediate having no memory of its source.³³ Thus there appears to be sufficient evidence to classify these base hydrolysis reactions as having D stoichiometric mechanisms (and by necessity a δ intimate mechanism).

It has been suggested^{31,32,34} that the amido group is formed *trans* to the leaving group and that interaction between a filled nitrogen p orbital and the empty $d_{x^2-y^2}$ Co orbital will cause stabilization and hence favour a trigonal bipyramidal structure for the intermediate. Sargeson has shown³⁵ that the base hydrolysis of 4-(aminoethyl)-1,4,7,10-tetraazadecane CoCl^{2+} goes with complete retention of optical activity at the assymetric nitrogen atom which is known to be *trans* to the chlorine. Since racemization will occur if a symmetrical bipyramidal intermediate is formed using this *trans*

nitrogen, the results of this experiment indicate that no appreciable $P_x - d_x^2 - 2 \pi$ stabilization with the *trans* nitrogen can occur. However this may be the result of the strongly chelated nature of the molecule and thus may not be a general conclusion.

Nordmeyer³⁶ has postulated an amido group forming *cis* to the leaving group for $(NH_3)_5CoX^{2+}$ and $(en)_2CoLX^{n+}$ base hydrolyses. This controversy about the specific structure (s) of the intermediate has not been resolved.

The base hydrolysis reactions of chelated oxyanions have been investigated for a few cases, namely the sulfato-,³⁷ phosphato-,³⁸ oxalato-,³⁹ and malonato-⁴⁰ bis(ethylenediamine) cobalt(III) complexes. Bond breaking experiments on the oxalato⁴¹ and phosphato⁴² base hydrolysis reactions showed that one C-O bond and approximately 0.35 of a P-O bond, respectively, were cleaved per complete loss of an oxyanion from the complex. As in the acid hydrolysis of chelated oxyanions, different positions of bond cleavage indicate different reaction paths. The opportunity to investigate the factors determining the choice of reaction path for the base hydrolysis of carbonate cobalt(III) ammine complexes led to the base hydrolysis studies on the $(NH_3)_5CoCO_3^+$, $(en)_2CoCO_3^+$, and $(phen)_2CoCO_3^+$ ions which are reported in Chapter 2.

To interpret and compare some of the data obtained in the acid and base hydrolysis studies, it was necessary to perform bond breaking and oxygen exchange experiments using $^{18}OH_2$. Chapter 4 is concerned with these studies although the results of the bond breaking experiments

are given and discussed with the relevant study.

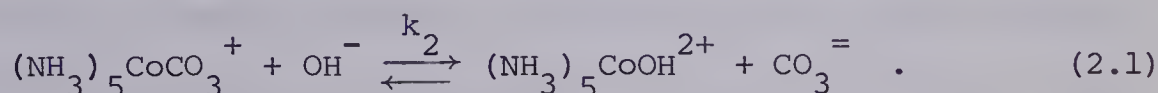
Each of the following chapters is made up of an introduction, an experimental section, a results section, and a discussion. Since two comprehensive reviews^{43,44} of carbonato complexes have appeared in the past year, only more recent results which are directly relevant to the particular study will be discussed in the introductions to the chapters.

The Appendices consist of a discussion of parameter error calculations, some derivations of equations, and tables of data.

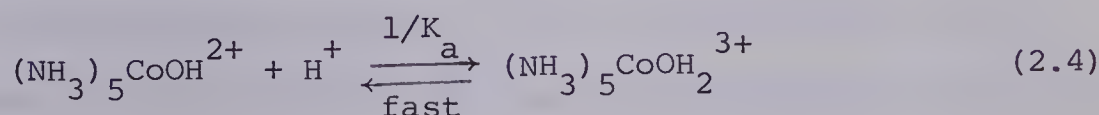
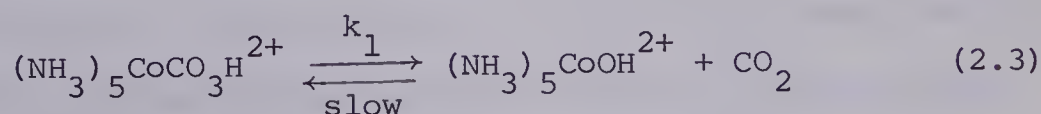
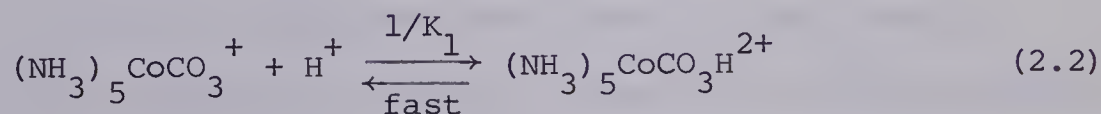
CHAPTER 2

THE BASE CATALYZED HYDROLYSIS OF CARBONATOCOBALT(III)AMMINE COMPLEXESIntroduction

If the intimate mechanism of the base hydrolysis of $(\text{NH}_3)_5\text{CoX}^{n+}$ ions is dissociative, as discussed in Chapter 1, a linear free energy relationship (LFER) with a slope of 1.0 should exist between the specific rate constant for the base hydrolysis reaction and the stability constant of $(\text{NH}_3)_5\text{CoX}^{n+}$ for a series of X's.¹⁸ The opportunity to test this relationship for $\text{X} = \text{CO}_3^{=}$ led in part to the kinetic study of the reaction given below



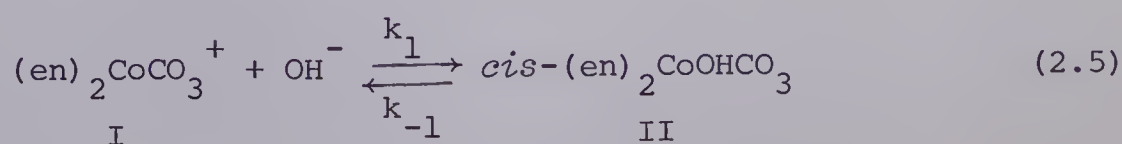
The LFER mentioned above requires the stability constant for the formation of $(\text{NH}_3)_5\text{CoCO}_3^+$ from $(\text{NH}_3)_5\text{CoOH}_2^{3+}$ and $\text{CO}_3^{=}$. This was determined when the equilibrium position of the acid hydrolysis reaction scheme given below

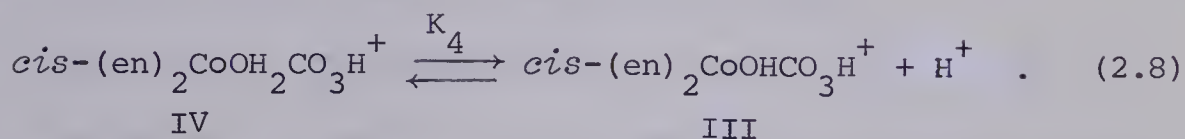
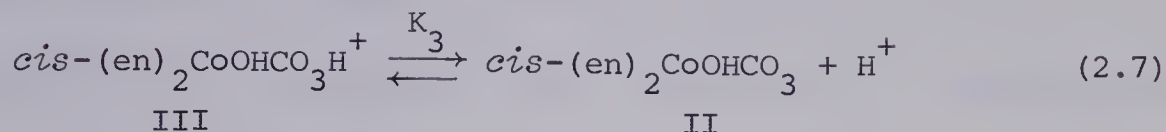
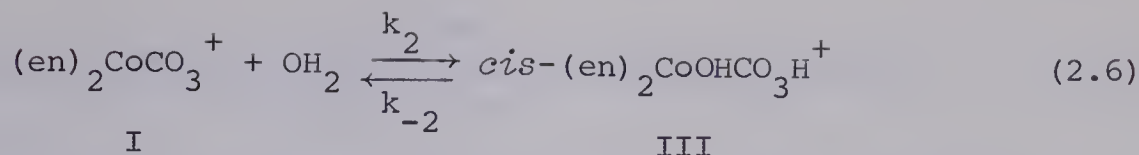


was forced partially to the left by the use of a carbonate buffer. The

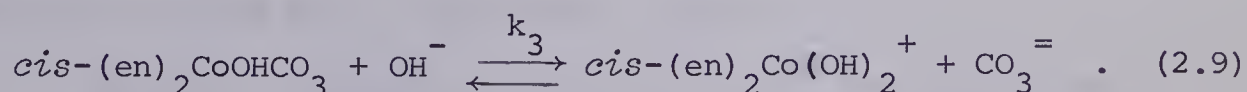
reaction scheme above is consistent with the acid hydrolysis studies,^{45,46} the bond cleavage position experiments,²⁰ and a $^{14}\text{CO}_3^{=}$ carbonate exchange study⁴⁷ which had been done on the $(\text{NH}_3)_5\text{CoCO}_3^+$ ion before the start of the experiments reported here. However, the values at 25° of k_1 reported were 7×10^{-3} ($\mu < 0.1$),^{45,46} 1.2×10^{-3} ($\mu < 0.1$),⁴⁷ and 7.8×10^{-4} ($\mu < 0.1$)⁴⁸ sec^{-1} , respectively, while the values of K_1 reported were 4×10^{-7} M⁴⁶ and 3.8×10^{-9} M,⁴⁸ respectively. A study of the kinetics of the attainment of equilibrium for reactions (2.2), (2.3), and (2.4) allowed calculation of values for k_1 (2.3×10^{-2} sec^{-1}) and K_1 (5.9×10^{-9} M), at 25° and 1.0 ionic strength (NaClO_4), which were used⁴⁹ in an attempt to resolve the differences in the reported values. After reference (49) had been published, Dasgupta and Harris⁵⁰ studied the acid hydrolysis of $(\text{NH}_3)_5\text{CoCO}_3^+$ by a stop-flow method which resulted in accurate values, at 25° and 0.5 ionic strength (NaClO_4), for k_1 and K_1 of 1.25 sec^{-1} and 4×10^{-7} M, respectively, thus finally resolving the issue.

As mentioned in Chapter 1, a study of the base hydrolysis of $(\text{en})_2\text{CoCO}_3^+$ can provide information about possible dual reaction paths, as has been indicated by different positions of bond cleavage, in the base hydrolysis of chelated oxyanions.^{41,42} The base hydrolysis of the $(\text{en})_2\text{CoCO}_3^+$ ion and of the related $(\text{tren})\text{CoCO}_3^+$ ion has been studied, at room temperature and low ionic strength ($\mu < 0.1$), over a limited pH range of 8.7-12.^{51,52} The data were found to be consistent with

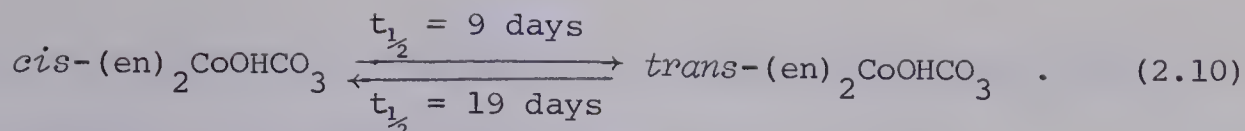




Pseudo first-order rate constants corresponding to $k_1[\text{OH}]$ and k_{-1} (at pH 12 and 25°) and k_{-2} (at pH 8.7 and 25°) were estimated as 1.28×10^{-4} , 6.4×10^{-5} , and $1.15 \times 10^{-2} \text{ sec}^{-1}$, respectively. The values of k_1/k_{-1} (pH 12) and $k_2[\text{H}_2\text{O}]/k_{-2}$ (pH 8.7) were $1.59 \times 10^2 \text{ M}^{-1}$ and 1.0×10^{-3} , respectively. The values of K_3 and K_4 were estimated to be $1.78 \times 10^{-9} \text{ M}$ and $4.79 \times 10^{-6} \text{ M}$, respectively. A slow *cis* \rightleftharpoons *trans* isomerization of species II, III, and IV was detected with *cis/trans* equilibrium ratios of 0.48, 17, and >3.5 , respectively. The hydroxycarbonato ring-opened species (II) was observed to undergo base hydrolysis, at a rate smaller than that of reaction (2.5), according to



A value for the equilibrium constant for reaction (2.9) was estimated to be $\sim 1 \times 10^{-3}$. A sodium bicarbonate buffer prevented reaction (2.9) from occurring thus allowing the half-time estimates for the *cis* \rightleftharpoons *trans* isomerization at pH 11, which are given below



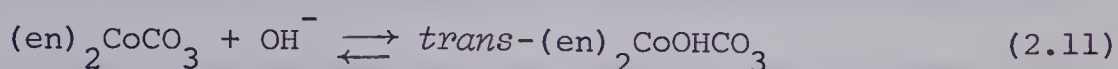
Notice that species III, $cis-(en)_2CoOHCO_3H^+$, could be written as $cis-(en)_2CoOH_2CO_3^+$ but it is believed⁵³ that in species IV, $(en)_2CoOH_2CO_3H^{2+}$, the water is more acidic than the bicarbonate ligand.

After most of the experiments on the base hydrolysis of $(en)_2CoCO_3^+$ which are reported in this thesis had been completed and reported,⁵⁴ two additional studies of the same reaction became available.^{40,55} Farago⁴⁰ does not observe the equilibration process described by Scheidegger, but does provide rate constants, at 24.8° and varying ionic strength, corresponding to reactions (2.5) and (2.9) in the hydroxide ion concentration range, 0.55-3.03 M. The values reported for k_1 and k_3 are $2.18 \times 10^{-3} \text{ M}^{-1} \text{ sec}^{-1}$ ($\Delta H^\ddagger = 21.4 \text{ kcal mole}^{-1}$) and $4.56 \times 10^{-5} \text{ M}^{-1} \text{ sec}^{-1}$ ($\Delta H^\ddagger = 23.4 \text{ kcal mole}^{-1}$), respectively. For additional runs at $[OH^-] > 3$, Farago observes a levelling off of the observed rate constant for reaction (2.5) and attributes this to complete formation of either an amido complex formed in an S_N1CB mechanism or an ion pair of the type, $(en)_2CoCO_3^+ \cdot OH^-$.

Hargis⁵⁵ studied the kinetics of the base hydrolysis of $(en)_2CoCO_3^+$ in the $[OH^-]$ range, 0.1-1.0 M, ($\mu = 1.0 \text{ NaClO}_4$) at 25.0, 35.0, and 45.0°. The rate of loss of $(en)_2CoCO_3^+$ ion was followed mainly by spectrophotometric means and these observed rate constants were confirmed by following the loss of optical activity of a basic solution of d- $(en)_2CoCO_3^+$. Since the O.R.D. spectrum of d- $(en)_2CoOHCO_3$ is not known, the loss of optical activity could be due to production

of 100% d-(en)₂CoOHCO₃, to production of more d-(en)₂CoOHCO₃ than l-(en)₂CoOHCO₃, or to production of some d-(en)₂CoOHCO₃ and some *trans*-(en)₂CoOHCO₃. Thus the stereochemical path of reaction (2.5) was not determined by this experiment.

The equilibration process involved in reaction (2.5) was not observed⁵⁵ but a direct production of *trans*-(en)₂CoOHCO₃ according to



was postulated as well as the other base hydrolysis and isomerization reactions proposed by Scheidegger. The existence of reaction (2.11) was based on the lack of agreement of a constant (r_i) in an empirical equation describing the data,

$$A = A_1 + A_2 e^{-r_2 t} + A_3 e^{-r_3 t} - A_4 e^{-r_4 t} \quad , \quad (2.12)$$

to the predicted rate constant for the *cis* \rightleftharpoons *trans* isomerization of the (en)₂Co(OH)₂⁺ ion. However, the molar extinction coefficient of *cis*-(en)₂Co(OH)₂⁺ is not greatly different from that of *trans*-(en)₂Co(OH)₂⁺ at 322 mμ⁵⁶ so that highly accurate measures of the *cis* \rightleftharpoons *trans* rate could not be expected. Thus good direct evidence for reaction (2.11) does not exist. Bearing this fact in mind, the half-times for reaction (2.10) in the forward and reverse directions are 2.6 and 12.0 days,⁵⁵ respectively, which do not agree with those reported by Scheidegger (9 and 19 days). Hargis' value of the rate constant corresponding to reaction (2.5), at 25°, of 3.20x10⁻³ M⁻¹ sec⁻¹ ($\Delta H^\ddagger = 21.0$ kcal mole⁻¹) is in fair agreement with the value of Farago (2.18x10⁻³ M⁻¹

sec^{-1} , $\Delta H^\ddagger = 21.4 \text{ kcal mole}^{-1}$) but Scheidegger's value determined at one pH ($1.28 \times 10^{-2} \text{ M}^{-1} \text{ sec}^{-1}$) is considerably different. The sum of Hargis' rate constants, k_{24} , k_{25} , k_{35} , and k_{34} ($6.205 \times 10^{-5} \text{ M}^{-1} \text{ sec}^{-1}$ at 25°) corresponds quite well to Farago's specific rate constant for reaction (2.9) ($4.56 \times 10^{-5} \text{ M}^{-1} \text{ sec}^{-1}$ at 24.8°).

The study of the base hydrolysis of the $(\text{en})_2\text{CoCO}_3^+$ ion reported here is an attempt to resolve the discrepancies noted above. The base hydrolysis kinetics over a wide range of $[\text{OH}^-]$, 0.002-1.00 M, were investigated, the geometrical structures of the intermediate, $(\text{en})_2\text{CoOHCO}_3$, and the products were determined, the amount of optical activity retention in reaction (2.5) was studied to provide information on the transition state and to determine if any *trans* species are produced in reaction (2.5), and the position of bond cleavage in reaction (2.5) was determined. The experiments of Farago in the $[\text{OH}^-]$ region, 1.0-3.7 M, were repeated.

While it has been established^{24,25} that the base hydrolysis reactions of $(\text{NH}_3)_5\text{CoX}^{n+}$ ions by the $\text{S}_{\text{N}}1\text{CB}$ mechanism requires an acidic ammine proton, the same mechanism may or may not hold for the first ring-opening step in the base hydrolysis reactions of $\text{N}_4\text{CoCO}_3^+$ species. The obvious test of the mechanism is to study the base hydrolysis behavior of an $\text{N}_4\text{CoCO}_3^+$ complex in which N lacks acidic protons. Therefore, the complex ion, $(\text{phen})_2\text{CoCO}_3^+$, where phen is 1,10- or o-phenanthroline, was prepared and the reaction of the complex in aqueous sodium hydroxide was studied.

Experimental

Base Catalyzed Hydrolysis of Carbonatopentaamminecobalt(III) Ion

Carbonatopentaamminecobalt(III) nitrate was prepared by the method of Lamb and Mysels⁴⁶ and stored in a vacuum desiccator over calcium sulfate. The analysis of the complex for cobalt,⁵⁷ ammonia,⁵⁸ carbon,⁵⁹ hydrogen,⁵⁹ and nitrogen⁵⁹ agreed with the formula, $[(\text{NH}_3)_5\text{CoCO}_3]\text{NO}_3 \cdot 1.5 \text{H}_2\text{O}$, reported by Lamb and Mysels. The analysis showed

	<u>%Co</u>	<u>%NH₃</u>	<u>%C</u>	<u>%H</u>	<u>%N</u>
exptl	20.9	29.1	4.4	6.1	29.2
calcd	20.1	29.1	4.1	6.2	29.1

The purity was also checked by comparing the extinction coefficients of the maxima in the visible absorption spectrum of the acid hydrolysis product of the carbonato complex to the known values⁶⁰ for $(\text{NH}_3)_5\text{Co}(\text{OH}_2)^{+3}$. The results gave a calculated molecular weight of 287.2 ± 1.5 (standard deviation). This deviation from the predicted value of 293.2 and the slight discrepancy in the other analyses is probably due to partial dehydration of the compound.

Solutions were prepared from water which had been redistilled from alkaline potassium permanganate in an all glass apparatus.

The temperature of solutions for kinetic runs was controlled with a Colora (Papst) constant temperature bath.

The ionic strength of the reaction solutions was controlled by addition of reagent grade sodium nitrate (Mallinckrodt) or addition

of a boiled solution of sodium perchlorate made by neutralizing perchloric acid (Baker and Adamson) with sodium bicarbonate (Shawinigan).

The sodium hydroxide solutions used were prepared by diluting a filtered 50% NaOH solution made by dissolving NaOH pellets (Fisher Scientific Co. Ltd.,) in redistilled water. The solutions were standardized against a standard HCl solution using phenolphthalein as an indicator.

For the high temperature-high pH kinetics, solutions containing sodium hydroxide and sodium nitrate ($\mu = 1.0$) of known concentration were brought to temperature equilibrium. At zero time, a weighed quantity of the complex was added to the reaction solution. Aliquots were taken at various times, filtered through a 0.45 μ Millipore filter (Millipore Filter Corp., Bedford, Mass.) to remove any cobalt oxide formed, and diluted to volume. Optical densities of the diluted filtrate were determined at 328 m μ on a Bausch and Lomb Spectronic 505 spectrophotometer.

For the low temperature-low pH kinetic study, a stock solution of complex in 0.05 M NaOH was syringed into a five cm spectrophotometer cell which contained known volumes of water, 0.05 M NaHCO₃, and 4.02 M NaClO₄ to give a final ionic strength of 1.0. The initial absorbance at 295 m μ was recorded within 15 sec after addition of the solution of complex. Infinite time optical densities were determined after at least 8 half-times. The final carbonate buffer concentration (0.0242M) was sufficiently high relative to the complex concentration (about 10^{-4} M) so that the pH remained constant during the hydrolysis reaction.

The pH of the buffered reaction medium was measured with a Beckman Expandomatic pH meter (Beckman Instruments Inc., Fullerton, California), on the one pH unit scale of expansion. The pH was measured at room temperature and corrected for sodium ion error. This correction was negligible below pH 9 and was 0.024 pH unit at the highest pH used. The pH meter was standardized using buffer solutions (Fisher Scientific Co. Ltd.,).

The value of the extinction coefficient of $(\text{NH}_3)_5\text{CoCO}_3^+$ at 295 m μ was determined by extrapolation of optical density-time plots to zero time. The concentrations of NaHCO_3 , $[(\text{NH}_3)_5\text{CoCO}_3]\text{NO}_3 \cdot 1.5 \text{ H}_2\text{O}$, NaOH , and NaClO_4 were 0.0242 M, 2.996×10^{-4} M, 0.15 M, and 0.826 M, respectively. As will be shown later, 0.15 M NaOH gives close to the minimum rate of hydrolysis of the complex. Thus the extrapolation to zero time was most accurate at this NaOH concentration.

Base Hydrolysis of Carbonatobis(ethylenediamine)cobalt(III) Ion

Preparation of Complexes and Reagents

Carbonatobis(ethylenediamine)cobalt(III) chloride was prepared as described by Schlessinger.⁶¹ The visible spectrum of *cis*-(en)₂Co(OH₂)₂³⁺ obtained by acid hydrolysis of $[(\text{en})_2\text{CoCO}_3]\text{Cl}$ (molecular weight = 274.5) compared well with the previously reported spectrum.⁵⁶ The corresponding perchlorate salt was precipitated directly by mixing a warm saturated solution of $[(\text{en})_2\text{CoCO}_3]\text{Cl}$ with a solution of sodium perchlorate. The $[(\text{en})_2\text{CoCO}_3]\text{ClO}_4$ was recrystallized from hot water, washed with methanol and stored in a vacuum

desiccator over calcium sulfate. The visible spectra of $[(en)_2CoCO_3]ClO_4$ and its acid hydrolysis product, *cis*- $(en)_2Co(OH)_2^{3+}$ compared well with reported spectra as shown in Table 2.1. The molecular weight of 338.7 for $[(en)_2CoCO_3]ClO_4$ was also consistent with the elemental analysis⁵⁹ which showed

	<u>%C</u>	<u>%H</u>	<u>%N</u>
exptl	17.9	5.2	16.8
calcd	17.4	4.7	16.6

The resolution of racemic $[(en)_2CoCO_3]Cl$ into its optical isomers was attempted⁶² by using (+)-antimonyl tartrate to remove the (-)(+)-diastereoisomer and then by using a 20% sodium iodide solution to precipitate the d- $[(en)_2CoCO_3]I$. The attempt failed. Other workers⁶³ also have been unable to repeat the resolution by this method.

A sample of resolved l- $[(en)_2CoCO_3]ClO_4$ which had been prepared⁶⁴ using d- $Na[(ox)_2enCo] \cdot H_2O$ as the resolving agent was obtained.⁶⁵ The visible absorption spectrum of the resolved complex agreed with that of the racemic complex so the resolved complex was used without further purification.

Sodium hydroxide solutions were prepared by dilution of ampoules of concentrated NaOH (Fisher Certified Reagent, Fisher Scientific Co. Ltd.,). The sodium perchlorate solutions were prepared either by neutralizing sodium carbonate with perchloric acid and boiling or by dissolving anhydrous sodium perchlorate (G. Frederick Smith Chemical Co.). The sodium perchlorate solutions were standardized by elution through a Dowex 50-X12 cation-exchange resin in the hydrogen ion form and the

TABLE 2.1

Comparison of the Visible Spectra of $(\text{en})_2\text{CoCO}_3^+$ and its Acid Hydrolysis Product,
 $\text{cis}-(\text{en})_2\text{Co}(\text{OH}_2)_2^{3+}$ to Previously Reported Spectra

Complex	$\lambda_{\text{max}}, \text{m}\mu$	ϵ_{max}	$\lambda'_{\text{max}}, \text{m}\mu$	ϵ'_{max}	Reference ^a
$(\text{en})_2\text{CoCO}_3^+$	358	120.8	512	131.5	(55)
$(\text{en})_2\text{CoCO}_3^+$	363	123.7	516	136.0	this work
$\text{cis}-(\text{en})_2\text{Co}(\text{OH}_2)_2^{3+}$	358	62.5	494	80.0	(56)
$\text{cis}-(\text{en})_2\text{Co}(\text{OH}_2)_2^{3+}$	360	66.3	496	82.2	this work acid hydrolysis product

^a All spectra were measured in solutions with $\mu = 1.0$.

resultant acid eluent solution titrated with standard sodium hydroxide. All reagents were prepared in water redistilled from alkaline permanganate in an all-glass apparatus.

Base Hydrolysis Kinetics

Solutions containing sodium hydroxide and sodium perchlorate (to adjust the ionic strength to 1.0) were added to a thermostated spectrophotometer cell and allowed to come to temperature equilibrium. The cell temperature was controlled by a water flow from a Colara (Papst) temperature bath. A stock solution of $[(en)_2CoCO_3]ClO_4$ and $NaClO_4$ was allowed to come to temperature equilibrium and then added to the cell with a syringe surrounded by a water jacket connected to the constant-temperature bath. The complex concentration was varied between 5×10^{-4} and 5×10^{-3} M, depending on the hydroxide ion concentration, which was always at least ten times the complex concentration. The change in absorbance with time at 300 m μ was followed continuously on a Bausch and Lomb Spectronic 505 spectrophotometer. The value of $[OH^-]$ at low concentrations was determined by titration of the reaction solution to pH 7 using a Beckman Expandomatic pH meter equipped with an Expandomatic Range Selector and a combination probe electrode (Cat. #13-639-90, Fisher Scientific Co. Ltd., Edmonton, Alberta). The electrolyte used in this standard sized electrode was a normal saturated KCl solution and the pH meter was standardized using buffer solutions.

The kinetic runs, at 24.5°, in which ionic strength was not

controlled and sodium hydroxide concentration varied from 1.00 to 3.71 M, were followed on a Bausch and Lomb Precision Spectrophotometer using the same procedure as in the runs with sodium hydroxide concentration less than 1.00 M. The temperature of the thermostated cell holder was controlled using a Colara (Papst) constant-temperature bath equipped with a Thermistemp temperature controller (Model 71, Yellow Springs Instrument Co., Inc., Yellow Springs, Ohio). The thermister bead temperature probe (Tele Thermometer, Model 423, Yellow Springs Instrument Co., Inc.,) was taped to the top of the cell holder and the bath temperature varied until the solution in the cell attained a constant temperature of 24.5°C as measured by a 0-100° mercury thermometer (uncalibrated). During these runs the reaction was followed past 90% completion, during which time the absorbance of the solution had quickly risen to a maximum and then had decreased slowly to a constant value.

Geometrical Isomerization

The reaction product was analyzed for possible geometrical isomerization during the reaction by hydrolyzing aliquots from the reaction solution with 1M HClO_4 at 10° under which conditions no isomerization occurs.⁶⁴ For each run an aliquot of an aqueous complex stock solution was directly hydrolyzed to get a spectrum of the $\text{cis}-(\text{en})_2\text{Co}(\text{OH})_2^{3+}$ ion for comparison. The first set of experiments were done by keeping the basic reaction solution at 44.0° for ten minutes and then hydrolyzing, diluting, and running the visible

spectrum of the resultant diaquo ion. The reaction solutions were initially 0.477, 0.667 and 0.954 M in NaOH. The final acidic solutions had an ionic strength of 1.0 (NaClO_4). For the second set of experiments the basic reaction solution was kept at 26.0° and aliquots of the solution hydrolyzed at various times during the course of the reaction. For these experiments the initial hydroxide concentrations were 0.4, 1.0 and 1.0 M, respectively and the ionic strengths of the final acid hydrolyzed solutions were 0.9, 1.0 and 1.0, respectively.

Optical Isomerization

The reaction product was analyzed for possible optical isomerization by allowing the base hydrolysis reaction to go to a stage which is 98% *cis*-(en)₂CoOHCO₃. The reaction solution was then slowly titrated with stirring to pH 7 with 1 M HClO₄, diluted to 25 ml with redistilled water, the visible and O.R.D. spectra recorded, and these spectra compared with those of 1-[(en)₂CoCO₃]ClO₄ in 1M NaClO₄. The spectra were recorded on a Jasco Model O.R.D./U.V-5 Optical Rotary Dispersion Recorder (Japan Spectroscopic Co., Ltd., Kitshachioji -Kojodanchi, Hachioji-City, Tokyo, Japan). The initial reaction solutions were 1.00 M in sodium hydroxide. The initial reaction solution (10 ml) was approximately 7.2×10^{-3} M in complex and all solutions were at room temperature.

Oxygen-18 Tracer Study

A solution of ^{18}O -enriched sodium hydroxide was prepared by diluting concentrated sodium hydroxide solution (Fisher Certified Reagent) with 1.7% ^{18}O -enriched water (Bio-Rad Laboratories). The molarity of the solution was determined by titration with standard HCl to a phenolphthalein end point. A stock solution of $[(\text{en})_2\text{CoCO}_3]\text{ClO}_4$ and NaClO_4 , in water of normal isotopic abundance, was prepared. The reaction was started by mixing about four ml of the stock solution with 21 ml of the ^{18}O -enriched sodium hydroxide solution. At various times, two ml samples of the solution were withdrawn with a syringe and injected into a gas bubbler containing 0.5 ml of concentrated perchloric acid. The apparatus, sampling technique and sample analysis are described in detail in Chapter 4. During the runs the complex was about 1×10^{-2} M, $[\text{OH}^-]$ varied from 0.50 to 1.00 M, μ was 1.0 (NaClO_4), and the temperature was 26° .

Base Catalyzed Hydrolysis of Carbonatobis(o-phenanthroline)cobalt(III) Ion Preparation and Characterization of o-Phenanthroline Complexes

The experimental details and results of the preparation and characterization of $[(\text{phen})_2\text{CoCO}_3]\text{Cl} \cdot 3\text{H}_2\text{O}$, *cis*- $[(\text{phen})_2\text{CoCl}_2]\text{Cl} \cdot 3\text{H}_2\text{O}$, *cis*- $[(\text{phen})_2\text{Co}(\text{OH}_2)_2]\text{Cl}_3 \cdot 2\text{H}_2\text{O}$, and $[(\text{phen})_3\text{Co}][\text{phenH}][\text{CoCl}_4]_2 \cdot \text{HCl} \cdot 5\text{H}_2\text{O}$ are given in Chapter 4.

Base Hydrolysis of Carbonatobis(o-phenanthroline)cobalt(III) Ion

Because of the very complicated nature of the base catalyzed hydrolysis of $(\text{phen})_2\text{CoCO}_3^+$, all of the kinetic runs consisted of complete scans of the spectrum of the reaction solution as the reaction proceeded. The spectra were run on a Cary Model 14 Recording Spectrophotometer (Applied Physics Corporation, Pasadena, Calif.) at room temperature. A known volume of sodium hydroxide and redistilled water was added to a five cm spectrophotometer cell. At zero time, 1.00 ml of a stock solution of $[(\text{phen})_2\text{CoCO}_3]\text{Cl}\cdot 3\text{H}_2\text{O}$ was syringed through a rubber serum cap into the cell. At appropriate time intervals, the spectrum of the solution between 400 m μ and 650 m μ was scanned. Blanks containing all the reagents except the complex were run to allow calculation of extinction coefficients. The stock solutions were generally around 2.0×10^{-2} M in complex and were used after varying periods of time to determine any ageing effects. The sodium hydroxide concentration varied between 0.867 and 1.0 M. In some runs, 2.0 M NaCl was added to give an ionic strength of 1.0. The zero time and infinite time spectra were used to determine the final product of the reaction. In order to test for catalysis by product a weighed amount of solid *cis*- $[(\text{phen})_2\text{Co}(\text{OH}_2)_2]\text{Cl}_3\cdot 2\text{H}_2\text{O}$ was added to the reaction mixture just prior to adding a weighed amount of the carbonato complex. After shaking, the spectral changes with time were followed by scanning as above. To test for catalysis by a Co(II) salt, a stock solution which was 1.496×10^{-3} M in *cis*-($\text{phen})_2\text{Co}(\text{OH}_2)_2^{2+}$ was prepared by dissolving known amounts of o-phenanthroline hydrate and cobaltous

chloride 6-hydrate in a 2:1 ratio in a known volume of redistilled water. After adding solid $[(\text{phen})_2\text{CoCO}_3]\text{Cl}\cdot 3\text{H}_2\text{O}$ to the solution in the cell, 0.1 ml of the stock Co(II) solution was syringed into the cell and the spectral changes with time were recorded.

Results

Base Catalyzed Hydrolysis of Carbonatopentaamminecobalt(III) Ion

The spectra of the carbonato-, aquo-, and hydroxypentaamminecobalt(III) ions are given in Figure 2.1. Because of the formation of brown cobalt oxide during the base hydrolysis reaction, it was not possible to scan the entire electronic absorption spectrum of the reaction solution. However, the infinite time sample of the reaction mixture was filtered and then rapidly scanned. The resultant spectrum had the same qualitative features as that of the hydroxypentaamminecobalt(III), shown in Figure 2.1, including the same wavelengths for the absorbance maxima and minima. This spectral evidence plus the fact that the $(\text{NH}_3)_5\text{CoOH}^{2+}$ ion is known to decompose to cobalt oxide, leads to the conclusion that the hydroxy species is the product of the base hydrolysis reaction.

The variation of the rate of hydrolysis of $(\text{NH}_3)_5\text{CoCO}_3^+$ with hydroxide ion concentration at 45-55° is consistent with a rate law developed from reactions (2.1), (2.2), and (2.3).

$$-\frac{d[T]}{dt} = k_1 [(\text{NH}_3)_5\text{CoCO}_3\text{H}^{2+}] + k_2 [(\text{NH}_3)_5\text{CoCO}_3^+][\text{OH}^-] \quad (2.13)$$

$$= \left(\frac{k_1 K_w}{K_1 [\text{OH}^-]} + k_2 [\text{OH}^-] \right) [(\text{NH}_3)_5\text{CoCO}_3^+] \quad (2.14)$$

$$= \left(\frac{k_1 K_w}{K_1 [\text{OH}^-]} + k_2 [\text{OH}^-] \right) \left(\frac{K_1}{K_1 + [\text{H}^+]} \right) [T] \quad (2.15)$$

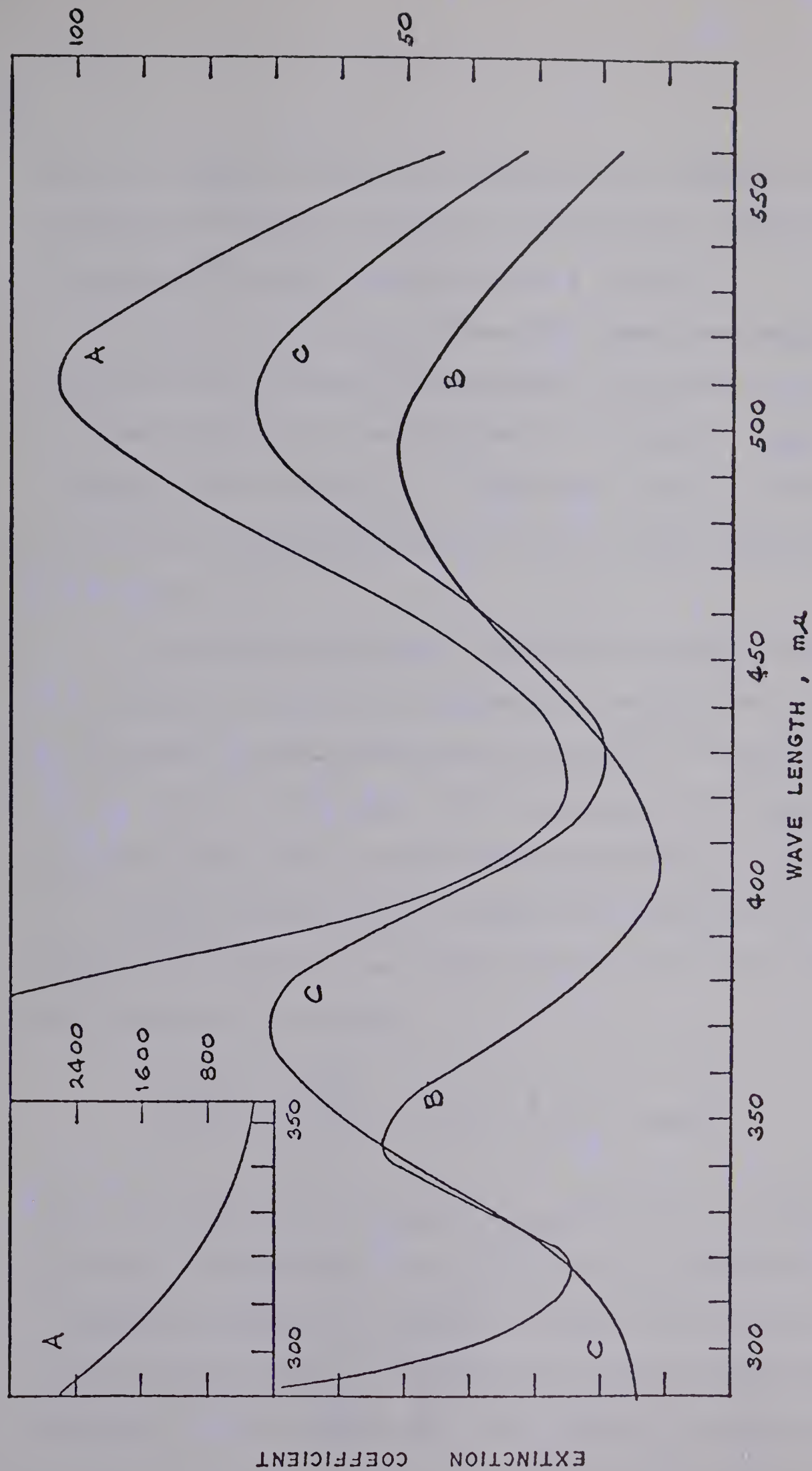


Figure 2.1: Electronic Absorption Spectra of $(\text{NH}_3)_5\text{CoCO}_3^+$, (A), $(\text{NH}_3)_5\text{CoOH}_2^{3+}$, (B), and $(\text{NH}_3)_5\text{CoCO}_3^{2+}$, (C). Inset-charge transfer region of the $(\text{NH}_3)_5\text{CoCO}_3^+$ spectrum.

where $[T]$ represents the total concentration of complex containing coordinated carbonate, K_1 is the acid dissociation constant of $(\text{NH}_3)_5\text{CoCO}_3\text{H}^{2+}$, and K_w is the ion product of water.

Under the conditions of these high temperature experiments the hydroxide ion was always in large excess over complex so that a pseudo first-order decrease in the absorbance was observed. Figure 2.2 shows a typical plot of $\log(A_t - A_\infty)$ vs. time where A_t and A_∞ are the absorbances of the reaction solution at time t and after complete reaction respectively.

The relationships between the physical property being measured, the concentration of the various species, the half-time of the reaction and the rate constant observed are well known⁶⁶ for simple first-order systems. These relationships will be used here and throughout other sections of this thesis without further derivation or justification.

Since the value of K_1 is likely to be between $1 \times 10^{-7} \text{ M}$ ⁴⁶ and $1 \times 10^{-9} \text{ M}$ ⁴⁸ and the $[\text{H}^+]$ was always less than $1 \times 10^{-11} \text{ M}$, $K_1 \gg [\text{H}^+]$.

Thus equation (2.15) becomes

$$-\frac{d[T]}{dt} = \left(\frac{k_1 K_w}{K_1 [\text{OH}^-]} + k_2 [\text{OH}^-] \right) [T] = k_{\text{obsd}} [T] \quad (2.16)$$

Figure 2.3 shows the variation of k_{obsd} with $[\text{OH}^-]$ at 55.0° along with the best fit line obtained from (2.16) using $K_w = 1.325 \times 10^{-13}$.⁶⁷

A computer program called ENLLSQ⁶⁸ has been used throughout these studies to obtain best fit parameters for linear and non-linear equations. A brief description of the program, its use, and the

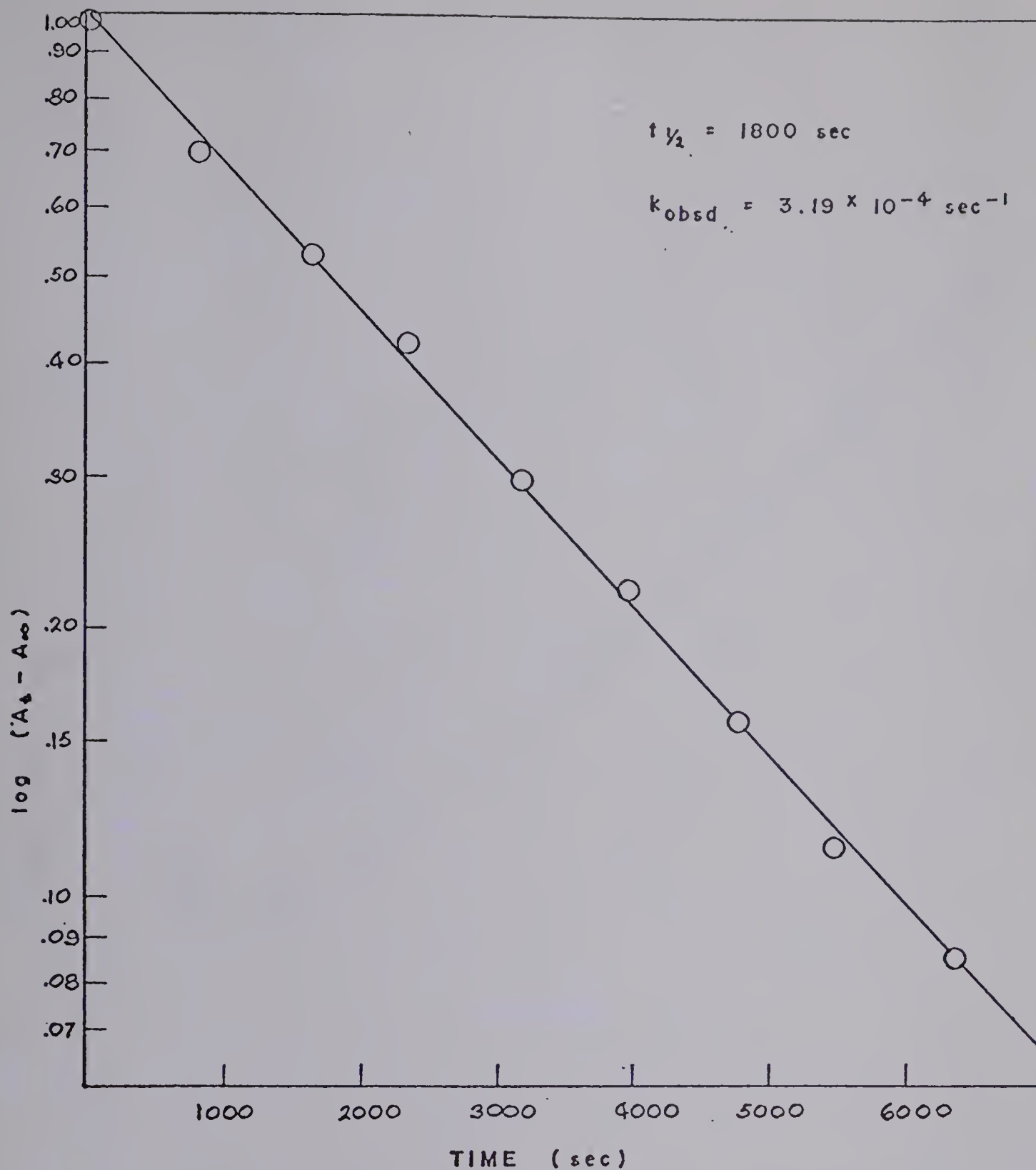


Figure 2.2: Variation of Absorbance with Time for the Reaction of

$(\text{NH}_3)_5\text{CoCO}_3^+$ Ion in Aqueous Sodium Hydroxide. $T = 55.0^\circ$,
 $[\text{OH}^-] = 0.020 \text{ M}$, $[\text{complex}] = 2.91 \times 10^{-3} \text{ M}$, $\mu = 1.0$.
 (NaNO_3) , $\lambda = 328 \text{ m}\mu$.

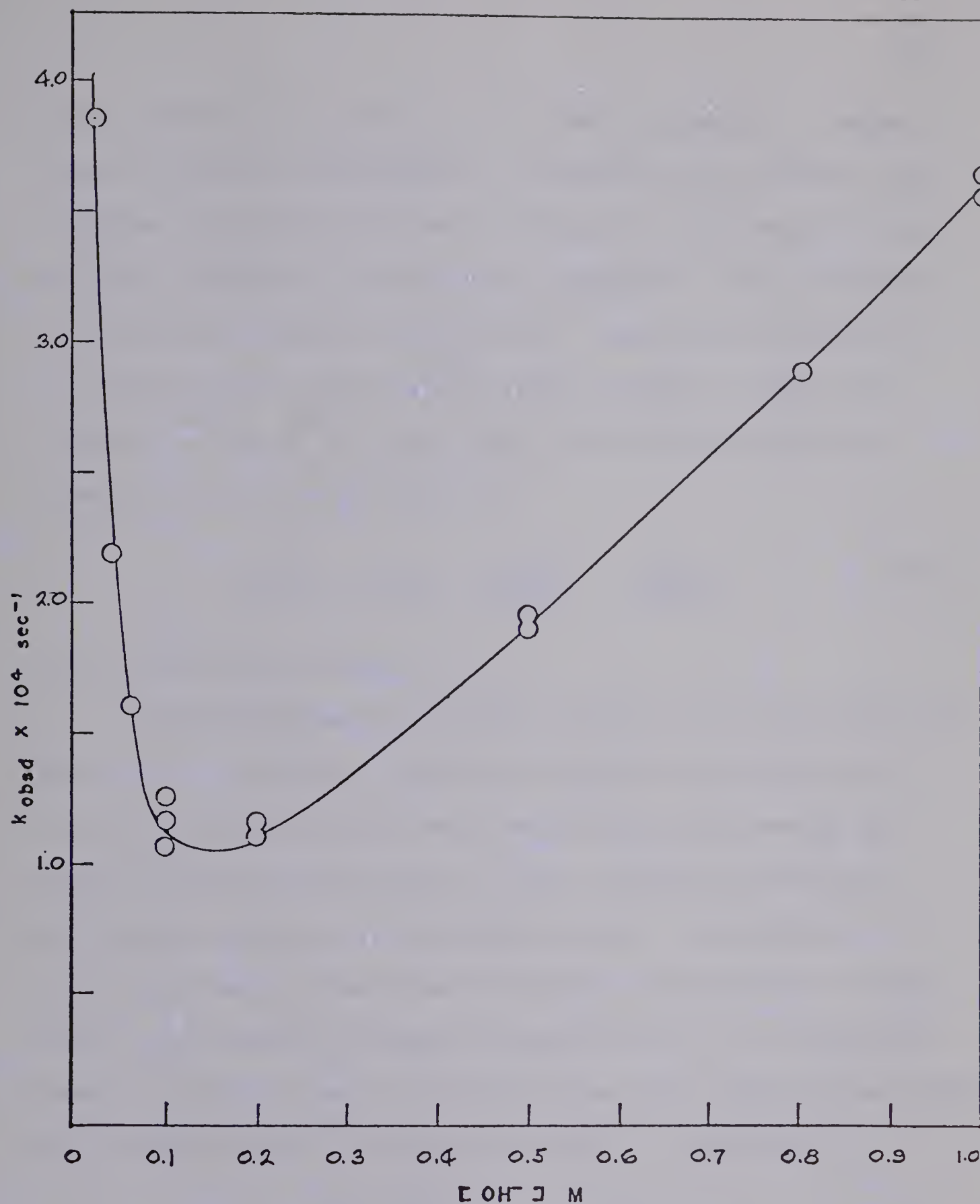


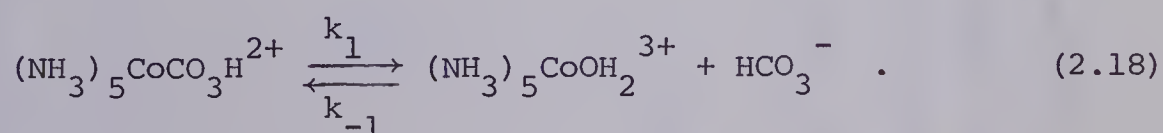
Figure 2.3: Variation of k_{obsd} with $[\text{OH}^-]$ for the Hydrolysis of $(\text{NH}_3)_5\text{CO}_3^+$ in Sodium Hydroxide. $T = 55.0^\circ$, $\mu = 1.0$ (NaNO_3).

error calculations it performs can be found in Appendix A. Tables giving the observed rate constant, the predicted rate constant, the hydroxide ion concentration, and the value of K_w used for 45.0, 50.0 and 55.0°, respectively, are located in Appendix D. All the values of K_w used were measured in 1.01 M KCl.⁶⁷ The values of k_1/K_1 and k_2 along with their 95% confidence limits are given in Table 2.2. Values of ΔH^\ddagger and ΔS^\ddagger for k_1/K_1 and k_2 were calculated from the standard transition state equation⁶⁹

$$\log\left(\frac{k_r}{T}\right) = \log\left(\frac{k_h}{h}\right) + \frac{\Delta S^\ddagger}{2.303R} - \frac{\Delta H^\ddagger}{2.303RT} \quad (2.17)$$

and are also given in Table 2.2.

Extrapolation of the 45.0-55.0° results to 25.0° shows that the second term in equation (2.16) will be negligible for the pH range, 8.5-9.4. A variation of the molar extinction coefficients of the reaction solution at zero time (ϵ_o) and at complete reaction (ϵ_∞) was observed indicating an equilibrium system. The variable ϵ_o is the optical density at zero time (obtained by extrapolation) divided by the total cobalt(III) complex concentration and ϵ_∞ is the optical density at infinite time also divided by the total complex concentration. The rate data have been interpreted in terms of the reaction



The rate of decomposition of carbonato and bicarbonato complexes is given by

TABLE 2.2

Specific Rate Constants and Activation Parameters for the Hydrolysis of $(\text{NH}_3)_5\text{CoCO}_3^+$

Temp, °C	$k_1/k_1 \times 10^{-7}, \text{M}^{-1} \text{sec}^{-1}$	$k_2 \times 10^4, \text{M}^{-1} \text{sec}^{-1}$
45.0	$2.074 \pm .286^a$	0.820 ± 0.147
50.0	$4.551 \pm .264$	$1.550 \pm .100$
55.0	$5.884 \pm .238$	$3.579 \pm .109$
$\Delta H^\ddagger, \text{kcal mole}^{-1}$	$17.6^b (16.9-18.7)$	$30.8 (28.2-33.9)$
$\Delta S^\ddagger, \text{cal mole}^{-1} \text{deg}^{-1}$	$30.4^b (28.3-33.7)$	$19.3 (11.1-28.9)$

^a Error limits calculated as in Appendix A.^b The value of k_1/k_1 determined at 25.0° was included in this activation parameter calculation.

$$-\frac{d[T]}{dt} = k_1[(\text{NH}_3)_5\text{CoCO}_3\text{H}^{2+}] - k_1[(\text{NH}_3)_5\text{CoOH}_2^{3+}][\text{HCO}_3^-] \quad (2.19)$$

where T is as defined previously. Use of the equilibrium and stoichiometry conditions results in

$$k_{\text{obsd}} = \frac{k_1[\text{H}^+]}{K_1 + [\text{H}^+]} \left\{ \frac{\epsilon_o}{\epsilon_o - \epsilon_\infty} \right\} \quad (2.20)$$

The derivation of equation (2.20) is given in Appendix C. The value of k_{obsd} was calculated in the standard way from a plot of $\log(A_t - A_\infty)$ vs. time. Rearrangement of (2.20) gives

$$\frac{1}{[\text{H}^+]} = \frac{k_1}{K_1} \left\{ \frac{\epsilon_o}{\epsilon_o - \epsilon_\infty} \right\} \frac{1}{k_{\text{obsd}}} - \frac{1}{K_1} \quad (2.21)$$

The results of the experiments at low pH and 25.0° are given in Table 2.3 which also gives values of the calculated rate constants using equation (2.20) and the best fit values of k_1 and K_1 obtained from a fit of the data to equation (2.21). Figure 2.4 shows the plot of equation (2.21) and the best fit straight line obtained by the use of ENLLSQ. The values of the slope and intercept parameters from Figure 2.4 are

	$k_1/K_1 \times 10^{-6}, \text{M}^{-1} \text{sec}^{-1}$	$K_1^{-1} \times 10^8, \text{M}^{-1}$
parameter	3.879	1.631
95% C.L.	±.430	±4.257

TABLE 2.3

Kinetic and Equilibrium Data for the Hydrolysis

of $(\text{NH}_3)_5\text{CoCO}_3^+$ at 25.0°

pH	$[\text{H}^+] \times 10^9$ M	$\epsilon_o \times 10^{-3}$	$\epsilon_\infty \times 10^{-3}$	$k_{\text{obsd}}^a \times 10^2$ sec ⁻¹	$k_{\text{calcd}}^b \times 10^2$ sec ⁻¹
8.492	3.222	2.318	1.628	2.618	2.780
8.648	2.245	2.440	1.645	1.899	1.955
8.695	2.020	2.341	1.581	1.775	1.815
8.763	1.728	2.325	1.575	1.593	1.620
8.855	1.398	2.399	1.588	1.184	1.301
8.960	1.097	2.384	1.515	1.050	0.987
9.013	0.971	2.575	1.573	0.970	0.836
9.148	0.711	2.388	1.440	0.587	0.632
9.237	0.580	2.405	1.415	0.468	0.498
9.294	0.508	2.390	1.387	0.468	0.433
9.338	0.460	2.220	1.355	0.423	0.425
9.390	0.407	2.280	1.328	0.375	0.365

^a $\mu = 1.0$ (NaClO_4).^b k_{calcd} calculated from equation (2.20) and the parameters in Table 2.2.

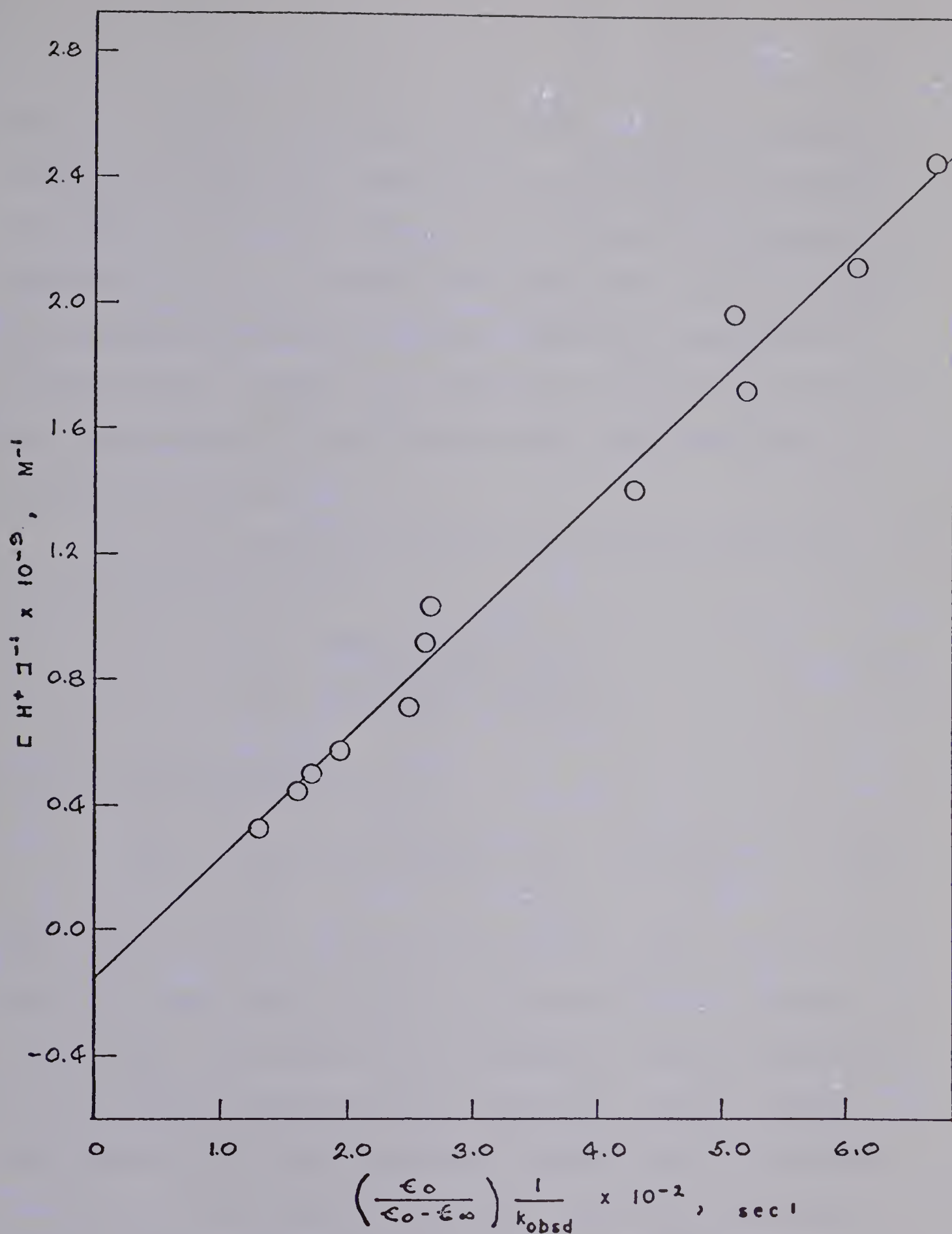


Figure 2.4: Variation of $[H^+]^{-1}$ with $[\epsilon_0/(\epsilon_0 - \epsilon_\infty)]k_{\text{obsd}}^{-1}$ for the Hydrolysis of $(\text{NH}_3)_5\text{CoCO}_3^+$ at 25.0° and at low pH.

Notice the large 95% confidence limits placed on the intercept (K_1^{-1}). These large limits cause a large degree of uncertainty in the values of k_1 and K_1 which can be calculated from the best fit parameters. Thus the value of k_1 , $2.375 \times 10^{-2} \text{ sec}^{-1}$, has a lower limit of 1.30×10^{-2} but an upper limit which can only be called large, corresponding to a zero intercept in Figure 2.4. Similarly the value of K_1 , $6.130 \times 10^{-9} \text{ M}$, has a lower limit of $3.02 \times 10^{-9} \text{ M}$ but an upper limit which again can only be called large.

It is also possible to calculate the formation constant K_f , for the bicarbonato complex

$$K_f = \frac{[(\text{NH}_3)_5\text{CoCO}_3\text{H}^{2+}][\text{OH}^-]}{[(\text{NH}_3)_5\text{CoOH}^{2+}][\text{HCO}_3^+]} \quad (2.22)$$

It can be shown (Appendix C) that

$$K_f = \frac{\epsilon_\infty K_w}{K_1(\epsilon_1 - \epsilon_\infty) + [\text{H}^+](\epsilon_2 - \epsilon_\infty)} \left(\frac{1}{[\text{HCO}_3^-]} \right) \quad (2.23)$$

where K_1 and ϵ_∞ are as defined previously and ϵ_1 and ϵ_2 are the extinction coefficients of the carbonato and bicarbonato complexes, respectively. The value of K_1 was determined as described later and ϵ_1 was measured as described in the experimental section. However the value of ϵ_2 could not be measured directly because the hydrolysis is too fast at low pH where $(\text{NH}_3)_5\text{CoCO}_3\text{H}^{2+}$ would be the predominant species. In principle, knowing ϵ_1 and K_1 it should be possible to calculate ϵ_2 from the ϵ_0 values, since at zero time the only absorbing species are the carbonato and bicarbonato complexes. However the ϵ_0

values in Table 2.3 do not show a smooth trend with pH. This randomness is most probably due to the error in extrapolating back to zero time of mixing. In fact, as can be shown in the subsequent treatment where a value of ϵ_2 is derived, very little variation is expected in ϵ_0 , and the observed values are generally within 10% of the expected values.

The values of ϵ_2 and K_f have been obtained by fitting the ϵ_∞ values to a rearranged form of (2.23)

$$\frac{K_1 \epsilon_1 - \epsilon_\infty (K_1 + [H^+])}{[H^+]} = \frac{1}{K_f} \left(\frac{K_w \epsilon_\infty}{[H^+][HCO_3^-]} \right) - \epsilon_2 \quad (2.24)$$

The value of $[HCO_3^-]$ was calculated using equation (4.50) found in Chapter 4 of this thesis. The values used for ϵ_1 , K_1 , K_w , K_{c1} , and K_{c2} are 2180, 3.28×10^{-7} M, 1.7×10^{-14} , 8.71×10^{-7} M, and 2.75×10^{-10} M, respectively. As was shown above, the value of K_1 determined in this study is subject to a large uncertainty. For this reason the value of K_1 used here was calculated from the value of k_1/K_1 which is known quite precisely, and the value of k_1 determined by Harris which is also quite precise. The details of this calculation are given in Chapter 4, p 176. The resulting plot of (2.24) was linear as shown in Figure 2.5. The best fit parameters obtained by the use of ENLLSQ are

	K_f	ϵ_2
parameter	5.408×10^{-6}	2.91×10^4
95% C.L.	$\pm 0.241 \times 10^{-6}$	$\pm 1.68 \times 10^4$

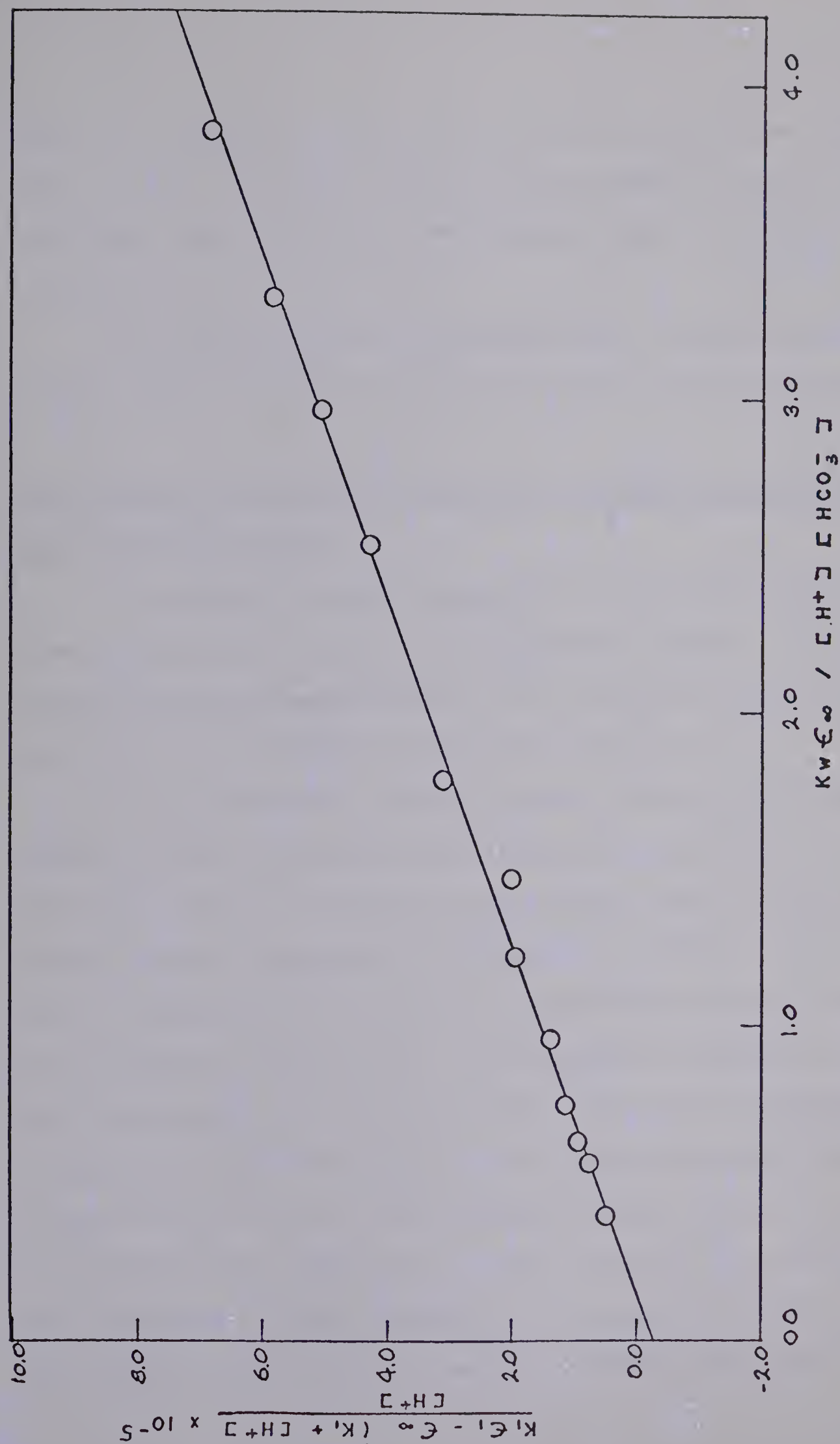


Figure 2.5: Variation of $[K_1 \epsilon_1 - \epsilon_\infty (K_1 + [H^+])]/[H^+]$ with $K_w \epsilon_\infty/[H^+] [HCO_3^-]$ for the $(NH_3)_5CoCO_3^+$ ion. $T = 25.0^\circ$, $\mu = 1.0$ (NaClO₄).

Table D.4 in Appendix D gives the experimental and calculated values of $[K_1\epsilon_1 - \epsilon_\infty(K_1 + [H^+])]/[H^+]$ corresponding to values of $(K_w\epsilon_\infty)/[H^+][HCO_3^-]$ which were used in determining the parameter values and the solid line in Figure 2.5.

The values of K_f and ϵ_2 reported here are not those reported by Francis and Jordan⁷³ due to the use of the more precise value of K_1 here.

Base Catalyzed Hydrolysis of Carbonatobis(ethylenediamine)cobalt(III) Ion

Base Hydrolysis Kinetics

The visible electronic spectra of the carbonatobis(ethylenediamine)cobalt(III) ion and its acid hydrolysis product, the *cis*-diaquobis(ethylenediamine)cobalt(III) ion are shown in Figure 2.6. Also shown is the spectrum of the *cis*-(en)₂Co(OH)₂⁺ ion.

It was found that a solution of [(en)₂CoCO₃]ClO₄ in water was stable and that no spectral change occurred for periods of at least one week. Figure 2.7 shows the spectral change which occurred when sodium hydroxide was added to the neutral stock solution of the complex. Over a time period of 115 minutes, the absorbance increased at 320 mμ and decreased at 360 and 515 mμ. By comparing the spectrum of the reaction solution at 115 minutes to those of the *cis*- and *trans*-(en)₂Co(OH)₂⁺ ions,⁵⁶ it can be seen that the initial product can be neither the *cis*- nor the *trans*-dihydroxy species. Following spectral changes during the reaction for a longer time at 300 mμ resulted in the curve shown in Figure 2.8 where A_t and A_∞ are the absorbance of the reaction solution at time t and the calculated absorbance of an

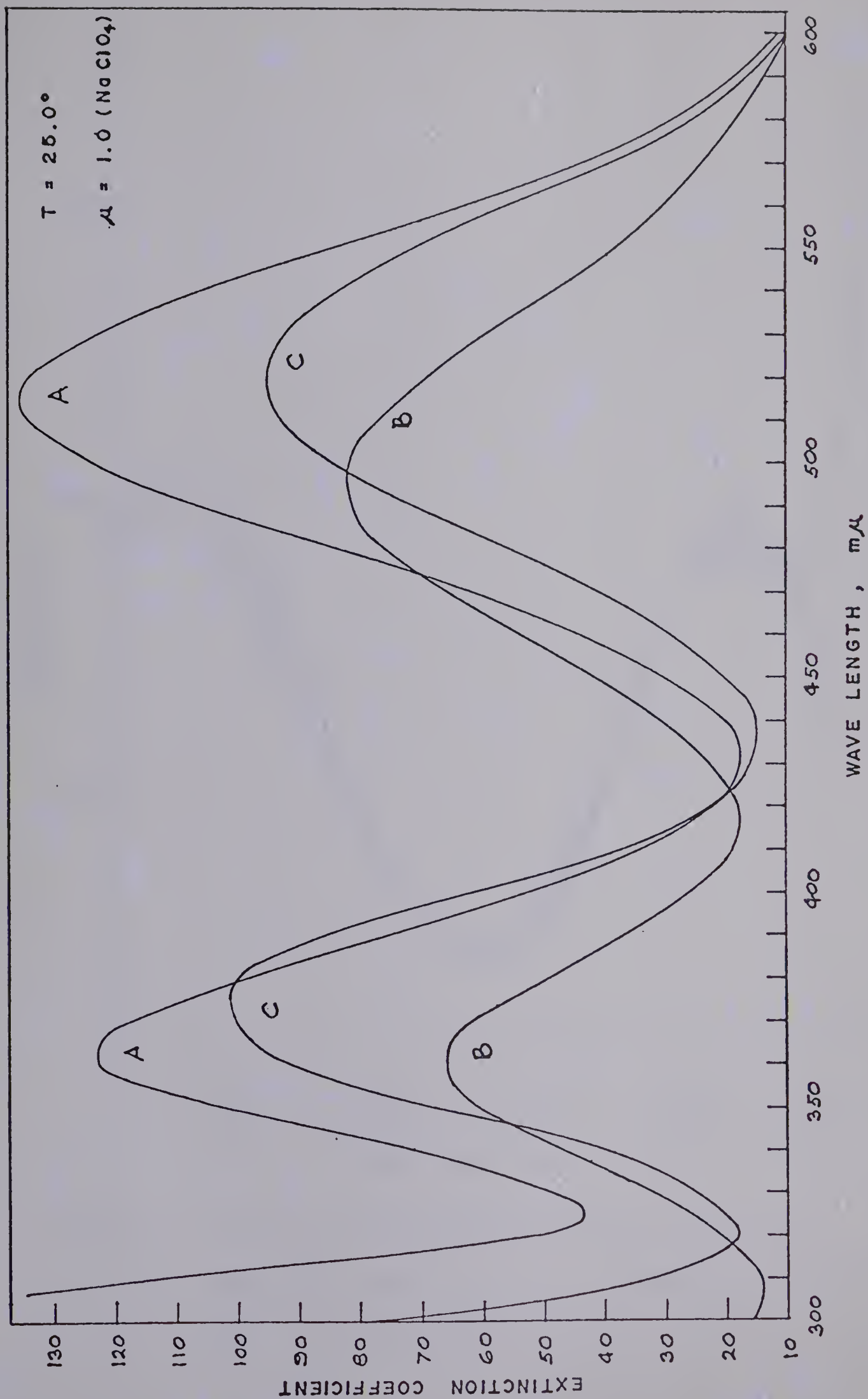


Figure 2.6: Visible Absorption Spectra of $(en)_2CoCO_3^+$, (A), $cis-(en)_2Co(OH)_2^{3+}$, (B) and $cis-(en)_2Co(OH)_2^+$, (C).

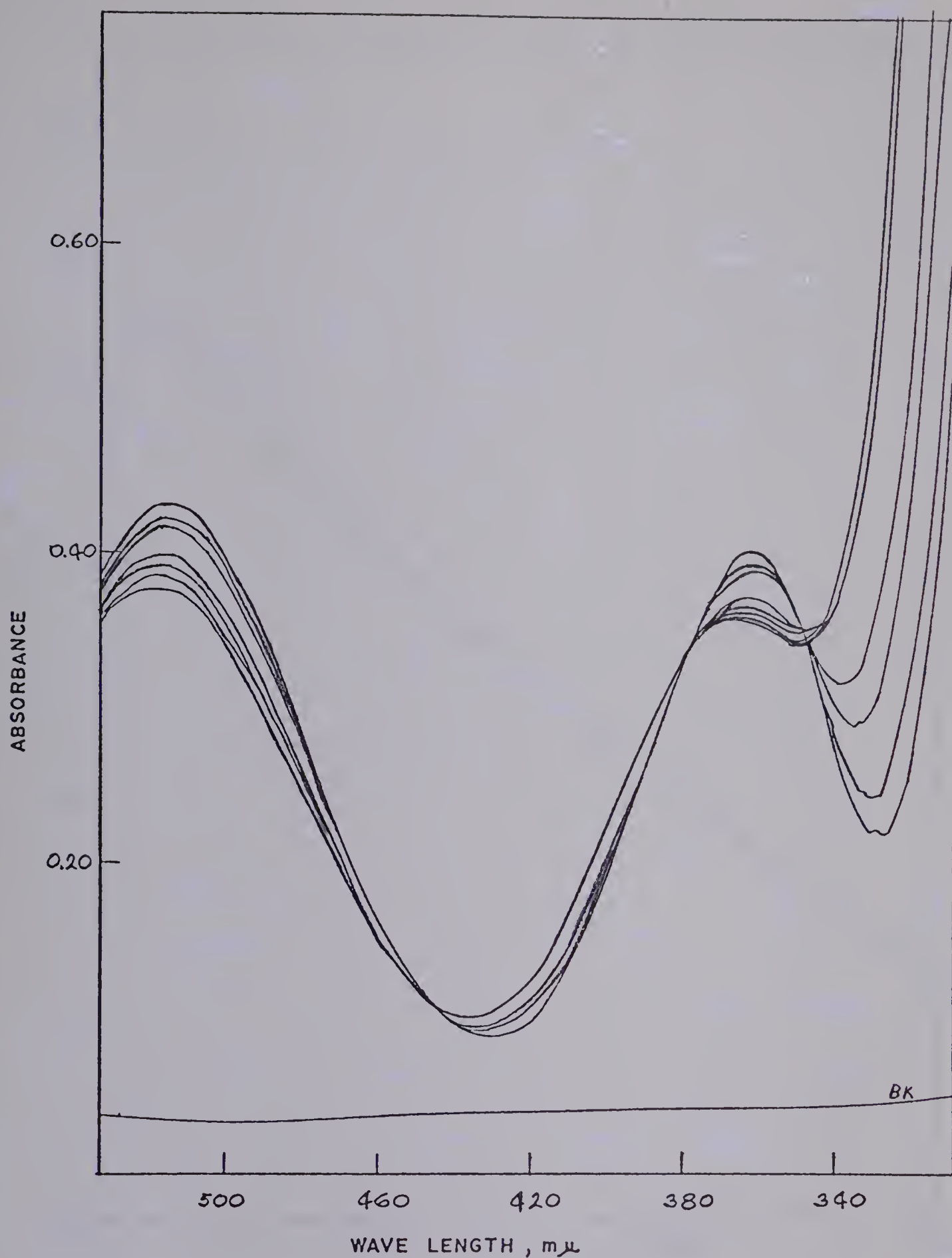


Figure 2.7: Variation of Absorbance with Time of a Solution of $(en)_2CoCO_3^+$ and NaOH at 26.0° . $[complex] = 3.05 \times 10^{-3} M$, $[OH^-] = 0.096 M$, 1 cm cell.

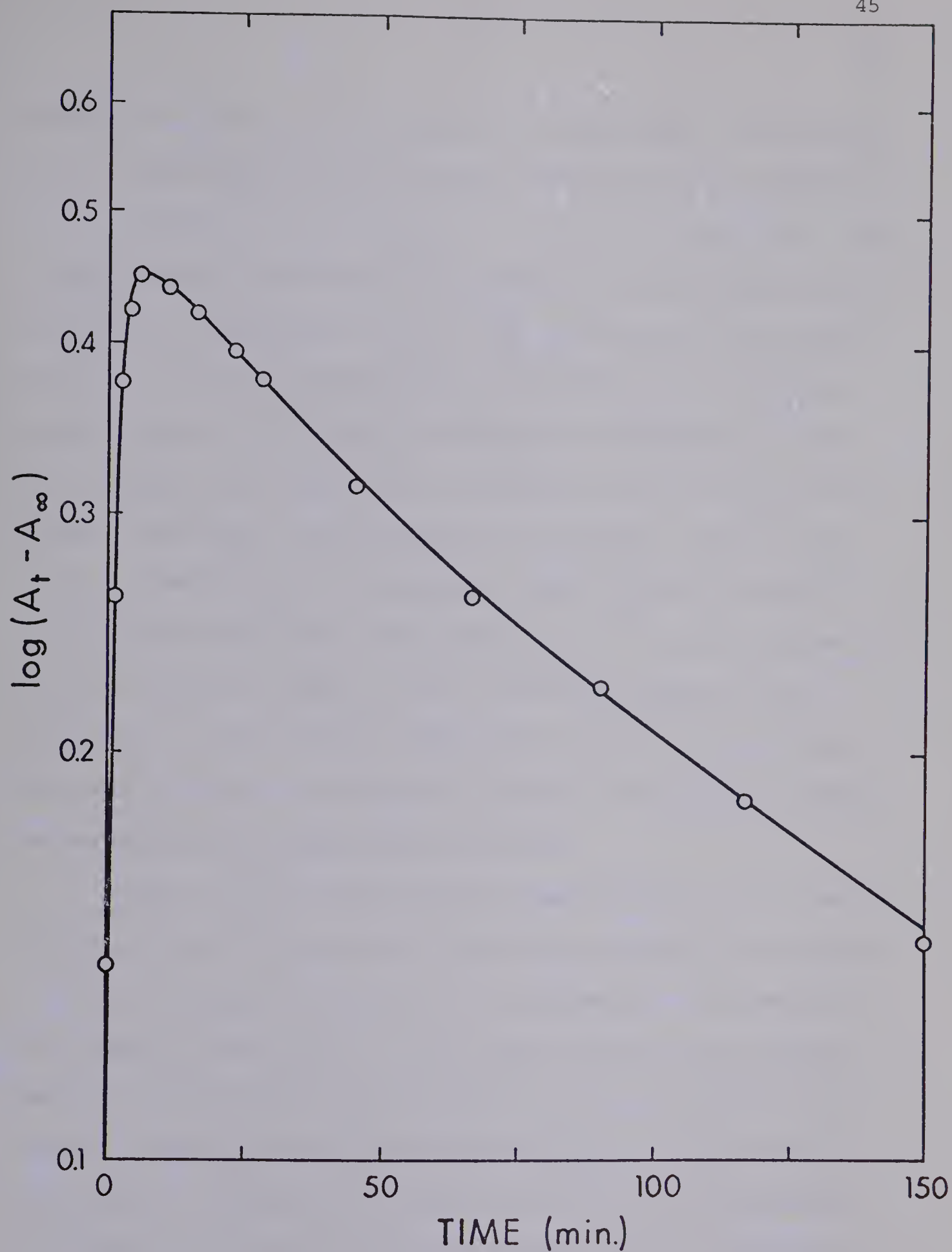


Figure 2.8: Variation of Absorbance with Time of a Solution of $(en)_2CoCO_3^+$ and NaOH at 34° . $[complex] = 2.70 \times 10^{-3} M$, $[OH^-] = 0.842 M$, $\lambda = 300 m\mu$.

equimolar solution of *cis*-(en)₂Co(OH)₂⁺, respectively. The initial rise in absorbance at 300 mμ has been attributed to the production of *cis*-(en)₂CoOHCO₃ via reactions (2.5), (2.6), (2.7), and (2.8). The slower decrease in absorbance corresponds to the production of *cis*-(en)₂Co(OH)₂⁺, reaction (2.9). The slight curvature in the second portion of the curve in Figure 2.8 corresponds to the *cis* \rightleftharpoons *trans* isomerization of (en)₂Co(OH)₂⁺ because the *trans*-dihydroxy isomer has a slightly higher extinction coefficient at 300 mμ than the *cis* isomer⁵⁶ and because the half-times of the second reaction, (2.9), and the isomerization, are comparable, being 1.49x10⁴ sec ([OH⁻] = 1.00 M) and 10.0x10⁴ sec, respectively at 25°. ⁷⁴ In the experiments at 24.5°, where [OH⁻] was > 1.0 M, no curvature appeared in the log(A_t-A_∞) vs. time plots even after two half-times of the second reaction indicating that the second reaction is essentially complete before appreciable isomerization can occur.

Figure 2.8 also shows that the second reaction, (2.9), cannot be ignored when determining the observed rate constant for the first reaction. If A_{max} is the value of the maximum observed absorbance, then plots of log(A_{max}-A_t) vs. time become nonlinear after approximately one half-time of the first reaction as seen in Figure 2.9, plot A. Provided the rate constants of consecutive first-order reactions are different by at least a factor of 10, it is possible to separate the concentration-time dependence data into components corresponding to each of the consecutive reactions.⁷⁵ For the 24.5° data this separation was done by extrapolating the log(A_t-A_∞) vs. time

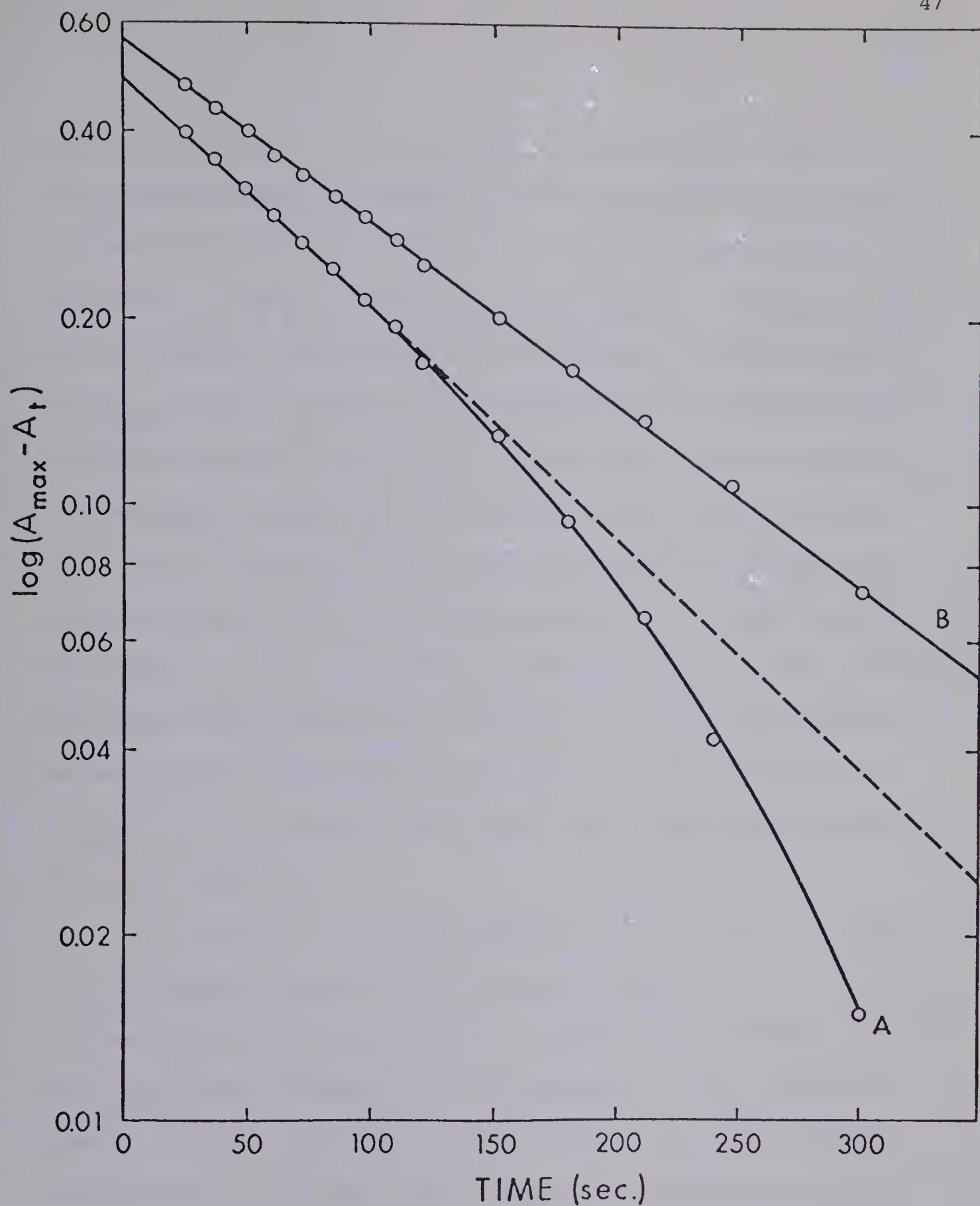


Figure 2.9: Variation of Absorbance with Time of a Solution of

$(en)_2CoCO_3^+$ in NaOH at 24.5° . $[complex] = 1.475 \times 10^{-4} M$,

$[OH] = 3.00 M$, $\lambda = 300 m\mu$. Plot A is $\log(A_{max} - A_t)$ vs.

time, Plot B is $\log(A'_{max} - A_t)$ vs. time.

plots to zero time to obtain a value for $\log(A'_{\max} - A_{\infty})$. A'_{\max} is the absorbance which the reaction solution would have shown at the completion of the first reaction if the second reaction had not occurred. As seen in Figure 2.9, plot B, a plot of $\log(A'_{\max} - A_t)$ vs. time is linear and has a different observed rate constant than the $\log(A_{\max} - A_t)$ vs. time plot. This "extrapolation" method was used to analyze the kinetic data at 24.5°. It was found that increasing A_{\max} to some A'_{\max} where A'_{\max} was sufficiently large to cause linearity in a plot of $\log(A'_{\max} - A_t)$ vs. time was equivalent to obtaining A'_{\max} by extrapolation. Since sufficient data for the extrapolation were not obtained, this second method of obtaining A'_{\max} was used to evaluate the kinetic data at 26.0, 34.0, and 44.0°. As the sodium hydroxide concentration decreased from 3.71 to 0.817 M, the corrections in k_{obsd} , at 24.5°, decreased from -32 to -16%, respectively and became negligible below 0.5 M.

The results of the kinetic study at 24.5° are given in Table 2.4. The observed rate constants for the second reaction, (2.9), were obtained from plots of $\log(A_t - A_{\infty})$ vs. time similar to Figure 2.8. In most good kinetic studies, the ionic strength is kept constant to prevent changes in activity of the reactants. Since this was not done for the 24.5° study, it was necessary to normalize all the observed rate constants by a factor N where

$$N = \frac{\gamma^{\pm} \text{ of } 1.0 \text{ M NaOH}}{\gamma^{\pm} \text{ of } x \text{ M NaOH}} \quad (2.25)$$

TABLE 2.4

Variation of k_{obsd} with $[\text{OH}^-]$ for the Complete Hydrolysis
of $(\text{en})_2\text{CoCO}_3^+$ in NaOH at 24.5°

Reaction	$[\text{OH}], \text{ M}$	$k_{\text{obsd}} \times 10^3, \text{ sec}^{-1}$	$k_{\text{obsd}}^{\text{N}^a} \times 10^3, \text{ sec}^{-1}$
(2.5)	1.00	3.18	3.18
	1.00	3.10	3.10
	2.00	5.05	4.91
	2.00	5.29	5.13
	3.00	7.08	6.21
	3.00	6.30	5.52
	3.00	6.79	5.95
	3.71	9.50	7.57
	3.71	10.2	8.14
	3.71	9.63	7.69
	3.71	10.2	8.14
(2.9)	1.00	0.0462	0.0462
	1.00	0.0465	0.0465
	2.00	0.0910	0.0883
	2.00	0.0924	0.0897
	3.00	0.193	0.168
	3.00	0.175	0.154
	3.00	0.173	0.151
	3.71	0.199	0.159

^a N is a correction factor for the change in activity coefficient
of NaOH as $[\text{NaOH}]$ goes from 1.00 M to 3.71 M.

where x M refers to the molarity of the particular NaOH solution and γ^\pm is the mean activity coefficient of NaOH. The normalization was done according to

$$k_{\text{obsd}}^N = k_{\text{obsd}} \cdot N \quad (2.26)$$

The value of γ^\pm for sodium hydroxide at concentrations of 1.0, 2.0, 3.0, and 3.71 M are 0.679, 0.698, 0.774, and 0.850, respectively.⁷⁶

It was observed that the corrected value of the absorbance of the reaction solution after completion of the first reaction (i.e. A'_{max}) varied both with temperature and with hydroxide ion concentration. Both of these effects indicate that the first step in the reaction is an equilibrium process. An equilibrium constant, K_1 , is defined by

$$K_1 = \frac{[(\text{en})_2\text{CoOHCO}_3]}{[(\text{en})_2\text{CoCO}_3^+][\text{OH}^-]} \quad (2.27)$$

It can be shown (Appendix C) that K_1 and $[\text{OH}^-]$ are related by

$$\frac{1}{[\text{OH}^-]} = K_1 (\epsilon_a - \epsilon_x) \left(\frac{bT_o}{A'_{\text{max}} - A_o} \right) - K_1 \quad (2.28)$$

where ϵ_x and ϵ_a are the extinction coefficients at 300 mμ of $(\text{en})_2\text{CoCO}_3^+$ and *cis*-($\text{en})_2\text{CoOHCO}_3$, respectively, T_o is the total complex concentration, b is the cell length in centimeters, A_o is the zero-time absorbance of the solution derived from the zero-time extrapolated value of $\log(A'_{\text{max}} - A_t)$ vs. time plot, and A_t and A'_{max} have been defined previously. Figure 2.10 shows the linear plot of equation (2.28) for 26.0°. Only data from solutions where

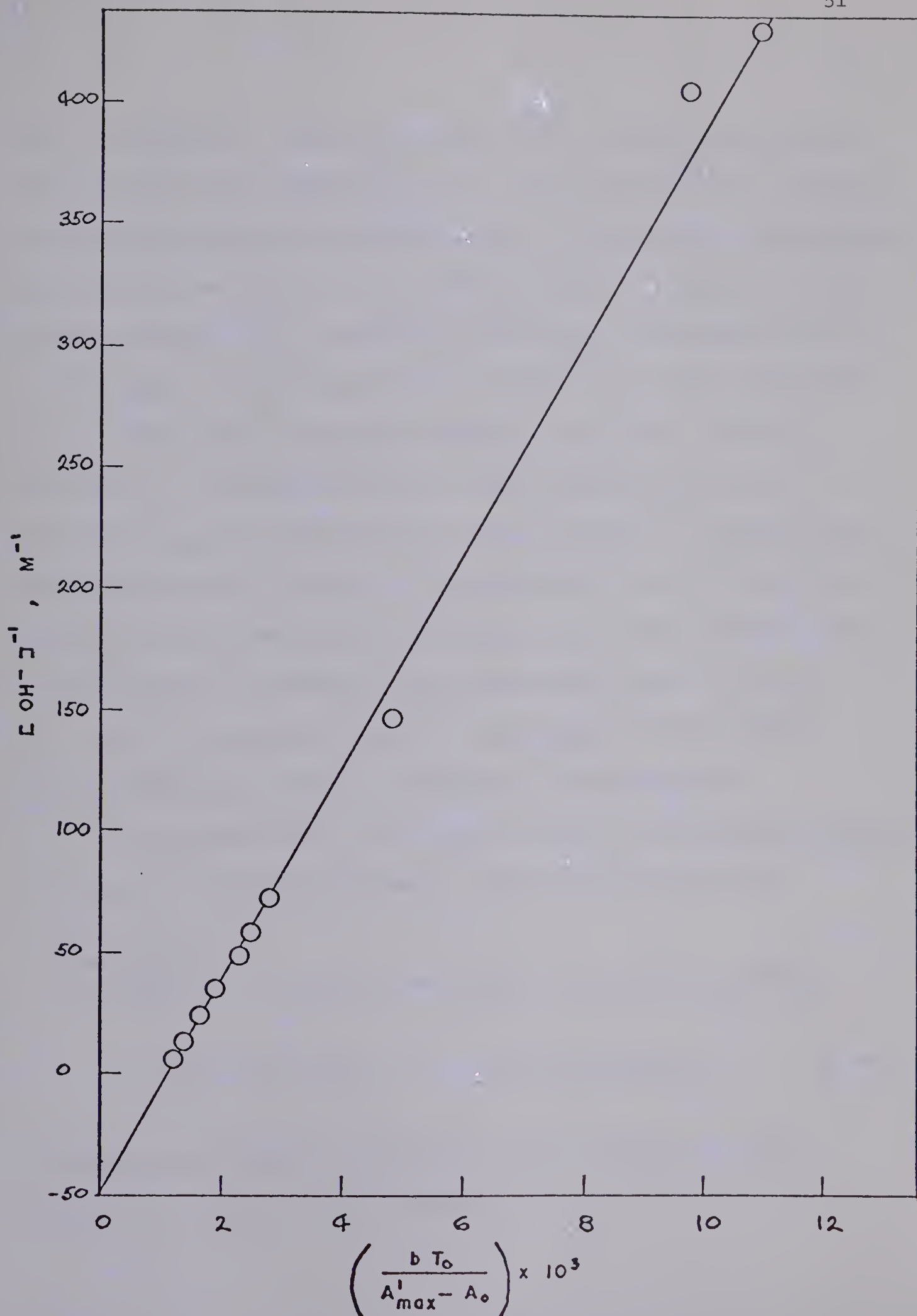


Figure 2.10: Plot of $[\text{OH}^-]^{-1}$ vs. $bT_0/(A'_{\max} - A_0)$ at 26.0° .

$(\text{en})_2\text{CoCO}_3^+$ in NaOH, K_1 is the -Y intercept.

90% > $[(\text{en})_2\text{CoCO}_3^+]$ > 10% were used in order to avoid large relative experimental errors in $bT_o/(A'_{\text{max}} - A_o)$. A first estimate of K_1 was used to eliminate points outside of this range. The best fit of the remaining data to equation (2.28) was obtained by using a modification of the computer program LSQ2,⁷⁷ which gives the linear least-squares fit to a polynomial. A weighting factor of $[\text{OH}^-]^{-1}$ was used to compensate for the large order of magnitude changes in the data. Tables D.5, D.6, and D.7 in Appendix D give the experimental values of $[\text{OH}^-]^{-1}$, T_o , and $bT_o/(A'_{\text{max}} - A_o)$ along with the values of $[\text{OH}^-]^{-1}$ calculated from equation (2.28) and the best fit parameters for 26.0, 34.0, and 44.0°. Table 2.5 gives these best fit parameters, their 95% confidence limits and the values of ΔH° and ΔS° calculated from a plot of $\log K_1$ vs. $1/T$. The 95% confidence limits are one-parameter limits assuming little correlation between the parameters (see Appendix A).

If reactions (2.5), (2.6), and (2.7) are the processes controlling the rate of equilibrium attainment, then the rate is given by

$$\begin{aligned}
 - \frac{d[(\text{en})_2\text{CoCO}_3^+]}{dt} &= k_1 [\text{OH}^-] [(\text{en})_2\text{CoCO}_3^+] - k_{-1} [\text{cis}-(\text{en})_2\text{CoOHCO}_3] \\
 &+ k_2 [\text{H}_2\text{O}] [(\text{en})_2\text{CoCO}_3^+] - k_{-2} [\text{cis}-(\text{en})_2\text{CoOHCO}_3\text{H}^+] \quad . \quad (2.29)
 \end{aligned}$$

Substitution for $[\text{cis}-(\text{en})_2\text{CoOHCO}_3\text{H}^+]$ using the equation for K_3 derived from reaction (2.7) results in

TABLE 2.5

Variation in K_1 with Temperature

Temp, °C	K_1, M^{-1}	95% Confidence Limits ^a
26.0	48.54	± 5.89
34.0	36.66	± 3.05
44.0	26.40	± 4.45
$\Delta H^\circ, \text{kcal mole}^{-1}$	-6.46	± 3.05
$\Delta S^\circ, \text{cal mole}^{-1} \text{ deg}^{-1}$	-13.9	± 9.5

^a Calcd as discussed in Appendix A.

$$\begin{aligned}
-\frac{d[(en)_2CoCO_3^+]}{dt} &= k_1[OH^-][(en)_2CoCO_3^+] - k_{-1}[cis-(en)_2CoOHCO_3] \\
&+ k_2[H_2O][(en)_2CoCO_3^+] - \frac{k_{-2}K_w}{K_3[OH^-]}[cis-(en)_2CoOHCO_3] \quad (2.30)
\end{aligned}$$

Let T_o be the initial complex concentration and assume that at any time, $[cis-(en)_2CoOHCO_3H^+]$ is small. Then

$$[cis-(en)_2CoOHCO_3] = T_o - [(en)_2CoCO_3^+] \quad (2.31)$$

Substitution in equation (2.30) for $[cis-(en)_2CoOHCO_3]$ yields an equation of the form

$$\begin{aligned}
-\frac{dA}{dt} &= \left(k_1[OH^-] + k_{-1} + k_2[H_2O] + \frac{k_{-2}K_w}{K_3[OH^-]} \right) A \\
&- \left(k_{-1} + \frac{k_{-2}K_w}{K_3[OH^-]} \right) A_o \quad (2.32)
\end{aligned}$$

which can be integrated directly.⁷⁸ The resultant expression for the observed rate constant is

$$k_{obsd} = k_1[OH^-] + k_{-1} + k_2[H_2O] + \frac{k_{-2}K_w}{K_3[OH^-]} \quad (2.33)$$

The principle of detailed balance⁷⁹ gives an equation relating the equilibrium constant, K_1 , to the various specific rate constants

$$K_1 = \frac{k_1}{k_{-1}} = \frac{k_2[H_2O]K_3}{k_{-2}K_w} \quad (2.34)$$

Substitution for k_{-1} and $k_2[\text{H}_2\text{O}]$ in equation (2.33) results in

$$k_{\text{obsd}} = k_1[\text{OH}^-] + \frac{k_1}{K_1} + \frac{k_{-2}K_wK_1}{K_3} + \frac{k_{-2}K_w}{K_3[\text{OH}^-]} \quad (2.35)$$

Over the temperature range, 26.0 to 44.0°, and over the hydroxide ion concentration range, 1.19×10^{-3} to 0.899 M, the observed rate constant determined from a plot of $\log(A'_{\text{max}} - A_t)$ vs. time followed the equation

$$k_{\text{obsd}} = k'[\text{OH}^-] + k'' + k'''[\text{OH}^-]^{-1} \quad (2.36)$$

A comparison of equations (2.35) and (2.36) shows that the rate law developed from reactions (2.5), (2.6), and (2.7) is consistent with the experimental rate law.

Values for the constants, k_1 and $k_{-2}K_w/K_3$ were obtained by fitting the experimental k_{obsd} values to equations (2.35) using the previously calculated value of K_1 at each temperature. The program ENLLSQ was used with a relative residuals minimization⁶⁸ option. The program results showed no parameter correlation between k_1 and $k_{-2}K_w/K_3$ and the non-linear and one-parameter confidence limits were equal so that the one-parameter 95% linear confidence limits were used (see Appendix A). The values of k_{-1} and $k_2[\text{H}_2\text{O}]$ were calculated from equation (2.34) using the value of K_1 at each temperature. The 95% confidence limits for k_{-1} and $k_2[\text{H}_2\text{O}]$ were calculated in the normal way⁸⁰ from the 95% confidence limits on k_1 , $k_{-2}K_w/K_3$, and K_1 . Figure 2.11 shows a representative plot of k_{obsd} vs. $-\log[\text{OH}^-]$ at 26.0°. The solid line was calculated from equation (2.33) and the best fit specific rate constants which are given in Table 2.6 for each temperature. Also

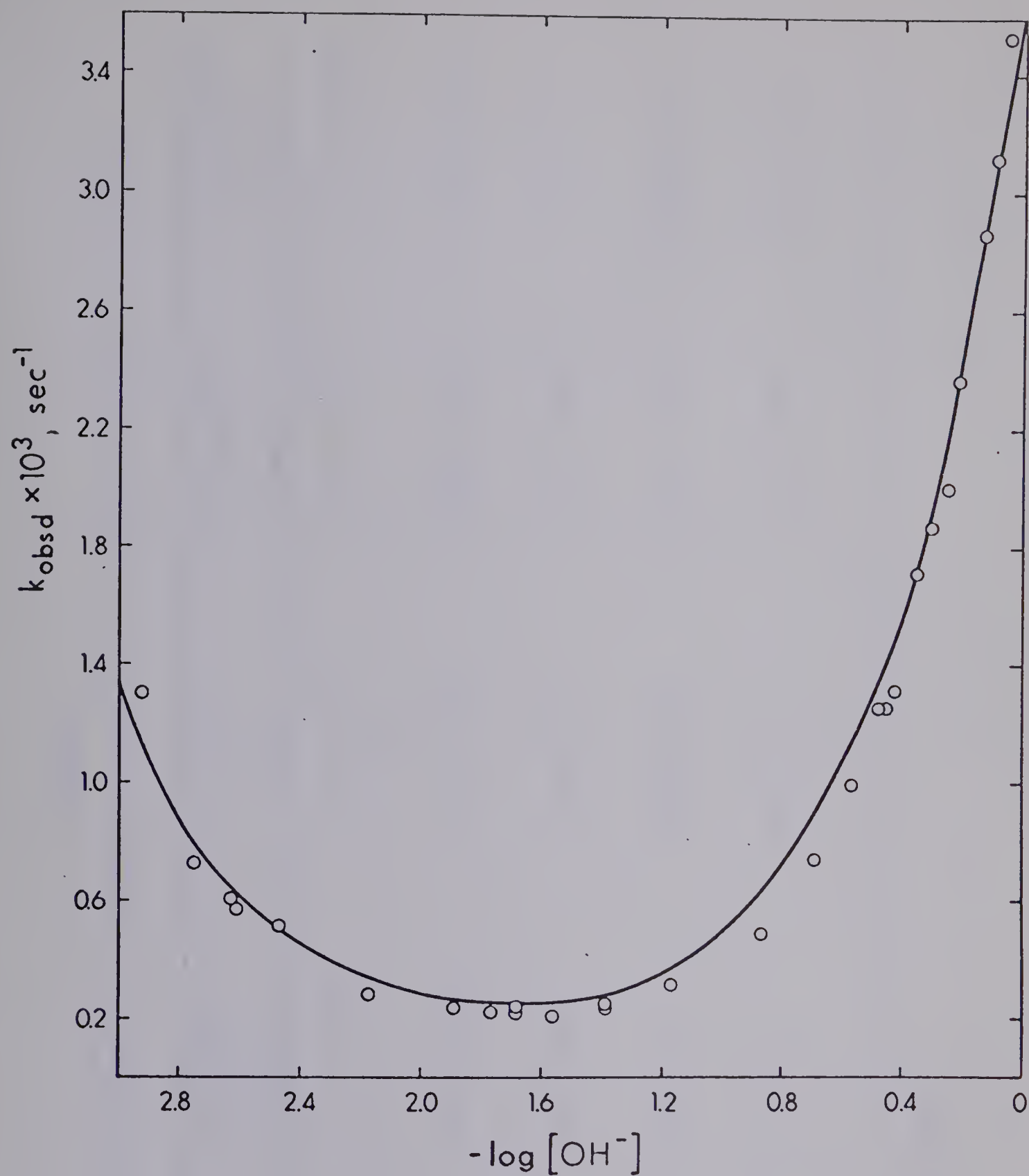


Figure 2.11: Variation of k_{obsd} with $-\log[\text{OH}^-]$ for $(\text{en})_2\text{CoCO}_3^+$ in NaOH at 26.0° . $\mu = 1.0$ (NaClO_4).

TABLE 2.6

Specific Rate Constants and Activation Parameters for the Base Hydrolysis of $(\text{en})_2\text{CoCO}_3^+$

Temp, °C	$k_1 \times 10^3$ $\text{M}^{-1} \text{sec}^{-1}$	$k_{-1} \times 10^5$ sec^{-1}	$k_2 [\text{H}_2\text{O}] \times 10^5$ sec^{-1}	$k_{-2}^{\text{K}} / K_3 \times 10^6$ M sec^{-1}
26.0	$3.17 \pm 0.140^{\text{a}}$	6.52 ± 1.08	5.40 ± 1.07	1.11 ± 0.085
34.0	8.69 ± 0.613	23.7 ± 3.65	13.4 ± 3.33	3.65 ± 0.601
44.0	27.4 ± 1.69	104 ± 24	43.1 ± 12.3	16.3 ± 1.93
ΔH^\ddagger , kcal mole $^{-1}$	22.0 ± 1.3	28.2 ± 4.5	21.4 ± 5.4	27.4 ± 2.2
ΔS^\ddagger , eu	$+3.6 \pm 4.3$	$+16.6 \pm 14.2$	-6.6 ± 12.3	$+10.6 \pm 5.5$

^a 95% confidence limits.

given in Table 2.6 are the 95% confidence limits for the parameters and the values of the activation parameters, ΔH^\ddagger and ΔS^\ddagger , which were determined in the standard way from plots of $\log k_r/T$ vs. $1/T$. Tables D.8, D.9, and D.10 in Appendix D give the observed and calculated values of k_{obsd} for each hydroxide ion concentration at 26.0, 34.0, and 44.0°, respectively.

Geometrical Products of the Base Hydrolysis of $(\text{en})_2\text{CoCO}_3^+$

The stereochemistry of the products of the base hydrolysis of $(\text{en})_2\text{CoCO}_3^+$, with respect to geometrical isomers, has been determined by treating the reaction solution with HClO_4 at 10°, thereby converting all the cobalt(III) complexes in solution to the corresponding diaquobis-(ethylenediamine)cobalt(III) complex. Since no isomerization occurs during the acid hydrolysis reaction,⁶⁴ any *cis*-diaquo isomer can only be derived from a *cis* species in the original reaction solution and any *trans* isomer must be derived from a *trans* species in the original reaction solution. From a comparison of the spectra of the *cis*- $(\text{en})_2\text{Co}(\text{OH}_2)_2^{3+}$ and *trans*- $(\text{en})_2\text{Co}(\text{OH}_2)_2^{3+}$ ions,⁵⁶ it is seen that the extinction coefficients of the resultant diaquo solution should decrease at 370, 480, 492, and 520 mμ, increase at 410 mμ, and remain constant at the isosbestic points of 380, 444, and 550 mμ, if any *trans* products are formed at any time during the total base hydrolysis of the $(\text{en})_2\text{CoCO}_3^+$ ion to the $(\text{en})_2\text{Co}(\text{OH})_2^+$ ion.

Table 2.7 shows the spectral characteristics of acidified base hydrolysis reaction solutions which were originally 0.477, 0.667, and

TABLE 2.7

Comparison of Molar Extinction Coefficients of
 $cis-(en)_2Co(OH_2)_2^{3+}$ and the Acidified Product of
 the Base Hydrolysis Reaction of $(en)_2CoCO_3^+$ at 44.0°

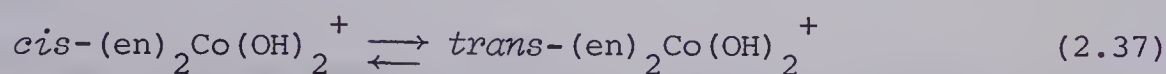
Wavelength, mμ	Extinction Coefficients			
	cis^a	I ^b	II ^b	III ^b
370	47.9	47.0	45.3	45.3
380	38.4	38.6	38.8	38.3
410	10.9	17.9	17.5	16.3
444	27.5	30.7	29.0	28.9
480	71.0	53.6	53.0	53.3
492	76.3	56.5	56.3	56.6
520	62.9	50.5	50.4	50.5
550	34.5	34.0	33.6	33.6

^a cis refers to $cis-(en)_2Co(OH_2)_2^{3+}$.

^b I, II, and III refer to reaction solutions initially 0.954, 0.667, and 0.477 M in NaOH, respectively.

^c Each initial reaction solution was kept at 44.0° for 600 sec.

0.954 M in NaOH and which had reacted at 44.0° for 600 sec. At 492 mμ, 35% *trans* base hydrolysis products are calculated based on *cis* and *trans* diaquo extinction coefficients of 77.3 and 19.2, respectively. Since, for a reaction time of 600 sec at 44.0° and 0.477, 0.667, and 0.954 M NaOH, reaction (2.9) will have occurred to some extent, three possible explanations for the *trans* product exist. There could be a direct production of *trans*-(en)₂CoOHCO₃ as in reaction (2.12) as suggested by Hargis,⁵⁵ there could be a direct production of *trans*-(en)₂Co(OH)₂⁺ from either *cis*-(en)₂CoOHCO₃ or *trans*-(en)₂CoOHCO₃, analogous to reaction (2.9), or the direct isomerization reaction



could occur. At 44°, at an ionic strength of approximately 0.1, the half time for reaction (2.37) is 4250 sec and is independent of hydroxide ion concentration.⁸¹ Thus the fact that 35% *trans* species was produced in 600 sec indicates that reaction (2.37) cannot be the only path for production of the *trans* species. The *cis* \rightleftharpoons *trans* isomerization reaction of the ring-opened species, *cis*-(en)₂CoOHCO₃, is very slow (t_{1/2} = 9 days) at pH 11.⁵¹ Even if the rate were first-order in [OH⁻], the rate at the [OH⁻] studied here would be much too slow to account for the production of the *trans*- species. The *cis/trans* ratios of the (en)₂CoOHCO₃H⁺ and (en)₂CoOH₂CO₃H²⁺ at equilibrium and room temperature are 17 and 3.5, respectively,⁵¹ so that no matter what the rate of the *cis* \rightleftharpoons *trans* isomerizations involving these species, the observed production of 35% *trans* species in the base

hydrolysis of $(en)_2CoCO_3^+$ at high $[OH^-]$ and 44° is not likely due to these isomerizations.

At 26.0° , the ring opening reaction, (2.5), at 0.40 and 1.00 M $[OH^-]$, is calculated to be 94% complete at 1992 and 884 sec, respectively. Using the spectral data reported in Tables 2.8 and 2.9 for the acidified reaction solutions at 26.0° , less than 9% *trans* product is produced, at 0.40 and 1.0 M NaOH in reaction times of 1453 and 690 sec, respectively, which correspond to slightly less than 94% completion for the reaction. Thus the base catalyzed ring-opening reaction goes mainly to the *cis*-(en) $_2$ CoOHCO $_3$ product as written in reaction (2.5).

The final aliquots sampled from the reaction solutions which were 0.40 M and 1.0 M in NaOH showed 28% (reaction time of 2.6×10^4 sec) and 24% (reaction time of 5.4×10^4 sec) *trans* product, respectively. The half-times of reaction (2.9), involving loss of coordinated carbonate, at 26.0° and 0.40 and 1.0 M NaOH are 3.8×10^4 and 1.49×10^4 sec, respectively, while the half-time for reaction (2.37) is 10×10^4 sec.⁷⁴ Thus, it is likely that in 0.40 and 1.0 M NaOH and at 26.0° , the *trans* product is being formed by reaction (2.37) as well as by an analagous reaction to (2.9), i.e.



Reaction (2.38) remains as the only probable explanation of the production of *trans* species in the study at 44.0° with a 600 sec reaction time.

TABLE 2.8

Comparison of Molar Extinction Coefficients of
 $cis-(en)_2Co(OH_2)_2^{3+}$ and the Acidified Product of the Base
 Hydrolysis Reaction of $(en)_2CoCO_3^+$ at 0.40 M NaOH and 26.0°

Wavelength, mμ	Extinction Coefficients					
	cis^a	I ^b	II ^b	III ^b	IV ^b	V ^b
370	59.1	59.0	58.0	59.3	57.6	57.0
380	46.5	46.7	45.7	47.0	45.6	46.6
410	16.3	17.9	18.8	18.5	19.2	23.5
444	33.7	34.7	34.1	34.8	34.7	36.1
480	75.2	73.5	71.2	71.1	68.8	60.7
492	80.7	77.6	75.0	75.2	72.3	63.4
520	63.7	61.5	60.1	61.1	58.3	52.8
550	33.9	33.9	33.9	33.9	33.9	33.9

^a cis refers to $cis-(en)_2Co(OH_2)_2^{3+}$.

^b I-V refer to the base hydrolysis reaction times 635, 1453, 2345, 3940, and 26100 sec, respectively.

TABLE 2.9

Comparison of Molar Extinction Coefficients of
 $cis-(en)_2Co(OH_2)_2^{3+}$ and the Acidified Product of the Base
 Hydrolysis Reaction of $(en)_2CoCO_3^+$ at 1.00 M NaOH and 26.0°

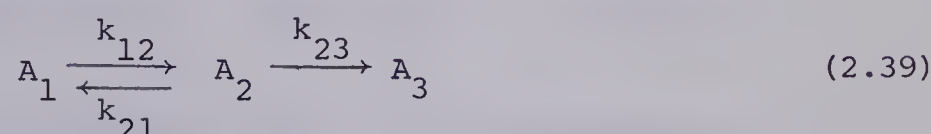
Wavelength, mμ	Extinction Coefficients						
	cis^a	I ^b	II ^b	III ^b	IV ^b	V ^b	VI ^b
370	57.8	59.8	60.2	59.2	58.8	58.5	58.0
380	46.6	48.7	48.2	47.2	47.5	47.3	46.9
410	15.9	16.2	15.3	15.8	16.6	17.3	22.0
444	30.5	31.0	30.2	31.9	31.6	31.7	32.6
480	70.4	70.8	71.4	69.9	68.4	66.6	58.4
492	77.3	76.4	78.4	75.2	73.4	71.6	61.8
520	64.0	61.5	66.3	63.9	62.9	61.4	52.6
550	35.5	35.5	35.5	35.5	35.5	35.5	35.5

^a cis refers to $cis-(en)_2Co(OH_2)_2^{3+}$.

^b I-VI refer to the base hydrolysis reaction times 190, 225, 485, 690, 4190, and 54000 sec, respectively.

Optical Isomerization

The method used to detect possible loss of optical activity in the base catalyzed ring-opening reaction consisted of opening the ring and then closing it by titrating with acid. A calculation⁸² of the relative amounts of $(en)_2CoCO_3^+$, $cis-(en)_2CoOHCO_3$, and $cis-(en)_2Co(OH)_2^+$ in solution after 1400 sec at 1.0 M NaOH using the specific rate constants reported previously shows that the complex will be 98% in the form $cis-(en)_2CoOHCO_3$, i.e. ring-opened. The calculation was done for the system



where A_1 , A_2 , and A_3 represent $(en)_2CoCO_3^+$, $cis-(en)_2CoOHCO_3$, and $cis-(en)_2Co(OH)_2^+$, respectively. The ring-opening reaction with water can be neglected at 1.0 M NaOH. The fraction of $cis-(en)_2CoOHCO_3$ as a function of time is given by

$$A_2 = -\frac{k_{12}e^{-\lambda_2 t}}{\lambda_2 - \lambda_3} + \frac{k_{12}e^{-\lambda_3 t}}{\lambda_2 - \lambda_3} \quad (2.40)$$

$$\text{where } \lambda_2 = \frac{1}{2} (p + q) \quad (2.41)$$

$$\lambda_3 = \frac{1}{2} (p - q) \quad (2.42)$$

$$p = k_{12} + k_{21} + k_{23} \quad (2.43)$$

$$q = (k_{12}^2 + k_{21}^2 + k_{23}^2 + 2k_{12}k_{21} - 2k_{12}k_{23} + 2k_{21}k_{23})^{\frac{1}{2}} \quad (2.44)$$

The values of k_{12} , k_{21} , and k_{23} used were 3.17×10^{-3} , 6.52×10^{-5} , and $4.65 \times 10^{-5} \text{ sec}^{-1}$, respectively. The ring-closing technique was checked experimentally by doing the experiment with racemic $[(\text{en})_2\text{CoCO}_3]\text{ClO}_4$ and comparing the final visible spectrum to that of known pure samples of $[(\text{en})_2\text{CoCO}_3]\text{ClO}_4$. The results are shown below

	$\lambda_{\text{max}}, \text{ m}\mu$	$\lambda'_{\text{max}}, \text{ m}\mu$	$\lambda_{\text{min}}, \text{ m}\mu$
I	516 (136.0)	363 (123.7)	324 (43.1)
II	518 (130.5)	366 (121.4)	329 (47.9)
III	518 (130.5)	364 (120.7)	325 (44.0)

where λ refers to the wavelength in $\text{m}\mu$, the bracketed values are the molar extinction coefficients and I, II, and III refer to the ring-opened then ring-closed racemic sample, pure $[(\text{en})_2\text{CoCO}_3]\text{ClO}_4$, and the 1- $[(\text{en})_2\text{CoCO}_3]\text{ClO}_4$ sample, respectively. All spectra were at ionic strength 1.0 (NaClO_4).

The O.R.D. spectrum of 1- $[(\text{en})_2\text{CoCO}_3]\text{ClO}_4$ was run in both water and 1.0 M NaClO_4 . The results are compared to the reported value^{64,83} below

Literature	Value ^{64,83}	This Study		
		H_2O	H_2O	1.0 M NaClO_4
$[\alpha]_{\text{D}}, ^\circ$	- 1250	- 1242	- 1237	- 1158
$[\alpha]_{\text{min}}, ^\circ$	-	- 1585	- 1575	- 1495

where D refers to the wavelength 589, $\text{m}\mu$, min refers to the peak minima in the O.R.D. spectrum, and $[\alpha]$ is defined by

$$[\alpha] = \frac{\alpha}{lb} \quad (2.45)$$

where α is the observed rotation of plane polarized light by the sample (in degrees), l is the cell length in decimeters and b is the concentration in gm/cc.

An experiment was performed in which all solutions were ice-cold and the titration with HClO_4 was started immediately after mixing in order to determine the amount of method induced racemization. Calculation of % retention, for the reaction in 1.0 M NaOH, was done by a comparison of $[\alpha]_{\text{min}}$ values to the previously measured value in 1.0 M NaClO_4 . The results of the retention experiment are given below.

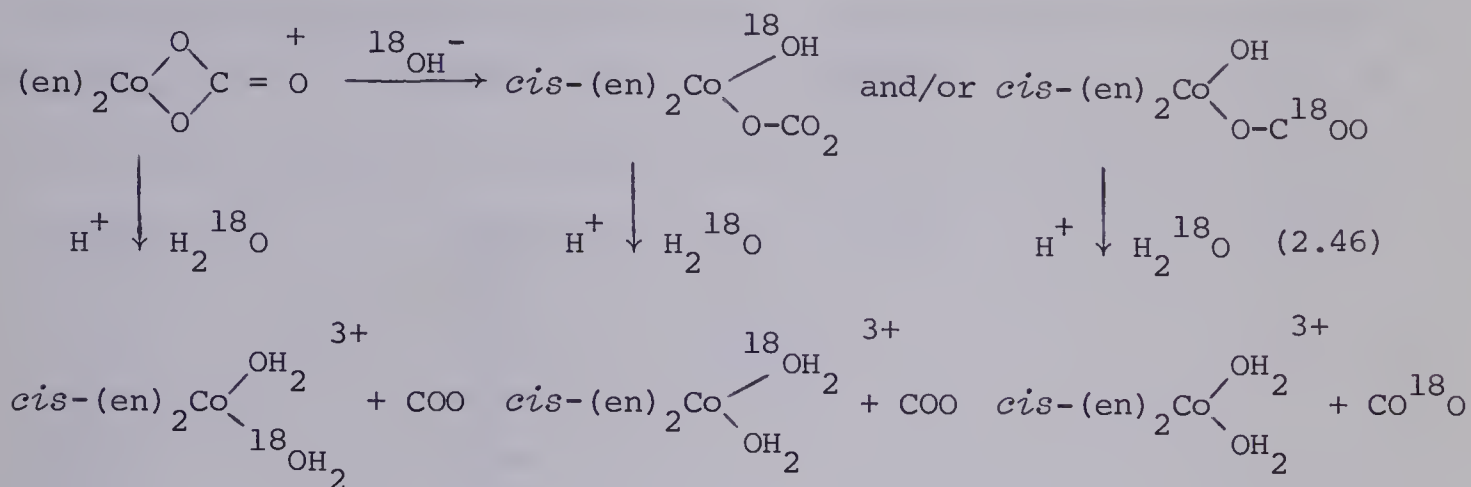
Reaction Time	$[\alpha]_{\text{min}}, ^\circ$	% retention
120 sec	- 1450	97.0
600 sec	- 1455	97.3
1420 sec	- 1450	97.0

The sample neutralized at 120 seconds indicates a method induced racemization of around 3%. Therefore the 600 and 1420 sec samples show that the ring-opening step (and thus the ring-closing step) goes with complete retention of optical activity.

Oxygen - 18 Tracer Study

The oxygen - 18 tracer study was carried out by acidifying the strongly alkaline reaction solution and collecting the carbon dioxide. Equation (2.46) shows the possible isotope distributions in the CO_2

product. A similar equation can be written for the reaction, (2.9), involving loss of coordinated carbonate.



It is known for the analagous tetraammine²¹ and pentaammine²⁰ species that acid hydrolysis goes without incorporation of solvent oxygen into the CO₂. Therefore ¹⁸O enrichment of the CO₂ would be consistent only with carbon-oxygen bond cleavage in the ring-opening step. At 26.0° and over a hydroxide ion concentration range of 0.50 to 1.00 M, no enrichment of CO₂ was observed. Table 2.10 shows the results of the three runs. The definition and measurement of R and R_∞ are described in detail in Chapter 4. If base catalyzed ring-opening occurs by C-O bond cleavage, values of R of 0.01677, 0.01812, and 0.02112 are predicted for the solutions which were 0.50, 0.957, and 0.993 M in NaOH, respectively. Therefore the base catalyzed ring-opening must occur by Co-O bond cleavage. The difference in R values for the reaction mixture and CO₂ of normal isotopic composition was found to be entirely due to dissolved carbonate in the concentrated sodium hydroxide solutions used for these experiments.

TABLE 2.10

Tracer Results on the Base Hydrolysis of $(en)_2CoCO_3^+$ at 26°

Time, min	$R^a \times 10^3$	$R_\infty^b \times 10^3$	$[OH^-], M$
5.5	5.68	29.7	0.50
27.5	6.50		
59.0	5.95		
215.5	6.69		
1043.5	6.62		
1127.0	6.31		
2495.0	5.62		
7.8	7.36	32.4	0.957
36.8	7.67		
72.3	8.05		
113.8	8.23		
161.8	8.47		
405.5	9.37		
1542.0	8.63		
1.7	6.90	38.4	0.993
18.7	6.96		
45.7	7.17		
170.7	7.11		
983.0	7.36		
2490.0	7.44		

^a R is the intensity ratio of mass 46 to mass 44 peaks in the mass spectrum of CO_2 . R of CO_2 of normal isotopic composition was found to be 0.00384.

^b R_∞ is the $^{18}O/^{16}O$ ratio of the NaOH used.

Since the reaction times of these experiments were sufficient for reaction (2.9) to occur, the results in Table 2.10 also show that the reaction involving loss of coordinated carbonate from the ring-opened species also involves Co-O bond cleavage.

Base Hydrolysis of Carbonatobis(o-phenanthroline)cobalt(III) Ion

The behavior of the $(\text{phen})_2\text{CoCO}_3^+$ ion in a solution of sodium hydroxide proved to be quite complicated. Figure 2.12 shows the results of a kinetic run in which the entire spectrum was scanned at various periods of time throughout the reaction. Only absorbance changes at one wavelength are shown. The $\log(A_t - A_\infty)$ vs. time plot, (A) is obviously curved. In fact the reaction appears to speed up with time. The stock solution of $(\text{phen})_2\text{CoCO}_3^+$ used in this run, (A) was approximately 30 minutes old. Figure 2.12 also shows the kinetic plot, (B), of a run using the same stock solution approximately 46 hours later. As the age of the stock solution increases, the spectral change occurs faster. The reaction velocity increases as the age of the stock solution increases. In Table 2.11, the spectra of the initial and final species in the reaction solution are compared to known spectra of the $(\text{phen})_2\text{CoCO}_3^+$ and *cis*-($\text{phen})_2\text{Co}(\text{OH})_2^+$ ions which are given in Chapter 3, Figure 3.1. λ_{max} and λ_{min} refer to the wavelength of the peak maxima and minima, respectively. ϵ_{max} and ϵ_{min} refer to the molar extinction coefficients of the peak maxima and minima, respectively. The comparison shows the initial and final species in the reaction solution to be the $(\text{phen})_2\text{CoCO}_3^+$ and *cis*-($\text{phen})_2\text{Co}(\text{OH})_2^+$ ions,

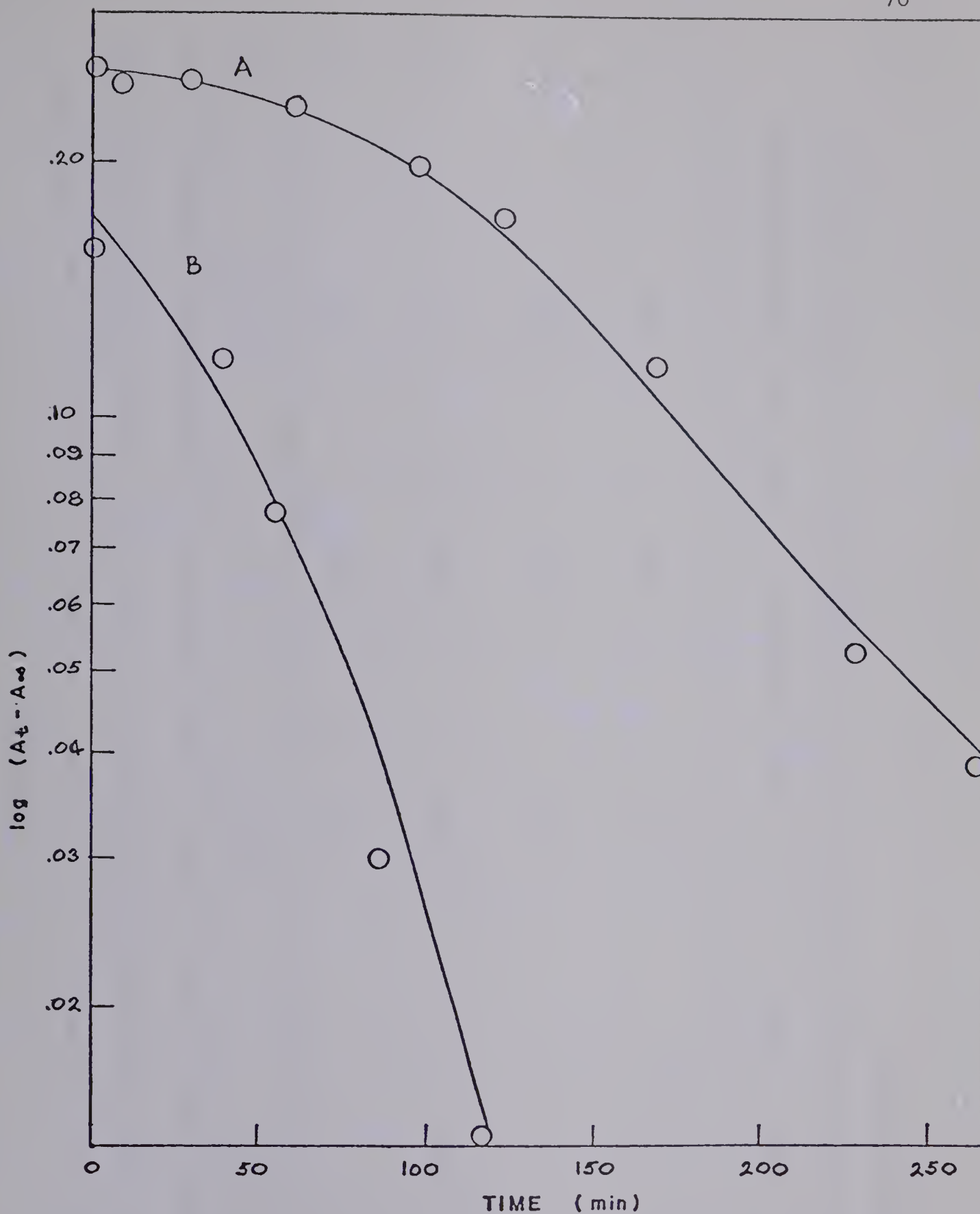


Figure 2.12: Variation of Absorbance with Time of Solutions of

$(\text{phen})_2\text{CoCO}_3^+$ in Aqueous Sodium Hydroxide.

$[\text{OH}^-] = 0.867$, $\mu = 1.0$ (NaCl), $T = 25^\circ$, $[\text{complex}] = 1.387 \times 10^{-3}$ M.

A - stock solution aged 30 min, $\lambda = 505$ m μ .

B - stock solution aged 46 hours, $\lambda = 512$ m μ .

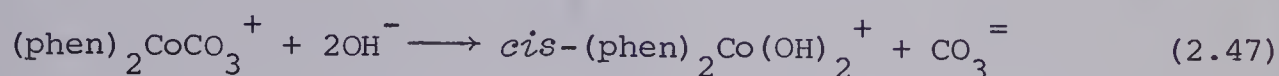
TABLE 2.11

Comparison of Spectral Characteristics of a Solution of $(\text{phen})_2\text{CoCO}_3^+$ Ion in Aqueous Sodium Hydroxide at Zero and Infinite Times with Spectral Characteristics of $(\text{phen})_2\text{CoCO}_3^+$ Ion and *cis*-(phen) $_2\text{Co}(\text{OH})_2^+$ Ion

Origin of Solution	$\lambda_{\text{max}}, \text{m}\mu$	ϵ_{max}	$\lambda_{\text{min}}, \text{m}\mu$	ϵ_{min}
E ^a 1.5 minutes	510	105.5	438	20.2
(phen) ₂ CoCO ₃ ⁺ , 1.0 M NaCl	509	109.1	437	24.6
E 18 hours	511	79.2	448	42.0
cis-(phen) ₂ Co(OH) ₂ ⁺ , 1.0 M NaOH	512	79.5	448	41.4

^a Solution E; $[\text{OH}^-] = 0.867 \text{ M}$, $\mu = 1.0 \text{ M (NaCl)}$, $[\text{complex}] = 1.508 \times 10^{-3} \text{ M}$, observed spectral changes with time in region 400-600 m μ , stock solution was 3 min old, no spectral change at all during first 40 min.

respectively. In all the runs, isosbestic behavior was observed for at least 70 percent reaction. The wavelength of the isosbestic points varied between 552 and 538 mμ for the high wavelength isosbestic point and between 478 and 454 mμ for the low wavelength isosbestic point. The predicted isosbestic points, from Chapter 3, Figure 3.1, for a direct reaction,



are 546 mμ and 460 mμ. Therefore it appears that the *cis*-(phen)₂Co(OH)₂⁺ ion is the only product of the hydrolysis of (phen)₂CoCO₃⁺ in aqueous NaOH.

The obvious explanation of the increase of reaction rate with time is catalysis of the reaction. The most probable catalyst is the product itself. It was thought that the more rapid reaction of solutions made from old stock solutions could then be explained by some slight hydrolysis in near neutral solutions. The resultant diaquo complex would be converted to the dihydroxy complex in basic solutions and thus be available for catalysis. This hypothesis was tested by adding solid [*cis*-(phen)₂Co(OH₂)₂]Cl₃·2H₂O to a solution made by dissolving solid [(phen)₂CoCO₃]Cl·3H₂O in a solution of NaOH and NaCl. Curve F in Figure 2.13 is nearly identical to curve A in Figure 2.12. As in all the kinetic runs using fresh (< 5 min old) stock solution, very little spectral change occurred during the first 40 minutes of reaction. The product, *cis*-(phen)₂Co(OH)₂⁺ is obviously not the cause of the reaction rate increase.

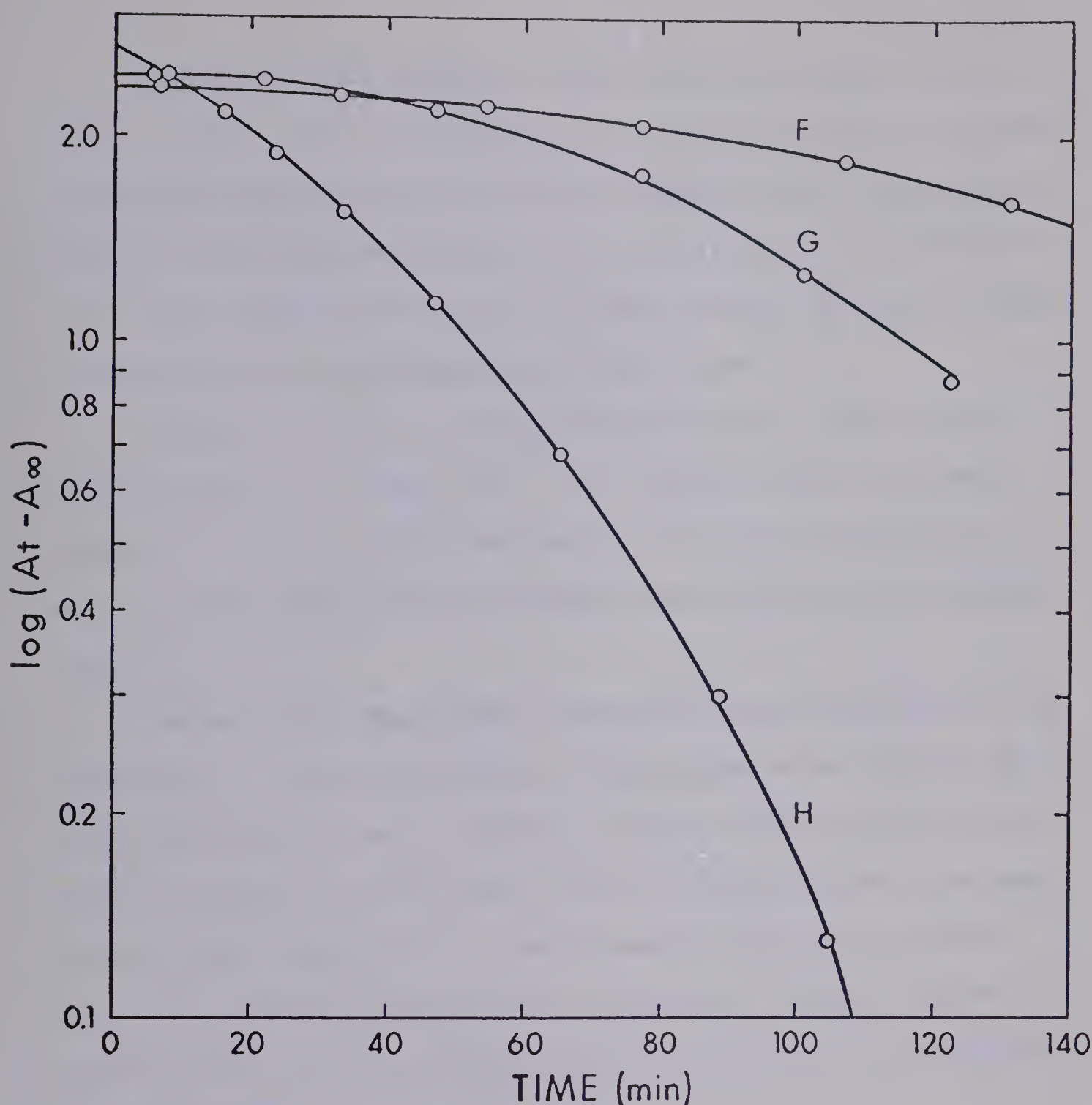


Figure 2.13: Variation of Absorbance with Time of Solutions of

$(\text{phen})_2\text{CoCO}_3^+$ in NaOH. $[\text{OH}^-] = 0.867$, $T = 25.0^\circ$,

$\lambda = 512 \text{ m}\mu$.

F; $[(\text{phen})_2\text{CoCO}_3^+] = 1.400 \times 10^{-3} \text{ M}$, $[\text{cis}-(\text{phen})_2\text{Co}(\text{OH})_2^+] = 2.0 \times 10^{-4} \text{ M}$,
test for product catalysis.

G; $[(\text{phen})_2\text{CoCO}_3^+] = 1.508 \times 10^{-3} \text{ M}$, test for chloride ion catalysis.

H; $[(\text{phen})_2\text{CoCO}_3^+] = 1.496 \times 10^{-3} \text{ M}$, $[\text{cis}-(\text{phen})_2\text{Co}(\text{OH})_2^{2+}] = 9.98 \times 10^{-6} \text{ M}$,
test for Co(II) catalysis.

Another possible catalyst is the chloride ion used to control the ionic strength. Curve G in Figure 2.13 is calculated from the spectral change with time in a solution made by dissolving solid $[(\text{phen})_2\text{CoCO}_3]\text{Cl}\cdot 3\text{H}_2\text{O}$ in aqueous sodium hydroxide with no NaCl added. The catalysis still occurs indicating that the Cl^- used to control the ionic strength is not the cause of the increase in reaction rate.

Figure 2.14 shows the complete absorbance vs. time scans used to calculate curve G in Figure 2.13. The isosbestic points and general behavior of the variation of absorbance with time are representative of most of the runs performed including those with other added complex ions.

Decomposition of reactants and products during the reaction was indicated by a thin brown film on the spectrophotometer cell and by a very small amount of brown colloidal material which could be filtered from the reaction solution with a 0.45 μm Millipore filter. The brown material, which was probably a form of cobalt oxide, did not affect the visible spectrum of the reaction solution so that the increase in reaction rate could not be due to any light scattering by the particles of cobalt oxide.

If the cobalt oxide decomposition product is formed by some type of redox reaction, the possibility of catalysis by a Co(II) species exists. Curve H in Figure 2.13 shows the effect on the reaction rate caused by adding a very small amount of a dilute solution of a Co(II) ion, $[\text{cis}-(\text{phen})_2\text{Co}(\text{OH}_2)_2]\text{Cl}_2$, resulting in a final cobalt(II) concentration of 9.98×10^{-6} M, to the reaction mixture. The amount

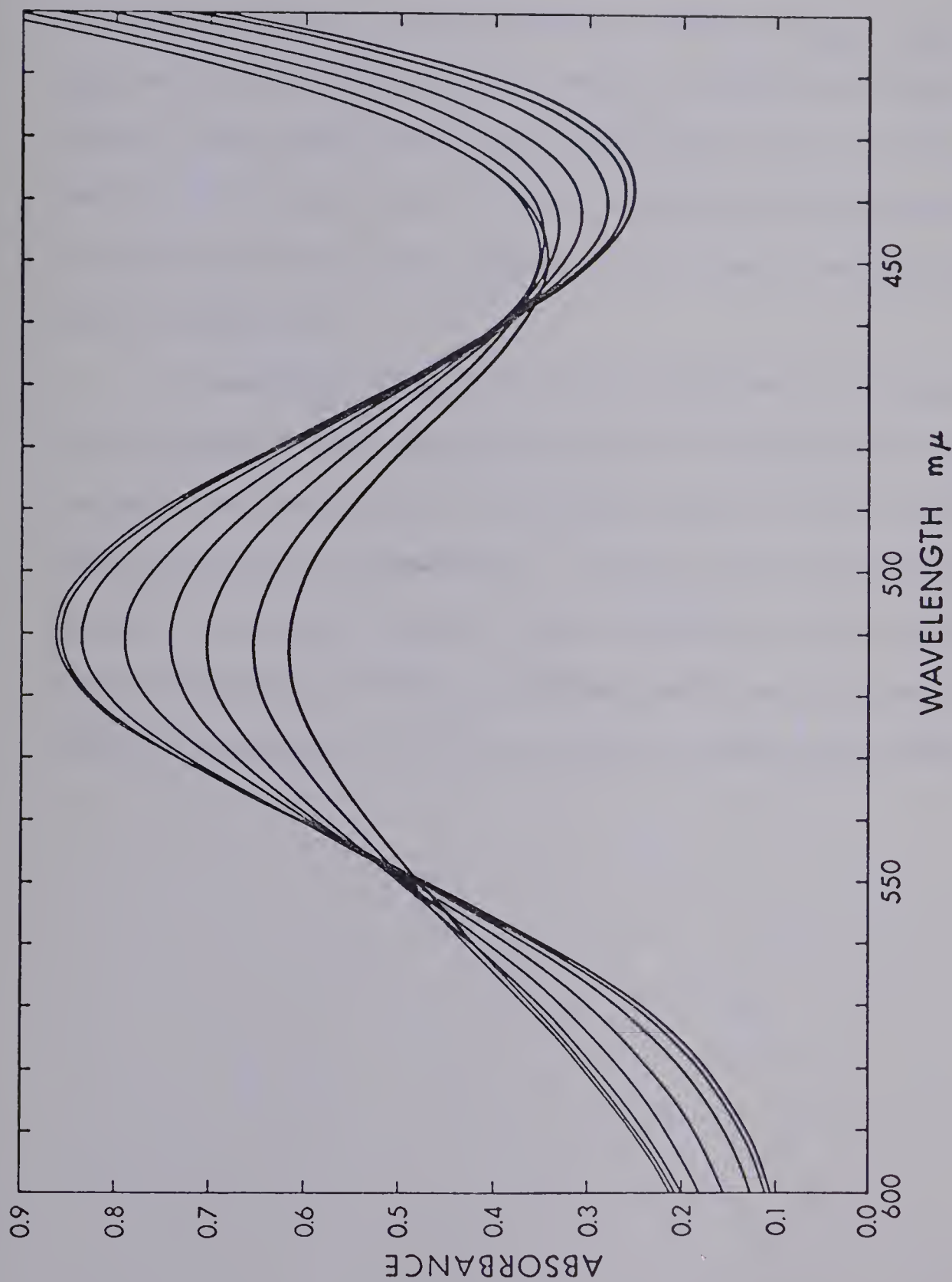


Figure 2.14: Variation of Absorption Spectrum of $(\text{phen})_2\text{CoCO}_3^+$ in Aqueous Sodium Hydroxide.
 $[\text{OH}^-] = 0.867 \text{ M}$, $[\text{complex}] = 1.508 \times 10^{-3} \text{ M}$, 5 cm cell, $T = 25.0^\circ \text{ C}$.

of cobalt(II) complex added was not enough to cause any change in the zero time spectrum yet it caused immediate initiation of the hydrolysis reaction. At zero time the values of λ_{\max} , ϵ_{\max} , λ_{\min} , and ϵ_{\min} were 510 m μ , 112.5, 438 m μ , and 27.6, respectively while the infinite time values were 513 m μ , 76.4, 448 m μ and 37.5, respectively. Comparison of these values to those in Table 2.11 shows that the initial reactant and final product are not changed by adding the Co(II) complex ion.

In summation, this study of the hydrolysis of the $(\text{phen})_2\text{CoCO}_3^+$ ion in aqueous sodium hydroxide allows the conclusion that the initial reactant goes completely to $\text{cis}-(\text{phen})_2\text{Co}(\text{OH})_2^+$ with no long-lived, high concentration intermediates. One can also conclude that the increase in reaction rate with time is caused by a Co(II) complex, specifically the $\text{cis}-(\text{phen})_2\text{Co}(\text{OH})_2$ molecule, and is caused by neither the chloride ion nor the reaction product, $\text{cis}-(\text{phen})_2\text{Co}(\text{OH})_2^+$.

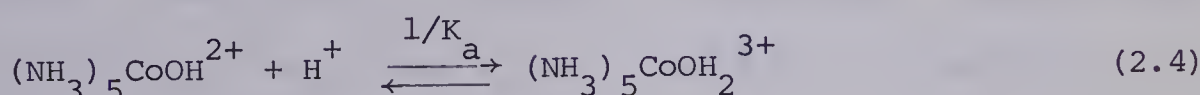
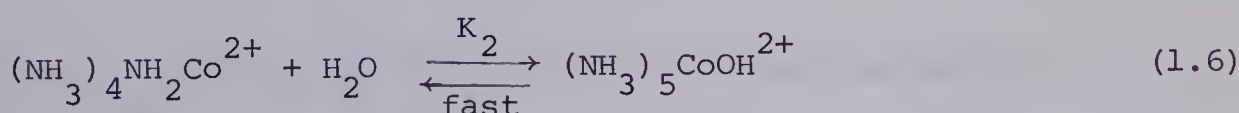
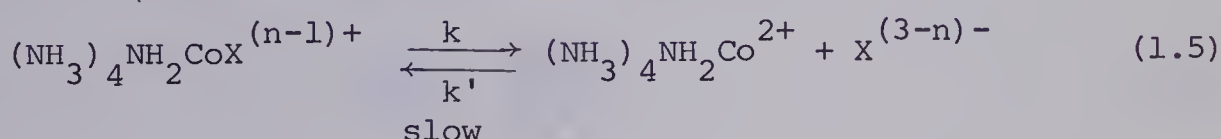
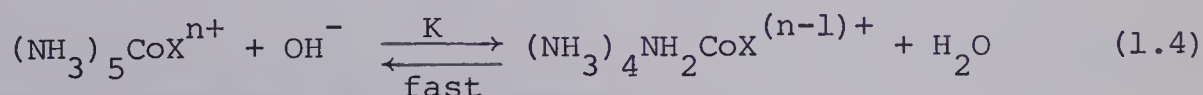
Discussion

The study of the base hydrolysis reaction of the $(\text{NH}_3)_5\text{CoCO}_3^+$ resulted in a value for the acid hydrolysis rate constant of the $(\text{NH}_3)_5\text{CoCO}_3\text{H}^{2+}$ ion, k_1 , of $2.375 \times 10^{-2} \text{ sec}^{-1}$ (25° , $\mu = 1.0$, NaClO_4) and a value for the acid dissociation constant of the $(\text{NH}_3)_5\text{CoCO}_3\text{H}^{2+}$ ion, K_1 of $6.130 \times 10^{-9} \text{ M}$ ($\mu = 1.0$, NaClO_4). Since both of the values of the constants reported here have large 95% confidence limits, they are consistent with the previously reported values for k_1 of 1.25 sec^{-1} ⁵⁰ and for K_1 of $4.0 \times 10^{-7} \text{ M}$ ^{46,50} and $3.8 \times 10^{-9} \text{ M}$ ⁴⁸. As has been mentioned previously, the values⁵⁰ for k_1 and K_1 of 1.25 sec^{-1} and $4 \times 10^{-7} \text{ M}$, respectively, are believed to be the most accurate. While the value of the intercept of Figure 2.4, K_1^{-1} , and hence the separated values of k_1 and K_1 , are not precise, the value of the slope, k_1/K_1 , is precise. Thus the value for k_1/K_1 of $3.88 \pm 0.43 \times 10^6 \text{ M}^{-1} \text{ sec}^{-1}$ compares well with Harris'⁵⁰ reported value of $3.13 \times 10^6 \text{ M}^{-1} \text{ sec}^{-1}$. Since Harris has shown that K_1 has a small temperature variability in the range $15\text{--}25^\circ$ ⁵⁰, the good agreement between the activation enthalpy for k_1/K_1 ($\Delta H^\ddagger = 17.6 \text{ kcal mole}^{-1}$) determined in this study and the activation enthalpy for k_1 ($\Delta H^\ddagger = 17.0 \text{ kcal mole}^{-1}$) determined by Harris⁵⁰ is expected. The large positive value of ΔS^\ddagger (+ 30.4 eu) for k_1/K_1 must be largely due to K_1 since for k_1 , as ΔS^\ddagger of -0.6 eu is found.⁵⁰ Thus the entropy change largely governs the value of K_1 .

Since the acid hydrolysis of $(\text{NH}_3)_5\text{CoCO}_3^+$ occurs via carbon-oxygen bond cleavage²⁰ with a ΔH^\ddagger of $17.0 \text{ kcal mole}^{-1}$, the activation

enthalpy of 30.8 kcal mole⁻¹ for the base hydrolysis of $(\text{NH}_3)_5\text{CoCO}_3^+$ indicates that reaction (2.1) occurs via cobalt-oxygen bond cleavage. Therefore the kinetic (k_2) and stability (K_f) constants measured here can be placed on a LFER plot of the logarithm of the specific rate constants of the base hydrolysis (via Co-X bond cleavage) vs. the negative logarithm of the stability constant (Q) of $(\text{NH}_3)_5\text{CoX}^{n+}$ complexes.

Referring to reactions (1.4), (1.5), (1.6), and (2.4)



the formation constant for the $(\text{NH}_3)_5\text{CoX}^{n+}$ ion can be defined as

$$Q = \frac{[(\text{NH}_3)_5\text{CoX}^{n+}]}{[(\text{NH}_3)_5\text{CoOH}_2^{3+}][\text{X}^{(3-n)-}]} \quad (2.48)$$

and written as

$$Q = \frac{k'K_a}{kK_2K_w} \quad (2.49)$$

Rearranging and taking the logarithm results in

$$\log kK = \log \frac{k'K_a}{K_2K_w} - \log Q \quad (2.50)$$

Since kK is the measured rate constant, k_2 , a plot of $\log k_2$ vs. $-\log Q$ should result in a straight line if the term $\log(k'K_a/K_2K_w)$ is independent of the nature of X .

For the $(\text{NH}_3)_5\text{CoCO}_3^+$ complex, Q is defined as

$$Q = \frac{[(\text{NH}_3)_5\text{CoCO}_3^+]}{[(\text{NH}_3)_5\text{CoOH}_2^{3+}][\text{CO}_3^{=}]}. \quad (2.51)$$

The formation constant, K_f , is related to Q by

$$Q = \frac{K_f K_1 K_a}{K_{c2} K_w} \quad (2.52)$$

where K_1 , K_a , and K_{c2} are the acid dissociation constants of $(\text{NH}_3)_5\text{CoCO}_3\text{H}^{2+}$, $(\text{NH}_3)_5\text{CoOH}_2^{3+}$, and HCO_3^- , respectively. Using values of K_1 ,⁵⁰ K_a ,⁸⁴ K_{c2} ,⁴⁹ K_w ,⁷⁰ and K_f of 3.28×10^{-7} M, 2.51×10^{-7} M, 2.75×10^{-10} M, 1.7×10^{-14} , and 5.41×10^{-6} , respectively, at 25° and $\mu = 1.0$ (NaClO_4), the calculated value of Q is $9.52 \times 10^4 \text{ M}^{-1}$. A value for the k_2 of $2.95 \times 10^{-6} \text{ M}^{-1} \text{ sec}^{-1}$ at 25° is obtained by extrapolation of a $\log(k_2/T)$ vs. $1/T$ plot. Figure 2.15 shows a LFER plot of $\log k_2$ vs. $-\log Q$ for the base hydrolysis of $(\text{NH}_3)_5\text{CoX}^{n+}$ ions. The slope of 1.0 in Figure 2.15 indicates¹⁸ that the role of the $X^{(3-n)-}$ group in the transition state of the base hydrolysis of $(\text{NH}_3)_5\text{CoX}^{n+}$ ions is similar to its role in the product, i.e. a solvated ion. Thus the data reported in Figure 2.15 is consistent with the $S_N1\text{CB}$

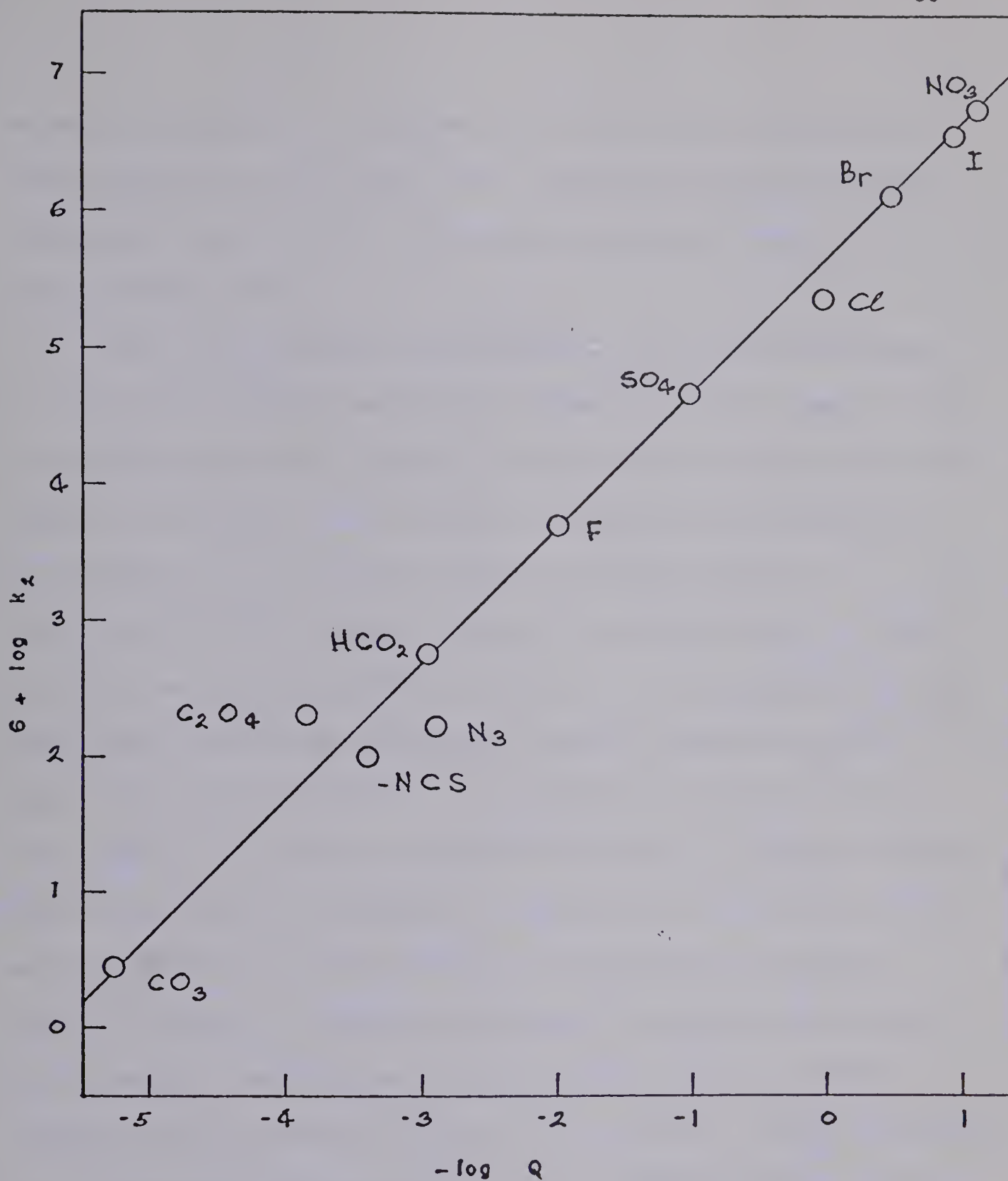


Figure 2.15: Plot of Log (specific rate constant) vs. Log (equilibrium constant) for the Base Hydrolysis of $(\text{NH}_3)_5\text{CoX}^{n+}$ Ions at 25° . Data taken mainly from Table IV, reference (85).

mechanism postulated in reactions (1.4), (1.5), and (1.6) for the base hydrolysis of $(\text{NH}_3)_5\text{CoX}^{n+}$ ions. Figure 2.15 does not provide information about the role of the entering groups, OH^- or H_2O , in the transition state.

Haim¹⁹ has suggested that LFER plots for the acid hydrolysis of $(\text{NH}_3)_5\text{CoX}^{n+}$ complexes will give a number of parallel lines of slope 1.0 but with increasing intercept, as the negative charge on the free ligand, X, increases. This increase in intercept was attributed to an increase in Q_o , an ion-pair formation constant for the $(\text{NH}_3)_5\text{CoOH}_2^{3+} \cdot \text{X}^{(3-n)-}$ ion pair, which is contained in the intercept portion of an equation similar to (2.50). Haim has assumed that the rate controlling step in the anation reaction forming $(\text{NH}_3)_5\text{CoX}^{n+}$ from $(\text{NH}_3)_5\text{CoOH}_2^{3+}$ and $\text{X}^{(3-n)-}$ is preceded by a reaction forming the ion-pair. For the base hydrolysis reactions, an ion-pair formation would occur prior to the reverse of reaction (1.5). The fact that no parallel, higher intercept LFER line is observed for divalent X ligands in Figure 2.15 may be explained by the absence of any ion-pair formation. However, even if an ion-pair did form preceding reaction (1.5), the expected increase in the ion-pair formation constant, Q_o , in going from $(\text{NH}_3)_4\text{NH}_2\text{Co}^{2+} \cdot \text{X}^-$ (2:2) to $(\text{NH}_3)_4\text{NH}_2\text{Co}^{2+} \cdot \text{X}^{2-}$ (2:1) is only 7 while the increase, for the acid hydrolysis Q_o , in going from $(\text{NH}_3)_5\text{CoOH}_2^{3+} \cdot \text{X}^-$ (3:2) to $(\text{NH}_3)_5\text{CoOH}_2^{3+} \cdot \text{X}^{2-}$ (3:1) is 20.¹⁰⁶ Thus, the small change in Q_o for the base hydrolysis reaction may not cause a detectable change in the intercept of the LFER plot.

The values of the specific rate constants and the equilibrium

constants, at 26° and ionic strength of 1.0 (NaClO₄), for the base hydrolysis of the (en)₂CoCO₃⁺ ion are compared to previously reported values in Table 2.12. The values of k_1 , k_{-1} , $k_2[\text{H}_2\text{O}]$, k_{-2} , K_1 and k_3 compare quite well considering the very limited pH range and low ionic strength of the study reported in reference (51). As will be discussed in Chapter 3, the acid hydrolysis of (en)₂CoCO₃⁺ in the pH range 1-5 yields a value for $k_2[\text{H}_2\text{O}]$ (called k_o in Chapter 3) of $1.2 \times 10^{-4} \text{ sec}^{-1}$ at 25° and 0.5 ionic strength (NaClO₄)⁸⁶ with activation parameters of $18 \pm 3 \text{ kcal mole}^{-1}$ (ΔH^\ddagger) and $-15 \pm 9 \text{ eu}$ (ΔS^\ddagger). These are in fair agreement with the values for $k_2[\text{H}_2\text{O}]$, ΔH^\ddagger , and ΔS^\ddagger of $4.9 \times 10^{-5} \text{ sec}^{-1}$, $21.4 \pm 5.4 \text{ kcal mole}^{-1}$ and $-6.6 \pm 12.3 \text{ eu}$, respectively, which are reported here. Thus kinetically, the values for the rate parameters of reactions (2.5), (2.6), and (2.9) seem to be fairly well substantiated as does the existence of equilibrium systems for reactions (2.5) and (2.6) in the pH range, 11-14.

Since the base hydrolysis of (NH₃)₅CoCO₃⁺ seems to go via the same mechanism as that of other (NH₃)₅CoXⁿ⁺ complexes, as indicated by the LFER plot, it would seem reasonable to expect reaction (2.9), the base hydrolysis of *cis*-(en)₂CoOHCO₃, to go via the same mechanism as the base hydrolysis of other *cis*-(en)₂CoOHXⁿ⁺ complexes. When $X = \text{Cl}^-$ or Br^- , the product of the base hydrolysis is 97% *cis*-(en)₂Co(OH)₂⁺. The constant amount of *cis* product is taken to be indicative of formation of a 5 coordinate intermediate which is independent of its source.³³ The production of some *trans*-(en)₂Co(OH)₂⁺ (approximately 35%) in the base hydrolysis of *cis*-(en)₂CoOHCO₃ is in

TABLE 2.12

Comparison of Kinetic Parameters for the Base Hydrolysis of $(en)_2CoCO_3^+$

T, °	$k_1 \times 10^3$, $M^{-1} \text{ sec}^{-1}$	$k_{-1} \times 10^5$, $k_2 [H_2O] \times 10^5$, $k_{-2} \times 10^2$, sec^{-1}	K_1 , M^{-1}	$k_3 \times 10^5$, $M^{-1} \text{ sec}^{-1}$	μ	reference		
26	3.17	6.52	5.40	11.6 ^a	48.54	4.65	1.0 (NaClO ₄)	this study
R.T.	12.8	6.4	1.15 ^b	1.15	159	slow	<.1 (reactants)	(51)
24.8	2.18	-	-	-	-	4.56 ^c	varied	(40)
25	3.20	-	-	-	-	6.2	1.0 (NaClO ₄)	(55)

^a Calcd from equation (2.34), $K_3 = 1.78 \times 10^{-9}$, $K_w = 1.7 \times 10^{-14}$ 70

^b Calcd from $k_2 [H_2O] / k_{-2} = 1 \times 10^{-3}$ and $k_{-2} = 1.15 \times 10^{-2} \text{ sec}^{-1}$ 51

^c Calcd from $k_3 = 1.9 \times 10^{13} \exp(-24000/RT) \text{ M}^{-1} \text{ sec}^{-1}$ 40

direct contrast to the results for $X = \text{Cl}^-$ and Br^- . However, a careful study of the rate of *cis* \rightleftharpoons *trans* isomerizations of the ring-opened species, $(\text{en})_2\text{CoOHCO}_3$ and $(\text{en})_2\text{CoOHCO}_3\text{H}^+$, at different temperatures, pH's, and ionic strengths is necessary before any meaningful conclusions can be made about this production of *trans* species.

Figure 2.16 compares the data obtained from the base hydrolysis of $(\text{en})_2\text{CoCO}_3^+$ at 24.8° and high hydroxide ion concentration with no ionic strength control to similar data obtained by Farago.⁴⁰ Contrary to what is observed by Farago, no distinct leveling of the $k_{\text{obsd}}^{\text{N}}$ vs. $[\text{OH}^-]$ plot is observed but a curvature does exist. The complete rate expression for the $\text{S}_{\text{N}}1\text{CB}$ mechanism is

$$-\frac{d[\text{T}]}{dt} = \frac{kK[\text{OH}^-]}{1 + K[\text{OH}^-]} \cdot [\text{T}] \quad (2.53)$$

which can be derived from reactions (1.4), (1.5), and (1.6). Normally the assumption is made that $1 \gg K[\text{OH}^-]$. Farago has attributed the leveling off of the $k_{\text{obsd}}^{\text{N}}$ vs. $[\text{OH}^-]$ plot to a saturation of the conjugate base equilibrium, reaction (1.4). Assuming that 1 equals $K[\text{OH}^-]$ at 3.0 M NaOH, one calculates a value of K of 0.33. K is related to the acid dissociation constant, K_{a} , of the ammine to amido reaction by

$$K = K_{\text{a}}/K_{\text{w}} \quad (2.54)$$

Using K_{w}^{70} of 1.7×10^{-14} , a value for K_{a} of 5.67×10^{-15} M is calculated which is reasonable in view of the fact that the $\text{p}K_{\text{a}}$'s of cobalt(III)

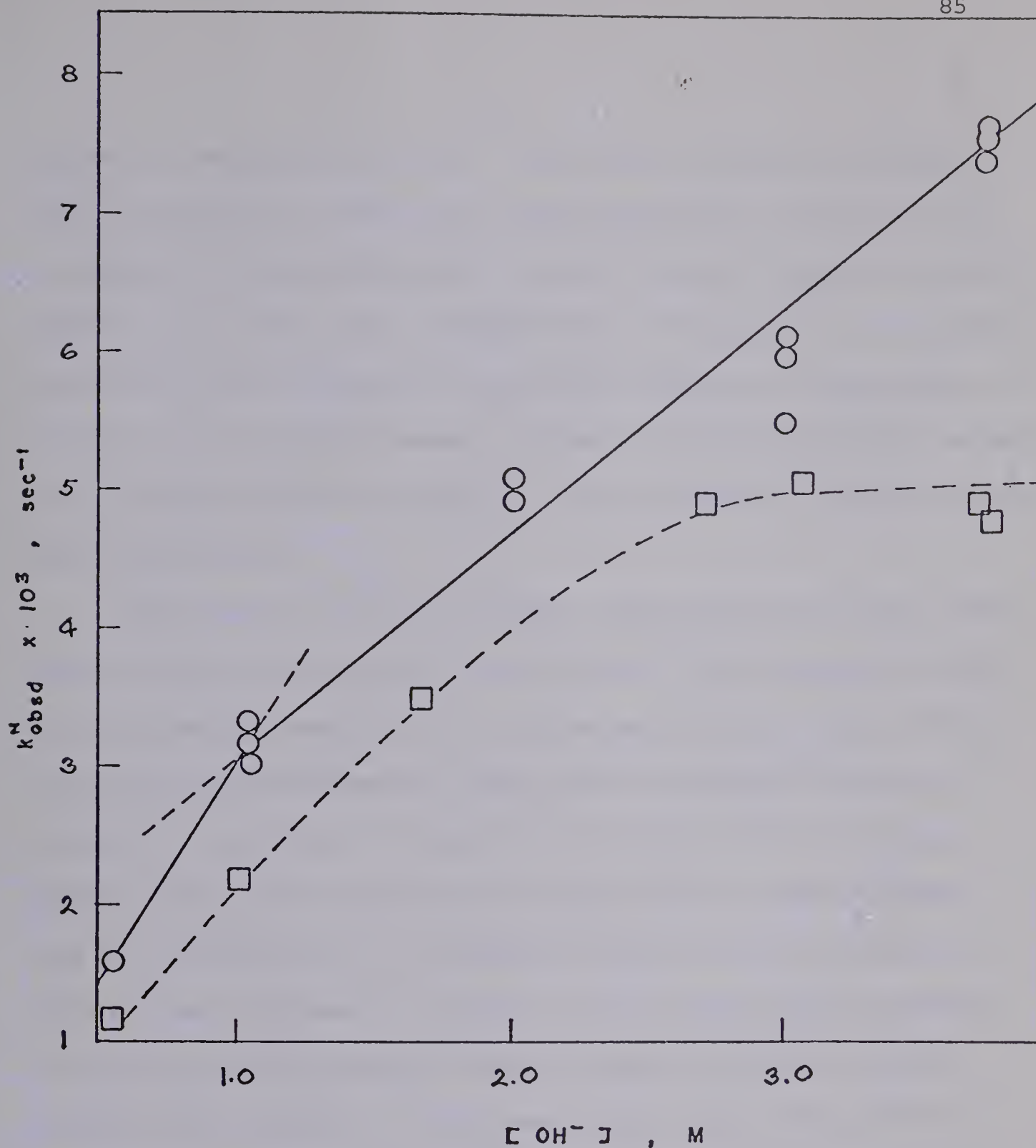


Figure 2.16: Plot of k_{obsd}^N vs. $[\text{OH}^-]$ at High Hydroxide Ion Concentration with No Ionic Strength Control at 24.5°. The results of this work (O) are compared to those of Farago⁴⁰ (□). k_{obsd}^N is defined by equations (2.25) and (2.26).

ammines are estimated to be >14 .⁸⁷ The curves in Figure 2.16 might also be explained by ion-pairing between hydroxide ion and $(\text{en})_2\text{CoCO}_3^+$ as suggested by Farago since the calculated ion-pair formation constant would be 0.33, which seems reasonable for a 1:1 system.⁸⁸ The curvature also could be due to a change in activity coefficient of the complex as the total ionic strength changes. Without a reliable independent measure of the ion-pair formation constant, it is not possible to decide between these alternatives.

The results of the bond cleavage experiments for the base catalyzed hydrolysis of $(\text{en})_2\text{CoCO}_3^+$ showed 100% Co-O bond cleavage for both the ring-opening, reaction (2.5), and carbonate loss, reaction (2.9), steps of the base hydrolysis. Both of the ring-opening reactions analagous to reactions (2.5) and (2.6), for the similar $(\text{en})_2\text{CoPO}_4$ complex proceed with 35% O-P bond cleavage while the base catalyzed loss of coordinated PO_4^{3-} , analagous to reaction (2.9), occurs with 100% Co-O bond cleavage.⁴² However, the ring-opening base catalyzed reaction for the $(\text{en})_2\text{CoC}_2\text{O}_4^+$ complex proceeds with 100% O-C bond cleavage while the loss of coordinated $\text{C}_2\text{O}_4^{2-}$ occurs with 100% Co-O bond cleavage.⁴¹ For the $[(\text{NH}_3)_4\text{CoCO}_3]\text{Br}$ complex, the X-ray crystal structure has shown the O-Co-O and O-C-O angles to be 70 and 110°, respectively,⁸⁹ as opposed to the normal values of 90 and 120°, respectively. Since the theoretical O-P-O angle in $(\text{en})_2\text{CoPO}_4$ would be expected to be near 109° (tetrahedral), less total ring strain could result in a stronger Co-O bond than for the $\text{N}_4\text{CoCO}_3^+$ complexes. Similarly the 5-membered oxalate ring would be expected

to be even less strained which could result in an even stronger Co-O bond. Thus, the observed increase of Co-O bond cleavage for the base catalyzed ring-opening reaction, in the series $(\text{en})_2\text{CoC}_2\text{O}_4^+ < (\text{en})_2\text{CoPO}_4 < (\text{en})_2\text{CoCO}_3^+$, could be explained on the basis of increasing ring strain. An increased susceptibility of the chelated ligand to nucleophilic attack by the hydroxide ion, in the order, $(\text{en})_2\text{CoC}_2\text{O}_4^+ > (\text{en})_2\text{CoPO}_4 > (\text{en})_2\text{CoCO}_3^+$, could also explain the observed shift in reaction path. A crystal structure on the $(\text{en})_2\text{CoPO}_4$ complex and more base hydrolysis and bond breaking studies on different cobalt(III) ammine complexes with chelated oxyanions are necessary before it will be possible to predict the reaction path of these base catalyzed ring-opening reactions.

Table 2.13 shows a comparison of the available rate data for the ring-opening and closing reactions of the oxalato-, carbonato-, and phosphato-bis(ethylenediamine)cobalt(III) complexes. In addition it has been observed that the base-catalyzed ring-opening reaction of the $(\text{en})_2\text{CoSO}_4^+$ ion is too fast to measure by conventional techniques.³⁷

It is generally observed that the ratio of the rate constants for hydroxide-catalyzed and uncatalyzed hydrolysis for cobalt(III) ammine complexes is of the order of 10^5 to 10^8 M^{-1} .⁹⁰ Since 65% Co-O bond cleavage occurs for both k_1 and $k_2[\text{H}_2\text{O}]$ in the $(\text{en})_2\text{CoPO}_4$ system, 65% of both k_1 and $k_2[\text{H}_2\text{O}]$ would be due to the "normally" observed path involving Co-X bond cleavage. Thus the ratio $k_1/k_2[\text{H}_2\text{O}]$ of $7 \times 10^4 \text{ M}^{-1}$ for $(\text{en})_2\text{CoPO}_4$ seems normal but the ratio for $(\text{en})_2\text{CoCO}_3^+$ is only 65 M^{-1} . Since the base catalyzed ring-opening step, reaction (2.5), has been shown to involve Co-O bond

TABLE 2.13

Comparison of Ring-Opening Kinetic Parameters for $(en)_2CoC_2O_4^+$, $(en)_2CoCO_3^+$, $(en)_2CoPO_4$, and $(en)_2CoSO_4^+$ at 22.5°

Complex	$k_1 \times 10^3$, $M^{-1} \text{ sec}^{-1}$	$k_{-1} \times 10^3$, sec^{-1}	$k_2 [H_2O] \times 10^3$, sec^{-1}	$k_{-2} \times 10^2$, sec^{-1}	K_1 , M^{-1}	ionic strength
$(en)_2CoC_2O_4^{+39}$	0.000568 ^a	-	-	-	-	<0.1
$(en)_2CoCO_3^+$	2.20 ^b	0.042 ^b	0.034 ^b	6.74 ^c	52.8 ^b	1.0 (NaClO ₄)
$(en)_2CoPO_4^{38}$	1750.0	2.48 ^d	0.025	0.83	707 ^c	1.0 (NaClO ₄)
$(en)_2CoSO_4^{+37}$	-	-	0.081 ^e	-	-	0.02 (KNO ₃)

^a Calcd from $k_{ox} = 9 \times 10^{19} \exp(-34000/RT)$ at 22.5°.³⁹

^b Calcd from activation parameters given in Tables 2.5 and 2.6.

^c Calcd from equation (2.34), $K_3 = 1.78 \times 10^{-9}$ ⁵¹ and $K_w = 1.7 \times 10^{-14}$ ⁷⁰.

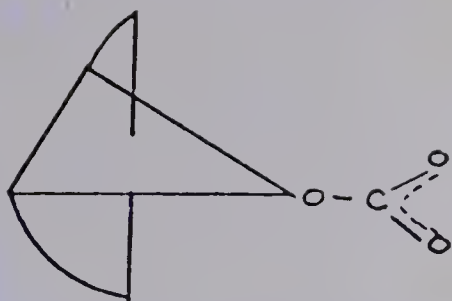
^d Calcd from equation (2.34).

^e Calcd at 22.5°, from $\Delta H^\ddagger = 19.6 \text{ kcal mole}^{-1}$ and $\Delta S^\ddagger = 10.0 \text{ eu}$.³⁷

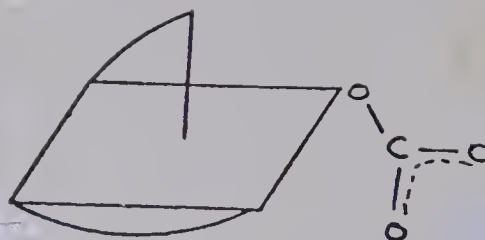
cleavage, this low $k_1/k_2[\text{H}_2\text{O}]$ ratio suggests a change in mechanism for the uncatalyzed ring-opening, reaction (2.6). Thus, it seems possible that the $k_2[\text{H}_2\text{O}]$ path occurs via C-O bond cleavage.

It is also interesting to compare the rate constants for the ring closing reaction (k_{-1}) in Table 2.13 for the phosphato and carbonato complexes. If one assumes a S_N1 mechanism for the ring-opening reaction (k_1), the principle of microscopic reversibility requires a S_N1 mechanism for the reverse reaction (k_{-1}). Thus the rate of the reverse reaction would be controlled by the rate of hydroxide ion exchange between the solvent and the ring-opened complex. The fact that k_{-1} for *cis*-(en) $_2\text{CoOHPO}_4^-$ is 59 times faster than for *cis*-(en) $_2\text{CoOHCO}_3$ is consistent with an I_d or D mechanism since the loss of the negative OH^- is expected to be easier from a negative than from a neutral species. However, the same reasoning would hold for an I_a mechanism involving simultaneous bond making and breaking so that the mechanism of the base catalyzed ring-opening and ring-closing reactions is still in question.

The base catalyzed ring-opening and ring-closing reactions have been shown to go with complete retention of optical activity. If the intimate mechanism of the rate controlling step is dissociative, either of the five coordinate intermediates, I or II, would give 100% retention of optical activity.

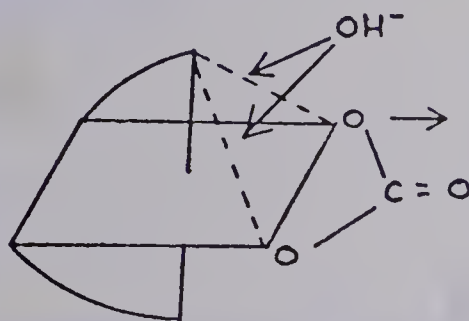


I



II

The other possible trigonal bipyramidal intermediate not having the carbonate in the trigonal plane would lead to complete racemization. If the intimate mechanism of the reaction was associative, a seven coordinate intermediate, III, generated by *cis* attack of the hydroxide



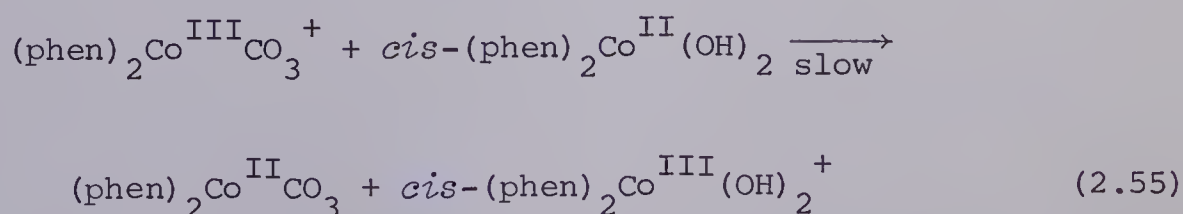
III

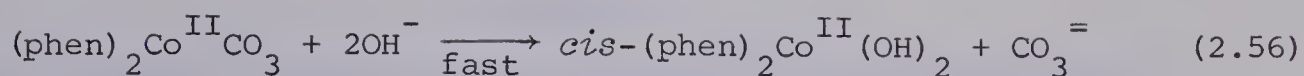
ion along an octahedral face or edge, would result in 100% retention of optical activity. Again, the data does not distinguish between the two possible mechanisms. However, the possibility of the direct production of *trans*-(en)₂CoOHCO₃ as suggested by Hargis⁵⁵ in reaction (2.12) has been definitely eliminated by the 100% retention of optical activity which is in agreement with the fact that less than 9% *trans* species is produced after the ring-opening reaction, (2.5), has

proceeded to 94% completion.

As has been mentioned in the introduction, the lack of a $[\text{OH}^-]$ term in the rate law for the ring-opening reaction of an $\text{N}_4\text{CoCO}_3^+$ complex in aqueous sodium hydroxide where the N ligand lacks acidic protons would be good evidence for the $\text{S}_{\text{N}}1\text{CB}$ mechanism being operative in the reactions of complexes having acidic ammine protons. The results of the study of the base hydrolysis of the $(\text{phen})_2\text{CoCO}_3^+$ ion, which has no acidic protons, can only be said to indicate a very, very slow reaction when no catalyzing Co(II) species is present. The complicated kinetic behavior prevented any test for a $[\text{OH}^-]$ term in the rate law. The very slow rate may be simply due to a much stronger Co-O bond caused by the very low basicity of the nitrogens in the ligand (discussed in detail in Chapter 3). Thus the reaction which was observed, while interesting in itself, unfortunately can shed no light on the general mechanism of base catalyzed ring-opening reactions in $\text{N}_4\text{CoCO}_3^+$ complexes. However, some other complex having ammine ligands with no acidic protons, and a similar basicity to NH_3 , would serve the same purpose.

A purely speculative reaction scheme can be postulated for the behavior of $(\text{phen})_2\text{CoCO}_3^+$ in aqueous sodium hydroxide with an added Co(II) salt.





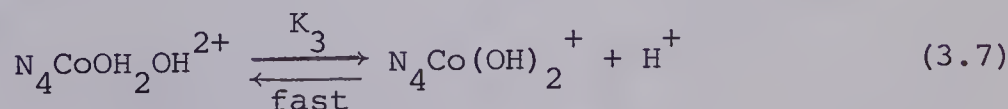
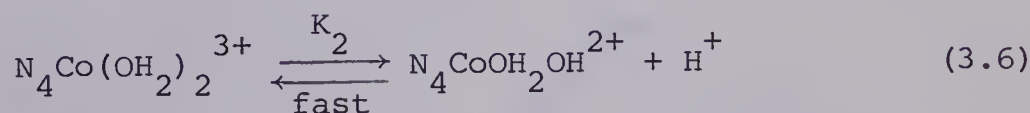
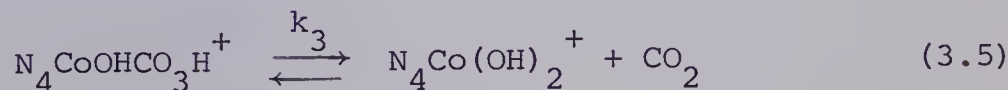
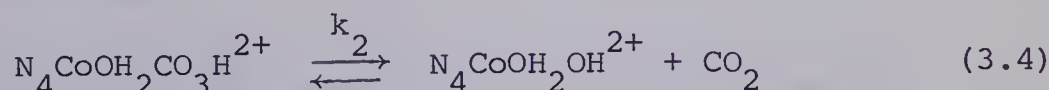
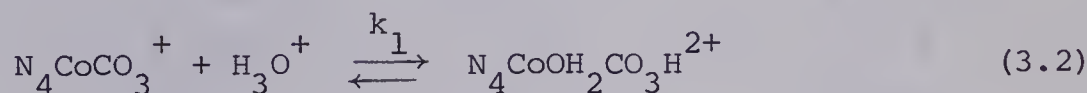
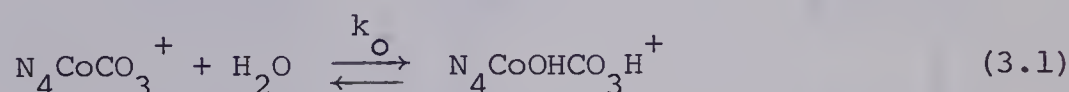
Additional *cis*-(phen)₂Co^{II}(OH)₂ could be generated by decomposition of the product or reactant, thus causing the observed rate increase with time. This decomposition must occur at near neutral pH's since aged stock solutions show a similar behavior to fresh stock solutions which have some added Co(II) salt. Further study is required before anything more definite can be said about the redox reactions involved here.

CHAPTER 3

ACID HYDROLYSIS STUDIES ON THE CARBONATOBIS(O-PHENANTHROLINE) -
AND (2,2'-BIPYRIDYL) COBALT(III) IONS

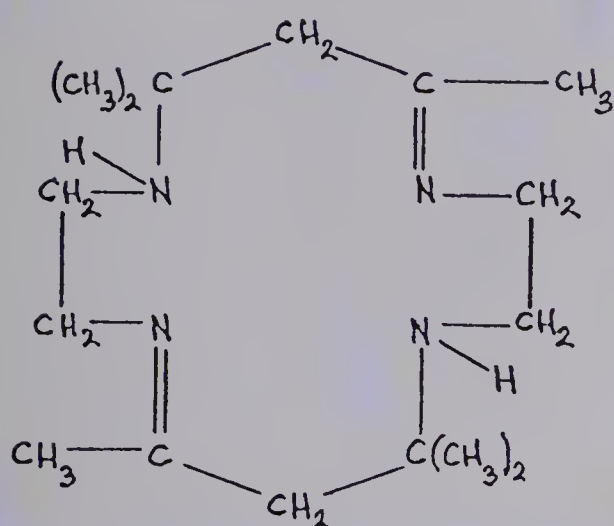
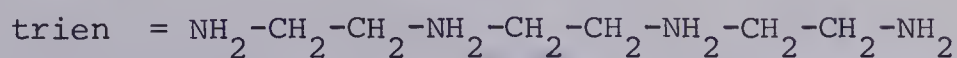
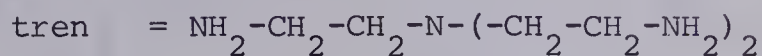
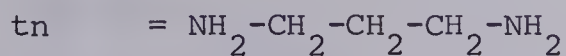
Introduction

The acid hydrolyses of $N_4CoCO_3^+$ ions, where N_4 represents $(NH_3)_4$,⁹¹⁻⁹³ $(en)_2$,⁹⁴⁻⁹⁶ $(pn)_2$,⁹⁷ $(tn)_2$,⁹⁷ $(tren)$,⁹⁸ α -(trien),⁹⁸ β -(trien),⁹⁸ *cis*-(NH_3)₂*en*,⁹⁸ *trans*-(NH_3)₂*en*,⁹⁸ *tet b*,⁹⁹ or *trans*[14] diene,⁹⁹ are consistent with the following general reaction scheme.

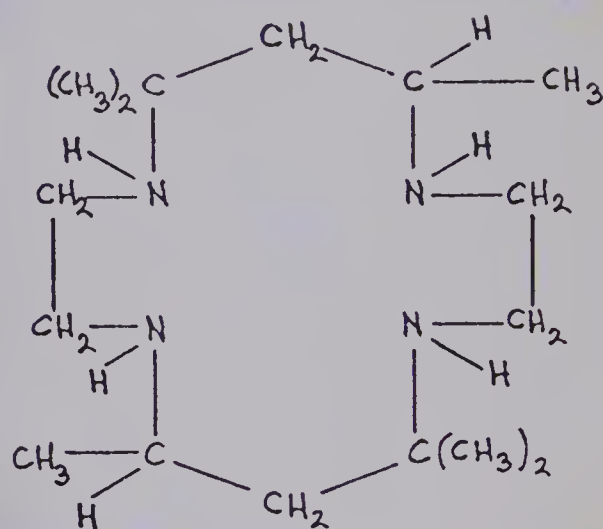


where all the species are assumed to have the *cis* configuration.

The ammine ligand abbreviations are given below,

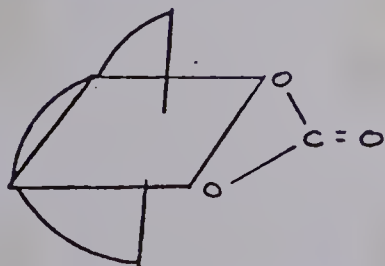


trans [14]diene

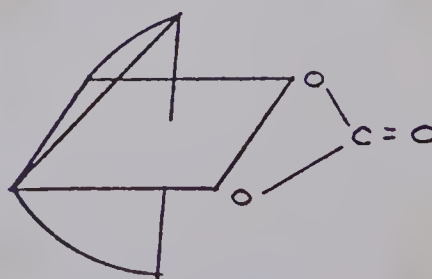


tet b

Indicating the $\text{NH}_2-(\text{CH}_2)_n-\text{NH}_2$ group as a curve, the α - and β -configurations of $(\text{trien})\text{CoCO}_3^+$ are,

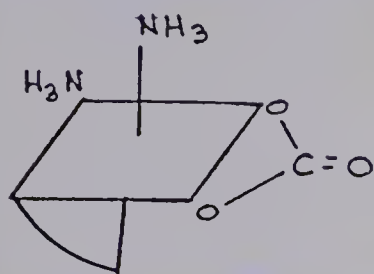


$\alpha-(\text{trien})\text{CoCO}_3^+$

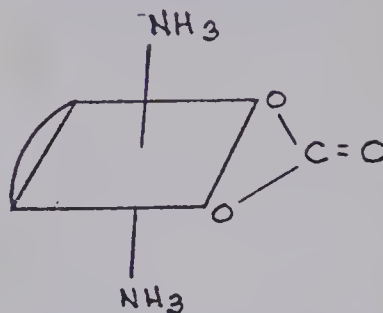


$\beta-(\text{trien})\text{CoCO}_3^+$

while the *cis* and *trans* isomers of $(\text{NH}_3)_2\text{enCoCO}_3^+$ are

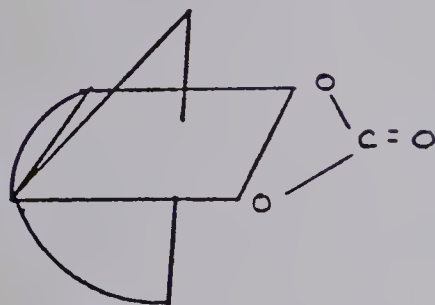


cis-(NH_3)₂enCoCO₃⁺



trans-(NH_3)₂enCoCO₃⁺

and (tren)CoCO₃⁺ has the structure



(tren)CoCO₃⁺

In the pH ranges usually studied for the acid hydrolysis, $2 < \text{pH} < 5$, the assumptions, $k_1[\text{H}^+] < k_2$, and $k_2 \gg k_3$, lead to the expression for the pseudo first-order rate constant

$$k_{\text{obsd}} = k_o + k_1[\text{H}^+] \quad (3.8)$$

The first assumption has been proven for the (tren)CoCO₃⁺ acid hydrolysis⁹⁸ and the second justified by assuming that the bicarbonato proton in $\text{N}_4\text{COOHCO}_3\text{H}^+$ is able to hydrogen bond to the hydroxy oxygen, thereby strengthening the carbon-oxygen bond which results in slower decarboxylation.¹⁰⁰ Table 3.1 shows the values of k_o and k_1 , with their

TABLE 3.1

Rate Parameters for the Acid Catalyzed Hydrolysis of

Various $N_4CoCO_3^+$ Ions at 25°

N_4	$k_o \times 10^4,$ sec^{-1}	$\Delta H_o^\ddagger,$ kcal mole^{-1}	$\Delta S_o^\ddagger,$ eu	$k_1,$ $\text{M}^{-1} \text{sec}^{-1}$	$\Delta H_1^\ddagger,$ kcal mole^{-1}	$\Delta S_1^\ddagger,$ eu
$(NH_3)_4$	1.3	12	-37	1.5	15.3	- 6.8
$(en)_2$	1.2	18	-15	0.6	13.8	- 7.4
$(pn)_2$	1.0	18	-15	0.5	14	-13
$(tn)_2$	0.8	16	-21	0.8	12	-19
$(tren)$	1.7	15	-25	2.0	11.1	-20.0
<i>cis</i> -(en) $(NH_3)_2$	0.3	17	-24	0.9	16.0	- 4.0
<i>trans</i> -(en) $(NH_3)_2$	1.1	19	-14	8.9	10.0	-20.0
α -trien	1.5	20	- 7	5.2	15.0	- 5.0
β -trien	0.1	17	-23	0.2	17.0	- 5.0
<i>trans</i> [14] diene	-	-	-	8×10^{-3}	24	-
tet <i>b</i>	-	-	-	$\sim 10^{-4}$	-	-

^a This table is a reproduction of a portion of Table VII,
reference (98).

activation parameters, for the $N_4CoCO_3^+$ acid hydrolyses studied to date.⁹⁸ The low value of k_o for the β -(trien) and *cis*-(NH_3)₂en complexes has been attributed⁹⁸ to a less strained O-Co-O bond angle since none of the ammine chelate rings are coplanar with the carbonate ring, as opposed to the α -(trien) and *trans*-(NH_3)₂en complexes. The (NH_3)₄, (en)₂, (pn)₂, (tn)₂, and *cis*-(NH_3)₂en complexes all have similar k_1 values and activation parameters. The lower ΔH_1^\ddagger for the tren complex, attributed to increased O-Co-O bond angle strain, is cancelled out by the more negative ΔS^\ddagger , resulting in a similar k_1 to the preceding complexes. The lower values of ΔH_1^\ddagger for the *trans*-(NH_3)₂en and (tren) complexes are also attributed to increased O-Co-O bond angle strain as well as steric hindrance for the case of the (tren) complex. The relative slowness of the *trans*[14]diene and tet *b* complex acid hydrolyses has been attributed⁹⁹ to steric hindrance of the fifth and sixth coordination positions by methyl groups of the macrocyclic ammine ligand.

During the course of preparing the (phen)₂CoCO₃⁺ for the base hydrolysis study described in Chapter 2, it was noticed that the acid hydrolysis of this carbonato complex was also unusually slow. Since, in the $N_4CoCO_3^+$ complexes, the ligands phen, tet *b* and *trans*[14]diene are all relatively rigid with respect to conformational changes of the N-C_n-N ring, as opposed to the en, pn, tn, tren, and trien ligands, this rigidity could be a cause of the slow acid hydrolysis if the N-C_n-N rings are required to go through a conformational change to reach the transition state. Therefore, a similar bis(2,2'-bipyridyl)

complex, $(\text{bipy})_2\text{CoCO}_3^+$, in which the ammine ligand is not as rigid, was prepared and the kinetics of the acid hydrolyses, as well as the position of bond cleavage, of the $(\text{phen})_2\text{CoCO}_3^+$ and $(\text{bipy})_2\text{CoCO}_3^+$ complexes were studied. The question of whether steric hindrance or ammine ring rigidity or carbonato ring strain or some other factor is causing the change in acid hydrolysis rates should be partially answered, at least, by the studies reported here.

Experimental

Preparation of o-Phenanthroline Complexes

Carbonatobis(o-phenanthroline)cobalt(III) chloride trihydrate was prepared by the method of Ablov and Palade.¹⁰¹ The general method of Ablov was modified in order to improve the yield. The modified method is given below.

Cobaltous chloride 6-hydrate (4.76 gm, Fisher Certified Reagent) was dissolved in a minimum amount (2.5 ml) of hot distilled water. O-phenanthroline hydrate (7.92 gm, Aldrich Chemical Co., Inc.) was dissolved in a minimum amount (47 ml) of hot distilled water. The two solutions were mixed hot and heated on a steam bath for a few minutes. The brown liquid was cooled rapidly (ice bath) with stirring to yield fine brown crystals which slowly (10 min) turned light pink. Chlorine gas was passed through the pink mixture for 50 minutes with stirring. Oxidation of the Co(II) to Co(III) was observed within 5 minutes resulting in a purple-green solution. The purple material precipitated leaving a green-brown solution. The purple precipitate, *cis*-[(phen)₂CoCl₂]Cl·3H₂O, was filtered, washed twice with 2 M HCl and air dried. The yield was 6.25 gm (54%). The crude product was recrystallized by attempting to dissolve a portion (5 gm) in 285 ml of hot water. The undissolved portion (1.7 gm) was filtered off and 50 ml of concentrated HCl added to the filtrate. The solution was evaporated to one-half of its original volume, allowed to cool to room temperature, filtered, and the product air dried to yield 4.3 gm of

small deep-violet crystals. The undissolved portion of the crude product (1.7 gm) was dissolved in 125 ml of hot water, 15 ml of concentrated HCl added, and treated as above to yield 1.6 gm of a gray powder. Only the violet crystals were used for further preparations and characterizations.

4.29 gm of *cis*-[(phen)₂CoCl₂]Cl·3H₂O were dissolved in 36 ml of hot redistilled water. 4.29 gm of anhydrous sodium carbonate (Analar) were added in portions to the solution which immediately turned red. Upon cooling, the red crystals were filtered off, washed with a small amount of ice-cold water and air dried to yield 4.07 gm of crude carbonato complex. 3.34 gm of crude product was recrystallized from 25 ml hot water containing one gm of dissolved sodium chloride. Upon cooling, red crystals formed and these were filtered off, washed with a small amount of ice-cold water and air dried to yield 2.87 gm (85% based on dichloro starting material) of pure [(phen)₂CoCO₃]Cl·3H₂O.

The original green-brown filtrate plus the 2 M HCl washings were placed in an evaporating dish. The addition of 15 ml of concentrated HCl changed the solution to bright green. When the solution was evaporated to one-half volume, green crystals precipitated. These crystals were filtered, washed with 95% ethanol and ether, and air dried to yield approximately 5 gm of [(phen)₃Co][phen H][CoCl₄]₂·HCl·5H₂O.

Cis-diaquobis(o-phenanthroline)cobalt(III) chloride dihydrate was prepared from the dichloro complex by the method of Ablov and Palade.¹⁰² All the complexes were stored in the dark to prevent possible photochemical decomposition.

Characterization of o-Phenanthroline Complexes

A microanalytical analysis for percentage of carbon, hydrogen, nitrogen, and chlorine was obtained⁵⁹ for each of the complexes. Table 3.2 gives the experimental and calculated percentages of C, H, N, and Cl for the four complexes. The calculated values are based on the molecular weights derived from the formulae given in Table 3.2. The reproducibility by the micro-analytical laboratory for these complexes was not good. All of the percentages varied by as much as one percent for the same sample. Because of this problem, other methods of characterization were necessary.

Electronic absorption spectra of the carbonato, diaquo, and dihydroxy compounds were run in 1.0 M NaCl, 1.0 M HCl, and 1.0 M NaOH, respectively, on a Cary 14 spectrophotometer. Because of the very low solubility of the dichloro complex, an accurate spectrum was not obtained.

60 MHz nmr spectra of the carbonato, diaquo, and tris(phen) complexes were run on either an A-60 or an A-56/60A NMR Spectrometer (Varian Associates, Analytical Instruments Division, Palo Alto, Calif.). The solvent and external reference used were D₂O and TMS, respectively. The spectrum of the free ligand, o-phenanthroline, was run in CDCl₃ with a TMS external reference. In order to fully interpret the nmr spectrum of the carbonato complex, spin decoupling experiments were performed at 100 MHz on an HA-100 NMR Spectrometer (Varian Associates, Analytical Instruments Division, Palo Alto, Calif.). The spectra were run in D₂O with 10% t-butanol as an internal reference. All spectra

TABLE 3.2

Molecular Weights and, Calculated and Experimental Percentage of Elements
for Various Cobalt(III) Complexes of o-Phenanthroline

Complex	Molecular Weight	%C		%H		%N		%Cl	
		exptl	calcd	exptl	calcd	exptl	calcd	exptl	calcd
$[(\text{phen})_2\text{CoCO}_3]\text{Cl}\cdot 3\text{H}_2\text{O}$	568.7	50.8	52.8	4.2	3.9	9.4	9.8	6.2	6.2
<i>cis</i> - $[(\text{phen})_2\text{CoCl}_2]\text{Cl}\cdot 3\text{H}_2\text{O}$	579.8	48.2	49.8	3.9	3.9	9.5	9.7	-	18.3
<i>cis</i> - $[(\text{phen})_2\text{Co}(\text{OH})_2]\text{Cl}_3\cdot 2\text{H}_2\text{O}$	598.0	48.2	48.3	4.3	4.1	9.2	9.4	15.8	17.8
$[(\text{phen})_3\text{Co}][\text{phen H}]$ $[\text{CoCl}_4]_2\cdot \text{HCl}\cdot 5\text{H}_2\text{O}$	1309.3	43.5	44.0	3.5	3.4	8.6	8.6	23.8	24.2

were run at normal probe temperature ($\sim 40^\circ$).

The infrared spectrum of the carbonato complex, in a KBr disk, was run on a Perkin-Elmer Model 421 IR Spectrophotometer (Perkin-Elmer Corporation, Norwalk, Connecticut).

Qualitative ion exchange experiments were carried out on the carbonato, diaquo, dichloro, and tris(phen) complexes as well as on $[(en)_2CoCO_3]Cl$ and $[(NH_3)_5CoCO_3]Cl \cdot 1\frac{1}{2}H_2O$. A column, eight cm long with a two cm diameter, was filled with Rexyn 102H cation exchange resin (Fisher Scientific Co. Ltd.) in the Na^+ form. After putting concentrated solutions (~ 0.1 gm in 0.5 ml) on the column, either NaCl or $NaHCO_3$ solutions, of increasing concentration from 0.005 M to saturated, were passed through the column.

Preparation of 2,2'-Bipyridyl Complexes

The preparations of the *cis*- $[(bipy)_2CoCl_2]Cl \cdot 2H_2O$ and $[(bipy)_2CoCO_3]Cl \cdot 3H_2O$ complexes were carried out by Gordon R. Thompson as a special project for the Advanced Inorganic Chemistry course, Chemistry 530. The *cis*- $[(bipy)_2CoCl_2]Cl \cdot 2H_2O$ complex was prepared by the method of Vlček¹⁰³ with a few modifications to improve the yield. For this reason, the detailed preparation is given below.

One gm of $CoCl_2 \cdot 6H_2O$ (Fisher Certified Reagent) and 1.6 gm of 2,2'-bipyridyl (Aldrich Chemical Co., Inc.) were dissolved in 50 ml dry methanol (The McArthur Chemical Co., Ltd.) to yield a dark red solution, presumably of the Co(II) complex, *cis*- $[(bipy)_2CoCl_2]$. Gaseous chlorine was bubbled through the stirred, ice cold solution

for 15 minutes. After addition of one gm of LiCl (Allied Chemical), a blue-gray mud precipitated. The precipitate was filtered off and recrystallized several times from large volumes of 98% ethanol (approximately one gm of complex per 100 ml). Dark violet-black crystals formed on slow evaporation (several days) of the violet solution. Only very small amounts of the green "*trans*" isomer reported by Vlček were precipitated, even after long periods of evaporation. This "*trans*" isomer has since been shown¹⁰⁴ to be *cis*-[Co(bipy)₂Cl₂]₂[CoCl₄]₂.

The [(bipy)₂CoCO₃]Cl·3H₂O complex was prepared by dissolving one gm of *cis*-[(bipy)₂CoCl₂]Cl·2H₂O in 25 ml of warm water. One gm of anhydrous sodium carbonate (Analar) was added in portions to the violet solution which immediately turned dark red. Dark red needles precipitated and were filtered. Upon air drying, the red needles became an orange-red powder which was recrystallized twice from re-distilled water.

The perchlorate salt of the (bipy)₂CoCO₃⁺ ion was prepared by dissolving [(bipy)₂CoCO₃]Cl·3H₂O in redistilled water, adding an equivalent weight of anhydrous NaClO₄ (G. Frederick Smith Chemical Co.) to the solution, and filtering and air drying the orange-red precipitate.

Characterization of 2,2'-Bipyridyl Complexes

The results of the elemental analysis⁵⁹ of the complexes for percentage of C, H, N, and Cl are shown in Table 3.3.

TABLE 3.3

Molecular Weights and, Calculated and Experimental Percentage of Elements
for Dichloro- and Carbonatobis(2,2'-bipyridyl)Cobalt(III) Complexes

Complex	Molecular Weight	%C		%H		%N		%Cl	
		exptl	calcd	exptl	calcd	exptl	calcd	exptl	calcd
<i>cis</i> -[(bipy) ₂ CoCl ₂]Cl·2H ₂ O	513.7	46.7	46.9	3.8	3.9	10.8	10.9	21.7	20.8
[(bipy) ₂ CoCO ₃]Cl·3H ₂ O	520.9	47.4	48.4	4.1	4.3	10.6	10.8	6.7	6.8
[(bipy) ₂ CoCO ₃]ClO ₄	530.8	45.6	46.9	2.9	3.0	10.7	10.4	6.6	6.6

The visible absorption spectrum of $[(\text{bipy})_2\text{CoCO}_3]\text{Cl}\cdot 3\text{H}_2\text{O}$ in 1.0 M sodium chloride was measured in a five cm cell at room temperature on a Cary 14 Spectrophotometer. A spectrum was also run of a solution of $[(\text{bipy})_2\text{CoCO}_3]\text{ClO}_4$ in 1.0 M HClO_4 which had been kept at 58° for 30 minutes, thus yielding the spectrum of the *cis*- $(\text{bipy})_2\text{Co}(\text{OH})_2^{3+}$ ion.

The ir spectrum of $[(\text{bipy})_2\text{CoCO}_3]\text{Cl}\cdot 3\text{H}_2\text{O}$ in a KBr disk was run on a Perkin-Elmer Model 421 I.R. Spectrophotometer.

The 100 MHz nmr spectrum of $[(\text{bipy})_2\text{CoCO}_3]\text{Cl}\cdot 3\text{H}_2\text{O}$ was run on a HA-100 nmr spectrometer in D_2O with 10% t-butanol as an internal reference. Spin decoupling experiments were done in order to fully assign the spectrum.

Acid Hydrolysis Kinetics of $(\text{bipy})_2\text{CoCO}_3^+$ and $(\text{phen})_2\text{CoCO}_3^+$ Ions

The same experimental method was used to follow the acid hydrolysis kinetics of the o-phenanthroline and 2,2'-bipyridyl carbonato cobalt(III) complexes.

Known amounts of 1.0 M HCl, 2.0 M NaCl, and redistilled water were added to a five cm spectrophotometer cell. After temperature equilibration has occurred, 1.00 ml of a stock solution of complex in redistilled water was injected with a syringe through a rubber serum cap on the neck of the cell. The HCl concentration was always at least 50 times greater than the complex concentration which was near 1.3×10^{-3} M. The change in absorbance with time for the o-phenanthroline and 2,2'-bipyridyl complexes was followed at 505 and 500 m μ , respectively, on Bausch and Lomb Spectronic 505 and Precision Spectrophotometers. The temperature of the reaction solution in the cell was controlled by water flowing through an aluminum cell block.¹⁰⁵ The water temperature was controlled by the same apparatus used for the 24.0° , high $[\text{OH}^-]$ base

hydrolysis kinetics of the $(en)_2CoCO_3^+$ ion. The solution temperature was measured directly with another thermistor bead temperature probe which was calibrated with a Hewlett-Packard Quartz Thermometer (2801A) and probe (2850-D) which had been factory calibrated from 0 to 100°.

Kinetic runs were also done by scanning the visible absorption spectra of reaction solutions in the wavelength region, 400-600 mμ, and observing the changes in spectra with time.

All water used was redistilled from a Corning AG1b Water Still (Corning Glass Works, Laboratory Products Division, Corning, New York). The 1.0 M HCl solutions were made by diluting ampoules of concentrated HCl (P-H Tamm, Bio-Rad Laboratories). The ionic strength of the reaction solutions was always 1.0 (NaCl). The 2.0 M NaCl was made by dissolving solid reagent grade NaCl (Fisher Certified Reagent) in redistilled water.

Oxygen - 18 Tracer Study

The oxygen - 18 enriched water, sample collection, sample analysis, and procedure for determination of solvent enrichment will be described in Chapter 4. The bubbler described in Chapter 4 was modified by adding a water jacket to allow temperature control by a water flow from a Colora (Papst) temperature bath. Hydrochloric acid enriched in ^{18}O was prepared by dilution of 0.419 ml of concentrated HCl (11.94 M, Canadian Industries Ltd.) to 5.0 ml with $^{18}OH_2$ enriched water.

A known weighed amount of solid complex was added to the dried

clean bubbler. After temperature equilibration, 1.00 ml of the 1.0 M HCl solution was syringed into the bubbler and the nitrogen stream immediately turned on and allowed to bubble through the solution for a set period of time. The nitrogen stream was then diverted and the resultant carbon dioxide sample collected and analyzed.

The acid hydrolysis bond breaking of the $(\text{phen})_2\text{CoCO}_3^+$, $(\text{bipy})_2\text{CoCO}_3^+$, and $(\text{en})_2\text{CoCO}_3^+$ (as a standard) ions was tested at 71.0° for reaction times of 5-10 minutes and at 25.0° for a reaction time of 31 minutes.

Results

Characterization of o-Phenanthroline Complexes

The visible absorption spectra of the carbonato, diaquo Co(III) and diaquo Co(II) bis(o-phenanthroline) complexes are shown in Figure 3.1. Also shown in Figure 3.1 is the spectrum of the *cis*-(phen)₂Co(OH)₂⁺ ion which was obtained by dissolving *cis*-[(phen)₂Co(OH₂)₂]Cl·2H₂O in 1.0 M NaOH. Table 3.4 compares the spectral characteristics of the compounds prepared here to those reported by Ablov.^{101,102} The agreement is quite good except for the minimum extinction coefficients of the diaquo and dihydroxy species. These differences may be due to the difference in ionic strength of the two studies. Ablov's spectra were run in redistilled water ($\mu \sim 0$) while the spectra reported here were measured in 1.0 M NaCl. High energy charge transfer bands may be shifted by changes in ionic strength due to ion-pair formation.¹⁰⁶ Since ion-pairing is more likely for the +3 diaquo species than the +1 dihydroxy or carbonato species, ion-pairing causing a charge transfer band shift could explain the difference in ϵ_{\min} value for the diaquo species but not for the dihydroxy species. The charge transfer band could also be shifted by a change in temperature.¹⁰⁶ However, the most likely explanation for these differences is that the low absorbance leads to larger errors in the calculated extinction coefficients and that the values actually do agree within experimental error.

The spectral maxima show the same trends with wavelength as the analagous bis(ethylenediamine)cobalt(III) complexes, i.e.,

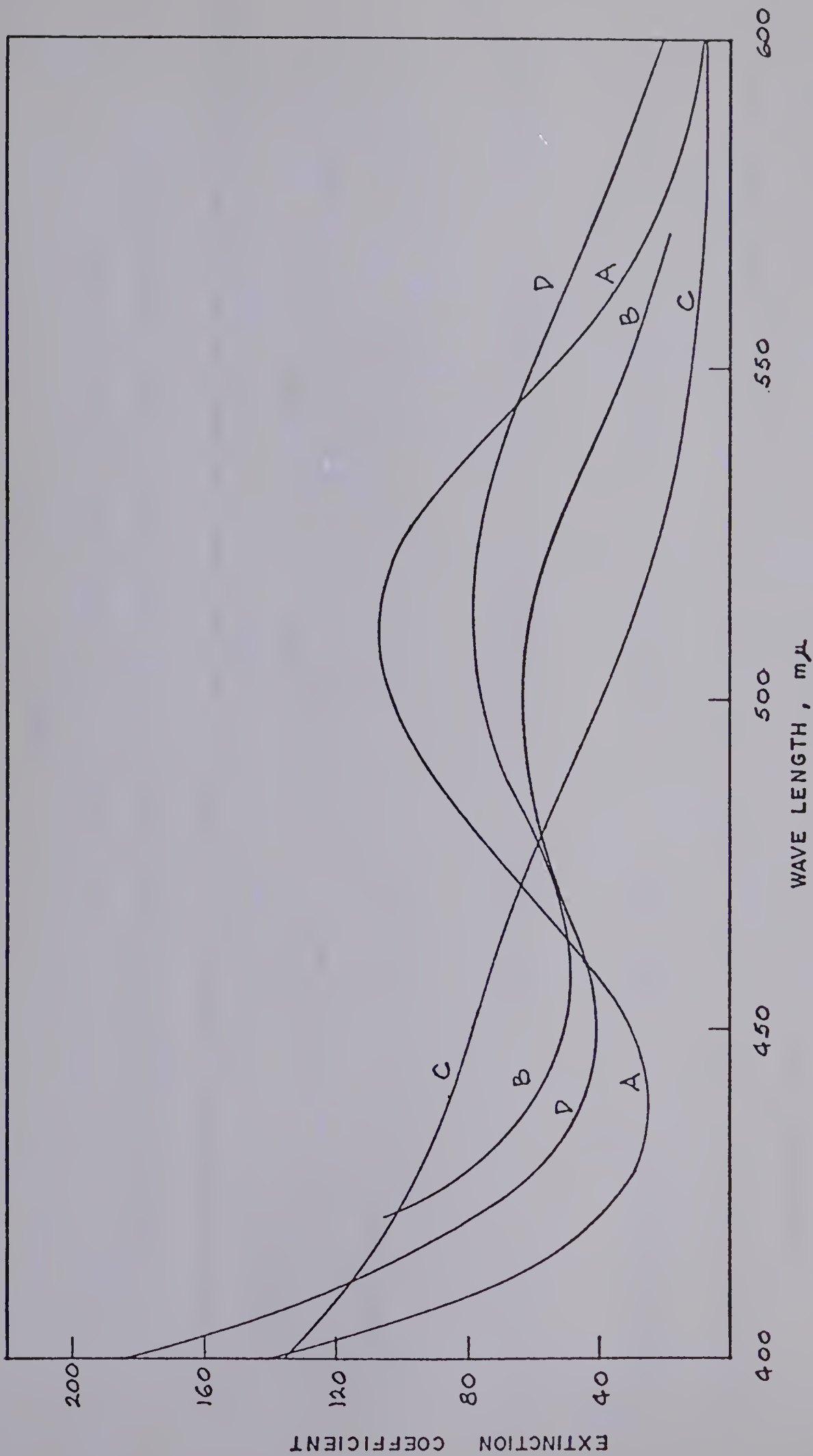


Figure 3.1: Electronic Absorption Spectra of $(\text{phen})_2\text{CoCO}_3^+$, (A), $\text{cis}-(\text{phen})_2\text{Co}(\text{OH}_2)_3^{3+}$, (B), $\text{cis}-(\text{phen})_2\text{Co}(\text{OH}_2)_2^{2+}$, (C), and $\text{cis}-(\text{phen})_2\text{Co}(\text{OH})_2^+$, (D).

TABLE 3.4

Visible Spectral Characteristics of *cis*-Dihydroxy-, *cis*-Diaquo-, and Carbonatobis(o-phenanthroline)Cobalt(III) Ions at 25° and 1.0 (NaCl) Ionic Strength

Complex Ion	$\lambda_{\text{max}}, \text{ m}\mu$	ϵ_{max}	$\lambda_{\text{min}}, \text{ m}\mu$	ϵ_{min}
<i>cis</i> -(phen) ₂ Co(OH) ₂ ⁺	512 ^a (517) ^b	79.5 (67.0)	448 (449)	41.4 (28.4)
(phen) ₂ CoCO ₃ ⁺	509 (510)	109.1 (105.7)	437 (438)	24.6 (25.4)
<i>cis</i> -(phen) ₂ Co(OH) ₂ ³⁺	500 (500)	63.0 (60.0)	458 (452)	48.2 (39.9)

^a Unbracketed values are from Figure 3.1.

^b Values in brackets are reported by Ablov^{101,102} in redistilled H₂O.

dihydroxy>carbonato>diaquo, (see Chapter 2, Figure 2.6).

Since all of these complexes are of the octahedral type, CoA_4B_2 , at least two electronic absorption bands are expected, corresponding to transitions from the ${}^1\text{A}_{1g}$ ground state to ${}^1\text{T}_{1g}$ and ${}^1\text{T}_{2g}$ excited states.¹⁰⁷ In *trans* complexes, the low energy band, ${}^1\text{A}_{1g} \rightarrow {}^1\text{T}_{1g}$, is expected to be split into ${}^1\text{A}_{1g} \rightarrow {}^1\text{A}_{2g}$ and ${}^1\text{A}_{1g} \rightarrow {}^1\text{E}_g$ bands while in *cis* complexes, the band is only expected to show some asymmetry due to some slight splitting of the ${}^1\text{T}_{1g}$ terms into ${}^1\text{A}_{1g}$, ${}^1\text{B}_{1g}$, and ${}^1\text{B}_{2g}$ terms under C_{2v} symmetry. Since no splitting is observed in the spectra, a *cis* configuration for the complexes is indicated but not proven.

A recent theoretical study¹⁰⁸ on the electronic structure of the tris(2,2'-bipyridyl)iron(II) complex shows that the very high wavelength charge transfer band (525 mμ) observed in the visible spectrum of this complex is due to an electronic transition from the metal $3d\pi$ (d_{xy} , d_{xz} , d_{yz}) atomic orbitals to the lowest vacant ligand π type molecular orbital. A shift of the π - π^* transition of the free ligand to a higher wavelength (from 281 mμ to 339 mμ) is attributed to the electrostatic effect of coordination.

The relatively high wavelength charge transfer band observed in these o-phenanthroline (and 2,2-bipyridyl) complexes is likely due to the latter ($\pi \rightarrow \pi^*$) internal ligand transition because Co(III), as opposed to Fe(II), is not easily oxidized, as would be required for the metal $d\pi \rightarrow$ ligand π transition.

The infrared spectrum of $[(\text{phen})_2\text{CoCO}_3]\text{Cl} \cdot 3\text{H}_2\text{O}$ is shown in Figure 3.2. The bands marked X are consistent with chelated carbonate

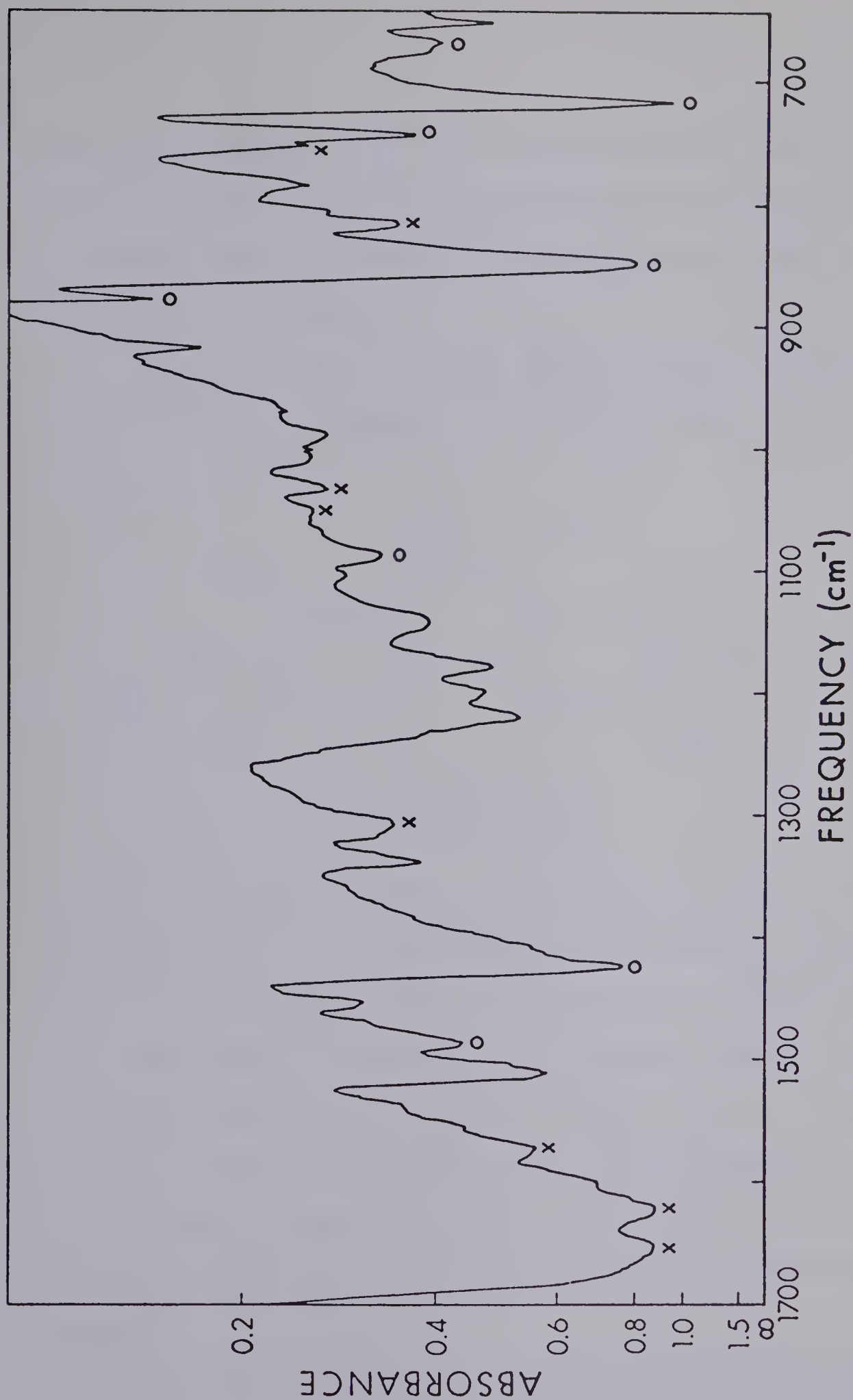


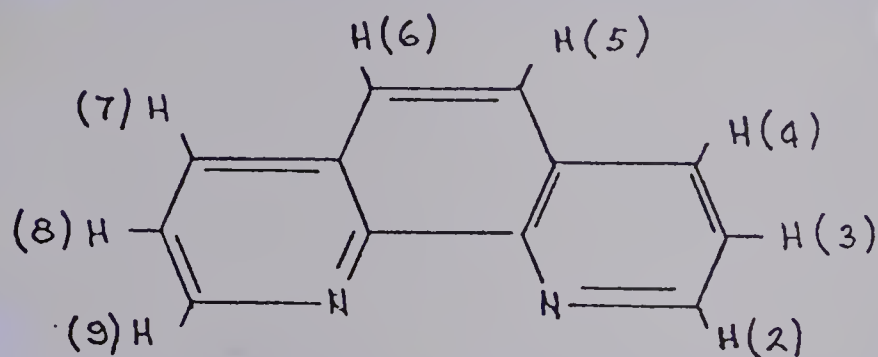
Figure 3.2: Infrared Spectrum of $[(\text{phen})_2\text{CoCO}_3][\text{Cl}\cdot 3\text{H}_2\text{O}]$ in KBr Disk.

x - consistent with chelated carbonate, references (109) and (110).

o - consistent with o-phenanthroline, reference (111).

cobalt(III) complexes^{109,110} while the bands marked o are consistent with those found in the tris(o-phenanthroline)cobalt(III) ion.¹¹¹ Thus the infrared spectrum confirms the bidentate nature of the carbonate ligand in the solid complex.

The nmr spectrum of the free ligand, o-phenanthroline, has been interpreted¹¹² with reference to the numbering system below.



1,10-phenanthroline

The nmr spectrum was assigned as an A_2 singlet (5,6) and an ABX system (4,3,2 and 7,8,9). Figure 3.3 shows the nmr spectrum of o-phenanthroline in $CDCl_3$ relative to TMS and the theoretical pattern¹¹³ expected from an ABX system. A comparison of the spectral data from this study to the data obtained by Rosenberger,¹¹² given in Table 3.5, shows good agreement between the two spectra. The slight differences may be due to the different solvent, CCl_4 , used by Rosenberger. Calculation of the chemical shifts and coupling constants was done using standard methods.¹¹³

Examination of a Framework Molecular Model (Prentice-Hall, Inc., Englewood Cliffs, New Jersey) of the $(phen)_3Co(III)^{3+}$ ion indicates that each half of each o-phenanthroline ligand is identical.

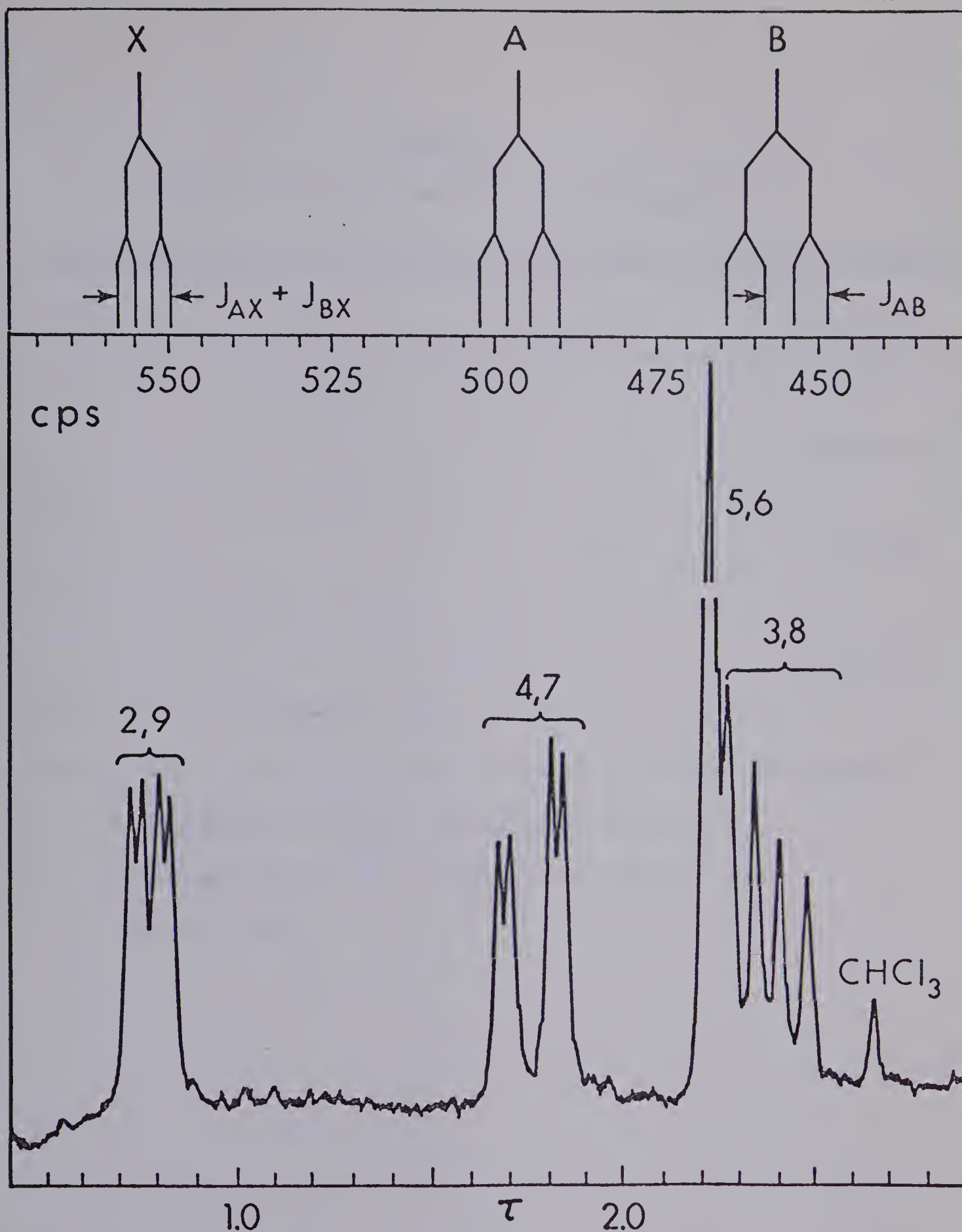


Figure 3.3: 60 MHz nmr Spectrum of o-Phenanthroline Monohydrate in CDCl_3 with TMS as an External Reference and a Schematic ABX Spectrum.

TABLE 3.5

60 MHz Nmr Spectral Data^{a,b} for o-Phenanthroline

Proton #	Tau	ij	J _{ij} , Hz
2,9	.76 (.93)		
		2,3	4.2 ^c (4.2)
3,8	2.37 (2.53)		
		2,4	1.3 (1.8)
4,7	1.76 (1.91)		
		3,4	8.5 (7.8)
5,6	2.23 (2.36)		

^a Spectrum run in CDCl₃, TMS external reference.

^b Bracketed values are in CCl₄, from reference (112).

^c Average value.

Each of the 2 and 9 protons lies directly over a pyridine ring of a different o-phenanthroline ligand. Thus the ring current (and hence opposing magnetic field) induced by the applied field would be expected to shift the 2,9 protons upfield from their free ligand position. Coordination is expected to shift all the protons downfield because of a loss of carbon σ electron density caused by σ bonding to the cobalt which results in a smaller opposing magnetic field and thus a lower resonance field. These two opposing effects should cause the resonance of the 2,9 protons to move closer to the other protons in the ligand. Figure 3.4 shows that the nmr spectrum of the tris complex is very similar to that of the free ligand except for the predicted upfield shift of the 2,9 protons relative to the others. Also notice that the 5,6 protons have shifted downfield relative to the 3,8 protons while the 4,7 protons have shifted upfield. These shifts are not readily explained but the pattern is assumed to be characteristic for coordination of o-phenanthroline to cobalt. The broad peak at 6.3 τ is attributed to broadening of the HDO in the D_2O by the Co(II) in the solution. The paramagnetic Co(II) ion may also cause large shifts in the total resonance position of the o-phenanthroline protons. For this reason, the chemical shifts in Figure 3.4 are not meaningful.

The molecular model of $(phen)_2CoCO_3^+$ shows that the halves of each o-phenanthroline are not identical. One half (say the 2,3,4,5 half) is similar to those in the tris complex in that the 2 proton lies directly over the center of a pyridine ring from the other o-phenanthroline ligand. The other half (say the 9,8,7,6 half) is similar to the

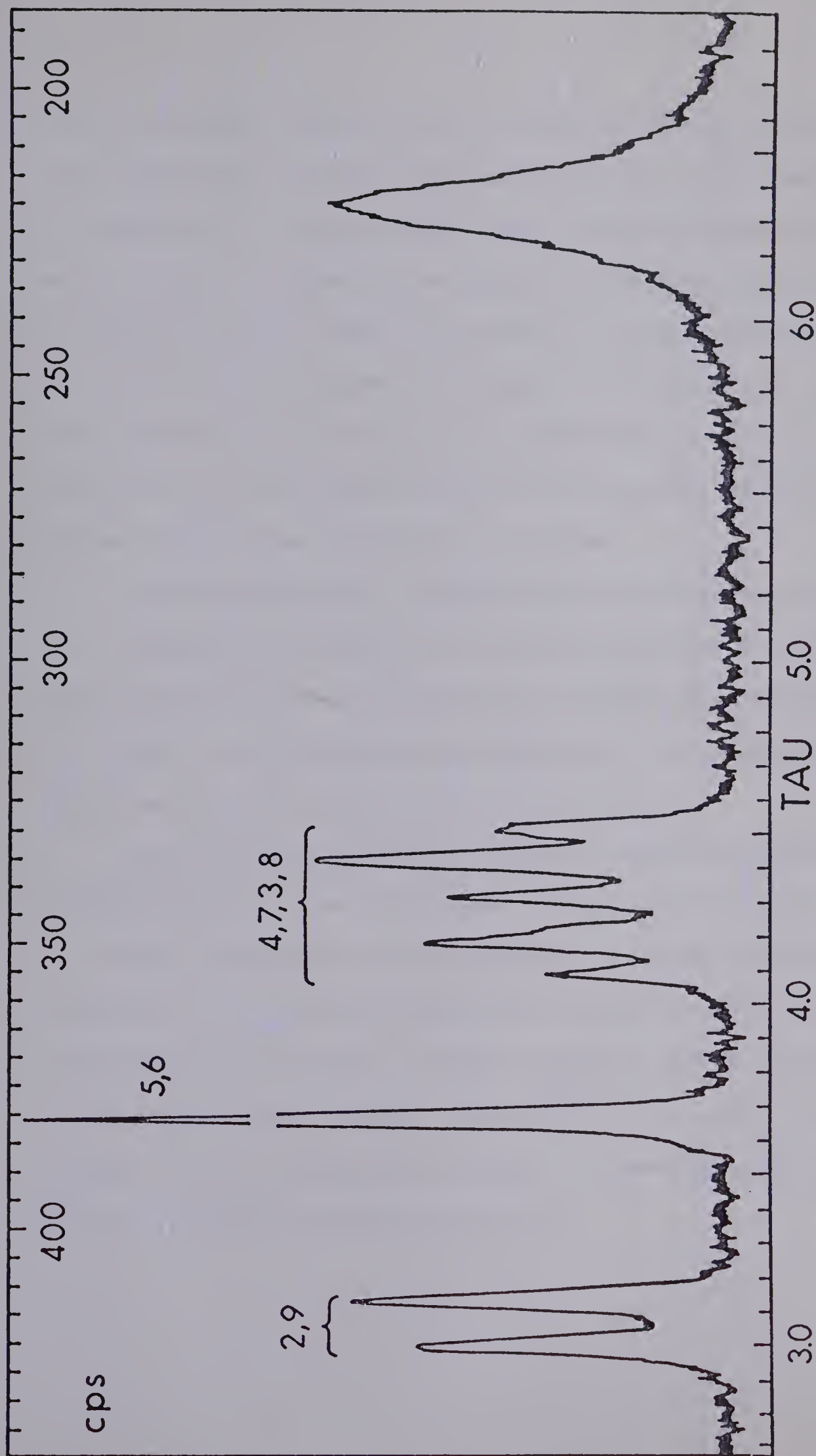


Figure 3.4: Nmr Spectrum of $[(\text{phen})_3\text{Co}][\text{CoCl}_4]_2 \cdot \text{HCl}$ in D_2O at 60 MHz. The broad

peak at 6.3 τ is due to broadening of the HDO in the D_2O by the paramagnetic $\text{Co}(\text{II})$ counter-ion.

free ligand except that it has the 2 proton of the other o-phenanthroline ligand lying over one of its pyridine rings. Since the two halves are different, the 5 and 6 protons are in slightly different environments. Figure 3.5 shows the nmr spectra of the $(\text{phen})_2\text{CoCO}_3^+$ and *cis*- $(\text{phen})_2\text{Co}(\text{OH}_2)_2^{3+}$ ions. In spectrum A, the characteristic AB pattern for the 5,6 protons can be seen centered at 486 Hz. The diaquo spectrum, B, can be seen to be qualitatively similar to the A spectrum so that any conclusions about the carbonato spectrum are assumed to apply also to the diaquo spectrum.

Because two slightly different halves exist for each o-phenanthroline ligand, it is expected that two ABX patterns will be seen. From Figure 3.6, which shows the 100 MHz nmr spectrum, the assignment, and the results of the spin decoupling experiment, two ABX systems are evident as is the AB pattern due to the 5,6 protons.

Since irradiation at 868 Hz causes the upfield multiplet to collapse to an AB system, the doublet at 868 Hz must be due to either 2 or a 4 proton. Assignment of the doublet to a 2 proton requires the assignment of the high field half of the multiplet at 765 Hz to a 4 proton because of the small (~ 1.5 Hz) coupling constant which is only consistent with meta coupling. Analysis¹¹³ of this part of the spectrum, which is called $\chi\alpha\beta$ in Figure 3.6, results in the chemical shifts and coupling constants given below.

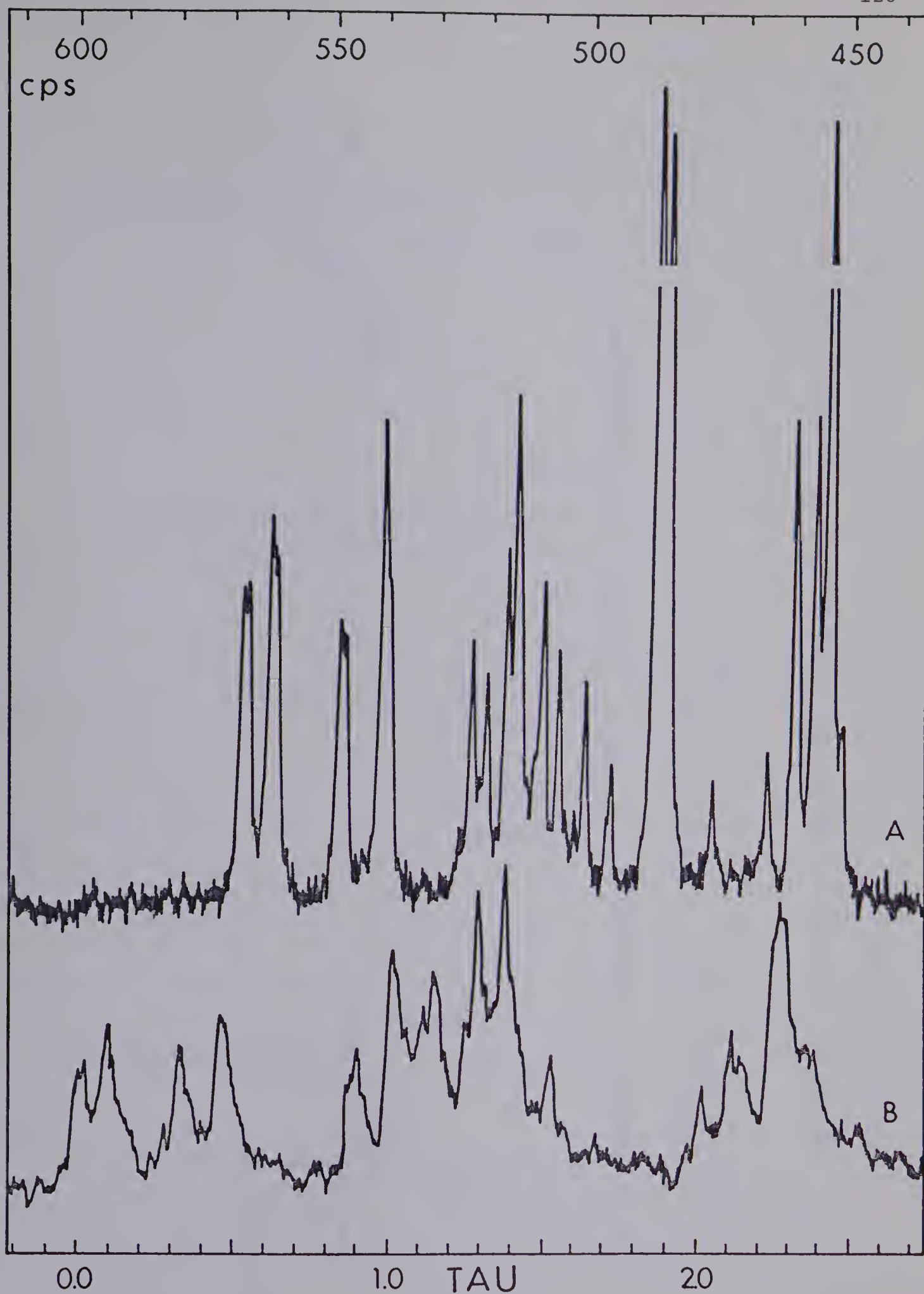


Figure 3.5: Nmr spectra of $[(\text{phen})_2\text{CoCO}_3]\text{Cl}\cdot 3\text{H}_2\text{O}$, (A), and $\text{cis}-[(\text{phen})_2\text{Co}(\text{OH}_2)_2]\text{Cl}_3\cdot 2\text{H}_2\text{O}$, (B), at 60 MHz in D_2O .

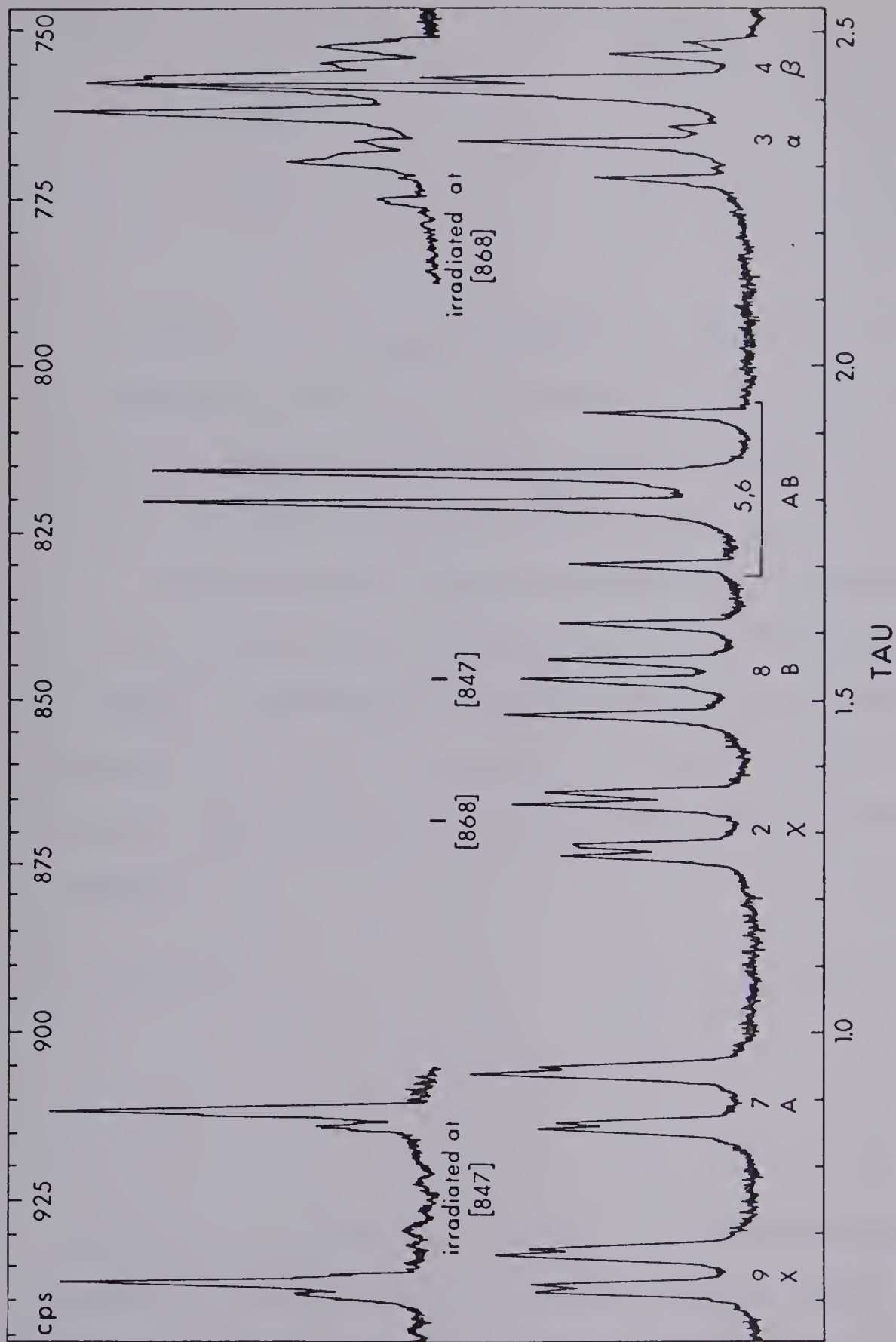


Figure 3.6: 100 MHz Nmr Spectrum of $[(\text{phen})_2\text{CoCO}_3]\text{Cl}\cdot 3\text{H}_2\text{O}$ in D_2O with 10% *t*-Butanol as an Internal Reference.

#	τ	ij	$J_{ij}, \text{ Hz}$
β 4	2.44	3,4	8.5
α 3	2.36	2,4	1.3
χ 2	1.32	2,3	4.2

The coupling constants are very similar to those for the free ligand. The similarity of the χ , AB, α , β pattern to the X, A₂, A, B pattern in the tris complex is consistent with the assignment of the χ proton as a 2 proton which lies over a pyridine ring.

Irradiation at 847 Hz causes collapse of the downfield multiplet to an AX uncoupled system. Thus the proton at 847 Hz must be the middle or 8 proton. Assuming the downfield proton to lie closest to the nitrogen results in the assignment 9,7,8 (X,A,B). Analysis¹¹³ of this portion of the spectrum gives the following chemical shifts and coupling constants;

#	τ	ij	$J_{ij}, \text{ Hz}$
B 8	1.58	8,9	5.5
A 7	0.90	7,9	1.1
X 9	0.65	7,8	8.2

The coupling constants are again close to the free ligand values. Because the 9 proton does not lie over a pyridine ring, it is not subject to shielding by a ring current. Thus the 9 proton's chemical shift value of 0.65 τ as compared to the 2 proton's value of 1.32 τ is consistent with the assignment. The downfield shift

of the 7 and 8 protons may be due to a specific electron withdrawing effect of the carbonate which is *trans* to the portion of the ligand containing the 7 and 8 protons. However the reasons for this effect are not obvious. Nor is the relatively greater downfield shift of the 7 proton easily explained.

While an explanation of some of the chemical shifts is not possible, the presence of two separate ABX systems, the presence of an AB system, the chemical shifts of the 2 and 9 protons, and the agreement of both sets of coupling constants, all agree with the assignment of a C_{2v} symmetry to the $(\text{phen})_2\text{CoCO}_3^+$ and *cis*- $(\text{phen})_2\text{Co}(\text{OH}_2)_2^{3+}$ ions.

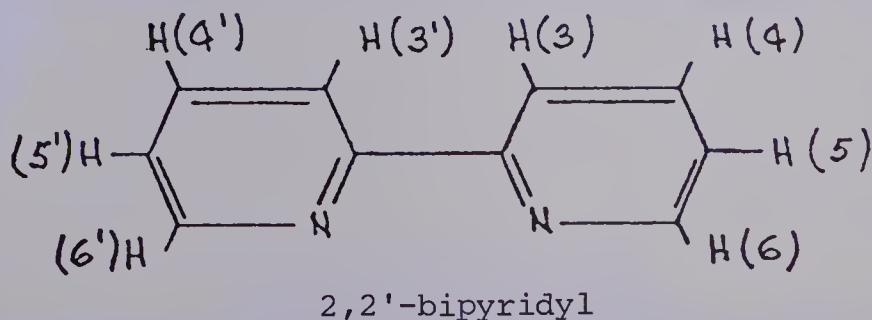
In the ion exchange experiments, the *cis*- $(\text{phen})_2\text{Co}(\text{OH}_2)_2^{3+}$ and *cis*- $(\text{phen})_2\text{CoCl}_2^+$ ions were not eluted from the column, even with concentrated hydrochloric acid. Some type of interaction occurred which made the complexes impossible to remove. The $(\text{phen})_3\text{Co}^{3+}$ ion was eluted with 1.0 M NaCl or NaHCO_3 . The $(\text{en})_2\text{CoCO}_3^+$ ion and the $(\text{NH}_3)_5\text{CoCO}_3^+$ ions were eluted with 0.2M NaHCO_3 and saturated NaHCO_3 , respectively. The $(\text{phen})_2\text{CoCO}_3^+$ ion was eluted with 0.02 M NaCl. When a faint yellow material could be eluted from the carbonato complex band with water, that particular preparation was discarded. For these very slightly impure preparations, a faint brown residue was often left on the column. The final criteria for purity of the carbonato complex was a lack of both yellow and brown impurities upon elution from the ion-exchange resin.

Characterization of 2,2'-Bipyridyl Complexes

The visible absorption spectrum of $[(\text{bipy})_2\text{CoCO}_3]\text{Cl}\cdot 3\text{H}_2\text{O}$ is given in Figure 3.7. The value of the extinction coefficient at 504 m μ (116.5) agrees fairly well with the value of 110 reported by Vlček.¹⁰³

The infrared spectrum of $[(\text{bipy})_2\text{CoCO}_3]\text{Cl}\cdot 3\text{H}_2\text{O}$, in a KBr disk, shows the characteristic bands near 760, 1450, and 1600 cm^{-1} which were observed¹¹¹ for the Mn(II), Fe(II), Fe(III), Co(II), Co(III), and Ni(II) tris (2,2'-bipyridyl)perchlorate complexes. The three bands in the observed spectrum at 770, 1445, and 1602 cm^{-1} are ascribed to out of plane bending of ring hydrogens, and to two C=C ring vibrations, respectively. The observed bands at 675, 750, 820, 1030, 1245-1275, and 1632 cm^{-1} have been assigned as the ν_6 , ν_3 , ν_8 , ν_2 , ν_5 , and ν_1 bands according to the assignment of Nakamoto.¹⁰⁹ These bands are consistent with the bidentate nature of the carbonato ligand in the solid complex.

The 100 MHz nmr spectrum of $[(\text{bipy})_2\text{CoCO}_3]\text{Cl}\cdot 3\text{H}_2\text{O}$ in D_2O is shown in Figure 3.8. The spectrum has been interpreted with reference to the numbering system below.



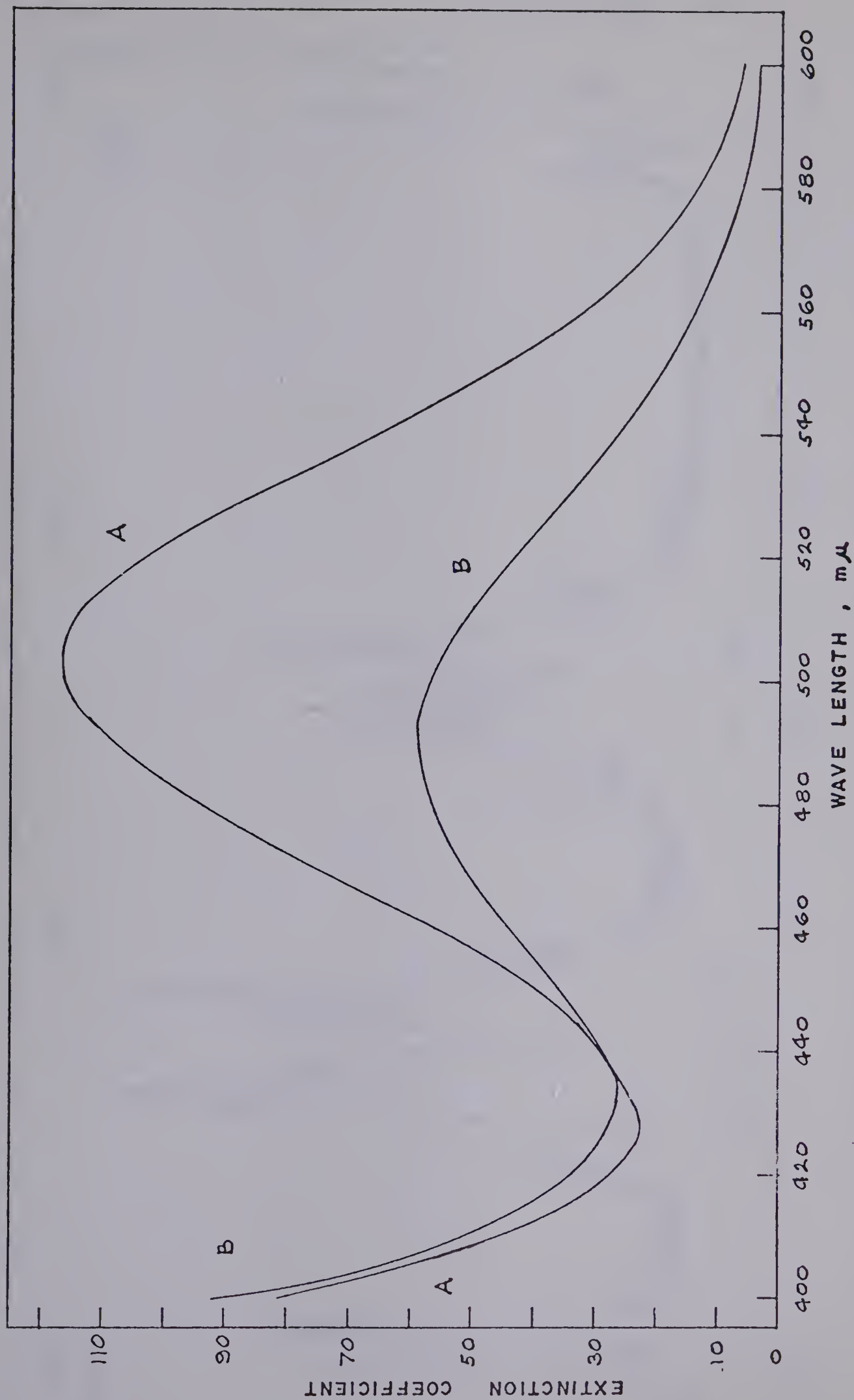


Figure 3.7: Visible Absorption Spectra of $(\text{bipy})_2\text{CoCO}_3^+$ in 1 M NaCl, (A), and $\text{cis}-(\text{bipy})_2\text{Co}(\text{OH})_2^{3+}$, (B). B is from $[(\text{bipy})_2\text{CoCO}_3]\text{ClO}_4$ hydrolyzed by 1.0 M HClO_4 .

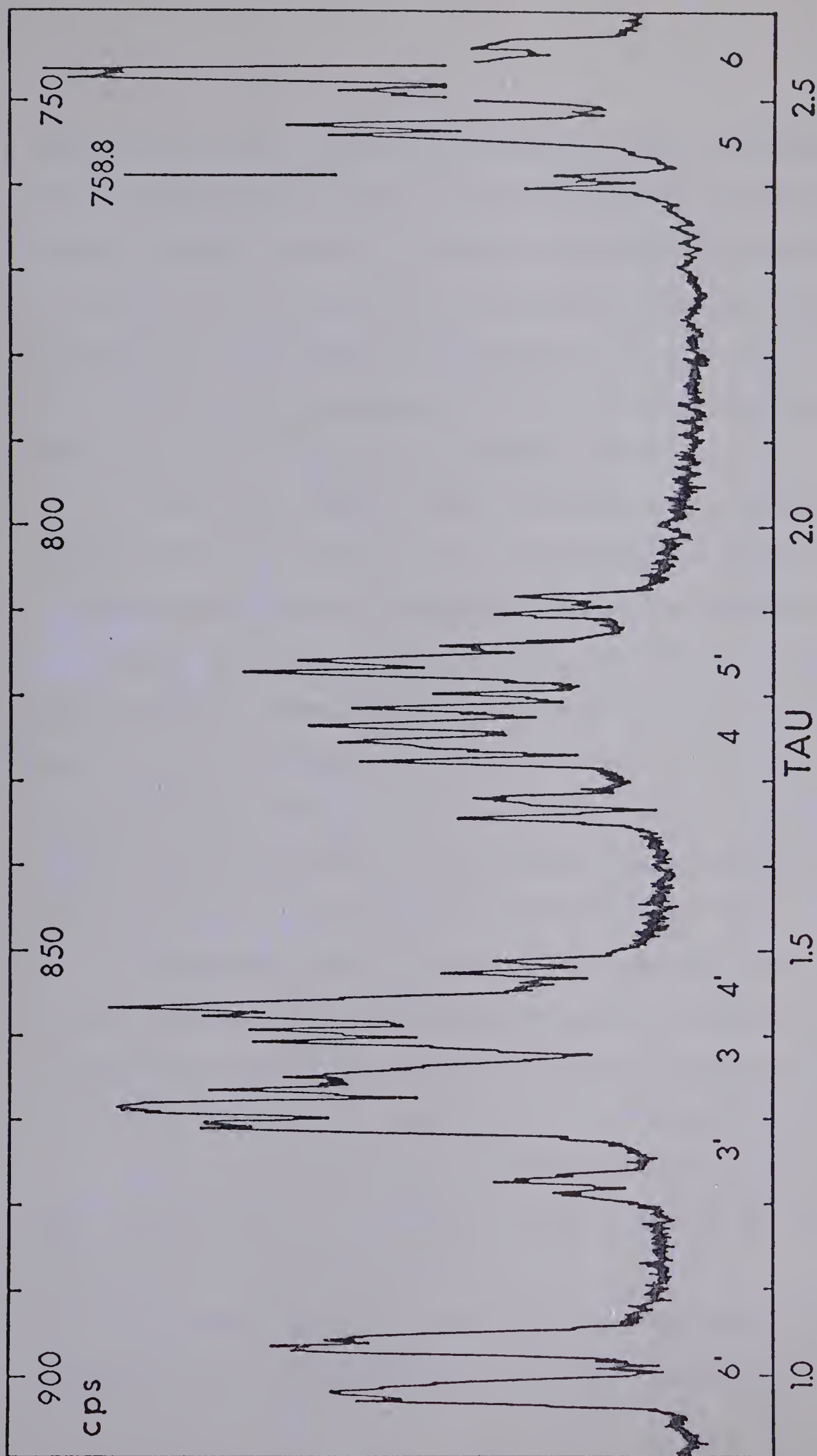


Figure 3.8: 100 MHz Nmr Spectrum of $(\text{bipy})_2\text{CoCO}_3^+$ in D_2O . The calibration line is 638 Hz from t-butanol, 758.8 from TMS.

Assuming the 6 proton lies over the pyridine ring of the other 2,2'-bipyridyl ligand, similar to the analagous o-phenanthroline complex, allows assignment of the downfield doublet (898 Hz) to the 6' proton since it does not lie over a pyridine ring and thus is not expected to be shielded by a ring current as is the 6 proton. The rest of the spectrum was interpreted with the aid of the spectrum of free bipyridyl¹¹⁴ and the spin decoupling experiments.

Irradiation at 898 Hz causes a collapse of the right hand side of the multiplet at 820 Hz to a pair of doublets. Since the large coupling ($J \sim 8$ Hz) expected for adjacent protons is removed, this right hand side of the multiplet must be due to the 5' proton. At the same time a collapse in the fine splitting ($J \sim 1.5$ Hz) of the right hand side of the multiplet centered at 863 Hz is seen. Therefore the right hand side of the 863 Hz multiplet is assigned to the 4' proton. No effect at all was observed in the 750 Hz multiplet therefore these protons must be on the other ring of the bipyridyl ligand.

Irradiation at 871 Hz causes the fine structure ($J \sim 1.5$ Hz) of the right hand side of the 820 Hz multiplet to collapse to a triplet. Therefore the quartet centered at 873 Hz must be due to the 3' proton since it is the only proton which can be ortho coupled to the 5' proton.

One of the protons in the high field multiplet is assumed to be the 6 proton because of the large shielding caused by the ring current effect of the underlying pyridine ring.

The middle four lines of the 862 Hz multiplet must belong to either the 3,4, or 5 protons because all the other protons have been

assigned. Irradiation at 862 Hz causes no change in the upfield half of the 750 Hz multiplet therefore it can be assigned to the 6 proton and the four lines at 862 Hz assigned to the 3 proton since these two are the only protons on the same ring which will not couple to each other. The fine structure ($J \sim 1.5$ Hz) on the left half of the 750 Hz multiplet collapses. Therefore this can be assigned to the 5 proton since it is the only one expected to show meta coupling to the 3 proton.

The left half of the 820 Hz multiplet is assigned to the 4 proton by elimination.

No attempt was made to calculate the chemical shifts and coupling constants for the $[(\text{bipy})_2\text{CoCO}_3]\text{Cl} \cdot 3\text{H}_2\text{O}$ complex because the spreading of the spectrum at 100 MHz was not sufficiently large, unlike the analagous o-phenanthroline complex.

Comparing this assignment to Drago's¹⁷⁵ for the $\text{cis-Ir}(\text{bipy})_2\text{Cl}_2^+$ ion shows that only the position of the 5 and 6 protons is reversed. Drago assigns the 6' proton to lie over a pyridine ring as opposed to the assignment used here. Thus it is necessary to switch the superscript primes before comparing the two assignments. The higher relative position of the 6 proton in the Co(III) complex may be reasonable since Ir is a larger atom than Co so that the 6 proton is expected to be farther away from the other pyridine ring and thus less shielded by the opposing magnetic field from the induced ring current.

This assignment of the nmr spectrum of $[(\text{bipy})_2\text{CoCO}_3]\text{Cl} \cdot 3\text{H}_2\text{O}$ provides additional evidence for the C_{2v} symmetry of the ion and the bidentate nature of the carbonate ligand in a D_2O solution.

Acid Hydrolysis Kinetics of $(\text{bipy})_2\text{CoCO}_3^+$ and $(\text{phen})_2\text{CoCO}_3^+$ Ions

Because of the poor nucleophilicity of perchlorate ion and because of the apparent instability of the *trans* isomers of bis(2,2'-bipyridyl)cobalt(III) complexes,¹⁰⁴ it was assumed that the product of the acid hydrolysis of $[(\text{bipy})_2\text{CoCO}_3]\text{ClO}_4$ with HClO_4 could only be the *cis*-diaquo- or *cis*-carbonatoaquobis-(2,2'-bipyridyl)cobalt(III) ion. Since it was observed that after 2 minutes at 71.0° in 1.0 M HCl, a large amount of CO_2 could be collected from a reaction solution (see ^{18}O - tracer study), complete loss of CO_2 or $\text{CO}_3^{=}$ occurs. Therefore a diaquo product, as opposed to a carbonatoquo product, is indicated.

Comparing the spectrum of *cis*- $(\text{bipy})_2\text{Co}(\text{OH}_2)_2^{3+}$, prepared as described above, the spectrum of the same ion given by Palade,¹¹⁶ and the spectrum of the final reaction product of the hydrolysis of $(\text{bipy})_2\text{CoCO}_3^+$ in HCl

Origin of Spectrum	$\lambda_{\text{max}}, \text{ m}\mu$	$\lambda_{\text{min}}, \text{ m}\mu$	ϵ_{500}
final hydrolysis product ($\mu = 1.0, \text{ NaCl}$)	488	435	56.5
<i>cis</i> - $(\text{bipy})_2\text{Co}(\text{OH}_2)_2^{3+}$ from HClO_4 hydrolysis ($\mu = 1.0, \text{ NaClO}_4$)	490	428	57.0
reference (116)	489	425	45.0

shows that the acid hydrolysis product is the *cis*- $(\text{bipy})_2\text{Co}(\text{OH}_2)_2^{3+}$ ion. ϵ_{500} is the molar extinction coefficient at 500 m μ . The extinction coefficients reported by Palade for the *cis*-(phen) $_2\text{Co}(\text{OH}_2)_2^{3+}$

ion were also lower than those for the diaquobis(o-phenanthroline) cobalt(III) complex prepared here so that the low value of ϵ_{500} is probably not significant.

The change in absorbance at 500 m μ with time was used to determine the observed pseudo first-order rate constants by doing the normal $\log(A_t - A_\infty)$ vs. time plot. A_t and A_∞ refer to the solution absorbance at any time t and at complete reaction, respectively. The dependence of the observed rate constant on $[H^+]$, in the range of $[H^+]$, 0.06 to 0.87 M, is given by

$$k_{\text{obsd}} = k_o + k_1 [H^+] \quad (3.9)$$

The observed rate constants were fitted to equation (3.9) by the program ENLLSQ, yielding best fit values for k_o and k_1 . Figure 3.9 shows the dependence of k_{obsd} on $[H^+]$ at 69.3° as well as the straight line calculated from the best fit values of the parameters. Table 3.6 gives the best fit values of k_o and k_1 at 52.0, 60.0, and 69.3, their 95% confidence limits and the activation parameters and error limits determined from a transition state plot of $\log k_r/T$ vs $1/T$. From the 95% confidence limits, it can be seen that the value of k_o is not necessarily >zero. No transition state activation parameters were calculated for k_o since the $\log k_r/T$ vs. $1/T$ plot was not linear. However, since the best fit value of k_o is always positive, it is felt that the k_o term in equation (3.9) is real, although inaccurately determined. Table D.11 in Appendix D gives the experimental values of k_{obsd} and the value of k_{obsd} calculated (k_{calcd}) from equation (3.9)

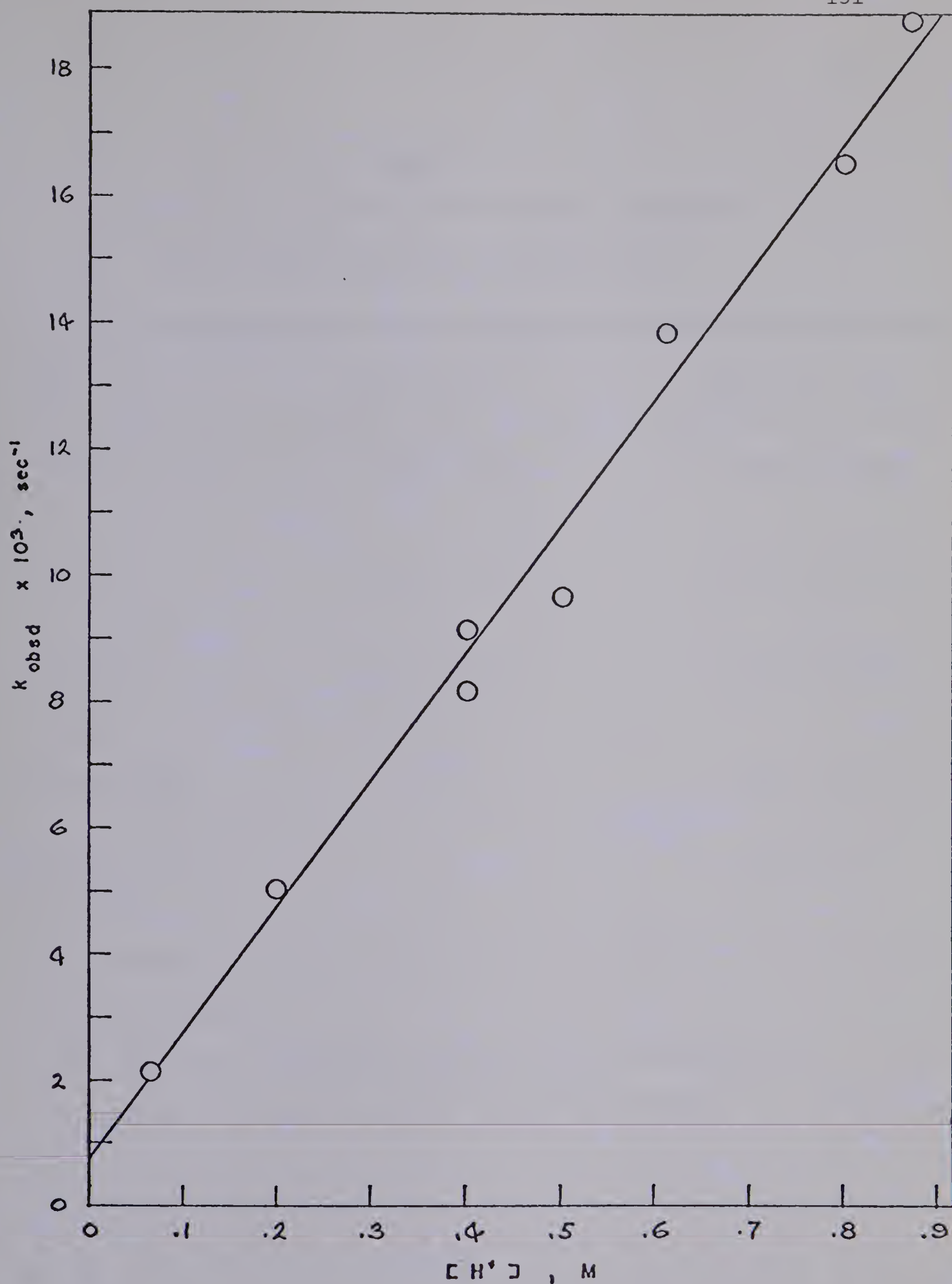


Figure 3.9: Variation of k_{obsd} with $[\text{H}^+]$ for the Reaction of $(\text{bipy})_2\text{CoCO}_3^+$ with HCl . $T = 69.3^\circ$, $\mu = 1.0$ (NaCl).

TABLE 3.6

Specific Rate Constants and Activation Parameters
for the Acid Hydrolysis of $(\text{bipy})_2\text{CoCO}_3^{+a}$

Temp, °C	$k_o \times 10^4, \text{sec}^{-1}$	$k_1 \times 10^2, \text{M}^{-1} \text{sec}^{-1}$
52.0	0.327 ± 2.03	0.343 ± 0.033
60.0	4.08 ± 3.40	0.931 ± 0.067
69.3	6.50 ± 10.25	2.03 ± 0.187
$\Delta H^\ddagger, \text{kcal mole}^{-1}$	b	22.3 ± 1.7
$\Delta S^\ddagger, \text{eu}$	b	-1.50 ± 4.8

^a $\mu = 1.0$ (NaCl).

^b No activation parameters because of non-linearity of $\log k_r/T$ vs. $1/T$ plot and large 95% confidence limits.

and the best fit parameters for each $[H^+]$ at 52.0, 60.0, and 69.3°.

The product of the reaction of $(phen)_2CoCO_3^+$ with HCl was determined to be the *cis*-($phen)_2Co(OH_2)_2^{3+}$ ion by comparison of the spectrum of the final reaction solution to the measured spectrum of *cis*-($phen)_2Co(OH_2)_2^{3+}$ (Figure 3.1). A solution of $[(phen)_2CoCO_3]Cl \cdot 3H_2O$ (1.050×10^{-3} M) in HCl (0.856 M) and NaCl (0.144 M) was allowed to react at 50° for 1243 min. The spectrum of the infinite time solution is compared below to that of the *cis*-diaquo complex.

Species	λ_{max} , mμ	ϵ_{max}	λ_{min} , mμ	ϵ_{min}
final acid hydrolysis reaction solution	504	60.2	466	49.1
<i>cis</i> -($phen)_2Co(OH_2)_2^{3+}$	500	63.9	458	48.1

The observed rate constant was determined in the same way as for the acid hydrolysis of the 2,2'-bipyridyl complex except that the absorbance change with time was followed at 505 mμ.

The dependence of the observed rate constant on $[H^+]$ for the acid hydrolysis of $(phen)_2CoCO_3^+$ is also given by equation (3.9). The values of k_o and k_1 for this system were determined in the same way as for the 2,2'-bipyridyl complex acid hydrolysis. However for this complex, while the 95% confidence limits still gave no reason for expecting $k_o > \text{zero}$, the $\log k_r/T$ vs. $1/T$ plot for k_o was linear so that values of ΔH^\ddagger and ΔS^\ddagger could be determined. The values are naturally subject to a large uncertainty. The values of the best fit parameters of k_o and k_1 at 50.0, 60.5 and 71.5°, their 95%

confidence limits, and the activation parameters and error limits are given in Table 3.7. Figure 3.10 shows the variation of k_{obsd} with $[\text{H}^+]$ at 50.0° . The solid line is calculated from equation (3.9) and the values of k_0 and k_1 at 50.0° . Tables D.12, D.13, and D.14 in Appendix D give the experimental value of k_{obsd} and value of k_{obsd} calculated (k_{calcd}) from equation (3.9) and the best fit values of k_0 and k_1 for each $[\text{H}^+]$ at 50.0 , 60.5 , and 71.1° , respectively.

Oxygen - 18 Tracer Study

In a reaction solution which is 1.0 M in $[\text{H}^+]$ and at 71° , the half-time calculated for the acid hydrolysis of $(\text{phen})_2\text{CoCO}_3^+$ is 51.9 sec . Under the same conditions the half-time for the acid hydrolysis of $(\text{bipy})_2\text{CoCO}_3^+$ is slightly less while that for the acid hydrolysis of $(\text{en})_2\text{CoCO}_3^+$ is very small.⁹⁵ Therefore a reaction (bubbling) time of 10 minutes is easily sufficient for complete hydrolysis of all three complexes. In fact most of the CO_2 was collected within 2 minutes of initiating the reaction.

R is defined as the $46/44$ mass ratio of the mass spectrum of the collected CO_2 . R_0 and R_∞ refer to the ratios for normal, un-enriched in ^{18}O , carbon dioxide and for the ^{18}O enriched solvent, respectively. F , the fraction of enrichment is defined by

$$F = \frac{R - R_0}{R_\infty - R_0} \quad . \quad (3.10)$$

Table 3.8 gives the results of the tracer experiments at 71° . The acid hydrolysis of $(\text{NH}_3)_4\text{CoCO}_3^+$ is known²¹ to go with no incorporation

TABLE 3.7

Specific Rate Constants and Activation Parameters

for the Acid Hydrolysis of $(\text{phen})_2\text{CoCO}_3^{+a}$

Temp, °C	$k_o \times 10^4, \text{sec}^{-1}$	$k_1 \times 10^2, \text{M}^{-1} \text{sec}^{-1}$
50.0	0.309 ± 0.605	0.167 ± 0.012
60.5	1.68 ± 1.31	0.514 ± 0.052
71.1	10.4 ± 8.88	1.23 ± 0.147
$\Delta H^\ddagger, \text{kcal mole}^{-1}$	37.9^b	20.4 ± 1.9
$\Delta S^\ddagger, \text{eu}$	$+27.5^b$	-8.6 ± 5.1

^a $\mu = 1.0$ (NaCl).^b Error calculation not done because of large 95% confidence limits on k_o .

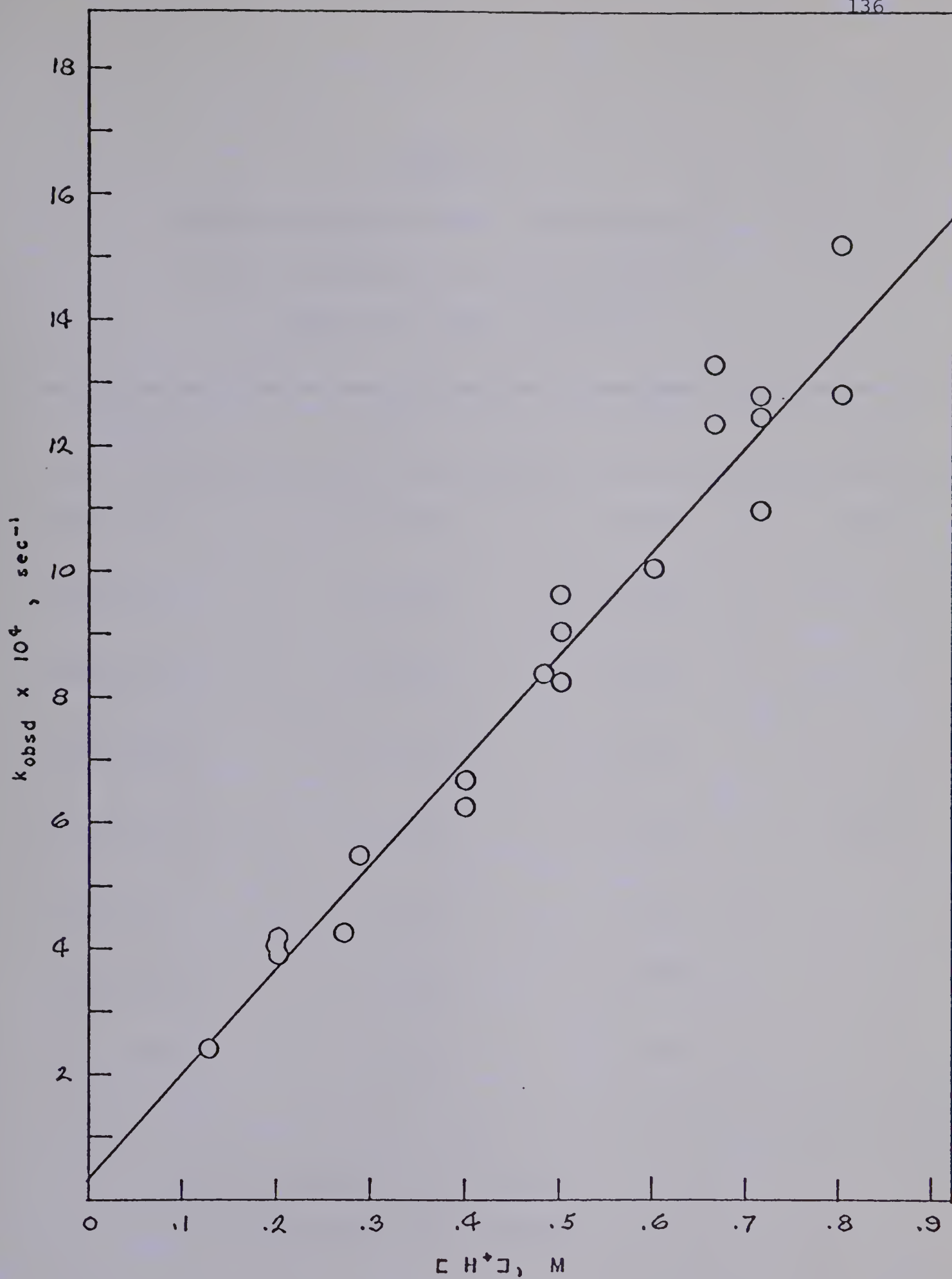


Figure 3.10: Variation of k_{obsd} with $[\text{H}^+]$ for the Reaction of $(\text{phen})_2\text{CoCO}_3^+$ with HCl . $T = 50.0^\circ$, $\mu = 1.0$ (NaCl).

TABLE 3.8

Tracer Experiments on the Bond Breaking in
the Acid Hydrolysis of $(\text{bipy})_2\text{CoCO}_3^+$ and
 $(\text{phen})_2\text{CoCO}_3^+$ at 1.0 M $[\text{H}^+]$

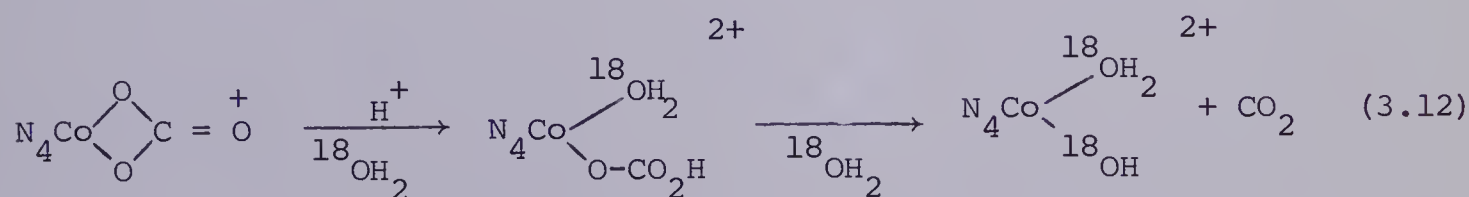
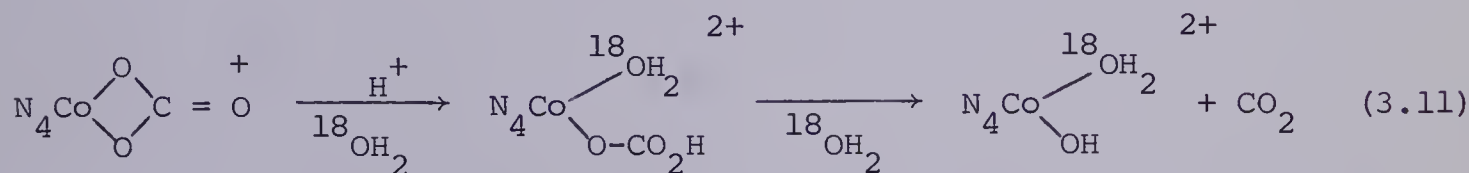
complex	R	F	T, °C
$(\text{en})_2\text{CoCO}_3^+$	0.01032	0.302	71.0 ^a
$(\text{en})_2\text{CoCO}_3^+$	0.00768	0.189	
$(\text{bipy})_2\text{CoCO}_3^+$	0.00806	0.208	
$(\text{phen})_2\text{CoCO}_3^+$	0.00973	0.291	
$(\text{en})_2\text{CoCO}_3^+$	0.00528	0.0690	25.0 ^b
$(\text{en})_2\text{CoCO}_3^+$	0.00582	0.0960	
$(\text{bipy})_2\text{CoCO}_3^+$	0.00441	0.0258	
$(\text{phen})_2\text{CoCO}_3^+$	0.00422	0.0164	

^a 71.0° runs bubbled for 10 minutes.

^b 25.0° runs bubbled for 31 minutes.

of solvent oxygen in the evolved CO_2 . Since the $(\text{en})_2\text{CoCO}_3^+$ ion is assumed to undergo acid hydrolysis by the same mechanism as the $(\text{NH}_3)_4\text{CoCO}_3^+$ ion, a low value of F for the $(\text{en})_2\text{CoCO}_3^+$ complex is expected. Thus there seems to be method induced incorporation of solvent oxygen at 71° .

Also given in Table 3.8 are the results of the tracer experiments at 25° with a reaction (bubbling) time of 31 minutes. At 25° , the half-time for the acid hydrolysis of $(\text{phen})_2\text{CoCO}_3^+$ at $1.0 \text{ M } [\text{H}^+]$ is 98 minutes. After 31 minutes, 20% of the reaction will have occurred. Since no solvent oxygen appears in the CO_2 evolved from the acid hydrolysis of either $(\text{bipy})_2\text{CoCO}_3^+$ or $(\text{phen})_2\text{CoCO}_3^+$, compared to the CO_2 evolved from the acid hydrolysis of $(\text{en})_2\text{CoCO}_3^+$, the reaction must go via Co-O and then either C-O or Co-O bond cleavage. These two possibilities are illustrated in equations (3.11) and (3.12).



In order to distinguish between the two possibilities, the rate of water exchange of the *cis*-(bipy) $_2$ - and *cis*-(phen) $_2\text{Co}(\text{OH}_2)_2^{3+}$ ions must be measured. Then a study to determine the number of solvent oxygens incorporated in the diaquo product of these $\text{N}_4\text{CoCO}_3^+$ acid hydrolyses

might be possible, thereby determining the correct reaction path. However, for purposes of discussion, the acid hydrolysis of these complexes will be assumed to go via reaction (3.11) which is the path for the acid hydrolysis of the $(\text{NH}_3)_4\text{CoCO}_3^+$ ion.²¹

Discussion

From Tables 3.6 and 3.7, it is apparent that the factor of ammine chelate ring rigidity cannot be important in determining the rate of acid hydrolysis of $N_4CoCO_3^+$ complexes since there is only a small difference in the rates yet the phen ligand is very much more rigid than the bipy ligand. Nor are the very slow rates for the acid hydrolysis of the bipy and phen $N_4CoCO_3^+$ complexes likely caused by steric hindrance, as has been suggested for the analogous *tet b* and *trans*[14] diene complexes,⁹⁹ since in both the bipy and phen complexes, the carbonato ring is only slightly sterically hindered, if at all. Although an increase in carbonato ring strain caused by a coplanar ammine chelated ligand is known to increase the rate of acid hydrolysis of $N_4CoCO_3^+$ complexes,⁹⁸ a decrease in rate, caused by a markedly less strained carbonato ring in the bipy and phen complexes than in the "normal" NH_3 complexes, seems unlikely.

A correlation between the basicity of the N ligand and the rate of acid hydrolysis at 25° is possible if those complexes are neglected which have ammine chelate rings coplanar to the carbonato ring, i.e., (tren)- $CoCO_3^+$, *trans*-(NH_3)₂en $CoCO_3^+$, and α -(trien)- $CoCO_3^+$. Table 3.9 gives the value of an average pK_a for each N ligand. This average pK_a was calculated to allow an estimate of the basicity of each nitrogen when all the other nitrogens are in the $-NR_2$ form. From Table 3.9 the order of basicity of the N ligands is

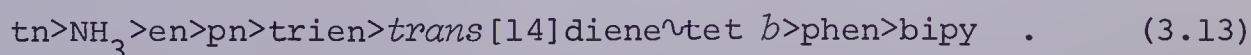


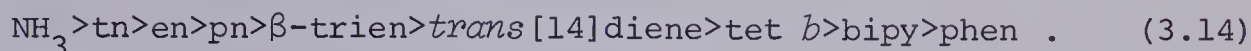
TABLE 3.9

The Basicity of Some Ammine Ligands^a

Ammine	Average pK_a	Reference
tn	9.7 ^b	117
NH ₃	9.3 ^c	118
en	8.6 ^b	119
pn	8.5 ^d	120
trien	7.3 ^b	121
$\left\{ \begin{array}{l} \text{tet } b \\ \text{trans[14]diene} \end{array} \right\}$	6.3 ^e	122
phen	5.0 ^b	123
bipy	4.5 ^b	124

^a All pK_a 's were measured at 20°C.^b Measured at ionic strength 0.1 (NaNO₃).^c Ionic strength 0.0 (corrected).^d Ionic strength 1.0 (KCl).^e Ionic strength <0.1 (reactants).

The order of the rate of acid catalyzed hydrolysis of the $N_4CoCO_3^+$ complexes is



A decreased basicity of the ammine nitrogen is expected to result in less ammine ligand Co σ electron donation, a higher charge on the Co and thus a stronger Co-O bond. Since the Co-O bond cleavage in reaction (3.2) is rate controlling, the stronger Co-O bond, caused by a lower basicity ammine, should result in a slower rate of acid catalyzed ring-opening, as is observed.

A more direct measure of the effect the ammine ligand has on the Co-O bond strength may be the value of the pK_a for the acid dissociation of $cis-N_4Co(OH_2)_2^{3+}$ complexes. A stronger Co-O bond should result in a weaker O-H bond and hence a greater acidity. Table 3.10 gives the pK_a values of some of the $cis-N_4Co(OH_2)_2^{3+}$ complexes. From Table 3.10 and equation (3.14), it appears that the greater the acidity of the $cis-N_4Co(OH_2)_2^{3+}$ complex, the slower the rate of acid catalyzed hydrolysis of the $N_4CoCO_3^+$ complex.

The discrepancy between the trends given by equations (3.13) and (3.14) for the bipy:phen pair becomes resolved when the data in Table 3.10 is used to predict the relative acid hydrolysis rates. Thus, the pK_a of the $cis-N_4Co(OH_2)_2^{3+}$ complexes seems a better indicator of Co-O bond strength than the ammine basicity, at least for the bipy:phen pair.

The discrepancy for the $NH_3:tn$ pair is probably due to the

TABLE 3.10

Acid Dissociation pK_a 's of Some
 $cis-N_4Co(OH_2)_2^{3+}$ Complexes at 25°

Complex	pK_a	Reference
$cis-(en)_2Co(OH_2)_2^{3+}$	6.1 ^a	56
$cis-(NH_3)_4Co(OH_2)_2^{3+}$	6.0 ^a	84
$\beta-(trien)Co(OH_2)_2^{3+}$	5.3 ^b	125
$cis-(bipy)_2Co(OH_2)_2^{3+}$	4.7 ^c	116
$cis-(phen)_2Co(OH_2)_2^{3+}$	4.5 ^c	102

^a Ionic strength 1.0 ($NaNO_3$).

^b Ionic strength 2×10^{-3} ($NaClO_4$).

^c Ionic strength 1.0 (KNO_3).

chelated nature of the tn complex. Referring to Table 3.1, the large activation entropy of -19.0 eu for k_1 of the tn complex may explain the slower than expected value of k_1 for $(tn)_2CoCO_3^+$ or the discrepancy may be due to slightly incorrect values for the pK_a 's of NH_3 or tn.

The general conclusion for these trends that the rate of acid catalyzed hydrolysis of $N_4CoCO_3^+$ complexes is sensitive to the strength of the Co-O bond allows a tentative classification of the intimate mechanism of the ring-opening portion of these reactions as *d* (dissociative). Further information about the nature of the transition state for reaction (3.2) is not available from the experiments performed to date.

CHAPTER 4

OXYGEN EXCHANGE STUDIES ON SODIUM BICARBONATE AND

CARBONATOCOBALT(III) AMMINE COMPLEXES

Introduction

An idealized chemical exchange reaction, given by

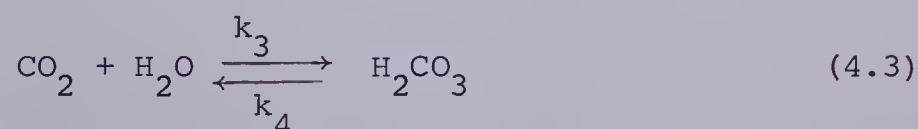


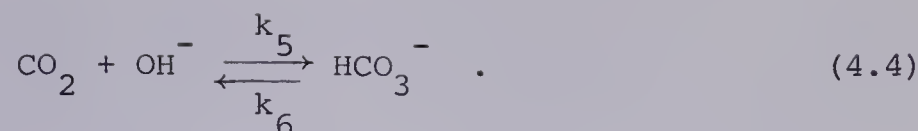
may proceed directly as written in one step. However, for cobalt(III) ammine complexes, reaction (4.1) generally proceeds through the intermediate solvent complex. For example, in water, the sequence



usually occurs. Few direct displacements of Y by Y have been observed in these systems.²³

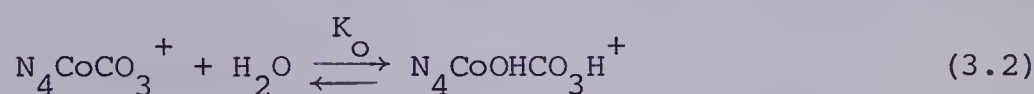
However, previous work^{47,48} on the exchange of carbon between free carbonate ion and $(NH_3)_5CoCO_3^+$ had shown that, as well as the normal aquation path, (4.2), a direct carbonate-carbonate exchange occurred. This latter path was indicated by the dependence of the exchange rate on the carbonate ion concentration. Recently, Harris⁵⁰ has reinterpreted these results as being due to the rate controlling reactions



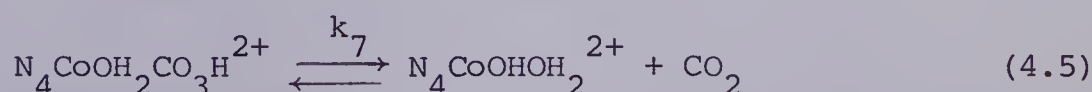


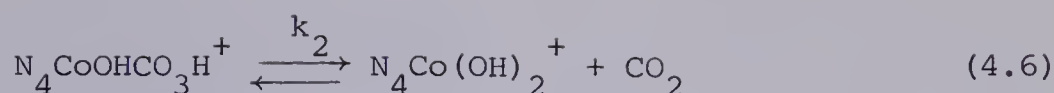
These reactions equilibrate the CO_2 released from decarboxylation of $(\text{NH}_3)_5\text{CoCO}_3^+$ with the free carbonate added to the system. The fit of the data⁴⁷ to this mechanism was not good at the lower pH's. Also the values of the specific rate constants for reactions (4.3) and (4.4) are not definitely agreed upon.¹²⁶ For these reasons the exchange of solvent oxygen with NaHCO_3 and with $(\text{NH}_3)_5\text{CoCO}_3^+$ was studied by using oxygen-18 enriched water to tag the solvent oxygens. Since the NaHCO_3 and $(\text{NH}_3)_5\text{CoCO}_3^+$ exchange studies are performed under exactly the same experimental conditions, they can be directly compared and should indicate the validity of Harris' mechanism since the rate of incorporation of solvent oxygen into $(\text{NH}_3)_5\text{CoCO}_3^+$ must be governed by the same reactions as the incorporation of carbon.

Studies of the detailed stoichiometric mechanism for the acid hydrolysis of $\text{N}_4\text{CoCO}_3^+$ ions, as discussed in Chapter 3, indicate that the ring-opening reaction, (3.2)



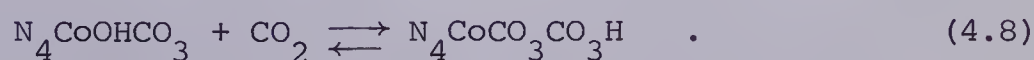
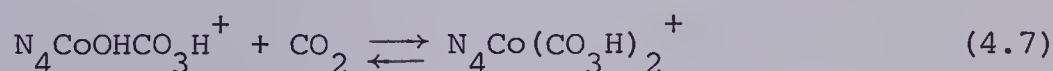
or one or both of two possible decarboxylation reactions, (4.5) and/or (4.6)





could be rate determining with respect to loss of CO_2 at near neutral pH's where the acid and base catalyzed ring-opening reactions are not important. The neutral ring-opened species, $(\text{en})_2\text{CoOHCO}_3$, has been shown in Chapter 1 to be relatively unreactive with respect to decarboxylation. Thus, if reactions (4.3) and (4.4) are not rate controlling with respect to incorporation of ^{14}C or ^{18}O , then exchange studies using $^{14}\text{CO}_3^{=}$ or $^{18}\text{OH}_2$ may allow independent checks of the values of the rate constants involved in reaction (3.2) or reactions (4.5) or (4.6), depending on the rate controlling reaction.

The exchange of ^{14}C between free carbonate and various $\text{N}_4\text{CoCO}_3^+$ ions has been extensively studied for N_4 equal to $(\text{NH}_3)_4$,^{127,128} $(\text{en})_2$,¹²⁹ $(\text{pn})_2$,⁴⁸ $(\text{tn})_2$,¹³⁰ *cis*- $(\text{NH}_3)_2\text{en}$ ^{100,131} and *trans*- $(\text{NH}_3)_2\text{en}$.¹⁰⁰ In all cases the rate law is first-order in [complex], $[\text{H}^+]$, and free $[\text{CO}_3^{=}]$. The data for all of these systems has recently been reinterpreted^{44,100} and the rate controlling reactions for $^{14}\text{CO}_3^{=}$ exchange taken to be reactions (4.5) and (4.6) along with two direct carbonate exchange reactions involving monodendate dicarbonato species

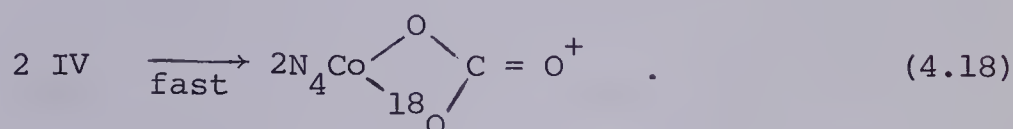
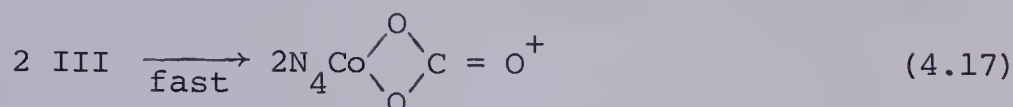
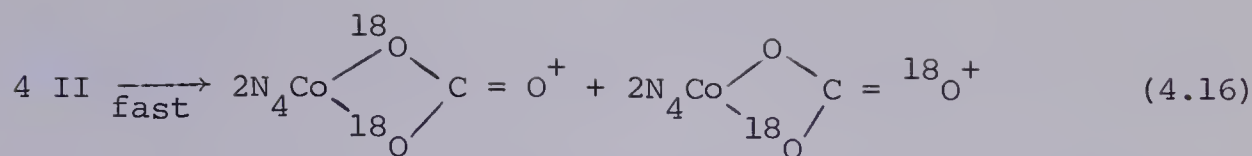


The $\text{CO}_3^{=}$ ion independent portion of the rate is given by

$$\frac{R}{[\text{complex}]} = \frac{k_7 K_O [H^+]}{K_1} + k_2 K_O \quad (4.9)$$

where K_1 is the acid dissociation constant for the $N_4CoOH_2CO_3H^{2+}$ ion. The values of K_O and K_1 for the $(en)_2CoCO_3^+$ system are estimated to be 1×10^{-3} and 4.8×10^{-6} M, respectively.⁵¹ Analysis of the data for the $(en)_2CoCO_3^+$ system yields a value for k_2 of $2.46 \times 10^{-3} \text{ sec}^{-1}$.¹³² The value of k_7 has been estimated as approximately $\sim 2 \text{ sec}^{-1}$ at 20° .⁵² Unfortunately, the exchange of ^{14}C between free carbonate and the $(en)_2CoCO_3^+$ ion was not studied over a wide enough pH range to estimate k_7 directly. However, the study of the *cis*-(NH_3)₂ $enCoCO_3^+ - ^{14}CO_3^{=}$ exchange over a wide pH range has provided an estimate for k_7 of 0.45 sec^{-1} which is in fair agreement with the value of $\sim 2 \text{ sec}^{-1}$ measured directly⁵² for the similar $(en)_2CoCO_3^+$ complex. Thus there remains little doubt that reactions (4.5) and (4.6) are rate controlling for the exchange of carbon between free carbonate and $N_4CoCO_3^+$ species.

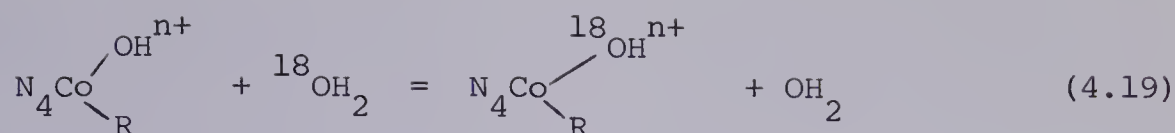
The exchange of oxygen between water and the $(NH_3)_4CoCO_3^+$ ion has been studied¹³³ and the rate was found to be first-order in $[\text{complex}]$, independent of $[H^+]$, and sensitive to the concentration of borax buffer used. All three oxygens in the complex were found to exchange at the same rate. The rate constant, $k_2 [H_2O]^n$, for the incorporation of *one* solvent oxygen into the complex at 24.8° was $3.00 \times 10^{-5} \text{ sec}^{-1}$ for those runs for which pH was reported and $1.80 \times 10^{-5} \text{ sec}^{-1}$ for those runs for which the pH was not reported. The value of $k_2 [H_2O]^n$ for free carbonate was found to be $4.21 \times 10^{-4} \text{ sec}^{-1}$ thus eliminating the possibility of reactions (4.3) and (4.4)



Analysis of the CO_2 acid hydrolysis products would give 0.75 solvent oxygens per ring-opening/ring-closing event. However, if the reverse of reaction (4.10) is fast enough to compete with reaction (4.11) for the $\text{N}_4\text{Co}^{18}\text{OHCO}_3\text{H}^+$ species, much less than 0.75 solvent oxygens would be incorporated per ring-opening/ring-closing event and the observed exchange rate constant would be less than that directly measured in an acid hydrolysis study. Thus the lack of agreement between the observed exchange rate constant of $3.0 \times 10^{-5} \text{ sec}^{-1}$ and the value of $1.4 \times 10^{-4} \text{ sec}^{-1}$ measured in a direct acid hydrolysis study⁹³ could be explainable.

Again assuming the mechanism outlined in reactions (4.10) to (4.18), the value of $k_2[\text{H}_2\text{O}]$ of $5.40 \times 10^{-5} \text{ sec}^{-1}$ measured in the base hydrolysis of $(\text{en})_2\text{CoCO}_3^+$ reported in Chapter 2, compares fairly well with O'Dell's value of $3.0 \times 10^{-5} \text{ sec}^{-1}$, considering the difference in ammine ligands.

Still another explanation is possible involving carbon-oxygen bond cleavage in reaction (4.10) as was mentioned in Chapter 2. This would require an exchange of the type



where R could be either OH_2 or CO_3H^- , to incorporate solvent oxygen in the Co-O-C position. When R is OH^- or OH_2 , the water exchange rates are 3.0×10^{-5} and $\sim 4.6 \times 10^{-4} \text{ sec}^{-1}$, respectively.⁷⁴ The exchange rate for $\text{R} = \text{CO}_3\text{H}^-$ could be expected to fall between these two values since hydroxide ion is a strongly labilizing ligand¹³⁴ and water is a weak one. Thus the observed rate constant of $3.0 \times 10^{-5} \text{ sec}^{-1}$ is also consistent with reaction (4.19) being the rate controlling step.

Although it seems likely that the exchange reactions of ^{14}C are controlled by the decarboxylation reactions, as suggested by Harris,¹⁰⁰ the above discussion points out several possible alternative mechanisms for the ^{18}O exchange. The study of the oxygen exchange between ^{18}O enriched water and $(\text{en})_2\text{CoCO}_3^+$, reported here, should resolve these ambiguities and possibly provide independent measurements of some of the rate constants.

Experimental

Oxygen Exchange Between Sodium Bicarbonate and Oxygen-18 Enriched Water

Oxygen-18 enriched H_2O of 1.58 atom % ^{18}O was obtained from Bio-Rad Laboratories, Richmond, Calif. After an exchange run, the water was recovered by distillation on a high vacuum system and purified by distillation from alkaline potassium permanganate in an all-glass apparatus. In this manner, the original oxygen-18 enriched water could be cycled three times before the isotope was too dilute to use.

Reagent grade sodium bicarbonate (Shawinigan) was used without further purification. Reagent grade 70% perchloric acid (Baker and Adamson) was used. Reagent grade anhydrous sodium perchlorate (G. Fredrick Smith Chemical Co.) was used to control the ionic strength of the reaction solutions.

The reaction solution temperature was controlled by keeping the reaction vessel in a Colora (Papst) constant temperature bath.

All unenriched water was redistilled from a Corning AGLb Water Still.

pH measurements were taken on a Beckman Expandomatic pH Meter equipped with an Expandomatic Range Selector and a combination probe electrode (Cat. #13-639-91, Fisher Scientific Co., Ltd., Edmonton, Alberta). A 2.0 M NaCl solution was used as the electrode electrolyte to prevent unstable pH readings caused by precipitation of KClO_4 which occurred when using the normal electrolyte, saturated KCl.

The pH meter was standardized with Certified Buffer Solution (Fisher Scientific Co., Ltd.).

For each run, an enriched (in $^{18}\text{OH}_2$) and an unenriched buffer solution (10 ml volumetric) were prepared by dissolving 0.17 gm of 2-amino-2-(hydroxomethyl)-1,3-propanediol (Eastman Organic Chemicals), henceforth called THM, in five ml of enriched water or unenriched re-distilled water, titrating to the required pH with 1.0M HClO_4 , and diluting to volume with water.

The reaction solution was made by weighing 1.08 gm NaClO_4 plus 0.015 gm NaHCO_3 into a 10 ml volumetric flask and dissolving the salts in a minimum amount (1 ml) of the unenriched buffer. The solution was temperature equilibrated in the water bath and at zero time, it was diluted to volume with the enriched buffer which had been previously temperature equilibrated.

Because the unprotonated form of THM is non-ionic, the ionic strength of the reaction solution varied from 1.00 at pH 7 to 0.888 at pH 9. However since at least one of the reactants (CO_2) in the rate controlling reactions is neutral, no primary kinetic salt effect was expected.

At appropriate times, 0.8 ml samples of the reaction solution were syringed into a nitrogen bubbler containing 0.5 ml 70% HClO_4 . The nitrogen stream carried the released carbon dioxide through a cold trap containing either mossy zinc (Fisher Scientific Co. Ltd.) or magnesium turnings (The British Drug Houses, Ltd.) which was cooled by a Dry Ice-acetone bath in order to remove water. The

nitrogen stream continued through a U-trap cooled by liquid nitrogen which trapped the CO_2 . After 5-10 minutes, the nitrogen stream was diverted and the U-trap evacuated to low pressure (5×10^{-6} torr, Pirani gauge, Consolidated Vacuum Corporation, Rochester, New York) with a combined oil and mercury diffusion pumping system. The CO_2 was then transferred to an evacuated sample tube immersed in liquid nitrogen, after having replaced the U-trap liquid nitrogen bath with a Dry Ice-acetone bath to prevent any residual water from being transferred. Figure 4.1 shows a schematic view of the apparatus.

After a sample had been withdrawn, the reaction vessel, which was capped with a rubber serum cap, was flushed with nitrogen to remove any O_2 or CO_2 from the atmosphere above the solution.

During the reaction, a one ml sample of the reaction solution was withdrawn and its pH measured at room temperature. The solution was degassed on the high vacuum line and the solvent distilled into the special sample tube. Gaseous unenriched CO_2 from a storage bulb was also distilled into this tube. The amount of CO_2 added to the tube gave a sample size similar to that of the reaction solution sample. The closed tube was heated at 80° for 10-20 hours and then the CO_2 distilled into a normal sample tube, ready for mass spectroscopic analysis. During the CO_2 transfer, the special sample tube was surrounded by a Dry Ice-acetone bath to prevent water transfer. This special sample of CO_2 was analyzed and used as the infinite time or solvent ^{18}O enrichment sample. Unenriched CO_2 from the storage bulb was distilled directly into a sample tube, analyzed, and used

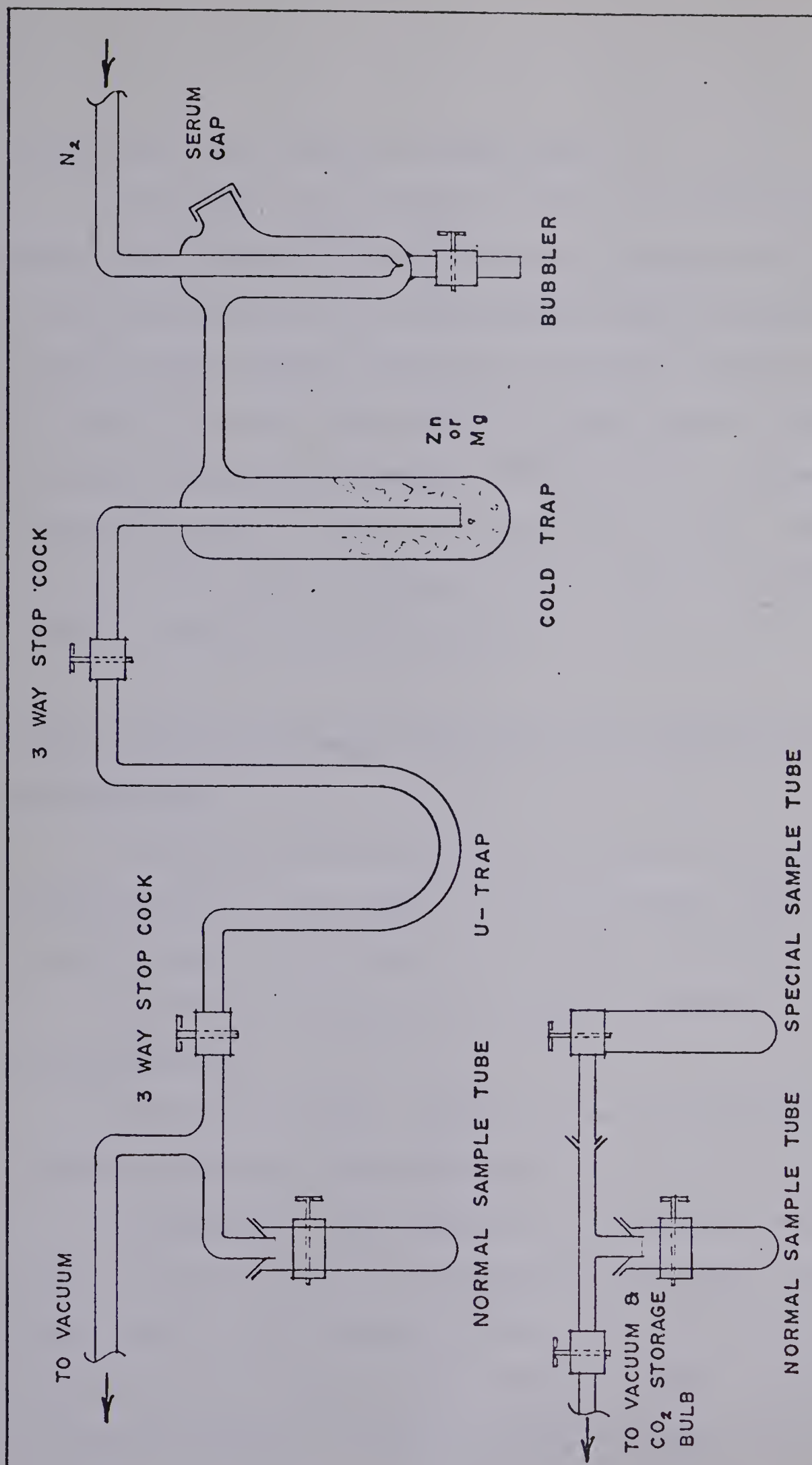


Figure 4.1: Schematic Diagram of the Sampling Apparatus used in Oxygen-18 Exchange and Tracer Experiments.

as the zero time or normal unenriched sample.

The samples were analyzed for $C^{16}O^{16}O$ and $C^{16}O^{18}O$ on a C.E.C. Model 21-614 low-resolution mass spectrometer equipped with a Penning-type pressure gauge on the inlet system (No. EW230a, Atlas MAT and Analysentechnik, Bremen, Germany) and a Honeywell Electronik 15 recorder. The average intensity ratio of the 44-46 mass peaks from three scans was used to determine the ratio $R = C^{16}O^{18}O / C^{16}O^{16}O$. The maximum experimental error for values of R was found to be $\pm 2\%$. The value of R for carbon dioxide of normal isotopic abundance was found to be 0.00401 ± 0.00005 (standard deviation).

Oxygen Exchange Study Between $(NH_3)_5CoCO_3^+$ Ion and Oxygen-18 Enriched Water

The carbonatopentaamminecobalt(III) nitrate used was from the same preparation as that used for the base hydrolysis study. Its preparation and characterization are described in Chapter 2.

All reagents and chemicals used were as described in the previous section.

The general procedure used was the same as described in the previous section except as noted below.

The THM buffers were prepared as in the previous section except that 1.06 gms of anhydrous sodium perchlorate was added to each buffer before titration and dilution to 10 mls. This was done to allow easy dissolution of the complex in the unenriched buffer. The reaction solution was prepared by weighing 0.04 gms of complex into a 10 ml

volumetric flask, dissolving the complex in a minimum amount of unenriched buffer (1 ml) and diluting the solution to volume with enriched buffer at zero time.

The sampling procedure and the apparatus was the same as that described in the previous section.

Oxygen Exchange Study Between $(en)_2CoCO_3^+$ Ion and Oxygen-18

Enriched Water

The preparation, characterization, and storage of the carbonato-bis(ethylenediamine)cobalt(III) chloride has been previously described in Chapter 2.

The general procedure and apparatus was the same as that in the previous sections except as noted below.

The unenriched THM buffer was made up without $NaClO_4$.

A stock solution was made containing 0.16657 gm complex diluted to 5 ml with unenriched buffer.

1.00 ml of the stock solution was syringed at zero time, into a volumetric flask containing 24.00 ml of an enriched buffer and enough anhydrous $NaClO_4$ to give a final $[NaClO_4]$ of 0.87 M.

Samples of the reaction solution were taken by syringing 2.0 ml into the bubbler containing 0.5 ml of 70% $HClO_4$.

Results

Oxygen Exchange Between Sodium Bicarbonate and Oxygen-18 Enriched Water

The general theory of exchange reactions involving species having more than one equivalent exchangeable atom is developed in Appendix B. Figure 4.2 shows both the exchange reactions, denoted by $=$, and the chemical equilibria, denoted by \rightleftharpoons , which are possible in the sodium bicarbonate-water system. Examination of Figure 4.2 shows that there are 4 different possible exchange systems. These are treated by the method developed in Appendix B. Let the central species in H_2CO_3 , HCO_3^- , $\text{CO}_3^{=}$, and CO_2 be called A_1 , A_2 , A_3 , and A_4 , respectively. The following definitions apply;

$$\begin{aligned}
 R_{Ti} &= \text{the rate of reaction between all } A_i \text{ species} \\
 &\quad \text{and all } \text{OH}_2 \text{ species} \\
 &= \text{the number of reactions of } A_i \text{ with water per} \\
 &\quad \text{unit time}
 \end{aligned}
 \tag{4.20}$$

$$\begin{aligned}
 R_T &= \text{the total number of reactions of } A, (A_1 \text{ or} \\
 &\quad A_2 \text{ or } A_3 \text{ or } A_4), \text{ species with water species} \\
 &\quad \text{per unit time} \\
 &= R_{T1} + R_{T2} + R_{T3} + R_{T4}
 \end{aligned}
 \tag{4.21}$$

$$\begin{aligned}
 a_1 &= \text{the concentration of O, } (^{16}\text{O} + ^{18}\text{O}), \text{ in the} \\
 &\quad A_1 \text{ form (gm atom l}^{-1}\text{)} \\
 &= 3[A_1^{18}\text{O}_3] + 3[A_1^{18}\text{O}_2^{16}\text{O}] + 3[A_1^{18}\text{O}^{16}\text{O}_2] \\
 &= 3 \cdot \text{initial molar concentration of } A_1
 \end{aligned}
 \tag{4.22}$$

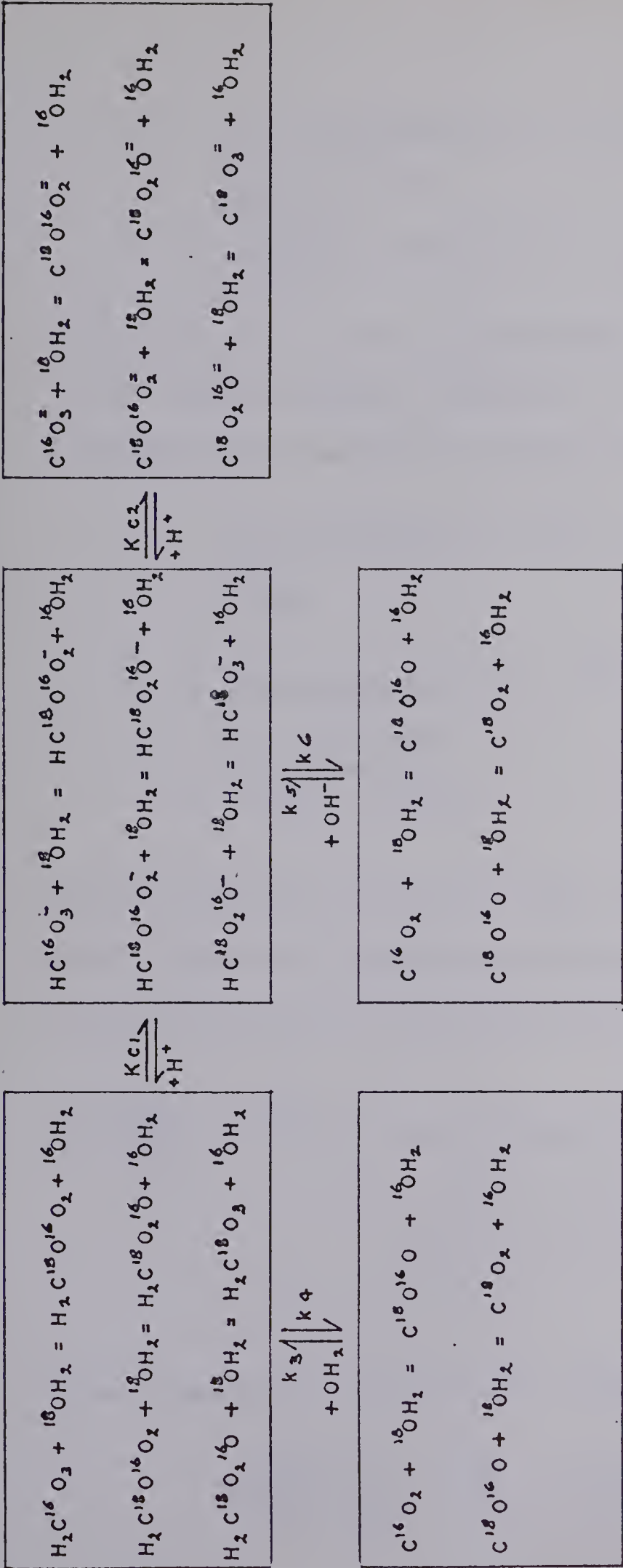


Figure 4.2: Exchange Systems and Chemical Equilibria for the Exchange of Oxygen Between Sodium

Bicarbonate and Water.

$$\begin{aligned}
 x_1 &= \text{the concentration of } ^{18}\text{O} \text{ in the } A_1 \text{ form} \\
 &\quad (\text{gm atom l}^{-1}) \\
 &= 3[A_1^{18}\text{O}_3] + 2[A_1^{18}\text{O}_2^{16}\text{O}] + [A_1^{18}\text{O}^{16}\text{O}_2] \quad .
 \end{aligned}
 \tag{4.23}$$

Let a_2 , a_3 , a_4 , x_2 , x_3 , and x_4 be similarly defined. Note that for A_4 (CO_2), the stoichiometric factor is 2. Let b and y be defined as in Appendix B substituting OH_2 for BX so that

$$\begin{aligned}
 y &= \text{the concentration of } ^{18}\text{O} \text{ in the water form} \\
 &= [^{18}\text{OH}_2]
 \end{aligned}
 \tag{4.24}$$

$$\begin{aligned}
 b &= \text{the concentration of O, } (^{18}\text{O} + ^{16}\text{O}), \text{ in} \\
 &\quad \text{the water form} \\
 &= [^{18}\text{OH}_2] + [^{16}\text{OH}_2] \quad .
 \end{aligned}
 \tag{4.25}$$

Since at any time all the species, H_2CO_3 , HCO_3^- , $\text{CO}_3^{=}$, and CO_2 , are present, they are all sampled when the solution is acidified. Thus the observed concentration-time differential is

$$\frac{d(x_1 + x_2 + x_3 + x_4)}{dt} = \text{rate of formation of all } ^{18}\text{O} \tag{4.26}$$

containing A species-rate of
destruction of all ^{18}O containing
A species.

Following exactly the methods used in Appendix B results in

$$\log\left(\frac{x_\infty - x}{x_\infty - x_0}\right) = -\frac{R_T}{2.303} \left(\frac{a + b}{ab}\right) t \tag{4.27}$$

where

$$a = \sum_{i=1}^4 a_i \quad (4.28)$$

and

$$x = \sum_{i=1}^4 x_i \quad (4.29)$$

Now it is necessary to replace the gm atom l^{-1} concentrations by the known molar concentrations.

$$a = 3[H_2CO_3] + 3[HCO_3^-] + 3[CO_3^{=}] + 2[CO_2] = GT \quad (4.30)$$

where T = initial concentration of $NaHCO_3$ and the G factor is defined as

$$G = (3[H_2CO_3] + 3[HCO_3^-] + 3[CO_3^{=}] + 2[CO_2])/T \quad (4.31)$$

Thus equation (4.27), under the condition of large excess of b , becomes

$$\log \left(\frac{x_{\infty} - x}{x_{\infty} - x_0} \right) = - \frac{R_T t}{2.303GT} \quad (4.32)$$

Now it is necessary to relate the experimentally measured mass 46/44 ratios R , R_{∞} , and R_0 and time to equation (4.32).

The analysis method (acidification) drives the equilibrium system shown in Figure 4.2 to the bottom by removing CO_2 in the nitrogen stream. No enrichment of the CO_2 species occurs upon acidification, relative to its parent molecules, H_2CO_3 , HCO_3^- , or $CO_3^{=}$, since these species lose an oxygen to the solvent when acidified. This amounts to a random picking of two oxygens and a carbon from the parent species. Thus the "sampling

reaction" samples each oxygen from the parent species. Since the % ^{18}O of the solvent is measured by the R value of an equilibrated CO_2 sample, R_∞ , 100% incorporation of the solvent oxygen into the molecule is indicated when the R value of sample CO_2 reaches R_∞ . This indicates that both the oxygens in the CO_2 are solvent derived even though only one is an oxygen-18 isotope.

Equation (4.32) requires measurement of the gm atom l^{-1} concentration of oxygen-18 in all A species. The mass spectral peak height for the $\text{C}^{16}\text{O}^{18}\text{O}$ peak (46 a.m.u.) is directly proportional to the *amount* of $\text{C}^{16}\text{O}^{18}\text{O}$ in the sample. The 44 peak height is directly proportional to the *amount* of $\text{C}^{16}\text{O}^{16}\text{O}$ in the sample. The ratio of the peak heights, 46/44, gives the ratio of the $^{18}\text{O}/^{16}\text{O}$ gm atom l^{-1} *concentrations* in the sample, which is defined as R. The required expression is

$$\frac{X_\infty - X}{X_\infty - X_\text{O}} = \frac{X_\infty/a - X/a}{X_\infty/a - X_\text{O}/a} \quad (4.33)$$

Define $R' = [^{18}\text{O}]/([^{18}\text{O}] + [^{16}\text{O}]) = X/a \quad (4.34)$

then $R' \approx R = [^{18}\text{O}]/[^{16}\text{O}] = 46/44 \quad (4.35)$

when $[^{16}\text{O}] \gg [^{18}\text{O}]$. This assumption will be true only when ^{18}O enriched water of less than 10% ^{18}O is used, which was always the case for these experiments. Therefore

$$\frac{X_\infty - X}{X_\infty - X_\text{O}} = \frac{R'_\infty - R'}{R'_\infty - R'_\text{O}} \approx \frac{R_\infty - R}{R_\infty - R_\text{O}} \quad (4.36)$$

Now define

$$(1-F) = \frac{R_{\infty} - R}{R_{\infty} - R_0} \quad (4.37)$$

and

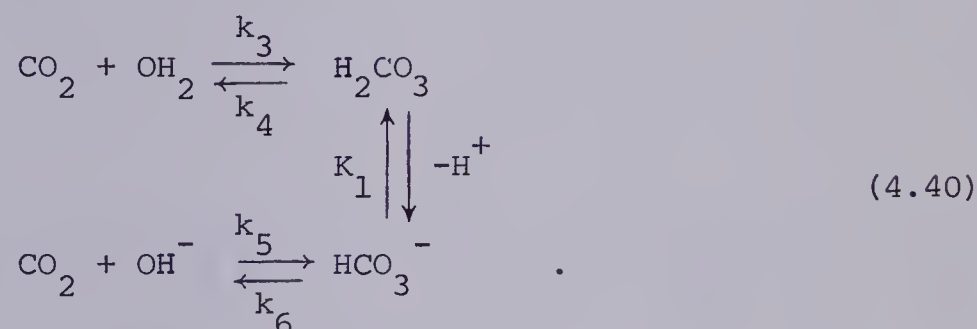
$$k_{\text{obsd}} = \frac{.693}{t_{1/2}} = \frac{R_T}{GT} \quad (4.38)$$

so that (4.32) becomes

$$\log(1-F) = - \frac{k_{\text{obsd}} t}{2.303} . \quad (4.39)$$

Figure 4.3 shows a typical plot of $\log(1-F)$ vs. time, which is linear as predicted by (4.39).

The chemical path for exchange of ^{18}O is postulated as



This scheme implies $R_{T3} = 0$, i.e. $\text{CO}_3^{=}$ does not directly exchange oxygens with water but only incorporates solvent oxygen via the acid-base equilibria and the reactions in equation (4.40). Since the system is at *chemical* equilibrium, the *net* rate of production of any chemical species is zero but the *dynamic* rate (i.e. the number of reactions/unit time) is not. Thus

$$-\frac{1}{2} \frac{d[\text{CO}_2]}{dt} = -\frac{d[\text{OH}_2]}{dt} = -\frac{d[\text{OH}^-]}{dt} = \frac{d[\text{H}_2\text{CO}_3]}{dt} = \frac{d[\text{HCO}_3^-]}{dt} = 0 . \quad (4.41)$$

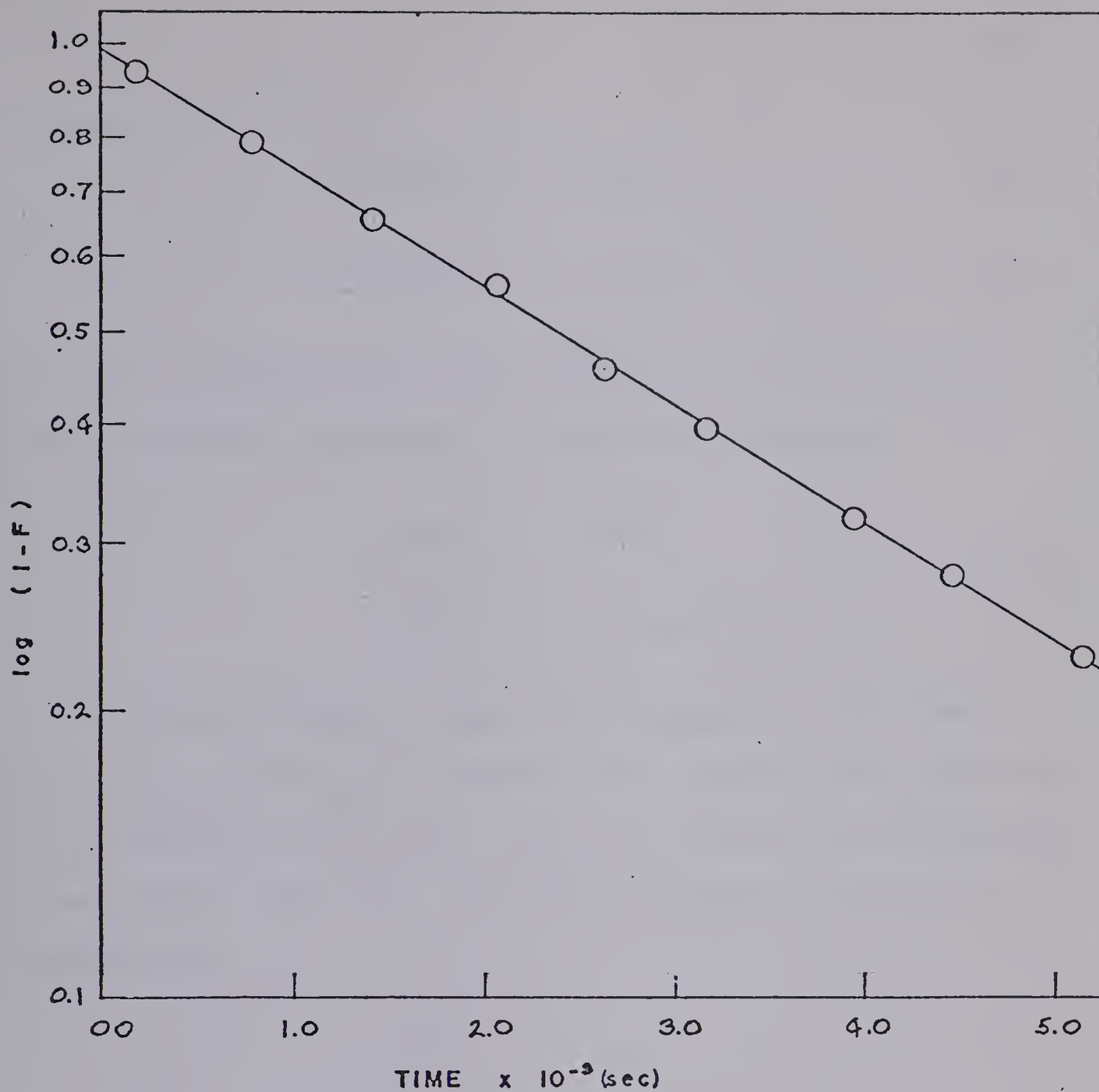


Figure 4.3: Variation of $\text{Log}(1-F)$ with Time for the Exchange of Oxygen Between NaHCO_3 and OH_2 at 26° .
 $\text{pH} = 7.705$, $[\text{T}] = 2.72 \times 10^{-3} \text{ M}$.

therefore

$$k_3 [\text{CO}_2] [\text{OH}_2] = k_4 [\text{H}_2\text{CO}_3] \quad (4.42)$$

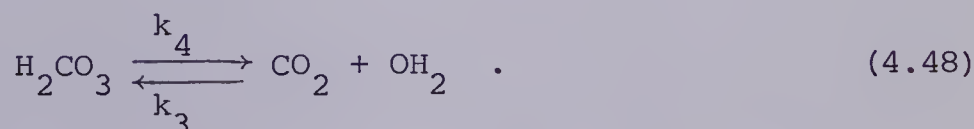
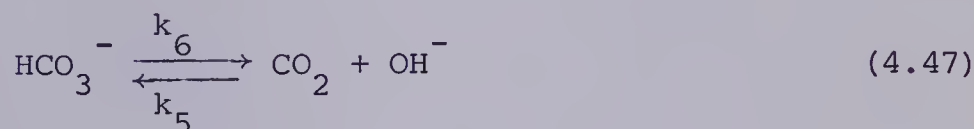
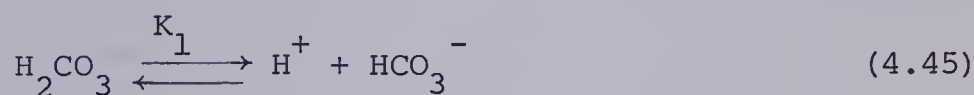
and

$$k_5 [\text{CO}_2] [\text{OH}^-] = k_6 [\text{HCO}_3^-] \quad (4.43)$$

The number of reactions per unit time occurring in a forward sense equals the number occurring in a reverse sense. Therefore

$$\begin{aligned} R_T &= k_4 [\text{H}_2\text{CO}_3] + k_6 [\text{HCO}_3^-] \\ &= k_3 [\text{CO}_2] [\text{OH}_2] + k_5 [\text{CO}_2] [\text{OH}^-] \end{aligned} \quad (4.44)$$

In order to directly compare the experimental R_T with the theoretical R_T and hence get values for the various kinetic parameters, it is necessary to write $[\text{HCO}_3^-]$ and $[\text{H}_2\text{CO}_3]$ as functions of the known concentrations T and $[\text{H}^+]$. The chemical equilibria which must be considered are



The apparent first dissociation constant for carbonic acid, K_{c1} , relates (4.45) and (4.48) by

$$K_{c1} = \frac{K_1}{1 + k_4/k_3} \quad (4.49)$$

The complete derivation, given in Appendix C, results in

$$[\text{HCO}_3^-] = \frac{K_{c1} T}{[\text{H}^+] + K_{c1} + \frac{K_{c1} K_{c2}}{[\text{H}^+]}} \quad (4.50)$$

and

$$[\text{H}_2\text{CO}_3] = \frac{\left\{ 1 - \frac{K_{c1} k_6}{K_w k_5} \right\} [\text{H}^+] T}{[\text{H}^+] + K_{c1} + \frac{K_{c1} K_{c2}}{[\text{H}^+]}} \quad (4.51)$$

In the pH region, 7 to 9, and using values of 9.13×10^{-7} M, 2.75×10^{-10} M, and 1.7×10^{-14} M for K_{c1} ,⁷² K_{c2} ,⁴⁹ and K_w ,⁷⁰ respectively, none of the terms in the denominator are negligible nor is the denominator constant.

Thus equation (4.44) becomes

$$R_T = \left\{ \frac{k_4 \left\{ 1 - \frac{K_{c1} k_6}{K_w k_5} \right\} [\text{H}^+]}{K_{c1} + [\text{H}^+] + \frac{K_{c1} K_{c2}}{[\text{H}^+]}} + \frac{k_6 K_{c1}}{K_{c1} + [\text{H}^+] + \frac{K_{c1} K_{c2}}{[\text{H}^+]}} \right\} T \quad (4.52)$$

and since

$$R_T = k_{\text{obsd}} GT \quad (4.53)$$

directly comparing (4.52) to (4.53) and solving for k_{obsd} gives

$$k_{\text{obsd}} = \frac{1}{G} \left\{ \frac{k_4 \left\{ 1 - \frac{K_{\text{cl}} k_6}{K_w k_5} \right\} [\text{H}^+] + k_6 K_{\text{cl}}}{K_{\text{cl}} + [\text{H}^+] + \frac{K_{\text{cl}} K_{\text{c2}}}{[\text{H}^+]}} \right\} . \quad (4.54)$$

The experimental data was fitted to (4.54) using the program ENLLSQ. Since G is a function of the rate constants, the equilibrium constants, $[\text{H}^+]$, and T , it must be calculated from estimated values of these parameters. G was calculated from (4.31), (4.50), (4.51), and equations for $[\text{CO}_3^{=}]$ and $[\text{CO}_2]$, which are given in Appendix C. Values for the parameters K_w , K_{cl} , K_{c2} , and k_4 were estimated for the experimental conditions and held constant while k_5 and k_6 were allowed to vary to obtain the best, self-consistent fit of (4.54) (including the G factor) to the experimental values of k_{obsd} , $[\text{H}^+]$, and T .

Since only two of the three kinetic parameters, k_4 , k_5 , and k_6 , can be independently determined from the data, it was necessary to decide which parameter to constrain to an estimated known value. The decision to estimate k_4 and hold it constant was based on some trial fits and on the fact that a fairly good estimate of k_4 was available.¹³⁵ The trial fits showed that constraining either k_5 or k_6 resulted in very unreasonable values for k_4 . It was also found that the values of k_5 and k_6 were fairly insensitive to changes in k_4 . Thus even if the estimated value of k_4 was slightly in error, the resultant values of k_5 and k_6 should be quite accurate.

The value of k_4 was estimated by using the value of Berger *et al*¹³⁵ at 25 and 37° and interpolating from a $\log (k_r/T)$ vs. $1/T$ plot

to obtain values at 20, 26, and 30°. The variation of k_4 with ionic strength at 25° was estimated¹³⁶ from Berger's data to be

$$\log k_4 = C - 0.187 \mu \quad (4.55)$$

where ; μ = ionic strength

C = a constant.

The value of the constant was determined from the value of k_4 at 0.11 ionic strength and then the value of k_4 at 1.0 ionic strength was calculated. Any effect on k_4 caused by changing the medium from KCl to NaClO₄ was neglected.

The value of K_w was estimated by using

$$K_w(\text{NaClO}_4) = C \cdot K_w(\text{NaCl}) \quad (4.56)$$

The values of $K_w(\text{NaClO}_4)$ ⁷⁰ and $K_w(\text{NaCl})$, at 25°C and ionic strength of 1.0 in their respective mediums, were used to determine the value of the constant C (0.905). Then the values of $K_w(\text{NaCl})$ at 20, 26, and 30°C were used with equation (4.56) to determine values of $K_w(\text{NaClO}_4)$.

The values of K_{c1} used were determined by the same method used for K_w . The value of the proportionality constant was 0.767. The value of $K_{c1}(\text{NaClO}_4)$ at 25°C and ionic strength 1.0 used is given in reference (72). Using an empirical equation¹³⁷ relating K_{c1} and temperature allowed calculation of values at 20, 26, and 30°C and ionic strength 1.0 (NaCl).

Since the pH of the experiments was always <9, the amount of $\text{CO}_3^{=}$ in solution was always small. Thus the fitted values of k_5 and

k_6 were expected to be insensitive to reasonable changes in K_{c2} . Trial fits varying K_{c2} from 1.11×10^{-9} to 6.85×10^{-11} gave no variation in the values of k_5 or k_6 . Because of this insensitivity, the same value⁴⁹ of K_{c2} , 2.75×10^{-10} , was used for all three temperatures.

Table 4.1 gives the experimental data and the values of k_{obsd} calculated using (4.54) with the parameter values given in Table 4.2. The values of $[H^+]$, T , the G factor, % CO_2 , % HCO_3^- , and % $CO_3^{=}$, for each kinetic run are also given in Table 4.1.

Oxygen Exchange Between $(NH_3)_5CoCO_3^+$ Ion and Oxygen-18 Enriched Water

The general method used in the previous section is applied again. Let $(NH_3)_5Co^{n+} = R$. Then Figure 4.4 gives the system of equations describing the $(NH_3)_5CoCO_3^+ + {}^{18}OH_2$ system. In exactly the same manner as for the preceeding $NaHCO_3$ experiment, an equation for the total rate as a function of the species concentrations and k_{obsd} can be obtained. Let

$$R_T = R_{T1} + R_{T2} + R_{T3} + R_{T4} + R_{T5} + R_{T6} \quad (4.57)$$

where the number subscripts refer to H_2CO_3 , HCO_3^- , $CO_3^{=}$, CO_2 , $ROCO_2H$, and $ROCO_2$, respectively. The possible exchange of oxygen between ROH and OH_2 is not considered since the sampling procedure does not analyze the oxygen next to the Co and it is known¹³⁸ that the Co-O oxygen does not exchange through rotation, with the carbonyl oxygens. Let

TABLE 4.1

Experimental and Calculated Data for the Exchange of Oxygen Between NaHCO_3 and OH_2

Temp, °	$T \times 10^2, \text{ M}$	$[\text{H}^+] \times 10^8, \text{ M}$	$k_{\text{obsd}} \times 10^4, \text{ sec}^{-1}$	$k_{\text{calcd}} \times 10^4, \text{ sec}^{-1}$	G factor	% CO_2 HCO_3^- $\text{CO}_3^{=}$		
						CO_2	HCO_3^-	$\text{CO}_3^{=}$
20	2.60	0.872	0.722	0.749	2.990	1.02	95.9	3.07
	2.32	1.550	1.135	1.112	2.982	1.83	96.5	2.66
	2.80	2.345	1.565	1.529	2.972	2.76	96.1	1.13
	1.84	3.560	2.134	2.156	2.959	4.15	95.1	0.74
26	2.19	0.310	0.987	0.990	2.997	0.32	91.6	8.07
	1.94	0.662	1.515	1.426	2.993	0.72	95.3	3.97
	2.07	0.768	1.470	1.552	2.992	0.84	95.7	3.45
	2.22	1.260	2.165	2.127	2.986	1.38	96.5	3.11
	2.72	1.886	2.828	2.845	2.979	2.07	96.5	1.42
	2.02	2.440	3.460	3.428	2.974	2.62	96.3	1.07

TABLE 4.1 (Cont'd)

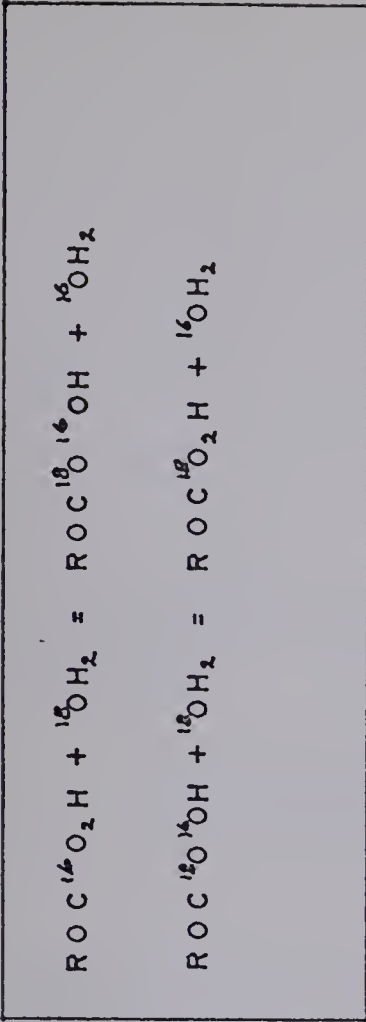
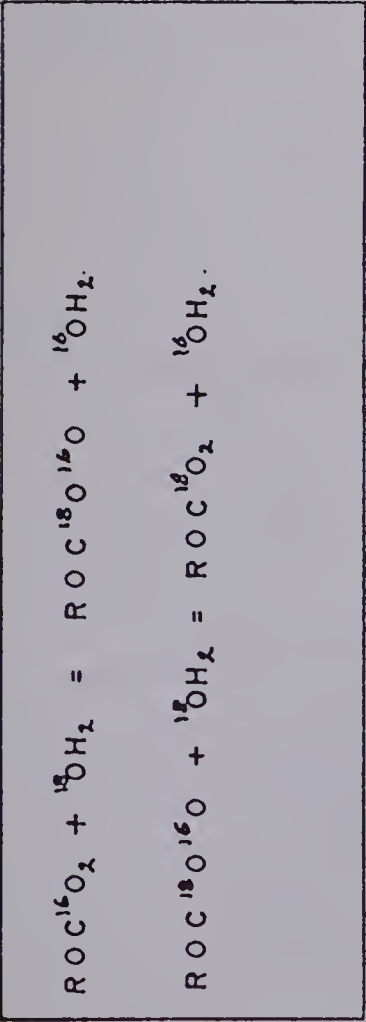
Temp, °	$T \times 10^2, M$	$[H^+] \times 10^8, M$	$k_{obsd} \times 10^4, sec^{-1}$	$k_{calcd} \times 10^4, sec^{-1}$	G factor	<div> <div>CO₂</div> <div>% HCO₃⁻</div> <div>CO₃⁼</div> </div>		
30	2.64	0.310	1.927	1.925	2.997	0.31	91.6	8.08
	1.97	0.538	2.348	2.389	2.995	0.55	94.6	4.84
	2.28	0.829	2.947	2.942	2.991	0.86	96.0	3.13
	2.44	1.350	4.005	3.901	2.986	1.41	96.6	1.98
	2.12	1.781	4.620	4.682	2.981	1.86	96.6	1.53

TABLE 4.2

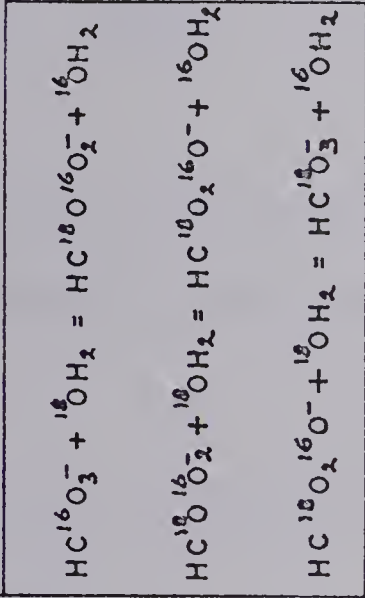
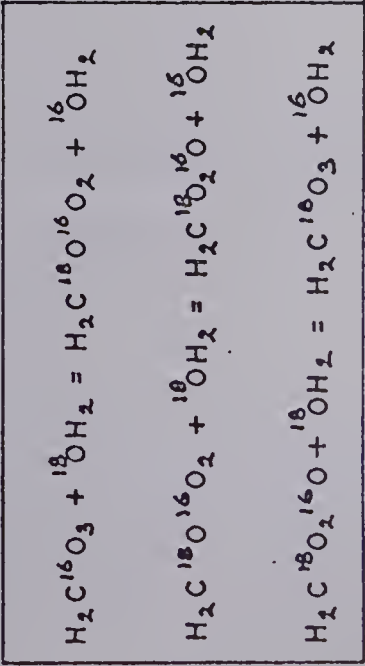
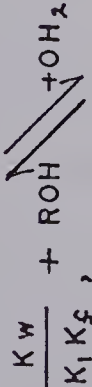
Best Fit Parameters with 95% Confidence Limits and Fixed Parameters for the
Exchange of Oxygen Between Sodium Bicarbonate and Water at 20, 26, and 30°

T, °	$k_5 \times 10^{-4}, \text{ M}^{-1} \text{ sec}^{-1}$	$k_6 \times 10^4, \text{ sec}^{-1}$	$k_4 \times 10^{-1}, \text{ sec}^{-1}$	$K_{\text{Cl}} \times 10^7, \text{ M}$	$K_{\text{C2}} \times 10^{10}, \text{ M}$	$K_{\text{W}} \times 10^{14}$
20	.679 (1.314-0.042) ^a	.971 (1.777-0.057)	1.016	8.150	2.750	1.103
26	1.056 (1.360-0.752)	2.150 (2.769-1.531)	1.806	8.790	2.750	1.792
30	1.734 (2.090-1.378)	4.583 (5.626-3.640)	2.602	9.220	2.750	2.442

^a Values in brackets are the 95% confidence limits calculated as described in Appendix A.



$$\frac{+H^+}{1/K_1}$$



$$\frac{K_{cl}}{+H^+}$$

$$\frac{K_{cl}}{+H^+}$$

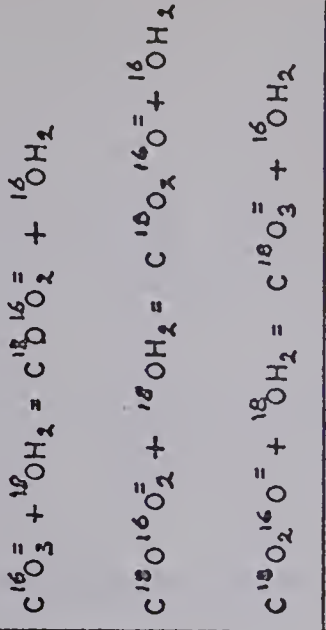
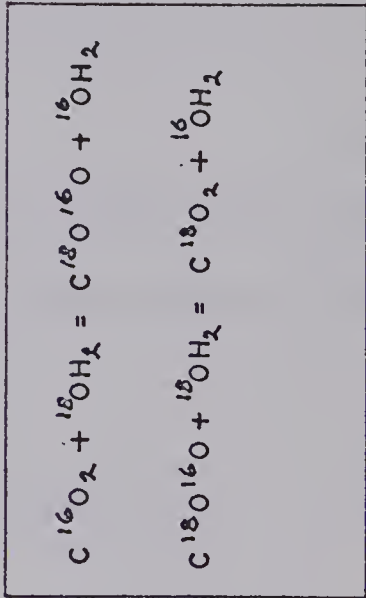
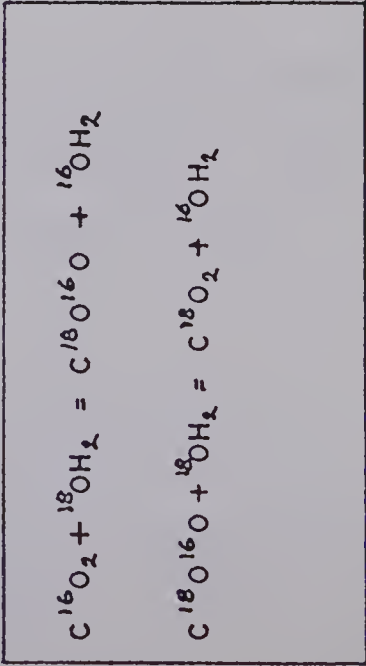
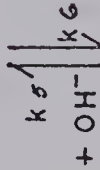
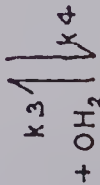


Figure 4.4: Exchange Systems and Chemical Equilibria for the Exchange of Oxygen Between

(NH₃)₅CoCO₃⁺ and OH₂.

$$X = \sum_{i=1}^6 X_i \quad (4.58)$$

and

$$a = \sum_{i=1}^6 a_i \quad (4.59)$$

After completing the derivation, the resultant equation, assuming $b \gg a$, is

$$\log \left(\frac{X_\infty - X}{X_\infty - X_0} \right) = - \frac{R_T t}{2.303} \left(\frac{1}{a_1 + a_2 + a_3 + a_4 + a_5 + a_6} \right) \quad (4.60)$$

Before converting the gm atom l^{-1} concentrations of ($^{18}\text{O} + ^{16}\text{O}$) into the known molar concentrations, it is necessary to note that for the complex species

$$\begin{aligned} a_6 &= 2[\text{ROC}^{18}\text{O}_2] + 2[\text{ROC}^{18}\text{O}^{16}\text{O}] + 2[\text{ROC}^{16}\text{O}_2] \\ &= 2[\text{ROCO}_2] \end{aligned} \quad (4.61)$$

This also applies for ROCO_2H , i.e. a_5 .

Since the complex hydrolyzes by carbon-oxygen bond cleavage²⁰ under acid conditions, the sampling method only samples 2 of the 3 oxygens in the complex. Substituting for a_i in terms of molar concentrations results in

$$\log(1-F) = - \frac{R_T t}{2.303} \left(\frac{1}{2[\text{ROCO}_2] + 2[\text{ROCO}_2\text{H}] + 3[\text{H}_2\text{CO}_3] + 3[\text{HCO}_3^-] + 3[\text{CO}_3^{=}] + 2[\text{CO}_2]} \right) \quad (4.62)$$

Defining

$$G = \frac{2[\text{ROCO}_2] + 2[\text{ROCO}_2\text{H}] + 3[\text{H}_2\text{CO}_3] + 3[\text{HCO}_3^-] + 3[\text{CO}_3^{=}] + 2[\text{CO}_2]}{T'} \quad (4.63)$$

where T' is the initial complex concentration results in

$$\log(1-F) = - \frac{R_T t}{2.303} \frac{1}{GT'} \quad (4.64)$$

and thus

$$R_T = k_{\text{obsd}} GT' \quad (4.65)$$

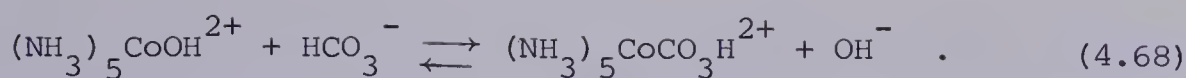
where

$$k_{\text{obsd}} = \frac{.693}{t_{1/2}} = \frac{R_T}{GT'} \quad (4.66)$$

If the rate controlling reactions for the exchange of oxygen between ROCO_2 and OH_2 are the same as the rate controlling reactions for the exchange of oxygen between NaHCO_3 and OH_2 , the rate will be given by (4.52). Comparing (4.52) and (4.65) results in

$$k_{\text{obsd}} = \frac{1}{T'G} \left\{ \frac{k_4 \left\{ 1 - \frac{K_{c1} k_6}{K_w k_5} \right\} [\text{H}^+] + k_6 K_{c1}}{K_{c1} + [\text{H}^+] + \frac{K_{c1} K_{c2}}{[\text{H}^+]}} \right\} T \quad (4.67)$$

where T is the total uncomplexed carbonates concentration at zero time. Notice that at zero time (w.r.t. exchange) some of the original complex has hydrolyzed hence there are some uncomplexed carbonates. Appendix C gives the derivation of the expressions giving $[\text{H}_2\text{CO}_3]$, $[\text{HCO}_3^-]$, $[\text{CO}_3^{=}]$, and $[\text{CO}_2]$ as functions of T' , $[\text{H}^+]$, K_{c1} , K_{c2} , k_5 , k_6 , K_w , K_1 (the acid dissociation constant for $(\text{NH}_3)_5\text{CoCO}_3\text{H}^{2+}$), and K_f , the formation constant for the reaction



Using these expressions allows calculation of T and the G factor.

The program ENLLSQ was used to fit the data to (4.67) to obtain best fit values for k_5 and k_6 at 20, 26, and 30°C. The values of the constant parameters k_4 , K_{c1} , K_{c2} , and K_w for each temperature were the same as those used for the NaHCO_3 study.

The value of K_1 at 20, 26, and 30°C was determined from values of k_1/K_1 ($\mu = 1.0$, NaClO_4) and k_1 ($\mu = 0.5$, NaClO_4) at each temperature. The values of k_1/K_1 were calculated from the activation parameters, ΔH^\ddagger (17.1 kcal mole⁻¹) and ΔS^\ddagger (+28.9 eu), given by Francis and Jordan.⁴⁹ The value of ΔS^\ddagger reported in the paper (+ 30.0 eu) is incorrect due to an arithmetic error. The values of k_1 were calculated from the data of Dasgupta and Harris⁵⁰ using the activation parameters, ΔH^\ddagger (16.75 kcal mole⁻¹) and ΔS^\ddagger (-1.93 eu). The ionic strength difference between the two studies was neglected.

The value of K_f used was 5.50×10^{-6} . This value was used for each temperature because no data was available on the temperature dependence of K_f . Trial fits at 26°C showed a mild sensitivity of k_5 and k_6 to the value of K_f . The fact that the temperature dependence for the formation constants of similar complexes^{37,39} is small plus the small temperature range makes the use of a single K_f value reasonable.

The program ENLLSQ was also used to calculate a predicted k_{calcd}^* using the best fit values of k_5 and k_6 from the NaHCO_3 study. This was done by forcing the convergence process to stop after one iteration.

Table 4.3 gives the values of k_{obsd} , k_{calcd} from best fit values of k_5 and k_6 , k_{calcd}^* from NaHCO_3 values of k_5 and k_6 , $[\text{H}^+]$, and $[\text{T}']$ at 20, 26, and 30°C, respectively. Table 4.4 gives the best fit values of k_5 and k_6 along with their 95% support plane confidence limits. Also given are the values of K_1 used for each temperature.

Since they are not given in Table 4.3, it may be useful to have an example of the self-consistent species concentrations which the program calculates in the process of fitting the data to equation (4.67). At 30.0° for a $[\text{H}^+]$ of 1.480×10^{-8} M and an initial complex concentration, T' , of 1.295×10^{-2} M, the calculated concentrations of ROCO_2 , ROCO_2H , H_2CO_3 , HCO_3^- , $\text{CO}_3^{=}$, and CO_2 are 4.61×10^{-3} , 2.08×10^{-4} , 5.01×10^{-6} , 7.86×10^{-3} , 1.46×10^{-4} , and 1.260×10^{-4} M, respectively. Thus the complex obviously hydrolyzes giving HCO_3^- as the major species, along with appreciable amounts of H_2CO_3 , $\text{CO}_3^{=}$, and CO_2 .

Comparing the best-fit values of k_5 and k_6 from the NaHCO_3 study to those of the $(\text{NH}_3)_5\text{CoCO}_3^+$ study, or the values of k_{calcd} to k_{calcd}^* in Table 4.3 shows that within the 95% confidence limits of the two studies, the exchange of oxygen-18 between water and HCO_3^- or $(\text{NH}_3)_5\text{CoCO}_3^+$ proceeds according to the same rate law.

Oxygen Exchange Between $(\text{en})_2\text{CoCO}_3^+$ Ion and Oxygen-18 Enriched Water

The exchange equations for this system are

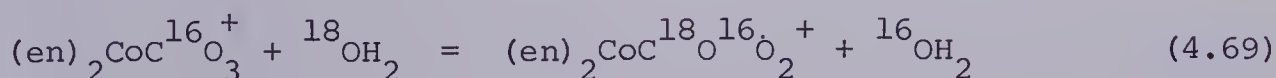


TABLE 4.3

Experimental and Calculated Data for the Exchange of Oxygen Between $(\text{NH}_3)_5\text{CoCO}_3^+$ and OH_2 at 20, 26, and 30°

Temp, °	$T' \times 10^2, \text{ M}$	$[\text{H}^+] \times 10^8, \text{ M}$	$k_{\text{obsd}} \times 10^4, \text{ sec}^{-1}$	$k_{\text{calcd}} \times 10^4, \text{ sec}^{-1}$	$k_{\text{calcd}}^* \times 10^4, \text{ sec}^{-1}$
20.0	1.188	6.030	2.330	2.312	2.312
	1.140	4.270	1.723	1.743	1.743
	1.356	2.500	1.042	1.063	1.063
	1.090	2.820	1.260	1.245	1.245
	1.402	1.380	0.660	0.662	0.662
26.0	1.160	1.098	0.577	0.591	0.591
	0.716	8.290	6.780	6.776	6.762
	0.578	6.175	5.410	5.548	5.494
	0.728	2.218	2.415	2.425	2.297
	0.783	1.150	1.490	1.572	1.427
	0.910	0.903	1.231	1.338	1.192
	1.012	0.279	0.781	0.815	0.678

TABLE 4.3 (Cont'd)

Temp, °	T'x10 ² , M	[H ⁺]x10 ⁸ , M	k _{obsd} x10 ⁴ , sec ⁻¹	k _{calcd} x10 ⁴ , sec ⁻¹	k _{calcd} [*] x10 ^{4a} , sec ⁻¹
30.0	1.295	1.480	2.350	2.363	2.277
	1.385	0.914	1.778	1.753	1.784
	1.348	0.604	1.440	1.436	1.530
	1.500	0.339	1.110	1.116	1.258

^a Calculated from the best fit values of k₅ and k₆ from the NaHCO₃ study.

TABLE 4.4

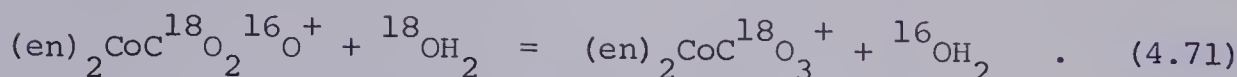
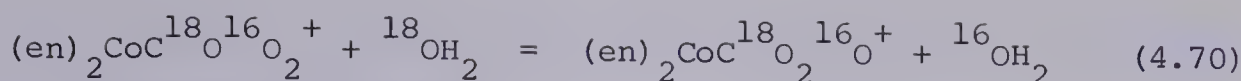
Best Fit Parameters with 95% Confidence Limits

for the Exchange of Oxygen Between $(\text{NH}_3)_5\text{CoCO}_3^+$ and OH_2 at 20, 26, and 30°

$T, ^\circ$	$k_5 \times 10^{-4}, \text{M}^{-1} \text{sec}^{-1}$	$k_6 \times 10^4, \text{sec}^{-1}$	$K_1^b \times 10^7, \text{M}$
20.0	0.679 (0.437-0.921)	0.971 (0.590-1.244)	3.47
26.0	1.254 (0.943-1.545)	2.552 (1.959-3.145)	3.30
30.0	1.372 (1.104-1.641)	3.629 (2.919-4.340)	3.20

^a Bracketed values are the 95% Confidence Limits as described in Appendix A.

^b K_1 is the value of the acid dissociation constant of $(\text{NH}_3)_5\text{CoCO}_3\text{H}^{2+}$ used in the fit.



These equations are treated by the method developed in Appendix B in the same way as in the two preceding studies. The plot of $\log(1-F)$ vs. time yields a value of an observed rate constant, k_{obsd} , which is related to the specific rate constant for the incorporation of one solvent oxygen into the complex

$$k_2[\text{H}_2\text{O}]^n = 3k_{\text{obsd}} \quad (4.72)$$

The results of the runs at 26.0° and ionic strength of 1.0 (NaClO_4) are

$k_2[\text{H}_2\text{O}]^n \times 10^5, \text{ sec}^{-1}$	$[\text{H}^+] \times 10^8, \text{ M}$	$[\text{complex}] \times 10^2, \text{ M}$
1.245	0.276	3.56
2.330	5.76	4.62

Assuming the decarboxylation reactions, (4.5) and (4.6) are rate controlling results in

$$k_2[\text{H}_2\text{O}]^n = \frac{k_7 K_O}{K_1} [\text{H}^+] + k_2 K_O \quad (4.73)$$

where the constants k_7 , k_2 , K_O , and K_1 are defined by equations (4.5), (4.6), (3.2) and (3.3), respectively.

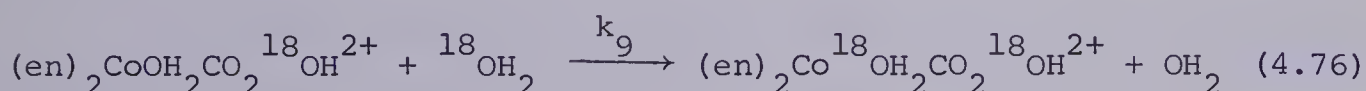
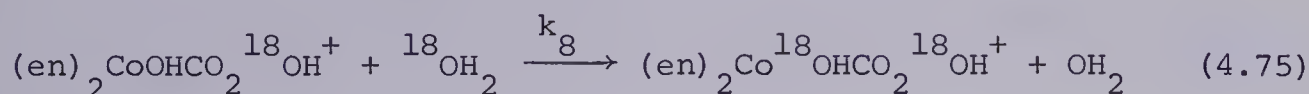
Analysis of the data above using equation (4.73) and the values for K_O and K_1 of 1×10^{-3} and 4.8×10^{-6} M, respectively,⁵¹ yields values for k_7 and k_2 of 0.94 sec^{-1} and $1.19 \times 10^{-2} \text{ sec}^{-1}$, respectively.

The assumption that the ring-opening reactions (3.1) and (3.2) are rate controlling results in

$$k_2 [\text{H}_2\text{O}]^n = k_1 [\text{H}^+] + k_o \quad (4.74)$$

where k_1 and k_o refer to the acid catalyzed ring-opening, (3.1), and the uncatalyzed ring-opening, (3.2), respectively. Analysis of the data above using (4.74) yields values for k_1 and k_o of $1.95 \times 10^2 \text{ M}^{-1} \text{ sec}^{-1}$ and $1.19 \times 10^{-5} \text{ sec}^{-1}$, respectively.

If the ring-opening reaction, (3.2), occurs via C-O bond cleavage and a direct water and/or hydroxide exchange step is rate controlling for the incorporation of solvent oxygen into the complex ($\text{R}=\text{CO}_3\text{H}$ in reaction 4.19),



the observed exchange rate constant is given by

$$k_2 [\text{H}_2\text{O}]^n = \frac{k_9 K_o [\text{H}^+]}{K_1} + k_8 K_o \quad (4.77)$$

where K_1 is the acid dissociation constant for the $(\text{en})_2\text{CoOH}_2\text{CO}_3\text{H}^{2+}$ complex. Using the same values for K_1 and K_o as above results in values for k_8 and k_9 of $1.19 \times 10^{-2} \text{ sec}^{-1}$ and 0.94 sec^{-1} , respectively.

Discussion

It has been shown that the exchange of oxygen between water and $(\text{NH}_3)_5\text{CoCO}_3^+$ proceeds by the same mechanism as the exchange of oxygen between water and NaHCO_3 . Thus the interpretation of Harris⁵⁰ that reactions (4.3) and (4.4) control the rate of oxygen or carbon exchange with the $(\text{NH}_3)_5\text{CoCO}_3^+$ ion is confirmed and the possibility of a direct carbonate-carbonate replacement reaction^{47,48} is removed.

The values of the specific rate constants for the reaction of carbon dioxide with hydroxide ion, reaction (4.4), are compared to other reported values, at 26° in Table (4.5). Since the values for k_5 and k_6 reported in this study are dependent on the value of k_4 used, a comparison of known k_4 values is also given in Table (4.5). The values for k_5 and k_6 compare quite well with the recent literature values, considering the wide variation in the rate constants of earlier studies.¹²⁶

The observed variation in exchange rate with pH for the exchange of ^{18}O between OH_2 and $(\text{en})_2\text{CoCO}_3^+$ has ruled out any mechanisms involving only the uncatalyzed ring-opening reaction, (3.1) as the rate controlling step. The possibility of rate control by both the acid catalyzed and uncatalyzed ring-opening reactions, (3.1) and (3.2) is eliminated since the calculated value for k_1 of $1.95 \times 10^2 \text{ M}^{-1} \text{ sec}^{-1}$ is much higher than the directly observed value for k_1 of $0.6 \text{ M}^{-1} \text{ sec}^{-1}$.⁹⁸

However, the $^{18}\text{OH}_2 - (\text{en})_2\text{CoCO}_3^+$ exchange data are consistent with rate control by the decarboxylation reactions, (4.5) and (4.6) since the calculated values for k_7 and k_2 of 0.94 and $1.19 \times 10^{-2} \text{ sec}^{-1}$ are

TABLE 4.5

Comparison of Values for Rate Constants^a of the Reactions of CO₂ with OH₂⁻ and OH⁻

$k_5 \times 10^{-4}, M^{-1} \text{ sec}^{-1}$	$k_6 \times 10^4, \text{ sec}^{-1}$	$k_4 \times 10^{-1}, \text{ sec}^{-1}$	T, °	Ionic Strength	Reference
1.056	2.15	1.806 ^a	26	~0.9 (NaClO ₄)	this study
0.840	-	-	25	0.5 (NaCl)	139
-	4.00	-	27.5	<0.1	140
0.980	-	-	20	1.0 (KCl)	141
0.850	2.00	2.0	25	<0.1	126

^a Calcd from reference (135) and used to calculate k₅ and k₆.

in fair agreement with the reported values of $\sim 2^{52}$ and $2.46 \times 10^{-3} \text{ sec}^{-1}$.¹³² The factor of five difference in the k_2 values may simply be due to the small number of runs done in the oxygen-18 exchange study.

A fast C-O bond cleavage in reaction (3.2) followed by the rate controlling reactions (4.75) and (4.76) might be eliminated if the assumption is made that OH^- and CO_3H^- have similar effects on the rates of exchange of ligands *cis* to themselves. Thus, the measured values for k_8 and k_9 of 1.19×10^{-2} and 0.94 sec^{-1} , respectively, do not agree with the estimated values⁷⁴ for the similar dihydroxy and hydroxyquo species of 3.0×10^{-5} and $4.6 \times 10^{-4} \text{ sec}^{-1}$, respectively. However, as discussed in Chapter 2, the relatively low value for the ratio of the rate constants for the base catalyzed and uncatalyzed ring-opening reactions of $(\text{en})_2\text{CoCO}_3^+$ might indicate a change in reaction path from Co-O to C-O bond cleavage. Thus the definite elimination of C-O bond cleavage for the uncatalyzed ring-opening reaction of $(\text{en})_2\text{CoCO}_3^+$ will require actual measurements of the rate constants for reactions (4.75) and (4.76). The rate controlling reactions for this C-O bond cleavage path for the ^{18}O exchange do not incorporate carbon into the complex so that the decarboxylation reactions, (4.7) and (4.8), are still likely rate controlling for the ^{14}C exchange reactions.

REFERENCES

1. P.E. Koefod, *"The Writing Requirements for Graduate Degrees"*, Prentice-Hall, Inc., Englewood Cliffs, New Jersey, 1964, chapter 2.
2. A.A. Frost and R.G. Pearson, *"Kinetics and Mechanism"*, 2nd ed., John Wiley & Sons, Inc., New York, 1961, p 2.
3. *Chemical & Engineering News*, 48, #20, 84 (1970).
4. *Chemical & Engineering News*, 48, #22, 11 (1970).
5. F. Basolo and R.G. Pearson, *"Mechanisms of Inorganic Reactions"*, 2nd ed., John Wiley and Sons, Inc., New York, 1967, p 125-129.
6. reference (2), p 11.
7. *ibid*, p 88.
8. C.H. Langford and H.B. Gray, *"Ligand Substitution Processes"*, W.A. Benjamin, Inc., New York, 1965, chapter 1.
9. reference (5), p 143.
10. *ibid*, p 96.
11. B.N. Figgis, *"Introduction to Ligand Fields"*, 1st ed., John Wiley & Sons, Inc., New York, 1966, p 184.
12. F. Aprile *et al.*, *Inorg. Chem.*, 7, 519 (1968).
13. U.D. Gomwalk and A. McAuley, *J. Chem. Soc.*, A, 1692 (1966).
14. U.D. Gomwalk and A. McAuley, *ibid*, 1796 (1967).
15. S.F. Lincoln and D.R. Stranks, *Aust. J. Chem.*, 21, 67 (1968).
16. reference (5), p 216.
17. *ibid*, p 164.
18. C.H. Langford, *Inorg. Chem.*, 4, 265 (1965).

19. A. Haim, *ibid*, 9, 426 (1970).
20. J.P. Hunt, A.C. Rutenberg, and H. Taube, *J. Amer. Chem. Soc.*, 74, 268 (1952)
21. F.A. Posey and H. Taube, *ibid*, 75, 4099 (1953).
22. reference (8), p 67.
23. reference (5), p 177.
24. R.G. Pearson, R.E. Meeker, and F. Basolo, *J. Inorg. Nucl. Chem.*, 1, 342 (1955).
25. V. Caglioti and G. Illuminati, Proceedings of the Eighth International Conference on Coordination Chemistry, Vienna, 1964, p 293.
26. R.G. Pearson, H.H. Schmidtke, and F. Basolo, *J. Amer. Chem. Soc.*, 82, 4434 (1960).
27. M. Green and H. Taube, *Inorg. Chem.*, 2, 948, (1963), *J. Phys. Chem.*, 67, 1565 (1963).
28. D.A. Buckingham, I.I. Olsen, and A.M. Sargeson, *J. Amer. Chem. Soc.*, 88, 5443 (1966).
29. D.A. Buckingham, I.I. Olsen, and A.M. Sargeson, *ibid*, 90, 6654 (1968).
30. D.A. Buckingham, I.I. Creaser, and A.M. Sargeson, *Inorg. Chem.*, 8, 655 (1969).
31. D.A. Buckingham, I.I. Olsen, and A.M. Sargeson, *J. Amer. Chem. Soc.*, 89, 5129 (1967).
32. D.A. Buckingham, I.I. Olsen, and A.M. Sargeson, *ibid*, 90, 6539 (1968).

33. R.B. Jordan and A.M. Sargeson, *Inorg. Chem.*, 4, 433, (1965).
34. reference (5), p 184, p 174.
35. D.A. Buckingham, P.A. Marzilli, and A.M. Sargeson, *Inorg. Chem.*, 8, 1595 (1969).
36. F.R. Nordmeyer, *ibid.*, 8, 2780 (1969).
37. C.G. Barraclough and R.S. Murray, *J. Chem. Soc.*, A, 7047 (1965).
38. S.F. Lincoln and D.R. Stranks, *Aust. J. Chem.*, 21, 57 (1968).
39. S. Sheel, D.T. Meloon, and G.M. Harris, *Inorg. Chem.*, 1, 170 (1962).
40. M.E. Farago, *Coord. Chem. Rev.*, 1, 66 (1966).
41. C. Andrade and H. Taube, *J. Amer. Chem. Soc.*, 86, 1328 (1964).
42. S.F. Lincoln and D.R. Stranks, *Aust. J. Chem.*, 21, 37 (1968).
43. C.R. Piriz Mac-Coll, *Coord. Chem. Rev.*, 4, 147 (1969).
44. K.V. Krishnamurty, G.M. Harris, and V.S. Sastri, *Chem Rev.*, 70, 171 (1970).
45. A.B. Lamb and R.G. Stevens, *J. Amer. Chem. Soc.*, 61, 3229 (1939).
46. A.B. Lamb and K.J. Mysels, *ibid*, 67, 468 (1945).
47. D.R. Stranks, *Trans. Faraday Soc.*, 51, 505 (1955).
48. G. Lapidus and G.M. Harris, *J. Amer. Chem. Soc.*, 85, 1223 (1963).
49. D.J. Francis and R.B. Jordan, *ibid*, 89, 5591 (1967).
50. T.P. Dasgupta and G.M. Harris, *ibid*, 90, 6360 (1968).
51. H.A. Scheidegger and G. Schwarzenbach, *Chimia*, 19, 166 (1965).
52. H.A. Scheidegger, Doctoral Thesis, E.T.H., Zurich, (1966) as given in reference (44).
53. reference (93), [reference (32) therein].

54. R.B. Jordan and D.J. Francis, Abstracts, 155th National Meeting of the American Chemical Society at San Francisco, Calif., April 1968, No. M35.
55. I.G. Hargis, Ph.D. Thesis, Ohio University, (1966).
56. J. Bjerrum and S.E. Rasmussen, *Acta Chem. Scand.*, 6, 1265 (1952).
57. R.E. Kitson, *Anal. Chem.*, 22, 664 (1950).
58. H.A. Horan and H.J. Eppig, *J. Amer. Chem. Soc.*, 71, 581 (1949).
59. Microanalytical Laboratory, Department of Chemistry, University of Alberta.
60. reference (50) and references therein.
61. G.S. Schlessinger, "*Inorganic Laboratory Preparations*", Chemical Publishing Co. Inc., New York, N.Y., 1962, p 230.
62. R.A. Haines, Ph.D. Thesis, University of Pittsburg, 1964.
63. R.A. Haines, personal communication.
64. F.P. Dwyer, A.M. Sargeson, and I.K. Reid, *J. Amer. Chem. Soc.*, 85, 1215 (1963) and references therein.
65. Courtesy of Dr. A.M. Sargeson, Institute for Advanced Studies, The Australian National University, Canberra, A.C.T., Australia.
66. reference (2), chapter 3.
67. H.S. Harned and B.B. Owen, "*The Physical Chemistry of Electrolytic Solutions*", 3rd ed., Reinhold Publishing Corporation, New York, 1958, p 638, Table (15-2-1A) p 752.
68. L.L. Rines, J.A. Plambeck, and D.J. Francis, "*ENLLSQ Reprogrammed*", Department of Chemistry Program Library, Department of Chemistry, University of Alberta, 1970.

69. reference (2), p. 99.
70. R. Näsänen and P. Mereläinen, *Suomen Kem.*, 33, B, 149 (1960), as reported in reference (71).
71. L.G. Sillén and A.E. Mortell, Ed., "*Stability Constants*", Special Publication No. 17, The Chemical Society, London, 1964.
72. M. Frydman *et al.*, *Acta. Chem. Scand.*, 12, 878 (1958), as reported in reference (71).
73. reference (49).
74. W. Kruse and H. Taube, *J. Amer. Chem. Soc.*, 83, 1280 (1961).
75. C.G. Swain, *ibid*, 66, 1696 (1944).
76. reference (67), p 498.
77. J.A. Plambeck and W.D. Ellis, October 1967 version, reprogrammed in double precision and listed as LSQ2, Department of Chemistry Program Library, Department of Chemistry, University of Alberta, 1969.
78. reference (2) p 186.
79. I. Amdur and G.G. Hammes, "*Chemical Kinetics*", McGraw-Hill Book Company, Toronto, 1966, p 16.
80. P.D. Lark, B.R. Craven, and R.C.L. Bosworth, "*The Handling of Chemical Data*", 1st ed., Pergamon Press, Oxford, London, 1968, p 128.
81. M.E. Farago, B.A. Page, and C.F.V. Mason, *Inorg. Chem.*, 8, 2270 (1969).
82. reference (2), p 173.

83. T.E. MacDermott and A.M. Sargeson, *Aust. J. Chem.*, 16, 334 (1963).
84. G.E. Schäffer, personal communication, 1957, as reported in reference (71).
85. W.E. Jones, R.B. Jordan, and T.W. Swaddle, *Inorg. Chem.*, 8, 2504 (1969).
86. V.S. Sastri and G.M. Harris, *J. Amer. Chem. Soc.*, 92, 2943 (1970).
87. reference (5), p 33.
88. *ibid*, p 37.
89. G.A. Barclay and B.F. Hoskins, *J. Chem. Soc.*, 586 (1962).
90. reference (5), p 780.
91. K.J. Pedersen, *J. Amer. Chem. Soc.*, 53, 18 (1931).
92. R. Ralea, G. Burlacu, and D. Giurgiu, *Revue de Chemie (Roumaine)*, 7, 1187 (1962).
93. T.P. Dasgupta and G.M. Harris, *J. Amer. Chem. Soc.*, 91, 3207 (1969).
94. J.Y. Tong, E. St. A. Kean, and B.B. Hall, *Inorg. Chem.*, 3, 1103 (1964).
95. G.M. Harris and V.S. Sastri, *ibid*, 4, 263 (1965).
96. R.B. Jordan and D.J. Francis, *ibid*, 6, 1605 (1967).
97. V.S. Sastri, Ph.D. Thesis, State University of New York at Buffalo (1966).
98. T.P. Dasgupta and G.M. Harris, *J. Amer. Chem. Soc.*, in press (1970).

99. J.A. Kernohan and J.F. Endicott, *J. Amer. Chem. Soc.*, 91, 6977 (1969).
100. R.J. Dobbins and G.M. Harris, *ibid*, in press (1970).
101. A.V. Ablov and D.M. Palade, *Rus. J. Inorg. Chem.*, 6, 306 (1961), [*Zhur. Neorg. Khim.*].
102. A.V. Ablov and D.M. Palade, *ibid*, 6, 567 (1961).
103. A.A. Vlček, *Inorg. Chem.*, 6, 1425 (1967).
104. J.G. Gibson, R. Laird, and E.D. McKenzie, *J. Chem. Soc.*, A, 14, 2089 (1969).
105. Machine Shop, Department of Chemistry, University of Alberta.
106. reference (5), p 36.
107. reference (11), p. 234.
108. I. Hanazaki and S. Nagakura, *Inorg. Chem.*, 8, 648 (1969).
109. K. Nakamoto, "*Infrared Spectra of Inorganic and Coordination Compounds*", John Wiley & Sons, Inc., New York, 1963, p 163.
110. J. Fujita, A.E. Martell, and K. Nakamoto, *J. Chem. Phys.*, 36, 339 (1962).
111. A.A. Schlitt and R.C. Taylor, *J. Inorg. Nucl. Chem.*, 9, 211 (1959).
112. H. Rosenberger and M. Pettig, *Ber. Bunsenges Phys. Chem.*, 78, 847 (1968).
113. H.J. Bernstein, J.A. Pople, and W.G. Schneider, *Can. J. Chem.*, 35, 65 (1957).
114. V.M.S. Gil, *Mol. Phys.*, 9, 97 (1965) as given in reference (115).
115. R.E. De Simone and R.S. Drago, *Inorg. Chem.*, 8, 2517 (1969).

116. D.M. Palade, *Rus. J. Inorg. Chem.*, 14, 231 (1969),
[*Zhur. Neorg. Khim.*].
117. H. Irving *et al.*, *J. Chem. Soc.*, 3494 (1954), as reported in
reference (71).
118. G. Schwarzenbach, A. Epprecht, and H. Erlenmeyer, *Helv. Chim.
Acta.*, 19, 1292 (1936), as reported in reference (71).
119. G. Schwarzenbach *et al.*, *ibid*, 35, 2337 (1952), as reported
in reference (71).
120. L.J. Edwards, Ph.D. Thesis, University of Michigan, (1950),
as reported in reference (71).
121. G. Schwarzenbach, *Helv. Chim. Acta.*, 33, 974 (1950), as
reported in reference (71).
122. N.F. Curtis, *J. Chem. Soc.*, 2644 (1964).
123. G. Anderegg, *Helv. Chim. Acta.*, 42, 344 (1959), as reported
in reference (71).
124. G. Anderegg, *ibid*, 46, 2397 (1963), as reported in reference
(71).
125. C.J. Hawkins, A.M. Sargeson, and G.H. Searle, *Aust. J. Chem.*,
17, 598 (1964).
126. D.M. Kern, *J. Chem. Educ.*, 37, 14 (1960).
127. G.M. Harris and D.R. Stranks, *Trans. Faraday Soc.*, 48, 137
(1952).
128. D.R. Stranks, *ibid.*, 48, 911 (1952).
129. J.S. Holden and G.M. Harris, *J. Amer. Chem. Soc.*, 77, 1934
(1955).

130. J.E. Boyle and G.M. Harris, *ibid*, 80, 782 (1958).
131. R.A.W. Pratt, E. Sherwin and G.J. Weston, *J. Chem. Soc.*, 476 (1962).
132. reference (100), Table II.
133. D. McKenzie, C. O'Connor, and A.L. Odell, *J. Chem. Soc.*, A, 184 (1966).
134. reference (5), p 171.
135. L. Rossi-Bernardi and R.L. Berger, *J. Biol. Chem.*, 6, 1297 (1968), Figure 5.
136. R.L. Berger, private communication. The decrease in $k_{\text{H}_2\text{CO}_3}^{(k_4)}$ with increasing ionic strength indicated in Figure 5 is correct as opposed to the text which gives the opposite trend.
137. H.S. Harned and F.T. Bonner, *J. Amer. Chem. Soc.*, 67, 1026 (1945).
138. R.B. Jordan, private communication. Preparation of $(\text{NH}_3)_5\text{Co}^{18}\text{OC}^{16}\text{O}_2^+$, equilibration in normal water, and acidification did not result in any enriched CO_2 .
139. D.J. Poulton and H.W. Baldwin, *Can. J. Chem.*, 45, 1045 (1967).
140. M.J. Welch, J.F. Lipton, and J.A. Seck, *J. Phys. Chem.*, 73, 3351 (1969).
141. B.R.W. Pinsent, L. Pearson, and F.J.W. Roughton, *Trans. Faraday Soc.*, 52, 1512 (1956).

APPENDIX A

The Determination of Parameter Confidence Limits and Their Use in Testing the Significance of a Theoretical Model

Throughout this thesis, raw experimental data is fitted to equations of the general form

$$y_i = f(b_j, x_{ij}) \quad (A.1)$$

where y_i is the i th dependent variable which is calculated from experimental data or is often the raw experimental data point itself, x_{ij} are the independent variables, and b_j are the parameters relating y_i and x_{ij} in the equation. Often it is helpful to have limits placed on the values of the parameters to indicate the confidence in the reported values. The computer program, ENLLSQ¹ is used to fit the raw experimental data to a theoretical model by a least-squares method in order to obtain values for the parameters. The documentation^{1,2} supplied with the program enables the user to run the program and to understand the theory of the method. However, because of the inadequate discussion of parameter error limits in the theoretical part of the documentation, it was decided to include comments on the ENLLSQ parameter error calculations in this section.

Throughout this discussion, it is assumed that the experimental error in a data point is indicated by its deviation from the true or mean value. A statistical analysis of these deviations leads to a

realistic estimate of the parameter error. The alternate approach is to actually estimate the experimental error on each point and then determine the parameter confidence limits (C.L.) which allow the fitted model to remain within these experimental errors. This approach was tried but often lead to unrealistic parameter errors so that the approach was abandoned except for transition state theory plots of $\log (k_r/T)$ vs. $1/T$. For these plots, the previously determined parameter limits on the specific rate constants (k_r) were used as "experimental" errors and the error limits on the activation parameters, ΔH^\ddagger and ΔS^\ddagger , were determined from the lines of maximum and minimum slope which could still pass through these "experimental" error limits.

A function, as in equation (A.1), can be treated as linear in its parameters, b_j , if it can be written as a polynomial in x_{ij} . Thus linear functions do not include functions which contain exponentials, logarithms, trigonometric expressions or roots. Many complicated algebraic equations cannot be represented exactly by a polynomial and thus are non-linear. However many functions can be represented by a polynomial closely within a certain range of x_{ij} and thus may be classed as linear in the region of x_{ij} which is of interest. The program ENLLSQ computes two linear parameter errors as well as one non-linear parameter error. The following sections discuss the calculation and use of these parameter errors.

For linear functions of the familiar form

$$y = mx + b \quad (A.2)$$

the least-squares estimates for one-parameter confidence limits³ are given by

$$100(1-P)\% \text{ C.L. of } m = m \pm t_{P,f} \cdot s_m \quad (\text{A.3})$$

and

$$100(1-P)\% \text{ C.L. of } b = b \pm t_{P,f} \cdot s_b \quad (\text{A.4})$$

where; f = no. of points - no. of parameters

= degrees of freedom

P = probability

t = two tailed $(1-P)$ point of Student's t distribution³

s_j = standard error of the j th parameter.

The s_j are calculated from the standard error of the fit, s_e , which is given by

$$s_e = ((Y_o - Y_p)^2 / (n - k))^{1/2} \quad (\text{A.5})$$

where; Y_o = observed y

Y_p = predicted y

n = no. of points

k = no. of parameters.

Expressions for the calculation of s_j from s_e are given by Marquardt¹ and Lark, Craven, and Bosworth.³

The one-parameter confidence limits do not consider the possibility of all parameters being at their maximum (or minimum)

values simultaneously. Taking this into consideration allows calculation of a joint confidence region (sometimes called support plane limits) for the parameters³ given by

$$100(1-P)\% \text{ C.L. of } m = m \pm (2F_{P,k/f} \cdot s_m)^{\frac{1}{2}} \quad (\text{A.6})$$

and

$$100(1-P)\% \text{ C.L. of } b = b \pm (2F_{P,k/f} \cdot s_b)^{\frac{1}{2}} \quad (\text{A.7})$$

where; $F_{P,k/f}$ = one tailed (1-P) point of variance ratio distribution.³

For linear functions, the Parameter Correlation Matrix, supplied as output by ENLLSQ, determines the proper set of limits to use. If the off-diagonal matrix elements are ≤ 0.1 , the parameters are taken to be uncorrelated and the one-parameter error limits are used. If the off-diagonal matrix elements are ≥ 0.1 , the parameters are correlated and the support plane limits are used. Uncorrelated parameters simply means that the model used is able to independently determine the parameters.

To determine if the model being used is close to being linear in the region of interest, it is only necessary to compare^{1,4} the one-parameter and non-linear confidence limits. If these sets of limits are equal, the model is deemed linear and the proper linear confidence limits are used. If the two sets of limits are not equal, it is necessary to use the non-linear limits.

It is important to note that the program does not automatically supply the correct value³ for $t_{P,f}$ and $F_{P,k/f}$. The user should input the correct values if any use is to be made of the parameter errors.

It is often useful to have error limits placed on the value of y_i predicted from the model and the parameters used. The standard error on the predicted value of y_i is given³ (for $y = mx + b$) by

$$s_{y_i} = s_e \left(1/n + (x_i - \bar{x})^2 / \sum X^2 \right)^{1/2} \quad (A.8)$$

and the confidence limits by

$$100(1-P)\% \text{ C.L. of } y_i = y_i \pm t_{P,f} \cdot s_{y_i} \quad (A.9)$$

or

$$100(1-P)\% \text{ C.L. of } y_i = y_i \pm (2F_{P,k/f} \cdot s_{y_i})^{1/2} \quad (A.10)$$

depending on the parameter correlation, where;

x_i = value of independent variable

\bar{x} = average of all experimental x_i 's

$$\sum X^2 = \sum (x_i)^2 - nx.$$

Two simple significance tests are used in this thesis. In some cases it was necessary to distinguish between a zero and non-zero y intercept for a linear function. A null hypothesis of intercept = 0 was assumed. If the 100(1-P)% C.L. includes the value assumed in the null hypothesis, then there is no reason why the null hypothesis can not be true.⁵ Therefore, even if the best

fit intercept was non-zero, the intercept must be reported as zero if the 95% C.L. include zero (unless there is other experimental evidence that the intercept is non-zero).

The other significance test was used to decide if a particular model agreed with the data within the experimental error. The error on the experimental points was estimated by the standard deviations on repeated points⁵ given by

$$s = (\sum (x - \bar{x})^2 / (n - 1))^{1/2} \quad (\text{A.11})$$

where; x = experimental value

\bar{x} = average value

n = no. of repeated points.

When s was not determined experimentally it was estimated from experience with similar systems or as a last resort when the variables were simple raw observed data points, s was estimated by the normal methods of experimental error assignment using statistical expressions and 2/3 of the 100% error.⁶ To insure the reality of these experimental errors, it was also required that they be smaller than the errors on the predicted points. For linear functions, error limits on predicted y_i were calculated as shown above. For non-linear functions the parameter limits were used directly to calculate error limits on predicted y_i .

The criteria for agreement of the data and the model was that the error limits of the experimental points must overlap with

the predicted line. Even with this criteria, chemical knowledge and separate experiments were often necessary to make the final decision as to the proper model.

REFERENCES

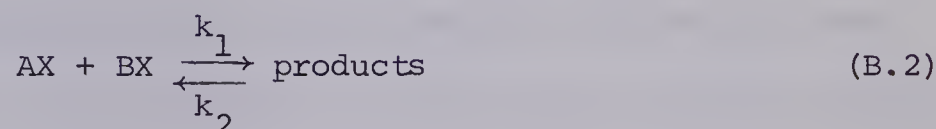
1. D.W. Marquardt, Share No. SDA 3094, E.I. Du Pont De Nemours and Co., Inc., Wilmington, Delaware, 1964.
2. L.L. Rines, J.A. Plambeck, and D.J. Francis, ENLLSQ Pre-programmed, Department of Chemistry Program Library, Department of Chemistry, The University of Alberta, 1970.
3. P.D. Lark, B.R. Craven, and R.C.L. Bosworth, "The Handling of Chemical Data," 1st ed., Pergammon Press, Oxford, London, 1968, p. 148.
4. D.W. Marquardt, R.G. Bennett, and E.J. Burrell, *J. Mol. Spectrosc.*, 7, 269 (1961).
5. reference (3), p. 106.
6. *ibid.*, p. 128.

APPENDIX B

Most derivations of the basic isotopic exchange equations found in the literature follow the method and terminology proposed by McKay.¹ The derivations refer to a total reaction rate,¹ a gross rate of exchange,² the rate of exchange of all exchanging atoms whether like or different isotopes,² the constant rate of exchange of exchanging atoms,³ or the rate of reaction between exchanging species in the dynamic equilibrium.⁴ For the simple case given by



this reaction rate, R , obviously refers to the rate of exchange of one X in an A type species for an X in a B type species. Looking at (B.1) from a net chemical reaction point of view results in



where "products" may simply be a short lived intermediate. If only exchange is observed, then regardless of what "products" is, the equilibrium must lie to the left and since the system is at chemical equilibrium

$$R = k_1 [AX] [BX] = k_2 [\text{products}] \quad (B.3)$$

where R is defined as

$$R = \text{number of collisions between } AX \text{ and } BX \text{ per unit time} \quad (B.4)$$

times some proportionality constant.

= number of reactions between AX and BX per unit time.

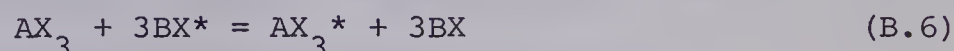
Since the only way X can exchange between AX and BX is through a collision between the two, the definitions of R are obviously identical.

However for the more complicated case when A contains more than one exchangeable species, the meaning of R has not been well defined by any of the references except perhaps by Wahl and Bonner although their definition is correct but not clear. Because of this lack of clarity a more precise definition of R is given, in addition to (B.4) as

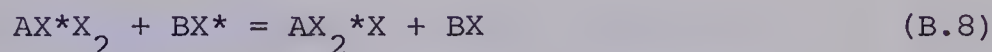
$$R = \text{rate of exchange of one X between A and B} \quad (\text{B.5})$$

$$\text{type species (gm atom l}^{-1} \text{ sec}^{-1}\text{)}.$$

This definition will be used to solve the following exchange system



where all the X's exchange by the same mechanism, i.e. at the same rate. Equation (B.6) may be looked at as the sum of 3 simple exchange reactions.



The following definitions will be used.

$$\begin{aligned}
 a &= \text{concentration of X, (X + X*) , in the A form (gm atom l}^{-1}\text{)} \\
 &= 3[AX_3^*] + 3[AX_2^*X] + 3[AX^*X_2] + 3[AX_3] \\
 &= 3 \cdot \text{total molar concentration of A species}
 \end{aligned}
 \tag{B.10}$$

$$\begin{aligned}
 x &= \text{concentration of X* in the A form (gm atom l}^{-1}\text{)} \\
 &= 3[AX_3^*] + 2[AX_2^*X] + [AX^*X_2]
 \end{aligned}
 \tag{B.11}$$

$$\begin{aligned}
 b &= \text{concentration of X, (X + X*) , in the B form (gm atom l}^{-1}\text{)} \\
 &= [BX] + [BX^*] \\
 &= \text{total molar concentration of B species}
 \end{aligned}
 \tag{B.12}$$

$$\begin{aligned}
 y &= \text{concentration of X* in the B form (gm atom l}^{-1}\text{)} \\
 &= [BX^*]
 \end{aligned}
 \tag{B.13}$$

Assuming that the analysis technique randomly samples the X's, the observed concentration-time differential is $-\frac{dy}{dt}$ or $\frac{dx}{dt}$.

If only the A species is sampled

$$\begin{aligned}
 \frac{dx}{dt} &= \text{rate of formation of X* containing A species -} \\
 &\quad \text{the rate of destruction of X* containing A species}
 \end{aligned}
 \tag{B.14}$$

where;

$$\begin{aligned}
 &\text{the rate of formation of } (AX_3^* + AX_2^*X + AX^*X_2) = \\
 &\text{total number of reactions per unit time} \cdot \text{fraction} \\
 &\text{of those occurring with X* containing B species} \cdot \\
 &\text{fraction of those occurring with X containing A species}
 \end{aligned}
 \tag{B.15}$$

$$= R \left(\frac{y}{b} \right) \left(\frac{a-x}{a} \right)$$

the rate of destruction of $(AX_3^* + AX_2^*X + AX^*X_2) =$ (B.16)

total number of reactions per unit time \cdot fraction

of those occurring with X containing B species \cdot

fraction of those occurring with X* containing A species

$$= R \left(\frac{y-b}{b} \right) \left(\frac{x}{a} \right)$$

therefore $\frac{dx}{dt} = R \left(\frac{y}{b} \right) \left(\frac{a-x}{b} \right) - R \left(\frac{y-b}{b} \right) \left(\frac{x}{a} \right)$

$$= R \left(\frac{y}{b} - \frac{x}{a} \right) . \tag{B.17}$$

At $t = \infty$, isotopic equilibrium is attained. Let

$$x = x_{\infty} \text{ and } y = y_{\infty} \tag{B.18}$$

therefore $x + y = x_{\infty} + y_{\infty}$ (B.19)

$$\frac{dx}{dt} = 0 = R \left(\frac{y_{\infty}}{b} - \frac{x_{\infty}}{a} \right)$$

$$\frac{y_{\infty}}{b} = \frac{x_{\infty}}{a}$$

$$y_{\infty} = \frac{bx_{\infty}}{a}$$

$$y = x_{\infty} + \frac{bx_{\infty}}{a} - x$$

$$\begin{aligned}
 \frac{dx}{dt} &= R \left(\frac{ax_{\infty} + bx_{\infty} - ax - bx}{ab} \right) \\
 &= R \left(\frac{x_{\infty}(a+b) - x(a+b)}{ab} \right) \\
 &= R \left(\frac{a+b}{ab} \right) \cdot (x_{\infty} - x) \quad .
 \end{aligned}
 \tag{B.20}$$

Solving this simple differential equation yields

$$\log \left(\frac{x_{\infty} - x}{x_{\infty} - x_0} \right) = - \frac{Rt}{2.303} \left(\frac{a+b}{ab} \right) \quad .
 \tag{B.21}$$

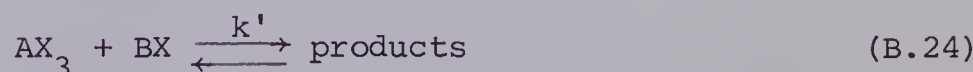
Equation (B.21) and the preceding derivation from (B.14) on is identical to that used by McKay. The known initial concentration of AX_3 , say T , is usually expressed in terms of mole l^{-1} of AX_3 . Thus it is necessary to replace a , (gm atom l^{-1}), by $3T$ as given by (B.10). Therefore

$$\log \left(\frac{x_{\infty} - x}{x_{\infty} - x_0} \right) = - \frac{Rt}{2.303} \left(\frac{3T+b}{3Tb} \right) \quad .
 \tag{B.22}$$

For cases when $b \gg 3T$, k_{obsd} is defined as

$$k_{\text{obsd}} = \frac{0.693}{t_{1/2}} = \frac{R}{3T}
 \tag{B.23}$$

where $t_{1/2}$ is the time required for $\log ((x_{\infty} - x)/(x_{\infty} - x_0))$ to decrease to one-half of its initial value. Note that k_{obsd} is now the specific rate constant for the exchange of 3 X's into AX_3 but R refers to the exchange of one X. Chemically we are usually interested in the rate of reaction for the incorporation of one X into an A species. That is



where

$$R = k' [BX] [AX_3] \quad (B.25)$$

$$= k' bT$$

$$R = kT \quad \text{since } b \text{ remains constant,} \quad (B.26)$$

$$b \gg 3T.$$

Now comparing (B.23) and (B.26), an equation relating the observed rate constant to the required specific rate constant is

$$k = 3k_{\text{obsd}} \quad (B.27)$$

The general procedure is to always directly compare equations of the type of (B.23) and (B.26) since the factor 3, called the G factor, is not always integral in more complicated systems.

REFERENCES

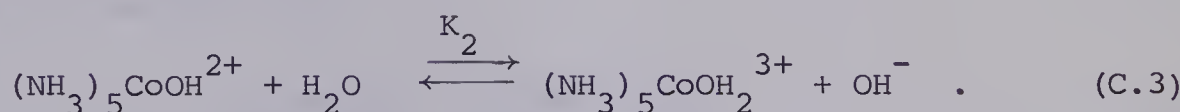
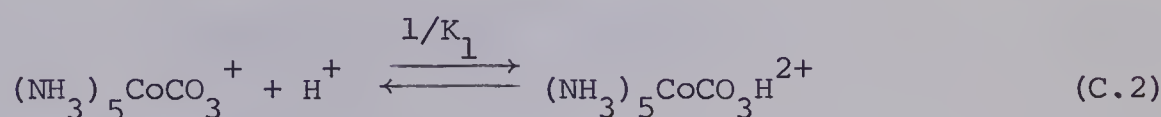
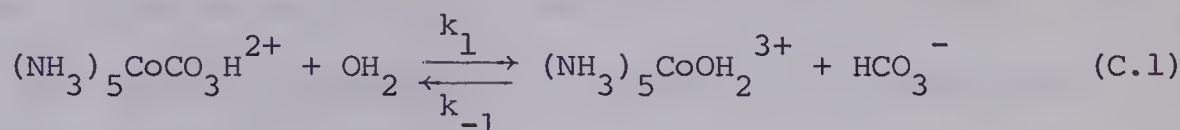
1. H.A.C. McKay, *J. Amer. Chem. Soc.*, 65, 702 (1943).
2. A.A. Frost and R.G. Pearson, "Kinetics and Mechanism", 2nd ed., John Wiley & Sons, Inc., New York, 1961, p. 192.
3. A.C. Wahl and N.A. Bonner, Ed., "Radioactivity Applied to Chemistry", 1st ed., John Wiley & Sons, Inc., New York, 1951, p. 8.
4. G. Friedlander, J.W. Kennedy, and J.M. Miller, "Nuclear and Radiochemistry", 2nd ed., John Wiley & Sons, Inc., New York, 1955, p. 196.

APPENDIX CDerivations of Expressions and Equations

This appendix contains the derivations of several kinetic expressions and equations which either do not fit in the thesis proper in a natural way or which were so long as to detract from the natural continuity of the section in which the derivations are used.

The Rate Law for the Hydrolysis of $(\text{NH}_3)_5\text{CoCO}_3^+$ in the pH range, 8.5-9.5, and at 25.0°

Assume that only the bicarbonatopentaamminecobalt(III) ion is reactive in the pH region, 8.5-9.5. The reactions to be considered are



Note that $K_2 = K_2'/K_w$ where K_2' is the acid dissociation constant of $(\text{NH}_3)_5\text{CoOH}_2^{3+}$. Define the following symbols as;

$$R = (\text{NH}_3)_5\text{Co}^{n+}$$

T_o = initial complex concentration

$T = [\text{ROCO}_2] + [\text{ROCO}_2\text{H}]$ at any time t

$T_e = [\text{ROCO}_2]_e + [\text{ROCO}_2\text{H}]_e$ at equilibrium.

Using the expression for K_1 from (C.2) yields

$$[\text{ROCO}_2\text{H}] = \frac{[\text{H}^+] T}{K_1 + [\text{H}^+]} \quad (\text{C.4})$$

Since (C.2) and (C.3) are fast proton transfer reactions, the rate expression can be written¹ as

$$-\frac{dT}{dt} = k_1 [\text{ROCO}_2\text{H}] - k_{-1} [\text{ROH}_2] [\text{HCO}_3^-] \quad (\text{C.5})$$

Substituting from (C.4) and (C.3) into (C.5) gives

$$-\frac{dT}{dt} = \frac{k_1 [H^+] T}{K_1 + [H^+]} - \frac{k_{-1} [ROH] [HCO_3^-]}{K_2 [OH^-]} \quad (C.6)$$

Because of the buffering of the carbonate-bicarbonate system, $[HCO_3^-]$ and $[OH^-]$ are constant throughout the reaction. At equilibrium

$$k_1 [ROCO_2H]_e = \frac{k_{-1} [ROH]_e [HCO_3^-]}{K_2 [OH^-]} \quad (C.7)$$

which can be rearranged to

$$\frac{k_{-1} [HCO_3^-]}{K_2 [OH^-]} = \frac{k_1 [ROCO_2H]_e}{[ROH]_e} \quad (C.8)$$

T_o has been defined as

$$T_o = [ROCO_2] + [ROCO_2H] + [ROH] + [ROH_2] \quad (C.9)$$

$$T_o = T + [ROH] + [ROH_2] \quad (C.10)$$

Substituting (C.10) into the equation for K_2 , as defined by (C.3), yields

$$[ROH] = \frac{K_2 [OH^-] (T_o - T)}{1 + K_2 [OH^-]} \quad (C.11)$$

Using the value for K_2' of $2.52 \times 10^{-7} \text{ M}^{-1}$, determined² in 1.0 M NaNO_3 at 25° and the value for K_w of 1.7×10^{-14} , determined³ in 1.0 M NaClO_4 at 25° to compare $K_2 [OH^-]$ to 1 at the pH 8.492 shows that $K_2 [OH^-] \gg 1$.

Therefore

$$[ROH] = (T_o - T) \quad (C.12)$$

and

$$[\text{ROH}]_e = (T_o - T_e) . \quad (\text{C.13})$$

Now using the expression for (C.4) at equilibrium and (C.13) transforms (C.8) into

$$\frac{k_{-1} [\text{HCO}_3^-]}{K_2 [\text{OH}^-]} = \frac{k_1 [\text{H}^+] T_e}{K_1 + [\text{H}^+]} \left(\frac{1}{T_o - T_e} \right) . \quad (\text{C.14})$$

Substituting (C.14) into (C.6) and simplifying gives

$$- \frac{dT}{dt} = \frac{k_1 [\text{H}^+]}{K_1 + [\text{H}^+]} \left(\frac{T_o}{T_o - T_e} \right) (T - T_e) . \quad (\text{C.15})$$

Integration gives the standard expression for a first order reaction

$$k_{\text{obsd}} = \frac{k_1 [\text{H}^+]}{K_1 + [\text{H}^+]} \left(\frac{T_o}{T_o - T_e} \right) . \quad (\text{C.16})$$

The total absorbance of the reaction solution is given by

$$A = \epsilon_1 b [\text{ROCO}_2] + \epsilon_2 b [\text{ROCO}_2\text{H}] \quad (\text{C.17})$$

where ϵ refers to the molar absorptivity index or extinction coefficient and b refers to the cell length in centimeters. The absorbance of ROH_2 can be neglected since it would be less than 1% at 295 m μ .⁵

Writing (C.17) in terms of T gives

$$A = \frac{\epsilon_1 b K_1 T}{K_1 + [\text{H}^+]} + \frac{\epsilon_2 b [\text{H}^+] T}{K_1 + [\text{H}^+]} \quad (\text{C.18})$$

$$A = \text{constant} \cdot T. \quad (\text{C.19})$$

Therefore

$$\frac{T_o}{T_o - T_e} = \frac{A_o}{A_o - A_\infty} \quad (C.20)$$

and

$$\frac{A_o}{A_o - A_\infty} = \frac{A_o/T_o}{(A_o/T_o - A_\infty/T_o)} = \frac{\epsilon_o}{\epsilon_o - \epsilon_\infty} \quad (C.21)$$

and therefore

$$k_{\text{obsd}} = \frac{k_1 [H^+]}{K_1 + [H^+]} \left(\frac{\epsilon_o}{\epsilon_o - \epsilon_\infty} \right) \quad (C.22)$$

An Equation Relating K_f to ϵ_1 , ϵ_∞ , $[HCO_3^-]$, $[H^+]$, K_1 and K_w

Define R , T_o , and T as in the previous section. Define ϵ_1 and ϵ_2 as the extinction coefficients at 295 mμ of $(NH_3)_5CoCO_3^+$ and $(NH_3)_5CoCO_3H^{2+}$, respectively. Define K_f by

$$K_f = \frac{[ROCO_2H][OH^-]}{[ROH][HCO_3^-]} \quad (C.23)$$

At equilibrium

$$A_\infty = \epsilon_1 b [ROCO_2]_e + \epsilon_2 b [ROCO_2H]_e \quad (C.24)$$

$$= \left(\frac{\epsilon_1 b K_1}{[H^+]} + \epsilon_2 b \right) [ROCO_2H]_e \quad (C.25)$$

$$\epsilon_\infty = \frac{A_\infty}{b T_o} = \left(\frac{\epsilon_1 K_1}{[H^+]} + \epsilon_2 \right) \frac{[ROCO_2H]_e}{T_o} \quad (C.26)$$

Now writing the equation for the concentration ratio of the carbonato/bicarbonato species and adding one to each side gives

$$\frac{[\text{ROCO}_2] + [\text{ROCO}_2\text{H}]}{[\text{ROCO}_2\text{H}]} = \frac{K_1 + [\text{H}^+]}{[\text{H}^+]} \quad . \quad (\text{C.27})$$

Substituting the stoichiometry relationship

$$[\text{ROCO}_2\text{H}] + [\text{ROCO}_2] = T_o - [\text{ROH}] \quad (\text{C.28})$$

into (C.27) and rearranging results in

$$\frac{[\text{ROH}]}{[\text{ROCO}_2\text{H}]} = \frac{T_o}{[\text{ROCO}_2\text{H}]} - \frac{K_1 + [\text{H}^+]}{[\text{H}^+]} \quad . \quad (\text{C.29})$$

At equilibrium, (C.26) can be rearranged and substituted into the first term on the r.h.s. of (C.29) to yield

$$\frac{[\text{ROH}]_e}{[\text{ROCO}_2\text{H}]_e} = \frac{\left(\frac{\epsilon_1 K_1}{[\text{H}^+]} + \epsilon_2 \right)}{\epsilon_\infty} - \frac{K_1 + [\text{H}^+]}{[\text{H}^+]} \quad . \quad (\text{C.30})$$

Rearrangement and inversion results in

$$\frac{[\text{ROCO}_2\text{H}]_e}{[\text{ROH}]_e} = \frac{\epsilon_\infty}{\frac{K_1}{[\text{H}^+]} (\epsilon_1 - \epsilon_\infty) + (\epsilon_2 - \epsilon_\infty)} \quad (\text{C.31})$$

Substitution into (C.23) under equilibrium conditions results in

$$K_f = \frac{\epsilon_{\infty} K_w}{K_1 (\epsilon_1 - \epsilon_{\infty}) + [H^+] (\epsilon_2 - \epsilon_{\infty})} \left(\frac{1}{[HCO_3^-]} \right) \quad (C.32)$$

after substitution of the water ion-product equation.

An Equation for the $(en)_2CoCO_3^+$ Study giving K_1 in Terms of $[OH^-]$, ϵ_a , ϵ_x , b , T_o , A'_{max} and A_o

Let $[(en)_2CoOHCO_3]$ and $[(en)_2CoCO_3^+]$ be represented by a and x , respectively. Then

$$K_1 = \frac{a}{x[OH^-]} \quad (C.33)$$

Let the following definitions hold;

- ϵ_x = extinction coefficient of $(en)_2CoCO_3^+$ at 300 m μ
- ϵ_a = extinction coefficient of $(en)_2CoOHCO_3$ at 300 m μ
- b = spectrophotometer cell length in centimeters
- T_o = initial complex concentration (C.34)
- = $a + x$.

Assuming only two species are present, the absorbance of a reaction solution after equilibration has been reached can be defined as

$$A'_{max} = \epsilon_a ba + \epsilon_x bx \quad (C.35)$$

Rearranging (C.33) and substituting (C.34) gives

$$a = \frac{K_1 [OH^-] T_o}{K_1 [OH^-] + 1} \quad (C.36)$$

and substitution of (C.36) into (C.35) yields

$$A'_{\max} = b\epsilon_x \left(T_o - \frac{K_1 [\text{OH}^-] T_o}{K_1 [\text{OH}^-] + 1} \right) + \frac{b\epsilon_a K_1 [\text{OH}^-] T_o}{K_1 [\text{OH}^-] + 1} . \quad (\text{C.37})$$

Dividing (C.37) by bT_o gives

$$\frac{A'_{\max}}{bT_o} = \epsilon_{\infty} = \epsilon_x \left(1 - \frac{K_1 [\text{OH}^-]}{K_1 [\text{OH}^-] + 1} \right) + \frac{\epsilon_a K_1 [\text{OH}^-]}{K_1 [\text{OH}^-] + 1} \quad (\text{C.38})$$

Writing (C.38) with the common denominator, $K_1 [\text{OH}^-] + 1$, and collecting terms results in

$$\epsilon_{\infty} = K_1 [\text{OH}^-] (\epsilon_a - \epsilon_{\infty}) + \epsilon_x \quad (\text{C.39})$$

Rearranging (C.39), adding K_1 to each side and collecting terms gives

$$\frac{1}{[\text{OH}^-]} = \left(\frac{\epsilon_a - \epsilon_x}{\epsilon_{\infty} - \epsilon_x} \right) K_1 - K_1 . \quad (\text{C.40})$$

Now the absorbance of the solution at zero time is defined by

$$A_o = \epsilon_x bT_o . \quad (\text{C.41})$$

Then substitution for ϵ_x and ϵ_{∞} from (C.41) and (C.38) into (C.40) yields

$$\frac{1}{[\text{OH}^-]} = K_1 (\epsilon_a - \epsilon_x) \left(\frac{bT_o}{A'_{\max} - A_o} \right) - K_1 . \quad (\text{C.42})$$

Equations Relating the Concentration of H_2CO_3 , HCO_3^- , $CO_3^{=}$, and CO_2 to $[H^+]$, the Initial $NaHCO_3$ Concentration and the Constants K_{C1} , K_{C2} , k_5 , k_6 , and K_w

Let the initial concentration of $NaHCO_3$ be defined as

$$T = [H_2CO_3] + [HCO_3^-] + [CO_3^{=}] + [CO_2] \quad . \quad (C.43)$$

The equilibrium constants used are

$$K_{C1} = \frac{[H^+][HCO_3^-]}{[H_2CO_3] + [CO_2]} \quad (C.44)$$

$$K_{C2} = \frac{[H^+][CO_3^{=}]}{[HCO_3^-]} \quad (C.45)$$

$$\frac{k_6}{k_5} = \frac{[OH^-][CO_2]}{[HCO_3^-]} = \frac{[H^+][CO_2]}{K_w[HCO_3^-]} \quad (C.46)$$

where K_w is the ion product for water.

Solving (C.46) for $[CO_2]$ gives

$$[CO_2] = \frac{k_6 K_w [HCO_3^-]}{k_5 [H^+]} \quad . \quad (C.47)$$

Then

$$T = [H_2CO_3] + [HCO_3^-] + [CO_3^{=}] + \frac{k_6 K_w [HCO_3^-]}{k_5 [H^+]} \quad (C.48)$$

and substituting in (C.44) for $[\text{CO}_2]$, and then using (C.48) gives

$$\begin{aligned}
 K_{C1} &= \frac{[\text{H}^+][\text{HCO}_3^-]}{[\text{H}_2\text{CO}_3] + \frac{k_6 K_w [\text{HCO}_3^-]}{k_5 [\text{H}^+]}} \\
 &= \frac{[\text{H}^+][\text{HCO}_3^-]}{[\text{T}] - [\text{HCO}_3^-] - \frac{K_{C2} [\text{HCO}_3^-]}{[\text{H}^+]}} \quad . \quad (\text{C.49})
 \end{aligned}$$

Therefore

$$[\text{HCO}_3^-] = \frac{K_{C1} T}{[\text{H}^+] + K_{C1} + \frac{K_{C1} K_{C2}}{[\text{H}^+]}} \quad . \quad (\text{C.50})$$

Expanding (C.44) using (C.47) yields

$$K_{C1} [\text{H}_2\text{CO}_3] + \frac{K_{C1} k_6 [\text{HCO}_3^-] [\text{H}^+]}{K_w k_5} = [\text{HCO}_3^-] [\text{H}^+] \quad . \quad (\text{C.51})$$

Solving for $[\text{H}_2\text{CO}_3]$ gives

$$[\text{H}_2\text{CO}_3] = \left\{ 1 - \frac{K_{C1} k_6}{K_w k_5} \right\} \frac{[\text{H}^+][\text{HCO}_3^-]}{K_{C1}} \quad . \quad (\text{C.52})$$

Substituting from (C.50) into (C.52) for $[\text{HCO}_3^-]$ yields

$$[\text{H}_2\text{CO}_3] = \frac{\left\{ 1 - \frac{K_{C1} k_6}{K_w k_5} \right\} [\text{H}^+] T}{[\text{H}^+] + K_{C1} + \frac{K_{C1} K_{C2}}{[\text{H}^+]}} \quad . \quad (\text{C.53})$$

Equations Giving the Concentrations of ROCO_2 , ROCO_2H , H_2CO_3 , HCO_3^- , $\text{CO}_3^{=}$ and CO_2 as Functions of $[\text{H}^+]$, the Initial Complex Concentration and the Constants K_{C1} , K_{C2} , k_5 , k_6 , K_w , K_f , and K_1

Let the initial concentration of ROCO_2 be defined in terms of the species concentration at any time as

$$T' = [\text{ROCO}_2] + [\text{ROCO}_2\text{H}] + [\text{ROH}] \quad (\text{C.54})$$

$$= [\text{ROCO}_2] + [\text{ROCO}_2\text{H}] + [\text{H}_2\text{CO}_3] + [\text{HCO}_3^-] + [\text{CO}_3^{=}] + [\text{CO}_2] \quad (\text{C.55})$$

In addition to (C.44), (C.45), and (C.46), the following equilibrium constants are used;

$$K_1 = \frac{[\text{H}^+][\text{ROCO}_2]}{[\text{ROCO}_2\text{H}]} \quad (\text{C.56})$$

$$\frac{K_1 K_f}{K_w} = \frac{[\text{ROCO}_2]}{[\text{ROH}][\text{HCO}_3^-]} \quad (\text{C.57})$$

Writing (C.55) in terms of $[\text{ROCO}_2]$ and $[\text{HCO}_3^-]$ using (C.56), (C.52), (C.47), and (C.45) results in

$$T' = [\text{ROCO}_2] + \frac{[\text{H}^+][\text{ROCO}_2]}{K_1} + [\text{HCO}_3^-] \left(1 + \frac{K_{C2}}{[\text{H}^+]} + \frac{k_6[\text{H}^+]}{k_5 K_w} + \frac{[\text{H}^+]}{K_{C1}} \left\{ 1 - \frac{K_{C1} k_6}{K_w k_5} \right\} \right) \quad (\text{C.58})$$

Solving for $[\text{HCO}_3^-]$ gives

$$[\text{HCO}_3^-] = \frac{T' - [\text{ROCO}_2] - \frac{[\text{H}^+][\text{ROCO}_2]}{K_1}}{1 + \frac{K_{C2}}{[\text{H}^+]} + \frac{k_6[\text{H}^+]}{k_5 K_w} + \frac{[\text{H}^+]}{K_{C1}} \left\{ 1 - \frac{K_{C1} k_6}{K_w k_5} \right\}} \quad (\text{C.59})$$

$$\text{Since} \quad [\text{ROH}] = T' - [\text{ROCO}_2] - [\text{ROCO}_2\text{H}] \quad (\text{C.60})$$

solving (C.57) for ROCO_2 using (C.56), (C.60), and (C.59) results in

$$[\text{ROCO}_2] = \frac{K_1 K_f T' \left\{ T' - [\text{ROCO}_2] - \frac{[\text{H}^+][\text{ROCO}_2]}{K_1} \right\}}{K_w Q + \left(T' - [\text{ROCO}_2] - \frac{[\text{H}^+][\text{ROCO}_2]}{K_1} \right) \left\{ K_1 K_f + K_f [\text{H}^+] \right\}} \quad (\text{C.61})$$

where

$$Q = 1 + \frac{K_{C2}}{[\text{H}^+]} + \frac{k_6[\text{H}^+]}{k_5 K_w} + \frac{[\text{H}^+]}{K_{C1}} \left\{ 1 - \frac{K_{C1} k_6}{K_w k_5} \right\} \quad (\text{C.62})$$

Rearrangement of (C.61) leads to a quadratic in $[\text{ROCO}_2]$, the solution of which is

$$[\text{ROCO}_2] = \frac{-b - (b^2 - 4ac)^{1/2}}{2a} \quad (\text{C.63})$$

where

$$a = \frac{K_f [\text{H}^+]^2}{K_1} + 2K_f [\text{H}^+] + K_1 K_f \quad (\text{C.64})$$

$$b = -2K_f [\text{H}^+] T' - 2K_1 K_f T' - K_w Q \quad (\text{C.65})$$

$$c = K_1 K_f T' \quad (\text{C.66})$$

Use of (C.63) allows the following expressions to be used;

$$[\text{ROCO}_2\text{H}] = \frac{[\text{H}^+][\text{ROCO}_2]}{K_1} \quad (\text{C.67})$$

$$[\text{HCO}_3^-] = \frac{T' - [\text{ROCO}_2] - [\text{ROCO}_2\text{H}]}{Q} \quad (\text{C.68})$$

$$[\text{CO}_2] = \frac{k_6[\text{H}^+][\text{HCO}_3^-]}{k_5 K_w} \quad (\text{C.47})$$

$$[\text{CO}_3^{=}] = \frac{K_{C2}[\text{HCO}_3^-]}{[\text{H}^+]} \quad (\text{C.69})$$

$$\begin{aligned} [\text{H}_2\text{CO}_3] &= T' - [\text{ROCO}_2] - [\text{ROCO}_2\text{H}] - [\text{HCO}_3^-] \\ &\quad - [\text{CO}_3^{=}] - [\text{CO}_2] \quad . \end{aligned} \quad (\text{C.70})$$

Therefore all the concentrations can be calculated from known concentrations and equilibrium constants if k_5 and k_6 are known. In cases when k_5 and k_6 are not known,⁶ they must be estimated and varied until self consistent values are attained.

REFERENCES

1. Equation (2.19), this thesis.
2. F. Basolo and R.G. Pearson, "Mechanisms of Inorganic Reactions", 2nd ed., John Wiley and Sons, Inc., New York, 1967, p. 32.
3. R. Näsänen and P. Meriläinen, *Suomen Kemistrilehti*, 33B, 149 (1960) as quoted in reference (4).
4. "Stability Constants", Special Publication No. 17, The Chemical Society, London, 1964.
5. Figure 2.1, this thesis.
6. Equation (4.54), G. factor, this thesis.

APPENDIX DTables of Data

This appendix contains tables of kinetic data for the base hydrolysis of $(\text{NH}_3)_5\text{CoCO}_3^+$, for the base hydrolysis of $(\text{en})_2\text{CoCO}_3^+$, for the acid hydrolysis of $(\text{phen})_2\text{CoCO}_3^+$, and for the acid hydrolysis of $(\text{bipy})_2\text{CoCO}_3^+$. Each table gives the observed rate constant, the hydroxide or hydrogen ion concentration, the predicted rate constant, k_{calcd} , calculated from the least-squares best fit parameters and the rate law, and the values of any constants required in these calculations.

Also given in this appendix are the equilibrium data for the $(\text{NH}_3)_5\text{CoCO}_3^+$ and $(\text{en})_2\text{CoCO}_3^+$ base hydrolysis systems. Here the subscript calcd refers to the value of an expression calculated from the best fit values of the parameters and the particular equation used.

TABLE D.1

Variation in the Rate of Hydrolysis of $(\text{NH}_3)_5\text{CoCO}_3^+$
with $[\text{OH}^-]$ at 45.0°

$[\text{OH}^-], \text{ M}$	$k_{\text{obsd}}^a \times 10^4, \text{ sec}^{-1}$	$k_{\text{calcd}}^a \times 10^4, \text{ sec}^{-1}$
0.010	1.360	1.489
0.020	0.935	0.757
0.040	0.528	0.403
0.050	0.360	0.337
0.099	0.229	0.231
0.100	0.292	0.230
0.300	0.257	0.295
0.400	0.353	0.365
0.500	0.437	0.440
0.700	0.602	0.595
0.800	0.673	0.675
1.000	0.835	0.835

(a) $\mu = 1.0$ (NaNO_3), $K_w = 7.140 \times 10^{-14}$.

TABLE D.2

Variation in the Rate of Hydrolysis of $(\text{NH}_3)_5\text{CoCO}_3^+$
with $[\text{OH}^-]$ at 50.0°

$[\text{OH}^-], \text{ M}$	$k_{\text{obsd}}^a \times 10^4, \text{ sec}^{-1}$	$k_{\text{calcd}}^a \times 10^4, \text{ sec}^{-1}$
0.020	2.230	2.265
0.040	1.220	1.179
0.060	0.900	0.838
0.100	0.597	0.602
0.100	0.537	0.602
0.200	0.612	0.534
0.500	0.900	0.865
0.800	1.260	1.296
0.800	1.260	1.296
0.900	1.475	1.445

(a) $\mu = 1.0 (\text{NaNO}_3), K_w = 9.820 \times 10^{-14}$.

TABLE D.3

Variation in the Rate of Hydrolysis of $(\text{NH}_3)_5\text{CoCO}_3^+$
with $[\text{OH}^-]$ at 55.0°

$[\text{OH}^-], \text{ M}$	$k_{\text{obsd}}^a \times 10^4, \text{ sec}^{-1}$	$k_{\text{calcd}}^a \times 10^4, \text{ sec}^{-1}$
0.020	3.850	3.970
0.040	2.200	2.093
0.060	1.610	1.514
0.099	1.180	1.141
0.099	1.075	1.141
0.100	1.180	1.138
0.100	1.260	1.138
0.199	1.125	1.103
0.200	1.160	1.106
0.497	1.920	1.934
0.497	1.960	1.934
0.794	2.920	2.941
0.993	3.660	3.633
0.993	3.580	3.633

(a) $\mu = 1.0$ (NaNO_3), $K_w = 1.325 \times 10^{-13}$.

TABLE D.4

Data for the Determination of $K_1 = [(\text{NH}_3)_5\text{CoCO}_3^+]$
 $[\text{H}^+]/[(\text{NH}_3)_5\text{CoCO}_3\text{H}^{2+}]$ at 25.0°

$\frac{K_w \epsilon_\infty}{[\text{H}^+][\text{HCO}_3^-]}$	$y_{\text{obsd}}^{a,b} \times 10^{-5}$	$y_{\text{calcd}}^b \times 10^{-5}$
0.387	0.546	0.424
0.579	0.765	0.780
0.626	0.957	0.867
0.734	1.133	1.084
0.956	1.373	1.477
1.215	1.973	1.955
1.462	2.035	2.412
1.781	3.134	3.003
2.528	4.312	4.382
2.957	5.106	5.178
3.307	5.869	5.825
3.842	6.853	6.813

(a) $T = 25.0^\circ$, $\mu = 1.0$ (NaClO_4), initial $[\text{HCO}_3^-] = 0.0242 \text{ M}$

(b) $y = \frac{K_1 \epsilon_1 - \epsilon_\infty (K_1 + [\text{H}^+])}{[\text{H}^+]}$

TABLE D.5

Data for the Determination of $K_1 = [(\text{en})_2\text{CoOHCO}_3] / [(\text{en})_2\text{CoCO}_3^+][\text{OH}^-]$ at 26.0°

$\left(\frac{bT_o}{A'_{\text{max}} - A_o} \right) \times 10^3$	$[\text{OH}^-]^{-1}, \text{M}^{-1}$		$T_o \times 10^4, \text{M}$
	Calculated	Experimental ^a	
10.85	431.3	432.0	2.08
9.72	381.3	407.0	2.08
4.80	163.8	147.0	3.28
2.77	73.97	73.40	2.82
2.50	62.03	58.60	2.49
2.33	54.51	48.90	3.40
1.91	35.93	36.80	4.68
1.60	22.22	24.50	2.51
1.39	13.07	14.70	3.41
1.26	7.320	7.340	3.13

(a) $\mu = 1.0$ (NaClO_4), 5 cm cell, $\lambda = 300 \text{ m}\mu$.

TABLE D.6

Data for the Determination of $K_1 = [(\text{en})_2\text{CoOHCO}_3] / [(\text{en})_2\text{CoCO}_3^+][\text{OH}^-]$ at 34.0°

$\left(\frac{bT_o}{A'_{\text{max}} - A_o} \right) \times 10^3$	$[\text{OH}^-]^{-1}, \text{M}^{-1}$		$T_o \times 10^4, \text{M}$
	Calculated	Experimental ^a	
6.10	180.7	191.0	2.28
5.00	141.5	134.0	2.23
3.00	70.22	71.70	2.09
2.40	48.85	52.30	2.02
2.31	45.64	45.00	2.07
1.99	34.24	35.80	2.00
1.99	34.24	30.50	2.16
1.95	32.82	28.60	2.50
1.44	16.43	18.10	4.79
1.43	14.29	14.20	4.61
1.37	12.15	11.90	6.00
1.27	8.590	7.110	5.50
1.18	5.383	5.820	8.05
1.13	3.602	4.450	6.36

(a) $\mu = 1.0$ (NaClO_4), 5 cm cell, $\lambda = 300 \text{ m}\mu$.

TABLE D.7

Data for the Determination of $K_1 = [(\text{en})_2\text{CoOHCO}_3]/$
 $[(\text{en})_2\text{CoCO}_3^+][\text{OH}^-]$ at 44.0°

$\left\{ \frac{bT_o}{A'_{\text{max}} - A_o} \right\}$	$\times 10^3$	Calculated	$\underbrace{[\text{OH}^-]^{-1}, \text{M}^{-1}}_{\text{Experimental}^a}$	$T_o \times 10^4, \text{M}$
7.15		143.5	129.5	3.94
3.54		57.7	63.0	2.38
2.86		41.6	44.1	2.80
2.71		38.0	45.6	2.22
2.65		36.6	45.6	1.84
2.29		28.0	20.1	2.14
2.27		27.6	34.8	2.11
2.25		27.0	27.6	2.88
2.23		26.6	34.8	2.04
2.02		21.6	23.3	2.31
1.90		18.8	15.8	2.75
1.80		16.4	13.1	3.78
1.67		13.3	14.3	1.46
1.49		9.01	10.5	2.52
1.48		8.77	8.20	3.41
1.47		8.54	9.65	2.25
1.46		8.30	7.40	2.19

TABLE D.7 (Cont'd)

$\left(\frac{bT_o}{A'_{\max} - A_o} \right) \times 10^3$	$[\text{OH}^-]^{-1}, \text{M}^{-1}$		$T_o \times 10^4, \text{M}$
	Calculated	Experimental ^a	
1.35	5.68	3.49	1.86
1.31	4.73	6.74	2.42
1.30	4.50	4.65	2.10
1.26	3.55	4.03	2.29

(a) $\mu = 1.0$ (NaClO_4), 5 cm cell, $\lambda = 300 \text{ m}\mu$.

TABLE D.8

Variation in the Rate of Hydrolysis of $(\text{en})_2\text{CoCO}_3^+$
with $[\text{OH}^-]$ at 26.0°

$[\text{OH}^-], \text{ M}$	$k_{\text{obsd}}^a \times 10^3, \text{ sec}^{-1}$	$k_{\text{calcd}}^a \times 10^3, \text{ sec}^{-1}$
0.00119	1.308	1.054
0.00179	0.729	0.745
0.00232	0.607	0.605
0.00246	0.577	0.577
0.00342	0.525	0.455
0.00681	0.285	0.304
0.0136	0.244	0.243
0.0171	0.229	0.238
0.0204	0.230	0.238
0.0272	0.214	0.246
0.0408	0.252	0.276
0.0408	0.259	0.276
0.0681	0.324	0.351
0.130	0.490	0.557
0.204	0.745	0.771
0.273	1.00	0.997
0.341	1.26	1.20
0.355	1.26	1.25

TABLE D.8 (Cont'd)

$[\text{OH}^-], \text{ M}$	$k_{\text{obsd}}^a \times 10^3, \text{ sec}^{-1}$	$k_{\text{calcd}}^a \times 10^3, \text{ sec}^{-1}$
0.381	1.32	1.32
0.445	1.72	1.53
0.508	1.87	1.73
0.572	2.04	1.93
0.603	2.15	2.03
0.613	2.37	2.23
0.680	2.64	2.37
0.748	2.86	2.80
0.817	3.12	3.24
0.886	3.53	3.32

(a) $\mu = 1.0 \text{ (NaClO}_4\text{)}, \lambda = 300 \text{ m}\mu, K_1 = 48.5 \text{ M}^{-1}$.

TABLE D.9

Variation in the Rate of Hydrolysis of $(\text{en})_2\text{CoCO}_3^+$
with $[\text{OH}^-]$ at 34.0°

$[\text{OH}^-], \text{ M}$	$k_{\text{obsd}}^a \times 10^3, \text{ sec}^{-1}$	$k_{\text{calcd}}^a \times 10^3, \text{ sec}^{-1}$
0.00228	4.56	1.99
0.00365	2.11	1.40
0.00496	1.00	1.15
0.00502	1.52	1.14
0.00523	1.18	1.11
0.00743	0.949	0.926
0.00773	1.17	0.910
0.0140	0.700	0.753
0.0191	0.737	0.728
0.0223	0.706	0.729
0.0227	0.618	0.729
0.0261	0.572	0.736
0.0279	0.753	0.744
0.0284	0.613	0.745
0.0328	0.711	0.766
0.0348	0.686	0.779
0.0350	0.739	0.780
0.0446	0.680	0.840

TABLE D.9 (Cont'd)

$[\text{OH}^-], \text{ M}$	$k_{\text{obsd}}^a \times 10^3, \text{ sec}^{-1}$	$k_{\text{calcd}}^a \times 10^3, \text{ sec}^{-1}$
0.0483	0.693	0.865
0.0552	0.906	0.917
0.0552	0.958	0.917
0.0702	0.950	1.03
0.0842	1.12	1.15
0.112	1.60	1.38
0.141	1.61	1.62
0.172	1.98	1.89
0.225	2.43	2.34
0.281	3.01	2.82
0.336	3.68	3.30
0.393	3.71	3.79
0.449	4.20	4.27
0.505	4.68	4.76
0.561	6.08	5.25
0.617	6.03	5.73
0.673	6.74	6.22
0.729	7.70	6.71
0.756	7.20	6.94
0.785	7.87	7.19

TABLE D.9 (Cont'd)

$[\text{OH}^-], \text{ M}$	$k_{\text{obsd}}^a \times 10^3, \text{ sec}^{-1}$	$k_{\text{calcd}}^a \times 10^3, \text{ sec}^{-1}$
0.785	7.45	7.19
0.842	9.12	7.68
0.842	8.45	7.68
0.842	8.65	7.68
0.899	8.45	8.18
0.899	8.80	8.18

(a) $\mu = 1.0$ (NaClO_4), $\lambda = 300 \text{ m}\mu$, $K_1 = 36.7 \text{ M}^{-1}$.

TABLE D.10

Variation in the Rate of Hydrolysis of $(\text{en})_2\text{CoCO}_3^+$
with $[\text{OH}^-]$ at 44.0°

$[\text{OH}^-], \text{ M}$	$k_{\text{obsd}}^a \times 10^3, \text{ sec}^{-1}$	$k_{\text{calcd}}^a \times 10^3, \text{ sec}^{-1}$
0.00365	6.88	6.03
0.00502	5.33	4.85
0.00773	3.85	3.79
0.0151	3.33	2.96
0.0159	2.70	2.93
0.0219	2.66	2.81
0.0219	2.50	2.81
0.0227	2.68	2.80
0.0287	2.83	2.82
0.0287	2.75	2.82
0.0362	2.59	2.91
0.0429	2.76	3.02
0.0497	3.13	3.16
0.0632	3.18	3.46
0.0698	3.50	3.62
0.0766	3.72	3.77
0.0949	4.58	4.24
0.104	4.88	4.27

TABLE D.10 (Cont'd)

$[\text{OH}^-], \text{ M}$	$k_{\text{obsd}}^a \times 10^3, \text{ sec}^{-1}$	$k_{\text{calcd}}^a \times 10^3, \text{ sec}^{-1}$
0.122	5.02	4.95
0.149	5.78	5.65
0.178	7.00	6.45
0.248	9.23	8.32
0.310	10.7	10.0

(a) $\mu = 1.0$ (NaClO_4), $\lambda = 300 \text{ m}\mu$, $K_1 = 26.4 \text{ M}^{-1}$.

TABLE D.11

Variation in the Rate of Hydrolysis of $(\text{bipy})_2\text{CoCO}_3^+$
 with $[\text{H}^+]$ at 52.0, 60.0, and 69.3°

$[\text{H}^+]$, M	$k_{\text{obsd}}^a \times 10^3$, sec^{-1}	$k_{\text{calcd}} \times 10^3$, sec^{-1}	T, °
0.0667	0.256	0.262	52.0
0.200	0.738	0.720	
0.334	1.15	1.18	
0.483	1.48	1.69	
0.551	1.96	1.92	
0.600	2.38	2.09	
0.800	2.81	2.78	
0.867	2.95	3.01	
0.867	2.95	3.01	60.0
0.0968	1.11	1.31	
0.226	2.47	2.51	
0.355	3.85	3.71	
0.467	4.95	4.75	
0.600	6.13	5.99	
0.867	8.25	8.48	69.3
0.0667	2.17	2.01	
0.200	5.06	4.71	

TABLE D.11 (Cont'd)

$[H^+], M$	$k_{obsd}^a \times 10^3, sec^{-1}$	$k_{calcd} \times 10^3, sec^{-1}$	$T, ^\circ$
0.400	8.16	8.76	69.3
0.400	9.13	8.76	
0.500	9.66	1.08	
0.613	13.8	13.1	
0.800	16.5	16.9	
0.867	18.8	18.3	

(a) $\mu = 1.0$ (NaCl).

TABLE D.12

Variation in the Rate of Hydrolysis of $(\text{phen})_2\text{CoCO}_3^+$
with $[\text{H}^+]$ at 50.0°

$[\text{H}^+]$, M	$k_{\text{obsd}}^a \times 10^3$, sec^{-1}	$k_{\text{calcd}} \times 10^3$, sec^{-1}
0.0666	0.133	0.142
0.0666	0.123	0.142
0.127	0.230	0.242
0.200	0.403	0.365
0.200	0.418	0.365
0.200	0.398	0.365
0.269	0.423	0.480
0.287	0.550	0.511
0.400	0.626	0.700
0.400	0.666	0.700
0.483	0.834	0.839
0.500	0.963	0.867
0.500	0.825	0.867
0.500	0.905	0.867
0.600	1.00	1.03
0.600	1.00	1.03
0.715	1.10	1.23
0.715	1.25	1.23

TABLE D.12 (Cont'd)

$[\text{H}^+], \text{ M}$	$k_{\text{obsd}}^a \times 10^3, \text{ sec}^{-1}$	$k_{\text{calcd}} \times 10^3, \text{ sec}^{-1}$
0.715	1.28	1.23
0.800	1.52	1.37
0.800	1.28	1.37

(a) $\mu = 1.0$ (NaCl).

TABLE D.13

Variation in the Rate of Hydrolysis of $(\text{phen})_2\text{CoCO}_3^+$
with $[\text{H}^+]$ at 60.5°

$[\text{H}^+], \text{ M}$	$k_{\text{obsd}}^a \times 10^3, \text{ sec}^{-1}$	$k_{\text{calcd}} \times 10^3, \text{ sec}^{-1}$
0.0666	0.529	0.510
0.133	0.842	0.851
0.200	1.07	1.19
0.267	1.66	1.54
0.333	1.98	1.88
0.400	2.31	2.22
0.500	2.56	2.74
0.600	3.12	3.25
0.700	3.75	3.76
0.800	4.38	4.28
0.840	4.50	4.48

(a) $\mu = 1.0$ (NaCl).

TABLE D.14

Variation in the Rate of Hydrolysis of $(\text{phen})_2\text{CoCO}_3^+$
with $[\text{H}^+]$ at 71.1°

$[\text{H}^+], \text{ M}$	$k_{\text{obsd}}^a \times 10^3, \text{ sec}^{-1}$	$k_{\text{calcd}} \times 10^3, \text{ sec}^{-1}$
0.0666	1.12	1.86
0.100	1.67	2.27
0.200	3.08	3.50
0.300	6.02	4.14
0.400	6.41	5.87
0.500	8.11	7.20
0.600	9.00	8.43
0.700	9.75	9.66
0.700	9.70	9.66
0.800	11.5	10.9
0.800	9.62	10.9
0.800	10.2	10.9
0.800	10.8	10.9
0.800	10.8	10.9

(a) $\mu = 1.0$ (NaCl) .

B29982